

Natural products from Myxococcales and
Bacillales & Description of a new
myxobacterial taxon

Dissertation

for the award of the degree

“Doctor of Philosophy (Ph.D.)”

Division of Mathematics and Natural Sciences
of the Georg-August-Universität Göttingen

within the Doctoral program Biology

of the Georg-August University School of Science (GAUSS)

submitted by

Sakshi Sood

born in

Jubbal, India

Göttingen 2014

Thesis committee

Prof. Dr. Rolf Daniel, Department of Genomic and Applied Microbiology and Genomics Laboratory, Institute of Microbiology and Genetics

Prof. Dr. Rolf Müller, Department of Microbial Drugs and Microbial Natural Products, Helmholtz Centre for Infection Research and Helmholtz Institute for Pharmaceutical Research Saarland

Members of the Examination Board

Reviewer

Prof. Dr. Rolf Daniel, Department of Genomic and Applied Microbiology and Genomics Laboratory, Institute of Microbiology and Genetics

Second Reviewer

Prof. Dr. Rolf Müller, Department of Microbial Drugs and Microbial Natural Products, Helmholtz Centre for Infection Research and Helmholtz Institute for Pharmaceutical Research Saarland

Further members of the Examination Board:

Prof. Dr. Stefanie Pöggeler, Department of Genetics of Eukaryotic Microorganisms, Institute of Microbiology and Genetics

PD Dr. Michael Hoppert, Department of General Microbiology, Institute of Microbiology and Genetics

PD Dr. Wilfried Kramer, Department of Molecular Genetics, Institute of Microbiology and Genetics

Jun.-Prof. Dr. Kai Heimel, Department of General Microbiology, Institute of Microbiology and Genetics

Date of Oral Examination: March 14, 2014

Time: 12:30-14:00

List of publications

Journal publications

Paenilarvins, iturin family lipopeptides from the honey bee pathogen *Paenibacillus larvae*

Sakshi Sood, Heinrich Steinmetz, Kathrin I. Mohr, Marc Stadler, Marvin Djukic, Rolf Daniel and Rolf Müller. (Manuscript in preparation for resubmission)

***Aggregicoccus edonensis* gen. nov., sp. nov., an unusually aggregating myxobacterium isolated from a soil sample**

Sakshi Sood, Ram Prasad Awal, Joachim Wink, Kathrin I. Mohr, Manfred Rohde, Marc Stadler, Peter Kämpfer, Stefanie P. Glaeser, Peter Schumann, Ronald Garcia and Rolf Müller.

Submitted to *International Journal of Systematics and Evolutionary Microbiology* on December 13th, 2013

Revised on February 5th, 2014

Pyrronazols, metabolites from the myxobacteria *Nannocystis pusilla* and *N. exedens* are unique chlorinated pyrrole-oxazole-pyrones.

Rolf Jansen, **Sakshi Sood**, Volker Huch, Brigitte Kunze, Marc Stadler and Rolf Müller. *Journal of Natural Products*, 2014. DOI: 10.1021/np400877r

Poster presentations

Antimicrobial compounds from *Paenibacillus larvae* and their role in pathogenesis

Sakshi Sood, Heinrich Steinmetz, Elzbieta Brzuszkiewicz, Kathrin Mohr, Rolf Daniel and Rolf Müller.

VAAM International Workshop on Drug Producing microorganisms, Braunschweig, Germany (2012)

Antimicrobial compounds from *Paenibacillus larvae* and their role in pathogenesis

Sakshi Sood, Heinrich Steinmetz, Elzbieta Brzuszkiewicz, Kathrin Mohr, Rolf Daniel and Rolf Müller.

Central European Symposium on Antimicrobials and Antimicrobial Resistance, Primosten, Croatia (2012)

Table of Contents

Abbreviations	IV
Chapter A Introduction	1
A.1 Natural products	1
A.1.1 Beginning of the era of Wonder Drugs	1
A.1.2 Natural products - much more than just antibiotics	2
A.1.3 Requisite for new natural products in future	3
A.1.4 Microbes as a source of novel natural products	3
A.2. <i>Paenibacillus</i> as a source of natural products	4
A.2.1 <i>Paenibacillus larvae</i> and its secondary metabolite potential	6
A.3 Myxobacteria: a promising source of natural products	8
A.3.1 Taxonomy of myxobacteria	9
A.3.2 Treasure from myxobacterial metabolome	10
A.3.3 Quest for novel myxobacteria and their metabolites	13
A.4 Process of drug development from microbial natural products	15
A.5 Challenges and benefits of microbial drug discovery program	16
A.6 Aim of this thesis	17
References	19
Chapter B Paenilarvins, iturin family lipopeptides from the honey bee Pathogen <i>Paenibacillus larvae</i>	26
B.1 Abstract	27
B.2 Introduction	27
B.3 Results and Discussion	29
B.3.1. Bioactivity screening of <i>P. larvae</i> DSM 25719 and DSM 25430	29
B.3.2 Structural analysis of paenilarvins	30
B.3.3 Mass spectrometric analysis	32
B.3.4 Antimicrobial and cytotoxic activity of paenilarvins	36
B.4 Conclusion	37
B.5 Experimental Section	40
B.5.1 General Experimental Procedures	40
B.5.2 Bacterial strain and growth conditions	41

B.5.3 Extraction and isolation of active compounds	41
B.5.4 Assignment of absolute stereochemistry of amino acid residues	42
B.5.5 Structural characteristics of paenilarvins	42
B.5.6 Antimicrobial assay	43
B.5.7 Cytotoxicity assay	43
Acknowledgements	44
References	45
Supplemental information	48
Chapter C <i>Aggregicoccus edonensis</i> gen. nov., sp. nov., an unusually aggregating myxobacterium isolated from a soil sample	69
C.1 Abstract	70
C.2 Introduction	70
C.3 Results and Discussion	71
C.4 Description of <i>Aggregicoccus</i> gen. nov.	83
C.5 Description of <i>Aggregicoccus edonensis</i> sp. nov.	84
Acknowledgements	84
References	85
Supplemental information	87
Chapter D Pyrronazols, Metabolites from the Myxobacteria <i>Nannocystis pusilla</i> and <i>N. exedens</i> are Unusual Chlorinated Pyrone-Oxazole-Pyrroles	96
D.1 Abstract	97
D.2 Introduction	97
D.3 Results and Discussion	98
D.4 Experimental Section	107
D.4.1 General Experimental Procedures	107
D.4.2 Isolation of Pyrronazols A, A2 and B from <i>N. pusilla</i> , strain Ari 7	107
D.4.3 Isolation of Pyrronazol C1 and C2 from <i>N. pusilla</i> , strain Na a174	109
D.4.4 X-Ray Structure Determination of Pyrronazol A (1)	109
D.4.5 Structural characteristics of compounds isolated	110
D.4.6 Antimicrobial Testing	111
D.4.7 Cytotoxicity assay	112
Acknowledgements	112

References	113
Supplemental information	114
Chapter E Discussion	127
E.1 Paenilarvins, antifungal peptides from honey bee pathogen, <i>Paenibacillus larvae</i>	127
E.2 <i>Aggregicoccus edonensis</i> gen. nov., sp. nov., a soil myxobacterium with characteristic aggregation	130
E.3 Pyrroazols and phenazines from <i>Nannocystis pusilla</i>	132
References	137
Summary	140
List of Figures	VII
List of Tables	X
Acknowledgements	XI

Abbreviations

[M+H] ⁺	Protonated molecular ions
[M+Na] ⁺	Molecular ions with sodium
[M-H] ⁺	Deprotonated molecular ions
[M-H ₂ O] ⁺	Dehydrated molecular ions
¹³ C HMQC	Carbon Heteronuclear Multiple Quantum Coherence
1D NMR	One dimensional Nuclear magnetic resonance
¹ H HMQC	Proton Heteronuclear Multiple Quantum Coherence
ACCs	Acetyl-CoA-carboxylase
adj.	adjective
AFB	American foulbrood
Asn	Asparagine
BCFAs	Branched chain fatty acids
BD	Becton Dickinson
BLAST	Basic Local Alignment Search Tool
Calcd.	Calculated
CD ₃ OH	Deuterated methanol
CDCl ₃	Deuterated Chloroform
CoA	Coenzyme A
COSY	Correlated Spectroscopy
CTAB	Cetyl trimethylammonium bromide
ddH ₂ O	Double distilled water
DMSO	Dimethyl sulfoxide
EDTA	Ethylenediaminetetraacetic acid
ERIC	Enterobacterial repetitive intergenic consensus
f. sp.	Formae specialis
FAs	Fatty acids
FASTA	DNA and protein sequence alignment software package
fem.	feminine
Fig.	Figure
FISH	Fluorescence in situ hybridization

FTMS	Fourier Transform Mass Spectrometry
GBF	Gesellschaft für Biotechnologische Forschung
GC-MS	Gas chromatography-mass spectrometry
gen. nov.	Genus novel
Gln	Glutamine
Gr.	Greek
HEPES	Buffering agent
HIV-1	Human immunodeficiency virus -1
HMBC	Heteronuclear Multiple-Bond Correlation
HRESIMS	High Resolution Electron Spray Ionization Mass spectrometry
IC ₅₀	Half maximal inhibitory concentration
IMG/ER	Integrated Microbial Genomes/Expert Review
IR	Infrared
Lat.	Latin
LD ₅₀	Lethal dose, 50%
LT ₁₀₀	Lethal time, 100%
<i>m/z</i>	Mass-to-charge ratio
MALDI-TOF	Matrix Assisted Laser Desorption Ionization-Time of Flight Mass Spectrometry
masc.	masculine
Mbp	Megabasepairs
MeOH	Methanol
MIC	Minimum inhibitory concentration
mp.	Melting point
n.i.	No inhibition
NCBI	National Center for Biotechnology Information
NCCB	The Netherlands Culture Collection of Bacteria
NMR	Nuclear Magnetic Resonance
NOE	Nuclear Overhauser effect
NOESY	Nuclear Overhauser effect spectroscopy
NRP	Nonribosomal peptides
NRPSs	Nonribosomal peptide synthetase
OAG	O-alkylglycerol
PK	Polyketides

PKSs	Polyketide synthetase
Pro	Proline
rDNA	Ribosomal DNA
ROESY	Rotating-frame nuclear Overhauser effect correlation spectroscopy
RP-HPLC	Reverse phase-High pressure liquid chromatography
rpm	Revolutions per minute
RP-MPLC	Reverse phase-Medium pressure liquid chromatography
rRNA	Ribosomal RNA
R_t	Retention time
SCFAs	Straight chain fatty acids
SDS	Sodium dodecyl sulfate
Ser	Serine
SHELX	Program for structure determination
Si	Silica
sp. nov.	Species novel
β -Aa	β -Amino acid
SSH	Suppression subtractive hybridization
Subsp.	Subspecies
Tab.	Table
TE buffer	Tris-EDTA buffer
TLC	Thin Layer chromatography
TOCSY	Total Correlation Spectroscopy
Tyr	Tyrosine
UV/Vis	Ultraviolet visible
v/v	Volume by volume
Ver.	Version
vvm	Volume gas per reaction volume per minute
w/v	Weight by volume
XAD	Adsorbent resins (Amberlite)
ϵ	Molar extinction coefficient
λ_{\max}	Wavelength of the most intense UV/Vis absorption

Chapter A

Introduction

A.1. Natural products

Chemical compounds isolated from natural origins are called natural products. These compounds may be products of primary or secondary metabolism of diverse living organisms. While primary metabolites like polysaccharides, proteins, nucleic and fatty acids are similar in all biological systems, the chemical and taxonomic diversity of secondary metabolites is enormous. Additionally, the bioactivities of secondary metabolites are versatile in contrast to primary metabolites (Berdy, 2005). Hence, in most cases the term, “natural products” refers to secondary metabolites, small molecules produced by an organism that are not essential for the survival of the organism. Secondary metabolites can include products of overflow metabolism as a result of nutrient limitation, shunt metabolism products during stationary phase, defense mechanism regulator molecules, etc. (Sarker *et al.*, 2005).

Natural products have been used to treat human diseases since the dawn of medicine through the use of traditional medicines predominantly derived from plants. Most early therapeutic drugs such as aspirin, digitoxin, morphine, quinine, and pilocarpine were results of clinical, pharmacological, and chemical studies on these traditional medicines (Butler, 2004).

Natural products have been reestablished as potential source of new medicines in scientific community in recent years. In spite of competition from other drug discovery methods, natural products still continue to provide novel therapeutic molecules. 40% of the modern drugs in use have been developed from natural products (Sarker *et al.*, 2005).

A.1.1. Beginning of the era of Wonder Drugs

Antibiotics are compounds of natural, semi-synthetic or synthetic origin which kill or inhibit the growth of microorganisms without significant toxicity to the human or

animal hosts. The search for antibiotics began in the late 1800s, with the growing acceptance of the 'germ theory of diseases', a theory given by Louis Pasteur which linked microbes to various infectious diseases. As a result, scientists began to devote time to search for drugs that would kill these infection causing agents. The goal of such research was to find compounds that would hamper microbial growth without toxicity to the patient. Sir Alexander Fleming discovered the production of penicillin by *Penicillium notatum* in 1929 as a substance killing cells of *Staphylococcus aureus* (Fleming, 1929). However, it was Florey, Chain and Heatley who were later successful in developing a stable form of penicillin which showed significant in vivo activity against many Gram positive bacterial pathogens. With the conjoined efforts between several universities and pharmaceutical companies, the commercial production of first chemotherapeutic agent, penicillin from a microbe became a reality, thus marking the beginning of the golden age of antibiotics i.e. the "wonder drugs" (Demain, 2006). The advent of penicillin was followed by discovery of many new antibiotics from actinomycetes by Selman Waksman. Streptomycin became one of the most famous amongst them. The tide began to change thereafter with the discovery of numerous antimicrobial drugs like cephalosporins, tetracyclines, aminoglycosides, chloramphenicol, macrolides and many others. All these compounds, or derivatives thereof, are still in use as drugs today.

A.1.2. Natural products - much more than just antibiotics

Natural products are widely recognized in the pharmaceutical industry for their broad structural diversity as well as their wide range of pharmacological activities. The activity may be highly specific or can be unspecific or even toxic in action. Although natural product discovery was mainly devoted to antibiotics in the early phase, but between the seventies and the nineties the exploration and the wide utilization of natural products began e.g. as enzyme inhibitors (lovastatin, pravastatin), immunosuppressants (cyclosporin, sirolimus, tacrolimus and mycophenolic acid), antiparasitic agents (ivermectins, narasin, lasalocid) bioherbicides (bialaphos), plant growth regulators (gibberellins), biopesticides (kasugamycin, polyoxins), bioinsecticides (spinosins and nikkomycin) and antitumor agents (doxorubicin, daunorubicin, mitomycin, bleomycin, etc.) (Demain, 2006). However, at subinhibitory concentrations these compounds can exhibit pleiotropic effects at different

concentrations (Romero *et al.*, 2011). They can act as signaling molecules that regulate gene expression in microbial population, or physiological functions such as motility, sporulation, pigmentation, quorum sensing, biofilm formation and virulence (Romero *et al.*, 2011).

A.1.3. Requisite for new natural products in future

New and reemerging infectious diseases for which an effective therapy is still unavailable are a matter of concern in modern times. In addition to this, emergence and rise of pathogens resistant to currently used drugs present a great threat to disease management. Development of multidrug resistance is now gathering pace and contributing more substantially to the problem. This conveys an overt message that a continual supply of structurally novel antibiotics with multiple modes of action needs to be part of the antimicrobial armamentarium. A similar situation exists with the need to develop new cancer chemotherapeutic agents. This has given rise to an urgent need for identification of novel molecular scaffolds which can serve as new leads for effective drug development. Natural products can contribute to the process of drug development by their application in unmodified state in as isolated from nature, by providing basic chemical scaffolds that can be used to derive new molecules, or by signifying novel modes of pharmacological action or targets that allow synthesis of entirely novel analogs (Sarker *et al.*, 2005).

With an insight into new molecular targets, it is essential to look and screen for natural molecular diversity against these targets. Products from natural origin can play a crucial role in meeting such demand since a lot of world's biodiversity such as marine environments and extreme environments still remain unexplored (Xiong *et al.*, 2013). Advances in technology can open access to untapped reservoir of genetic and metabolic diversity within the eukaryotic as well as microbial world.

A.1.4. Microbes as a source of novel natural products

Due to technical improvements in screening programs and chromatographic techniques, biological activity is observed for ~20-25% of the reported natural products, and 10% of these active natural products are obtained from microbes (Demain and Sanchez, 2009). The versatility of microbial drugs is gigantic. Microbes keep on producing novel metabolites as they move into the diverse ecological units.

From the microbes that have been used so far to obtain the biologically active compounds, filamentous actinomycetes and fungi in particular, are the source for the majority of commercially exploited natural products while unicellular bacteria like *Bacillus* sp. on the other hand, more commonly, but not exclusively, produce peptide antibiotics like gramicidin, surfactin and subtilin.

The fact that the secondary metabolite producing ability is not evenly distributed in the microbial world is indicated by the number of bioactive compounds obtained from fungi (Keller *et al.*, 2005) (61%) followed by actinobacteria (Watve *et al.*, 2001) (28%) both of which represent the largest groups of producers (Berdy, 2012). Mycobacteria, Mycoplasmatales and Spirochaetes are occasional producers unlike *Bacillus* (Fickers, 2012) and *Pseudomonas* species (Gross and Loper, 2009) which are most frequent producers amongst the prokaryotic, unicellular bacteria. Myxobacteria and Cyanobacteria species seem to join these distinguished organisms as recognized-prolific species producing chemically diverse compounds (Weissmann and Müller, 2010; Singh *et al.*, 2011) However, the bias observed in production of bioactive compounds can also be attributed to the amount of work done on each of these groups of microorganisms over the years.

A.2. *Paenibacillus* spp. as a source of natural products

Paenibacillus is a group of endospore forming, aerobic or facultative anaerobic, rod shaped bacteria which belonged to the genus *Bacillus* until 1993 when Ash *et al.* reassigned some of the bacilli to a new genus *Paenibacillus* using a battery of phenotypic characters and a highly specific gene probe based on 16S rRNA. At present a total of 152 species (including subspecies) belong to this genus according to the Leibniz Institute DSMZ (German Collection of Microorganisms and Cell Cultures). Diverse ecological niches like soil, rhizospheres, diseased insect larvae, food, animal faeces etc. have been used as a source for isolation of novel *Paenibacillus* sp. (Saha *et al.*, 2005).

Paenibacillus species are notable for their ability to produce secondary metabolites such as antibacterial and antifungal compounds, pigments, toxins, along with inductors of competition and symbiosis, enzyme inhibitors, pheromones and promoters of vegetable and animal growth (Li-jing *et al.*, 2011). Production of such

secondary metabolites can confer special benefits to the producing organisms such as biocontrol of the competitors by scavenging minerals and nutrients and inhabiting the colonization sites in their natural environment (Lorentz *et al.*, 2006). Therefore, a number of *Paenibacillus* species have been studied as a source of biologically active novel natural compounds and for their potential application as biocontrol agents in the recent past.

The type species of genus *Paenibacillus*, *Paenibacillus polymyxa* produces peptide antibiotics like polymyxins, polypeptins, jolipeptin, gavaserin, saltavalin and fusaricidins active against bacteria, actinomycetes and fungi (Raza *et al.*, 2009). Polymyxins (Stansly *et al.*, 1947) were found to be produced by *Paenibacillus polymyxa* (formerly known as *Bacillus polymyxa*) and selectively active against Gram negative bacteria by disruption of bacterial cell membrane lipopolysaccharides. Polymyxins B and E (colisitin) have been regularly used in clinical practice against a number of pathogenic bacteria (Falagas and Kasiakou, 2006). In recent years, polymyxins have been shown to be effective in treatment of patients infected with multidrug-resistant Gram negative bacteria (Falagas *et al.*, 2008). Martin *et al.* described another cyclic peptide antibiotic belonging to polymyxins, mattacin (polymyxin M) produced by *P. kobensis* and active against a wide variety of Gram positive and negative bacteria including several human and plant pathogens.

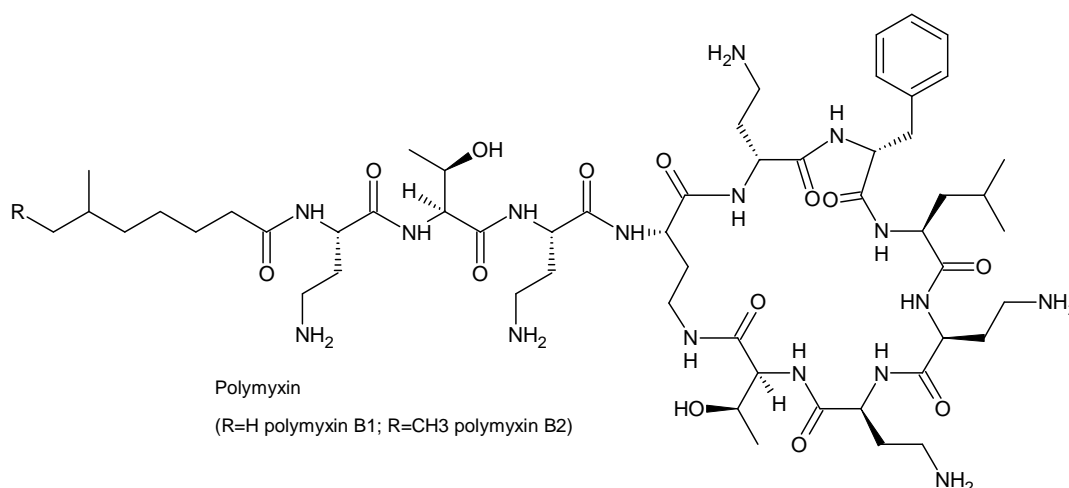


Fig. A1. Structure of Polymyxin B isolated from *B. subtilis*

P. alvei, strain NP75 has been reported to coproduce two new peptide antibiotics, paenibacillin P and paenibacillin N active against Gram positive and negative

bacteria, respectively (Anandraj *et al.*, 2009). A soil isolate of *P. tianmuensis* produces battacin, a cationic lipopeptide antibiotic active against some critical multi drug-resistant Gram negative bacterial strains of *Pseudomonas aeruginosa* and *E. coli* (Qian *et al.*, 2011). In 2010, paenimacrolidin, a polyunsaturated macrolactone showing bacteriostatic activity against methicillin-resistant *Staphylococcus aureus* was discovered from *Paenibacillus sp.* (Wu *et al.*, 2011). Additionally, *P. peoriae* (Weid *et al.*, 2003), *P. brasiliensis* (Fortes *et al.*, 2008), *P. koreensis* (Chung *et al.*, 2000) and many other species have been described to demonstrate antimicrobial activity though their active components have not yet been isolated.

In conclusion, a number of *Paenibacillus* species continue to be studied as a source of biologically active novel natural compounds for their potential application in therapeutics and as biocontrol agents against phytopathogens like *Fusarium oxysporum* f. sp. *neivium*, the causative agent of fusarium wilt of watermelons (Raza *et al.*, 2009).

A.2.1. *Paenibacillus larvae* and its secondary metabolite potential

Paenibacillus larvae is the etiological agent of a disastrous honey bee epidemic, American Foulbrood (AFB). AFB is an economically significant and a very contagious disease which can lead to the collapse of entire bee colonies. It is a notifiable disease in many countries and the effective measures for control usually involve burning of infected colonies to prevent the spread to other healthy colonies. Efforts to study the complete pathogenesis of *P. larvae* have thrown light on many aspects of the infectious disease in last few decades but a comprehensive understanding of disease progression and virulence factors employed by the pathogen is still lacking.

Bacillus larvae was first described as the causative agent of AFB in honey bees (*Apis mellifera*) by Whites in 1906. Another organism named *Bacillus pulvifaciens* was later accounted for causing powdery scale disease in honey bee larvae. But both these species along with many others were correctly classified into genus *Paenibacillus* in 1993 based on comparative 16S rRNA sequence analysis (Ash *et al.*, 1993). However, strains belonging to species *Paenibacillus larvae* were reclassified into two subspecies as *P. larvae* subsp. *larvae* and *P. larvae* subsp. *pulvifaciens* based on possible phenotypic and genotypic differentiation and distinguished pathologies

(Heyndrickx *et al.*, 1996). It was in 2006 that conclusive evidence based on polyphasic taxonomic study on strains from both the subspecies was presented that justified bringing the two subspecies together into a single species, *Paenibacillus larvae*.

Four different genotypes of *P. larvae* (ERIC I – IV) have been described on the basis of repetitive-element PCR using enterobacterial repetitive intergenic consensus (ERIC) primers (Genersch and Otten, 2003). The four genotypes show phenotypic differences in metabolism as well as in colony and spore morphology. But most importantly, they show differences in their level of virulence on larval and colonial level (Genersch *et al.*, 2005; Ashiralieva and Genersch, 2006; Rauch *et al.*, 2009). Strains of the genotype ERIC I and ERIC II are the most common field isolates from AFB diseased colonies while genotypes ERIC III and ERIC IV are rarely isolated. Experimental bioassays accomplished on honey bee larvae infected with *P. larvae* spores have revealed that *P. larvae* ERIC I strains have LT₁₀₀ of around 13 days while the other three genotypes ERIC II-IV have LT₁₀₀ of 5-7 days (Genersch *et al.*, 2005). Owing to their higher virulence and the frequency with which genotype ERIC I and ERIC II are encountered in diseased colony samples in nature, they are mostly used for in depth study of the disease.

Paenibacillus larvae infects the honey bee larvae in their first instar stage through the ingestion of food contaminated with spores (Yue *et al.*, 2008). The spores germinate inside the midgut lumen followed by proliferation of the vegetative cells. The vegetative cells then breach the epithelial barrier and colonize haemocoel. The cells of bacteria degrade the larvae body after its death into a thick ropy mass which later dry to form hard scales containing a huge number of infectious bacterial spores which can spread to other healthy bee colonies through various means.

Many virulence factors like toxins (Fünfhaus *et al.*, 2013), S-layer protein (Poppinga *et al.*, 2012) and proteases (Antunez *et al.*, 2010; Antunez *et al.*, 2011) have been described in the recent years for their potential involvement in pathogenesis. Four fragments showing homology to the various nonribosomal peptide synthetases from *Bacillus* sp. were identified in the genome of *P. larvae* ERIC I and ERIC II. Precisely, partial sequences showing homology to the mycosubtilin synthetase subunit, iturin A synthetase subunit and bacitracin synthetase subunit were identified during the

comparative genome analysis (Fünfhaus *et al.*, 2009). The products of these gene clusters have been suggested to be putative virulence factors of the pathogen but have not yet been recognized and purified.

A.3. Myxobacteria: a promising source of natural products

Myxobacteria were discovered by Roland Thaxter in 1892. They are a fascinating group of gram negative, aerobic, δ -proteobacteria with noteworthy features like social behavior, gliding on solid surfaces and formation of fruiting bodies under starvation. The cells within the fruiting bodies become metabolically dormant and environmentally resistant exhibiting an impressive morphological complexity. Myxobacteria are found in various habitats including soil, bark of trees, decomposing insects and lichens, decaying plant material, dung of herbivores and marine environments since they can utilize a diverse array of natural macromolecules as food sources by secretion of exo-enzymes. In addition, they can also utilize living or dead bacterial, fungal or yeast cells as food in their natural surroundings. They are known to possess one of the largest genomes amongst bacteria (9-13 Mbp) with a DNA of high GC content of 66-72 mol% (Reichenbach, 1999; Goldman *et al.*, 2006).

However, in the last three decades the myxobacteria attracted much attention as promising producers of compounds with both, unique structures and bioactivities owing to their rich secondary metabolome. *Sorangium cellulosum* So ce56 which has one of the largest bacterial genomes is known to have around 20 secondary metabolite gene clusters (Schneiker *et al.*, 2007). Secondary metabolite gene clusters account for 9% of genome of *Myxococcus xanthus* which is comparatively higher than many species of actinomycetes (Bode and Müller, 2005).

The biosynthetic potential of these microbes is remarkable and has an immense room for exploration and exploitation. They have hitherto yielded at least 100 different core structures and 500 different derivatives (Garcia *et al.*, 2009a). The majority of the secondary metabolites produced by myxobacteria are polyketides, nonribosomal peptides, or their hybrids while other structural metabolite types comprise terpenoids, phenylpropanoids, and alkaloids (Nett and König, 2007). Distinctive modes of action against a broad range of both prokaryotic and eukaryotic cells can often be observed by compounds isolated from myxobacteria (Weissmann and Müller, 2010).

A.3.1. Taxonomy of myxobacteria

All known myxobacteria are included in the order Myxococcales, which is further divided into three suborders, Sorangiineae, Cystobacterineae and Nannocystineae (Reichenbach, 2005). Novel myxobacterial taxa continue to be discovered from strains isolated in varied locations worldwide signifying that the myxobacterial diversity is yet unexplored. Availability of the 16S rRNA sequences of cultured strains of halophilic (Iizuka *et al.*, 2003a,b), halotolerant (Iizuka *et al.*, 2006) and anaerobic (Coates *et al.*, 2002; Sanford *et al.*, 2002) myxobacteria suggest the wide-ranging physiological and ecological niches which can be inhabited by myxobacteria. Dawid and colleagues isolated some psychrophilic myxobacterial species from Antarctic soil samples with optimal growth temperatures ranging from 4°C to 9°C (Dawid *et al.*, 1988). 16S rDNAs of many myxobacteria is also detected during the metagenomic studies but these bacteria are often termed as viable but not cultivable (VBNC) environmental strains (Garcia *et al.*, 2010). Such strains are not significantly represented and described currently due to their unfamiliar and slightly complex physiological and nutritional growth requirements. A combination of new sophisticated isolation techniques, selective culture media, and other methods may make culturing such bacteria possible under laboratory conditions in future.

With the continuous discovery of new and reclassification of some known myxobacterial taxa, it is immensely important to revise and update the current phylogeny of this group. The unique morphological traits of myxobacteria are the primary basis for isolation and characterization of families, genera and species and to identify the taxonomic status of novel strains within the order Myxococcales. However, such characteristics are often lost or become aberrant when the strains are repeatedly subcultured under laboratory conditions and so, are unreliable for taxonomic classification (Garcia *et al.*, 2010). Exploration and application of some new molecular taxonomic approaches along with the traditional ones is necessary to alleviate some of these problems and to clearly delineate a potential new taxon from its closest relatives (Shimkets and Woese, 1992). The novel tools available for systematics include the complete 16S rRNA gene sequencing and its comparative analysis by phylogenetic trees, DNA-DNA hybridization studies with related organisms, analyses of molecular markers and signature pattern(s), biochemical

assays, physiological and morphological tests. All these genotypic, chemotaxonomic and phenotypic tools in combination with each other or all together can furnish substantial information for elucidating the reliable taxonomic position of a microbe and constitute a polyphasic approach for taxonomic studies.

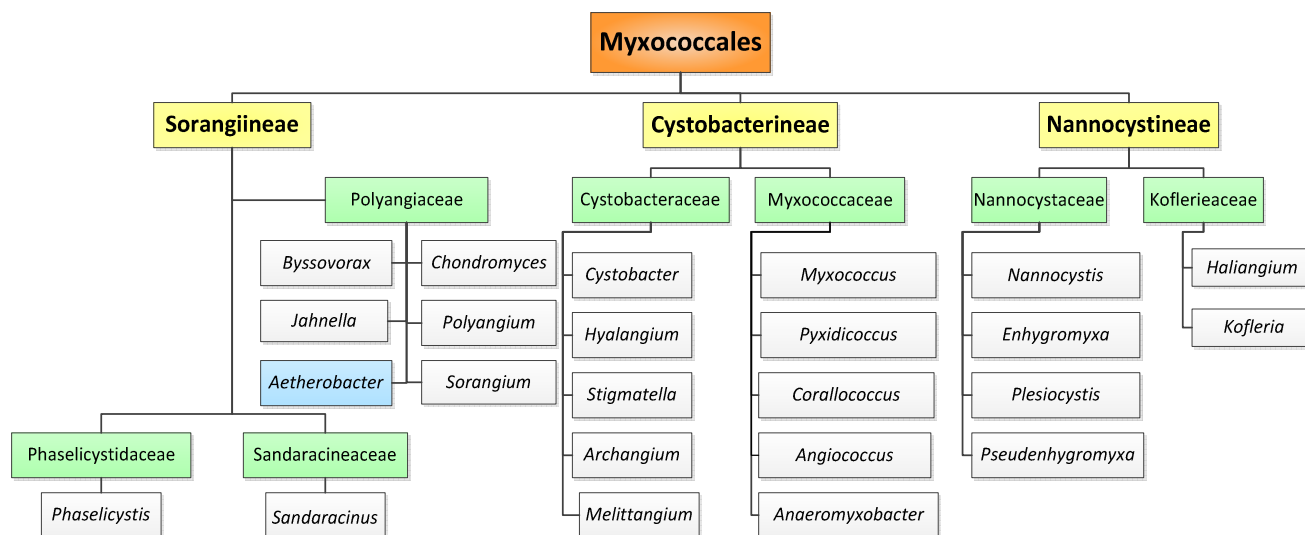


Fig.A2. Systematic description of myxobacteria within order Myxococcales (orange). Three suborder (yellow) and seven families (green) are also indicated. *Aetherobacter* (blue) is a novel unpublished genus. (Garcia *et al.*, 2009b; Mohr *et al.*, 2011; Iizuka *et al.*, 2003; Iizuka *et al.*, 2013)

Progress in polyphasic approach has become an important tool in bacterial systematics and should be applied more effectively for myxobacteria to classify newly isolated strains as well as reclassification of strains placed under invalid taxa. Recently, cellular fatty acid analysis has been used for chemo-taxonomic classification of myxobacteria and it has been proven to be a valid tool to verify the rDNA based phylogeny (Garcia *et al.*, 2011). More such molecular markers or methods need to be determined for deciphering accurate phylogenetic relationships between the closely related taxa. Following a polyphasic approach will progressively pave the way for modern myxobacterial systematics rooted in the genetic lineages of the organisms.

A.3.2. Treasure from myxobacterial metabolome

The myxobacterial metabolome is unique both in structural diversity and biological activities. About 40% of the myxobacterial compounds that have been described

represent novel chemical scaffolds while others comprise structural elements already known from other organisms like streptomycetes and cyanobacteria but modified by myxobacteria into new compounds (Reichenbach, 2001). Only in very rare events, structures exactly identical to compounds known from other sources were identified from myxobacteria suggesting the diverse chemical space of the myxobacterial metabolome.

These findings have motivated more research efforts to identify lead compounds amongst the myxobacterial secondary metabolites for clinical application. One of the most celebrated compounds from myxobacteria is epothilone B which was isolated from *Sorangium cellulosum*. It was found to possess cytotoxic activity against mouse fibroblast cell line L929 and human T-24 bladder carcinoma cell line (Gerth *et al.*, 1996a). It was hence further investigated and exhibited selective activity against breast and colon tumor cell lines in the *in vitro* antitumor screening program of the National Cancer Institute (Höfle *et al.*, 1996). A semi-synthetic analogue of epothilone B, ixabepilone (Ixempra[®]) was the first natural product of myxobacterial origin approved for clinical use in 2007 for treatment of breast cancer (Hunt, 2009). Disorazols, (Elnakady *et al.*, 2004), tubulysins (Sasse *et al.*, 2000), rhizopodin (Jansen *et al.*, 2008), chivosazols (Diestel *et al.*, 2009) and chondramides (Sasse *et al.*, 1998) all act on cytoskeletal elements and need to be evaluated for development to potential anticancer drugs (Kaur *et al.*, 2006; Elnakady *et al.*, 2004; Khalil *et al.*, 2006). In addition to affecting the cytoskeletal elements, myxobacterial compounds can also act on a number of other target sites inside the eukaryotic cells. Argyrins (Nickeleit *et al.*, 2008) and gephyronic acid (Sasse *et al.*, 1994), for example, both isolated from the myxobacterium *Archangium gephyra* exhibit cytotoxic activities by inhibition of proteasome activity and inhibition of protein synthesis, respectively.

Approximately 54% of the bioactive myxobacterial metabolites exhibit antifungal activity (Gerth *et al.*, 2003) following varied mechanism of actions. The main target of such compounds like stigmatellin (Thierbach *et al.*, 1984), myxothiazol (Thierbach and Reichenbach, 1981), haliangicin (Fudou *et al.*, 2001) and myxalamid (Gerth *et al.*, 1983) is the mitochondrial respiratory chain. Soraphen, a polyketide metabolite produced by *Sorangium cellulosum* came into limelight upon revelation of its unique mode of action which targeted the fungal Acetyl-CoA-carboxylase (Gerth *et al.*,

1994). Its mechanism of action became a model for novel test systems, e.g. showing small-molecule inhibitors of human ACCs have potential in the treatment of metabolic syndromes like obesity (Schreurs *et al.*, 2009) and cancer (Beckers *et al.*, 2007).

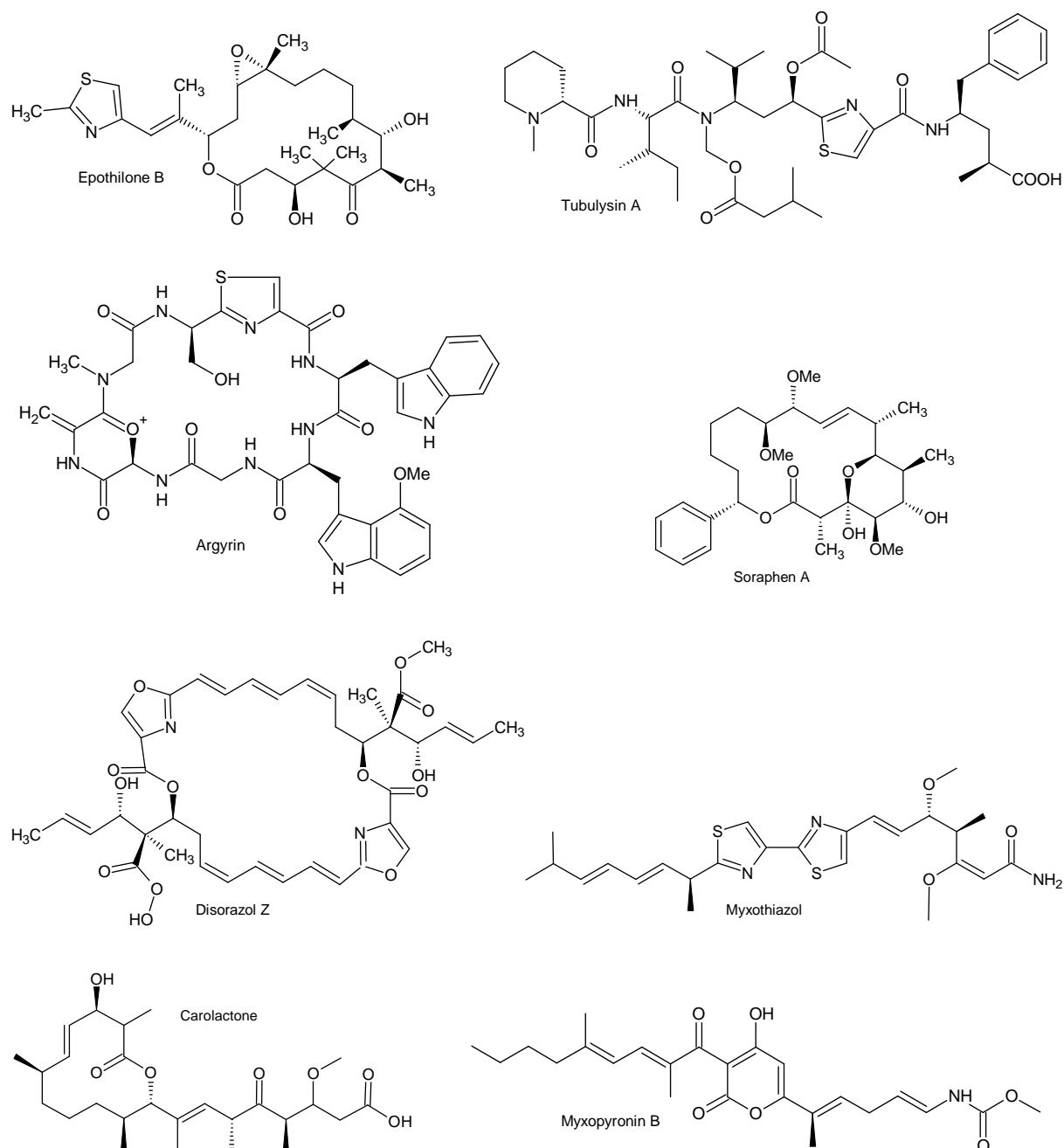


Fig.A3. Natural compounds from myxobacteria with cytotoxic, antifungal and antibacterial activity (Weissman and Müller, 2010)

Out of the huge repertoire of myxobacterial metabolites, around 29% show activities against various bacteria (Gerth *et al.*, 2003) and these antibacterial compounds use varied mode of actions. DNA-dependent RNA polymerase is the key enzyme of

transcription in all living organisms, and hence, also a crucial target for antibacterial therapy. Myxobacterial compounds like coralopyronin (Irschik *et al.*, 1985), myxopyronin (Irschik *et al.*, 1983a), ripostatins (Irschik *et al.*, 1995) and sorangicins (Irschik *et al.*, 1987) can serve as lead structures for development to effective drugs specifically targeting the eubacterial RNA polymerase. Etnangien (Irschik *et al.*, 2007a) has the ability to inhibit bacterial RNA polymerase as well as DNA polymerase, making it an interesting lead molecule for further investigation.

Thuggacins (Irschik *et al.*, 2007b) show activity against selective Gram positive bacteria by inhibition of the cellular electron-transport chain (Steinmetz *et al.*, 2007). Protein synthesis is inhibited by angiolam (Kunze *et al.*, 1985), althiomycin (Kunze *et al.*, 1982) and myxovalargin (Irschik *et al.*, 1983b). Myxovirescins (Gerth *et al.*, 1982) specifically inhibit incorporation of N-acetyl-glucosamine during murein synthesis leading to disruption of the cell wall synthesis.

In the continuing efforts to exploit the myxobacterial secondary metabolism, many new compounds have been identified and described recently including roimatacenes produced by *Cystobacter ferrugineus* (Zander *et al.*, 2011), hyaladione isolated from *Hyalangium minutum* (Okanya *et al.*, 2012) and icumazoles (Barbier *et al.*, 2012) which were described as a new class of antifungals from *Sorangium cellulosum*. Another highly potent compound, carolactone (Jansen *et al.*, 2010) which inhibits biofilm formation by *Streptococcus mutans* was isolated from *Sorangium cellulosum* (Müller and Wink, 2013).

A.3.3. Quest for novel myxobacteria and their metabolites

The strain collection at the Helmholtz Centre for Infection Research has continued to expand over the last few decades and currently comprises more than 8000 isolates of myxobacteria and other gliding bacteria. Our ongoing screening of this huge strain collection for bioactive molecules, which can serve as potential drug candidates or leads in future, has revealed the remarkable ability of myxobacteria to synthesize novel natural products with unique structures. A bulk of the compounds isolated from myxobacteria come from selected genera, such as *Sorangium*, *Myxococcus* and *Chondromyces* sp., reflecting the non-uniform potential to produce secondary metabolite within the myxobacterial species (Garcia *et al.*, 2009). However, this

conclusion is based upon the production under laboratory conditions and may vary in their natural environments. Another striking feature is the commonly observed similarity in the secondary metabolite profiles of strains belonging to the same suborder (Gerth *et al.*, 2007). This aspect can be exploited for chemotaxonomy of myxobacteria using selected secondary metabolites as biomarkers.

Additionally, production of a family of closely related metabolites with varied biological activity rather than a single natural product with unique structure is often observed for myxobacteria (Gerth *et al.*, 2007). For example, *Sorangium cellulosum* can produce at least 30 different variants of epothilone upon fermentation (Gerth *et al.*, 2007). In contrast, a single myxobacterial strain can also produce a huge repertoire of structurally unrelated secondary metabolites based on their genetic potential.

Sampling from biologically complex or extreme environments increases the likelihood of isolation of novel myxobacterial taxa (Dawid, 2000). Forest soil samples which are usually enriched with decaying plant matter and animal dung can serve as an excellent source for isolation of novel strains (Garcia *et al.*, 2009). Such extremely intricate environments seem to be ideal for fostering new myxobacteria and their interaction and competition for limited common resources act as important factors for the development of bioactive secondary metabolites. Recently, 58 halotolerant strains were isolated using conventional isolation methods from saline-alkaline soil samples collected in Xinjiang, China (Zhang *et al.*, 2013). Some of these strains could grow at salt concentration as high as 2% while others formed fruiting bodies at 1% salt concentration displaying their osmotolerance, which is quite unusual in terrestrial myxobacteria.

Additionally, refined isolation and baiting techniques, selective culture media, and other methods could possibly lead to discovery of novel taxa (Garcia *et al.*, 2010). For example, *Anaeromyxobacter dehalogenans* was isolated on the basis of its ability to grow using acetate as an electron donor and 2-chlorophenol as an electron acceptor (Sanford *et al.*, 2002). It was described as first myxobacteria taxon with the ability to grow under facultative anaerobic conditions. Isolation methods involving different prey strains as bait for myxobacteria and imitating natural predatory environment are also often helpful in myxobacterial isolation (Li *et al.*, 2013).

Identification, isolation and screening of new myxobacteria over the last three decades have led to the discovery of many new compounds. This implies that the probability of finding uncharacterized metabolites increases with isolation and screening of novel families, genera or species of myxobacteria. Isolation of aetheramides, potent HIV inhibitory molecules isolated from the novel myxobacterial genus, *Aetherobacter* (not validly published) clearly exemplifies the potential of new taxa in production of new molecules (Plaza *et al.*, 2012). Aetheramides were found to be active against fungi and human colon tumor cell line (HCT-116) but most importantly against the virus, HIV-1. Indiacens were also isolated and purified as compounds with antibiotic activity against certain bacteria and filamentous fungi from another novel myxobacterial genus, *Sandaracinus amylolyticus*, (Steinmetz *et al.*, 2012).

Bioassay-based screening and fractionation, and HPLC-coupled mass spectrometry of the crude extracts from selected strains form a part of conventional methods in drug discovery. Apart from these commonly used screening and de-replication processes for identification of novel myxobacterial products, new approaches need to be implemented in order to discover yet unidentified metabolites. Co-cultivation with other soil bacteria and mimicking the natural environment during cultivation could be employed as new strategies for screening for potential new bioactive compounds from already known taxa as well as novel taxa.

A.4. Process of drug development from microbial natural products

In a classic microbe-based natural product program, microbiologists isolate pure cultures of microorganism from environmental samples collected from the biosphere. Environmental samples can vary from the traditional soil samples to leaf litter, tree barks, animal dung and beetle carcasses but each kind of environmental sample has its own characteristic microbial spectrum (Borris, 1996).

Extracts from small scale fermentations of the isolated pure cultures are then screened on a panel of preliminary assays. Cultures that are found to be active in one or more assays are again grown under similar conditions to check the reproducibility of the original activity before the culture extract is subjected to some

form of dereplication.

Dereplication, the process of determining whether the active compound is novel is a vital part of any natural product program. A finely designed and executed dereplication process helps to avoid wasting resources and allows focusing on unique molecules and activities. Isolation and identification of the active constituent follows the dereplication process for the positive extracts. Optimization of media and growth conditions is also often crucial to obtain higher yields of compounds. Isolation of the active compounds is performed by various subsequent chemical processes guided at each step by bioassay data. The molecular structure of the compound is determined using various spectroscopic and chemical techniques like NMR spectroscopy and X-Ray crystallography. Isolation of the pure compound at larger scale is then carried out after optimization of all the biological as well as chemical procedures.

After the isolation and identification of the compound, it must be evaluated against the entire spectrum of specific assays to identify its molecular targets and potential toxicity or side effects to normal eukaryotic cells. Eventually, the potential lead compound has to undergo a rigorous safety assessment program which involves tests on several species of animal and with high doses of compound. Any significant toxicity in any species of test animals even at very high doses of compound can lead to termination of active interest in a compound by a pharmaceutical company. In case the compound passes through safety assessment, it has to undergo clinical trials before it reaches the market.

A.5. Challenges and benefits of microbial drug discovery program

High-throughput screening from all natural sources presents a number of challenges. The problem of reliable access and supply is of utmost concern. Even slight variations in growth conditions of the microbes can sometimes cause difficulties with production and initial detection of active compounds as well as subsequent repetition of assays or purification. Loss of production of the anticipated compound is also possible upon repeated sub-culturing under laboratory conditions. Even if supply is consistent, the initial raw extract usually consists of a complex mixture of various compounds including media components which need to be separated from the

desired compound using successive separation techniques. The raw extract might also contain only very small quantities of a bioactive substance and often as a mixture with structurally related molecules or its own derivatives and the initial concentration might be too low to be effectively detected by high-throughput screening. Additionally, the primary screening assays may be disguised by poor solubility of the compound or by fluorescent or colored false positives. Furthermore, the activity observed from a raw extract during the primary screening could be due to the synergistic activity of two constituents that may then diminish or disappear upon separation. The key compound can also be unstable making isolation a challenging task. Finally, extensive study is often required for complete structural elucidation of the compound to be absolutely sure that the molecule is novel.

Microorganisms also implicate a number of advantages in a natural products discovery program compared to other sources of natural products. Firstly, the diversity of the microbes taxonomically as well as biochemically is enormous. The accessibility of a wide range of microbes makes a high screening throughput both practical and lucrative. One of the major advantages of working with microorganisms is the ability to screen vast numbers of cultures on a small scale and production of large quantities of microbial products by fermentation. It is unlikely that continuous supply becomes a hurdle in the development of a microbial product. The innumerable antibiotics derived from microbial natural products currently in use imply the real potential of microbes as source of lead drugs in future.

A.6. Aim of this thesis

The main goals embedded in this thesis include identification of novel microbial natural products and myxobacterial taxa. In this framework, one of the first objectives was to screen two *Paenibacillus larvae* and 50 myxobacterial strains using a comprehensive reactivation-process with up-to-date methods. After the screening was accomplished, the focus was set on *P. larvae* ERIC II (DSM 25430) and *Nannocystis pusilla*, Ari7 for purification of uncharacterized secondary metabolites. Large scale fermentations were carried out for *P. larvae* ERIC II (DSM 25430) and *N. pusilla*, Ari7 followed by bioassay guided separation for purification of compounds. Structure elucidation of the pure compounds was done using NMR spectroscopy and mass spectrometry. Furthermore, amino acid composition, sequence and

stereochemistry were analyzed for the compounds obtained from *P. larvae*. Finally, the biological activities of the pure compounds which were isolated in sufficient amounts were tested against a panel of bacteria, fungi and yeasts along with various cell lines.

Additionally, 16S rRNA gene sequences of the same set of 50 myxobacterial strains were analyzed. Strain MCy1366^T (Ar1733) was found to be branching out from rest of the known strains in the family Myxococcaceae and was selected for further investigation. MCy1366^T along with the 9 type strains from family Myxococcaceae was also studied and compared for antibiotic resistance, fatty acid composition using GC-MS and cytoplasmic proteome using MALDI-TOF analysis. In addition, strain MCy1366^T was subjected to many physiological tests to ascertain its position as a new genus.

References

- Anandaraj, B., Vellaichamy, A., Kachman, M., Selvamanikandan, A., Pegu, S., and Murugan, V. (2009) Co-production of two new peptide antibiotics by a bacterial isolate *Paenibacillus alvei* NP75. *Biochemical and Biophysical Research Communications* 379,179–185
- Antunez, K., Anido, M., Arredondo, D., Evans, J. D., and Zunino, P.(2010) *Paenibacillus larvae* enolase as a virulence factor in honey bee larvae infection. *Veterinary microbiology*, 147, 83-89
- Antunez, K., Arredondo, D., Anido, M., and Zunino, P. (2011) Metalloprotease production by *Paenibacillus larvae* during the infection of honeybee larvae. *Microbiology*, 157, 1474-1480
- Ash, C., Priest, F. G., and Collins, M. D. (1993) Molecular identification of rRNA group 3 bacilli (Ash, Farrow, Wallbanks and Collins) using a PCR probe test. Proposal for the creation of a new genus *Paenibacillus*. *Antonie van Leeuwenhoek* 64, 253–260
- Ashiralieva, A., and Genersch, E. (2006) Reclassification, genotypes and virulence of *Paenibacillus larvae*, the etiological agent of American foulbrood in honeybees - a review. *Apidologie*, 37, 411–420
- Barbier, J., Jansen, R., Irschik, H., Benson, S., Gerth, K., Böhlendorf, B., Höfle, G., Reichenbach, H., Wegner, J., Zeilinger, C., Kirschning, A., and Müller, R., (2012) Isolation and structure elucidation (by total synthesis) of icumazoles and noricumazoles – new antifungal antibiotics and cation channel blockers from *Sorangium cellulosum*. *Angew. Chem. Int. Ed.* 51, 1256–1260
- Beckers, A., Organe, S., Tinunermans, L., Scheys, K., Peters, A., Brusselmans, K., Verhoeven, G., and Swinnen, J.V., (2007) Chemical inhibition of Acetyl-CoA Carboxylase induces growth arrest and cytotoxicity selectively in cancer cells. *Cancer Res.* 67, 8180 -8187
- Berdy, J. (2012) Thoughts and facts about antibiotics: Where we are now and where we are heading. *J. Antibiot.* 65, 385–395
- Berdy, J., (2005) Bioactive Microbial Metabolites. *J. Antibiot.* 58(1): 1–26
- Bode, H.B. and Muller, R. (2005) The impact of bacterial genomics on natural product research. *Angew. Chem. Int. Ed.*,44(42):6828–6846
- Borris, R. P. (1996) Natural products research: perspectives from a major pharmaceutical company. *Journal of Ethnopharmacology* 51, 29-38
- Butler, M. S., (2004). The Role of Natural Product Chemistry in Drug Discovery. *J. Nat. Prod.* 67, 2141-2153
- Chung, Y.R., Kim, C. H., Hwang, I., and Chun, J. (2000) *Paenibacillus koreensis* sp. nov., a new species that produces an iturin-like antifungal compound. *Intern. J. Syst. Evol. Microb.* 50, 1495–1500
- Coates, J.D., Kimberly, A., Chakraborty, C.R., O' Connor, S.M., and Achenbach, L.A. (2002) Diversity and ubiquity of bacteria capable of utilizing humic substances as electron donors for anaerobic respiration. *Appl. Environ. Microbiol.* 68, 2445–2452
- Dawid, W. (2000) Biology and global distribution of myxobacteria in soils. *FEMS Microbiol. Rev.* 24,403–427
- Dawid, W., Gallikowski, C.A., and Hirsch, P. (1988) Psychrophilic myxobacteria from Antarctic soils. *Polarforschung.* 58, 271–278
- Demain, A. L. (2006) From natural products discovery to commercialization: a success story *J. Ind. Microbiol. Biotechnol.* 33, 486-495

- Demain, A. L. and Sanchez, S. (2009) Microbial drug discovery: 80 years of progress. *J. Antibiot.* 62, 5–16
- Diestel, R., Irschik, H., Jansen, R., Khalil, M. W., Reichenbach, H., and Sasse, F., (2009) Chivosazoles A and F, Cytostatic Macrolides from Myxobacteria, Interfere with Actin. *ChemBioChem* 10, 2900 – 2903
- Elnakady, Y. A., Sasse, F., Lünsdorf, H., and Reichenbach, H., (2004) Disorazol A1, a highly effective antimitotic agent acting on tubulin polymerization and inducing apoptosis in mammalian cells. *Biochemical Pharmacology* 67, 927–935
- Falagas, M. E., and Kasiakou, K. S., (2006) Toxicity of polymyxins: a systematic review of the evidence from old and recent studies. *Critical Care* 10, 1-13
- Falagas, M.E., Grammatikos, A. P., and Michalopoulos, A., (2008) Potential of old-generation antibiotics to address current need for new antibiotics. *Expert Rev. Anti- Infect. Ther.* 6(5), 593-600
- Fickers, P. (2012) Antibiotic compounds from Bacillus: why are they so amazing? *Am. J. Biochem. Biotechnol.* 8, 40–46
- Fleming, A. (1929) On the antibacterial action of cultures of a penicillium, with special reference to their use in the isolation of *B. influenzae*. *Br. J. Exp. Pathol.* 10 (3), 226–36
- Fortes, T.O., Alviano, D.S., Tupinamba, G., Padron, T.S., Antonioli, A. R., Alviano, C.R., and Seldin, L. (2008) Production of an antimicrobial substance against *Cryptococcus neoformans* by *Paenibacillus brasiliensis* Sa3 isolated from the rhizosphere of *Kalanchoe brasiliensis*. *Microbiological Research* 163, 200–207
- Fudou, R., Iizuka, T., and Yamanaka, S., (2001) Haliangicin, a novel antifungal metabolite produced by a marine myxobacterium- Fermentation and biological characteristics. *J. Antibiotics* 54(2), 149-152
- Fünfhaus, A., Ashiralieva, A., Borriss, R. and Genersch, E. (2009) Use of suppression subtractive hybridization to identify genetic differences between differentially virulent genotypes of *Paenibacillus larvae*, the etiological agent of American Foulbrood of honeybees. *Environ. Microbiol. Rep.*,1, 240-250
- Fünfhaus, A., Poppinga, L., and Genersch, E. (2013) Identification and characterization of two novel toxins expressed by the lethal honey bee pathogen *Paenibacillus larvae*, the causative agent of American foulbrood. *Environ. Microbiology*. doi:10.1111/1462-2920.12229
- Garcia, R. O., Reichenbach, H., Ring, M. W., and Müller, R. (2009b) *Phaselicystis flava* gen. nov., sp. nov., an arachidonic acid-containing soil myxobacterium, and the description of *Phaselicystidaceae* fam. nov. *Int. J. Syst. Bacteriol.* 59, 1524-1530
- Garcia, R., Gerth, K., Stadler, M., Dogma, I. J., Jr. & Müller, R., (2010) Expanded phylogeny of myxobacteria and evidence for cultivation of the 'unculturable'. *Mol. Phylogenet. Evol.* 57, 878-887
- Garcia, R., Gerth, K., Stadler, M., Dogma, I. J., Jr. and Müller, R., (2010) Expanded phylogeny of myxobacteria and evidence for cultivation of the 'unculturable'. *Mol. Phylogenet. Evol.* 57, 878-887
- Garcia, R., Pistorius, D., Stadler, M., and Müller, R. (2011) Fatty acid related phylogeny of myxobacteria as an approach to discover polyunsaturated omega-3/6 fatty acids. *J. Bacteriol.* 193, 1930-1942
- Garcia, R.O., Krug, D., and Müller, R. (2009a) Discovering natural products from Myxobacteria with emphasis on rare producer strains in combination with improved analytical methods. *Methods Enzymol.* 458, 59–91

- Garcia, R.O., Krug, D., and Müller, R. (2009a) Discovering natural products from Myxobacteria with emphasis on rare producer strains in combination with improved analytical methods. *Methods Enzymol.* 458, 59–91
- Genersch, E., Ashiralieva, A., and Fries, I. (2005) Strain- and genotype-specific differences in virulence of *Paenibacillus larvae* subsp. *larvae*, a bacterial pathogen causing American foulbrood disease in honeybees. *Appl. Environ. Microbiol.* 71:7551–7555.
- Genersch, E., and Otten, C. (2003) The use of repetitive element PCR fingerprinting (rep-PCR) for genetic subtyping of German field isolates of *Paenibacillus larvae* subsp. *larvae*. *Apidologie* 34: 195–206
- Genersch, E., Forsgren, E., Pentikäinen, J., Ashiralieva, A., Rauch, S., Kilwinski, J., and Fries, I. (2006) Reclassification of *Paenibacillus larvae* subsp. *pulvificiens* and *Paenibacillus larvae* subsp. *larvae* as *Paenibacillus larvae* without subspecies differentiation. *Int. J. Syst. Evol. Microbiol.* 56:501–511.
- Gerth K., Irschik H., Jansen R., Kunze B., Müller R., Sasse F. (2007). Myxobakterien, vom Aussenseiter zum Geheimfavoriten, in Vorbild Natur, G. Kreysa, D. Sell (Eds.) Dechema e.V., Frankfurt am Main, 64 – 71
- Gerth, K., Bedorf, N., Höfle, G., Irschik, H., and Reichenbach, H., (1996a) Epothilons A and B: Antifungal and cytotoxic compounds from *Sorangium cellulosum* (Myxobacteria). Production, physico-chemical and biological properties. *J. Antibiotics*, 49, 560–3
- Gerth, K., Bedorf, N., Irschik, H., Höfle, G., and Reichenbach, H., (1994) The Soraphens: A family of novel antifungal compounds *Sorangium cellulosum* (Myxobacteria). *J. Antibiot.* 47(1), 23-31
- Gerth, K., Irschik, H., Reichenbach, H., and Trowitsch, W., (1982) The Myxovirescins, a family of antibiotics from *Myxococcus virescens* (Myxobacteriales). *J. Antibiot.* 35, 1454–1459
- Gerth, K., Jansen, R., Reifenthal, G., Höfle, G., Irschik, H., Kunze, B., Reichenbach, H., and Thierbach, G., (1983) The Myxalamides, new antibiotics from *Myxococcus Xanthus* (Myxobacteriales). *J. Antibiotics* 36(9), 1150-1156
- Gerth, K., Pradella, S., Perlova, O., Beyer, S., and Müller, R., (2003) Myxobacteria: proficient producers of novel natural products with various biological activities—past and future biotechnological aspects with the focus on the genus *Sorangium*. *J. Biotechnol.* 106, 233–253
- Goldman, B. S., Nierman, W. C., Kaiser, D., Slater, S.C., Durkin, A. S., Eisen, J. A., Ronning, C. M., Barbazuk, W. B., Blanchard, M., Field, C., Halling, C., Hinkle, G., Iartchuk, O., Kim, H. S., Mackenzier, C., Madupu, R., Miller, N., Shvartsbeyn, A., Sullivan, S. A., Vaudin, M., Wiegand, R., Kaplan, H. B., (2006) Evolution of sensory complexity recorded in a myxobacterial genome. *Proc. Nat. Acad. Sci.* 103, 15200–15205
- Gross, H., Loper, J. E. (2009) Genomics of secondary metabolite production by *Pseudomonas* spp. *Nat. Prod. Rep.* 26, 1408–1446
- Heyndrickx, M., Vandemeulebroecke, K., Hoste, B., Janssen, P., Kersters, K., De Vos, P., Logan, N. A., Ali, N. & Berkeley, R. (1996). Reclassification of *Paenibacillus* (formerly *Bacillus*) *pulvificiens* (Nakamura 1984) Ash et al. 1994, a later subjective synonym of *Paenibacillus* (formerly *Bacillus*) *larvae* (White 1906) Ash et al. 1994, as a subspecies of *P. larvae*, with emended descriptions of *P. larvae* as *P. larvae* subsp. *larvae* and *P. larvae* subsp. *pulvificiens*. *Int. J. Syst. Bacteriol.* 46, 270–279
- Höfle, G., Bedorf, N., Steinmetz, H., Schomburg, D., Gerth, K., and Reichenbach, H., (1996) Epothilone A and B—Novel 16-Membered Macrolides with Cytotoxic Activity: Isolation, Crystal Structure, and Conformation in Solution. *Angew. Chem. Int. Ed. Engl.* 35, 13-14
- Hunt, J. T. (2009) Discovery of Ixabepilone. *Mol. Cancer Ther.* 8,275-281

Iizuka, T., Fudou, R., Jojima, Y., Ogawa, S., Yamanaka, S., Inukai, Y., and Ojika, M. (2006) Miuraenamides A and B, novel antimicrobial cyclic depsipeptides from a new slightly halophilic myxobacterium: taxonomy, production, and biological properties. *J. Antibiot.* 59, 385–391

Iizuka, T., Jojima, Y., Fudou, R., Hiraishi, A., Ahn, J.W. and Yamanaka, S. (2003a) *Plesiocystis pacifica* gen. nov., sp. nov., a marine myxobacterium that contains dihydrogenated menaquinone, isolated from the pacific coasts of Japan. *Int. J. Syst. Evol. Microbiol.* 53, 189–195

Iizuka, T., Jojima, Y., Fudou, R., Tokura, M., Hiraishi, A. and Yamanaka, S. (2003b) *Enhygromyxa salina* gen. nov., sp. nov., a slightly halophilic myxobacterium isolated from the coastal areas of Japan. *Syst. Appl. Microbiol.* 26, 189–196

Iizuka, T., Jojima, Y., Fudou, R., Tokura, M., Hiraishi, A., and Yamanaka, S. (2003) *Enhygromyxa salina* gen. nov., sp. nov., a slightly halophilic myxobacterium isolated from the coastal areas of Japan. *System. Appl. Microbiol.* 26, 189–196

Iizuka, T., Jojima, Y., Hayakawa, A., Fujii, T., Yamanaka, S., and Fudou, R. (2013) *Pseudenhygromyxa salsuginis* gen. nov., sp. nov., a myxobacterium isolated from an estuarine marsh. *Int. J. Syst. Bacteriol.* 63, 1360–1369

Irschik, H., Augustiniak, H., Gerth, K., Höfle, G., and Reichenbach, H., (1995) Ripostatins, novel inhibitors of eubacterial RNA polymerase isolated from Myxobacteria. *J. Antibiot.* 48, 787–792

Irschik, H., Gerth, K., Höfle, G., Kohl, W., and Reichenbach, H., (1983a) The myxopyronins, new inhibitors of bacterial RNA synthesis from *Myxococcus fulvus* (Myxobacterales). *J. Antibiot.* 36, 1651–8

Irschik, H., Gerth, K., Kemmer, T., Steinmetz, H., and Reichenbach, H., (1983b) The myxovalargins, new peptide antibiotics from *Myxococcus fulvus* (Myxobacterales). *J. Antibiot.* 36, 6–12

Irschik, H., Jansen, R., Gerth, K., Höfle, G., and Reichenbach, H., (1987) Sorangicins, novel and powerful inhibitors of eubacterial RNA polymerase isolated from myxobacteria. *J. Antibiot.* 40, 7–13

Irschik, H., Jansen, R., Hofle, G., Gerth, K., and Reichenbach, H., (1985) The coralopyronins, new inhibitors of bacterial RNA synthesis from *Myxobacteria*. *J. Antibiot.* 38, 145–52

Irschik, H., Reichenbach, H., Höfle, G., and Jansen, R., (2007b) The Thuggacins, novel antibacterial macrolides from *Sorangium cellulosum* acting against selected Gram positive bacteria. *J. Antibiot.* 60, 733–738

Irschik, H., Schummer, D., Höfle, G., Reichenbach, H., Steinmetz, H., and Jansen, R., (2007a) Etnangien, a macrolide-polyene antibiotic from *Sorangium cellulosum* that inhibits nucleic acid polymerases. *J. Nat. Prod.* 70, 1060–1063

Jansen, R., Irschik, H., Huch, V., Schummer, D., Steinmetz, H., Bock, M., Schmidt, T., Kirschning, A., and Müller, R., (2010) Carolacton – a macrolide ketocarboxylic acid reducing biofilm formation by the caries- and endocarditis-associated bacterium *Streptococcus mutans*. *European J. Org. Chem.* 7, 1284–1289

Jansen, R., Steinmetz, H., Sasse, F., Schubert, W. D., Hagelüken, G., Albrecht, S. C., and Müller, R., (2008) Isolation and structure revision of the actin-binding macrolide rhizopodin from *Myxococcus stipitatus* (Myxobacteria). *Tetrahedron Letters* 49, 5796–5799

Katznelson, H. (1950). *Bacillus pulvifaciens* (n. sp.), an organism associated with powdery scale of honeybee larvae. *J. Bacteriol.* 59, 153–155

Kaur, G., Hollingshead, M., Holbeck, S., Schauer-Vukasinovic, V., Camalier, R. F., Domling, A., and Agarwal, S., (2006) Biological evaluation of tubulysin A: a potential anticancer and antiangiogenic natural product. *Biochem. J.* 396, 235–242

- Keller, N. P., Turner, G., and Bennett, J. W. (2005) Fungal secondary metabolism—from biochemistry to genomics. *Nat. Rev. Microbiol.* 3, 937-947
- Khalil, M. W., Sasse, F., Lünsdorf, H., Elnakady, Y. A., and Reichenbach, H., (2006) Mechanism of action of tubulysin, an antimitotic peptide from myxobacteria. *Chembiochem.* 7, 678–683
- Kunze, B., Kohl, W., Höfle, G., and Reichenbach, H., (1985) Production, isolation, physico-chemical and biological properties of Angiolam A, a new antibiotic from *Angiococcus Disciformis* (Myxobacteriales). *J. antibiot.* 38, 1649–1654
- Kunze, B., Reichenbach, H., Augustiniak, H., and Höfle, G., (1982) Isolation and identification of althiomycin from *Cystobacter fuscus* (myxobacteriales). *J. antibiot.* 35, 635–636
- Li, B., Xie, X., Zhang, X., Cai, Z., and Zhu, H. (2013) Influence of different prey strains on isolation myxobacteria in saline-alkaline soils of Xinjiang. *Wei Sheng Wu Xue Bao.* 53(4), 379-89
- Li-jing, Z., Xiao-nan, Y., Xiang-ying, L., Wei, M. and Feng, L. (2011) Antifungal, Insecticidal and Herbicidal Properties of Volatile Components from *Paenibacillus polymyxa* Strain BMP-11. *Agricultural Sciences in China*, 10(5): 728-736
- Lorentz, R.H., Artico, S., Silveira, A.B., Einsfeld, A., and Corcao, G. (2006) Evaluation of antimicrobial activity in *Paenibacillus* spp. strains isolated from natural environment. *Lett. Appl. Microbiol.* 43, 541–547
- Martin, N.I., Hu, H., Moake, M.M., Churey, J. J., Whittal, R., Worobo, R. R., and Vederas, J. C. (2003) Isolation, structural characterization, and properties of mactacin (polymyxin M), a cyclic peptide antibiotic produced by *Paenibacillus kobensis* M. *J. Biol. Chem.* 278 (15), 13124–13132
- Mohr, K. I.; Garcia, R. O.; Gerth, K.; Irschik, H.; Müller, R. (2011) *Sandaracinus amylolyticus* gen. nov., sp. nov., a starch degrading soil myxobacterium, and description of *Sandaracinaceae* fam. nov. *Int. J. Syst. Bacteriol.* 62, 1191-1198
- Müller, R., and Wink, J., (2013) Future potential for anti-infectives from bacteria – How to exploit biodiversity and genomic potential. *Int. J. Med. Microb.*
- Nett, M. and König, G. M. (2007) The chemistry of gliding bacteria. *Nat. Prod. Rep.*, 24, 1245–1261
- Nickeleit, I., Zender, S., Sasse, F., Geffers, R., Brandes, G., Sörensen, I., Steinmetz, H., Kubicka, S., Carlomagno, T., Menche, D., Gütgemann, I., Buer, J., Gossler, A., Manns, M. P., Kalesse, M., Frank, R., and Malek, N. P., (2008) Argyrin A reveals a critical role for the tumor suppressor protein p27^{kip1} in mediating mntitumor activities in response to proteasome inhibition. *Cancer Res.* 14, 23–35
- Okanya, P.W., Mohr, K.I., Gerth, K., Steinmetz, H., Huch, V., Jansen, R., and Müller, R., (2012) Hyaladione, an S-methyl cyclohexadiene-dione from *Hylangium minutum*. *J. Nat.Prod.* 75, 768–770
- Plaza, A., Garcia, R., Bifulco, G., Martinez, J.P., Hüttel, S., Sasse, F., Meyerhans, A., Stadler, M., and Müller, R., (2012) Aetheramides A and B, potent HIV-inhibitory depsipeptides from a myxobacterium of the new genus “*Aetherobacter*”. *Org. Lett.* 14, 2854–2857
- Poppinga L, Janesch B, Fünfhäus A, Sekot G, Garcia-Gonzalez E, et al. (2012) Identification and Functional Analysis of the S-Layer Protein SplA of *Paenibacillus larvae*, the Causative Agent of American Foulbrood of Honey Bees. *PLoS Pathog.* 8(5): e1002716. doi:10.1371/journal.ppat.1002716
- Qian, C. D., Wu, X. C., Teng, Y., Zhao, W. P., Li, O., Fang, S. G., Huang, Z. H. and Gao, H. C. (2011) Battacin (Octapeptin B5), a new cyclic lipopeptide antibiotic from *Paenibacillus tianmuensis* active against multidrug-resistant gram-negative bacteria. *Antimicro. Agents and Chemother.* 56(3), 1458–1465
- Rauch, S., Ashiralieva, A., Hedtke, K., and Genersch, E., (2009) Negative Correlation between

- Individual-Insect-Level Virulence and Colony-Level Virulence of *Paenibacillus larvae*, the Etiological Agent of American Foulbrood of Honeybees. *Applied and Environmental Microbiology*, 75, 3344–3347
- Raza, W., Yang, X., Wu, H., Wang, Y., Xu, Y., and Shen, Q., (2009) Isolation and characterisation of fusaricidin-type compound-producing strain of *Paenibacillus polymyxa* SQR-21 active against *Fusarium oxysporum f.sp. neivium*. *Eur J Plant Pathol* 125, 471–483
- Reichenbach, H. (1999) The ecology of the myxobacteria. *Environmental Microbiology* 1: 15–21
- Reichenbach, H. (2001) Myxobacteria, producers of novel bioactive substances. *J. Ind. Microbiol. Biotechnol.* 27(3), 149–156
- Reichenbach, H. (2005) In *Bergey's Manual of Systematic Bacteriology*, Eds, Brenner, D. J.; Krieg, N. R.; Staley, J. T. Springer, 2, 1059 – 114
- Romero, D., Traxler, M. F., López, D. and Kolter, R. (2011) Antibiotics as Signal Molecules. *Chem. Rev.*, 111(9), 5492–5505
- Saha, P., Mondal, A.K., Mayilraj, S., Krishnamurthi, S., Bhattacharya, A., and Chakrabarti, T. (2005) *Paenibacillus assamensis* sp. nov., a novel bacterium isolated from a warm spring in Assam, India. *Int. J. Syst. Evol. Microbiol* 55, 2577–2581
- Sanford, R., Cole, J. and Tiedje, J. (2002) Characterization and description of *Anaeromyxobacter dehalogenans* gen. nov., sp. nov., an aryl-halo-respiring facultative anaerobic myxobacterium. *Appl. Environ. Microbiol.* 68, 893–900
- Sanford, R., Cole, J. and Tiedje, J. (2002) Characterization and description of *Anaeromyxobacter dehalogenans* gen. nov., sp. nov., an aryl-halo-respiring facultative anaerobic myxobacterium. *Appl. Environ. Microbiol.* 68, 893–900
- Sarker, S.D., Latif, Z., and Gray, A. I. (2005) Natural Product isolation– An overview. In *Natural Products Isolation: Methods in Biotechnol. 2nd ed. Humana Press Inc., Totowa, NJ.* 20, 1-25
- Sasse, F., Kunze, B., Gronewold, T. M. A., and Reichenbach, H., (1998) The Chondramides: Cytostatic agents from myxobacteria acting on the actin cytoskeleton. *Journal of the National Cancer Institute* 90, 20
- Sasse, F., Steinmetz, H., Heil, J., Höfle, G., and Reichenbach, H., (2000) Tubulysins, new cytostatic peptides from myxobacteria acting on microtubule. *J. Antibiot.* 53, 879–885
- Sasse, F., Steinmetz, H., Höfle, G., and Reichenbach, H., (1994) Gephyronic Acid, a Novel Inhibitor of Eukaryotic Protein Synthesis from *Archangium gephyra* (Myxobacteria) *J. Antibiotics* 48, 26-30
- Schneiker, S., Perlova, O., Kaiser, O., Gerth, K., Alici, A., Altmeyer, M. O., Bartels, D., Bekel, T., Beyer, S., Bode, E., et al. (2007) Complete genome sequence of the myxobacterium *Sorangium cellulosum*. *Nat. Biotechnol.* 25(11):1281–1289
- Schreurs, M., van Dijk, T. H., Gerding, A., Havinga, R., Reijngoud, D. J., and Kuipers, F., (2009) Soraphen, an inhibitor of the acetyl-CoA carboxylase system, improves peripheral insulin sensitivity in mice fed a high-fat diet. *Diabetes, Obes. and Metab.* 11, 987-991
- Shimkets, L., and Woese, C. S., (1992) A phylogenetic analysis of the myxobacteria: Basis for their classification. *Proc. Natl. Acad. Sci. USA.* 89, 9459-9463
- Singh, R. K., Tiwari, S. K., Rai, A. K., and Mohapatra, T. M. (2011) Cyanobacteria: an emerging source for drug discovery, *The Journal of Antibiotics*, 64, 401–412
- Stansly, P. G., Shepard, R. G., and White, H. J., (1947) Polymyxin: a new chemotherapeutic agent. *Bull. Johns Hopkins Hosp.* 81, 43–54

- Steinmetz, H., Irschik, H., Kunze, B., Reichenbach, H., Höfle, G., and Jansen, R., (2007) Thuggacins, macrolide antibiotics active against *Mycobacterium tuberculosis*: isolation from myxobacteria, structure elucidation, conformation analysis and biosynthesis. *Chemistry* 13(20), 5822–5832
- Steinmetz, H., Mohr, K. I., Zander, W., Jansen, R., Gerth, K., and Müller, R. (2012) Indiacens A and B: Prenyl Indoles from the Myxobacterium *Sandaracinus amylolyticus*. *J. Nat. prod.* 75, 1803–1805
- Thierbach, G., and Reichenbach, H., (1981) Myxothiazol, a new antibiotic interfering with respiration. *Antimicrobial agents and chemotherapy* 19(4), 504-507
- Thierbach, G., Kunze, B., Reichenbach, H., and Hofle, G., (1984) The mode of action of stigmatellin, a new inhibitor of the cytochrome b–c1 segment of the respiratory chain. *Biochim. Biophys. Acta.* 765,227–235
- Watve, M. G., Tickoo, R., Jog, M. M. and Bhole, B. D. (2001) How many antibiotics are produced by the genus *Streptomyces*? *Arch. Microbiol.* 176, 386–390
- Weid, I., Alviano, D. S., Santos, A. L. S., Soares, R.M.A., Alviano, C.S., and Seldin, L. (2003) Antimicrobial activity of *Paenibacillus peoriae* strain NRRL BD-62 against a broad spectrum of phytopathogenic bacteria and fungi. *Journal of Applied Microbiology* 95, 1143–1151
- Weissmann, K. J. and Müller, R. (2010) Myxobacterial secondary metabolites: bioactivities and modes-of-action, *Nat. Prod. Rep.*, 27, 1276–1295
- White, G. F. (1906) The bacteria of the apiary with special reference to bee disease. In Bureau of Entomology, Technical Series no. 14, pp. 1–50. Washington, DC: US Department of Agriculture
- Wu, X. C., Qian, C. D., Fang, H. H., Wen, Y. P., Zhou, J. Y., Zhan, Z. J., Ding, R., Li, O., and Gao, H. (2011) Paenimacrolidin, a novel macrolide antibiotic from *Paenibacillus* sp. F6-B70 active against methicillin-resistant *Staphylococcus aureus*. *Microb. Biotech.* 4(4), 491–502
- Xiong, Z. Q., Wang, J. F., Hao, Y. Y. and Wang, Y. (2013) Recent Advances in the discovery and development of marine microbial natural products. *Mar. Drugs* 11, 700-717
- Yue, D., Nordhoff, M., Wieler L. H. and Genersch, E. (2008) Fluorescence in situ hybridization (FISH) analysis of the interactions between honeybee larvae and *Paenibacillus larvae*, the causative agent of American foulbrood of honeybees (*Apis mellifera*). *Environmental Microbiology*, 10, 1612-1620
- Zander, W., Gerth, K., Mohr, K.I., Kessler, W., Jansen, R., and Müller, R., (2011) Roimatacene: an antibiotic against gram-negative bacteria isolated from *Cystobacter ferrugineus* Cb G35 (myxobacteria). *Chemistry* 17, 7875–7881
- Zhang, X., Yao, Q., Cai, Z., Xie, X., and Zhu, H. (2013) Isolation and Identification of Myxobacteria from Saline-Alkaline Soils in Xinjiang, China. *PLoS ONE* 8(8):e70466. doi:10.1371/journal.pone.0070466

Chapter B

Paenilarvins, iturin family lipopeptides from the honey bee pathogen *Paenibacillus larvae*

Sakshi Sood, Heinrich Steinmetz, Kathrin I. Mohr, Marc Stadler, Marvin Djukic, Rolf Daniel and Rolf Müller

(**Current Status** – Published online in ChemBioChem on July 28th, 2014)

Author's contribution to this work

Performed and analyzed genomic data: MD

Purified compounds: SS, HS

Performed and analyzed biological assay data: SS

Analyzed chemical and NMR data: HS

Wrote the paper: SS, HS

Provided research facilities and supervised the project: MS, RD, RM

Conceived and designed the experiments: HS (chemical), KM (biological)

B.1. Abstract

Paenibacillus larvae has been extensively studied in past few decades as an appalling honey bee pathogen. In the present work, we screened *P. larvae* genotype ERIC I and II crude methanol extracts for antimicrobial activity based on the detection of 4 secondary metabolite gene clusters showing homology to various known antibiotic clusters during complete genome sequencing project. Paenilarvins, iturinic lipopeptides exhibiting strong antifungal activity were identified and purified guided by bioactivity assays from cultures of *P. larvae* ERIC II. The molecular structures were determined using 1D, 2D NMR spectroscopy and mass spectrometry. Nonribosomally synthesized peptides can yield a plethora of advantages to the producing organisms from survival benefits to regulation of metabolism and virulence, apart from some being pharmaceutically significant, e.g. in the form of antibiotics. Paenilarvins represent the first secondary metabolites isolated and characterized from *P. larvae*. These lipopeptides may play a role in *P. larvae* survival and pathogenesis but further studies are needed to investigate their function in detail.

B.2. Introduction

American foulbrood (AFB), one of the most catastrophic honey bee (*Apis mellifera*) epidemics, is a notifiable disease in many countries and strict laws are enforced for its regulation. Burning of infected or diseased colonies is considered the most effective control measure against AFB in most countries bringing huge losses. Despite being a deleterious and economically significant disease for honey bees, the complete molecular pathogenesis of AFB remains obscure.

Paenibacillus larvae, a Gram positive, rod shaped and spore forming bacterium which only infects the larvae in first instar stage through its spores, is the etiological agent of AFB. Genotyping of *P. larvae* isolates on the basis of repetitive-element PCR using enterobacterial repetitive intergenic consensus (ERIC) primers identified four genotypes of *P. larvae* (*P. larvae* ERIC I – IV) (Genersch *et al.*, 2006) which vary in varied aspects

but most importantly, in their level of virulence (Genersch, 2010; Genersch *et al.*, 2005; Rauch *et al.*, 2009). Strains of the genotypes ERIC I and ERIC II are the most common field isolates and account for most of the AFB outbreaks worldwide, making them most significant genotypes for study.

Fluorescence in situ hybridization (FISH) using *P. larvae*-specific, 16S rRNA targeted oligonucleotide probes was used to study the interaction between the host and the pathogen (genotype ERIC I and II) in detail (Yue *et al.*, 2008). This study gave a deep insight of the disease progression starting from the ingestion of spores of *P. larvae* by the honey bee larvae through contaminated food to the formation of hard scales from dead larval remains. These hard scales are the source for millions of bacterial spores, which can further be transmitted by use of contaminated equipment or by adult honey bees feeding on contaminated honey within a colony as well as between colonies.

A number of potential virulence factors have been described to be instrumental in *P. larvae* pathogenesis in recent years. The *P. larvae* secretome was studied in detail and established as a source of some of these factors (Antunez *et al.*, 2010). Enolase, produced by *P. larvae* was identified as a highly toxic and immunogenic protein to *Apis mellifera* larvae (Antunez *et al.*, 2011a). *P. larvae* was also detected to produce metalloprotease *in vivo* during bee larvae infection (Antunez *et al.*, 2011b). Both aforementioned enzymes have been reported to be possibly involved in larval degradation during and after infection. Poppinga *et al.* (2012) recently established the functional S-layer protein, SplA of *P. larvae* ERIC II as an important virulence factor. The latest report on the subject has affirmed that *P. larvae* ERIC I strains produce AB binary toxins, Plx1 and Plx2 as virulence factors (Fünfhaus *et al.*, 2013).

Lately in an attempt to identify all the putative virulence genes in *P. larvae*, suppression subtractive hybridization (SSH) was applied for comparative genomics of *P. larvae* genotypes (Fünfhaus *et al.*, 2009) and several fragments showing homology to nonribosomal peptide synthetases (NRPSs) and polyketide synthetases (PKSs) subunits belonging to the iturin family lipopeptides, bacitracin and bacillomycin were

identified in different genotypes. Open reading frames showing close homology to NRPSs of the antibiotic plipastatin and surfactin were also observed in another study on *P. larvae* genome using a combination of bioinformatics and proteomics (Chan *et al.*, 2011). NRPS and PKS are giant multifunctional enzyme systems with numerous domains bundled together into functional modules responsible for nonribosomal assembly of secondary metabolites. The end products of such complex multistep biosynthetic process are nonribosomal peptides (NRP) or polyketides (PK) or their hybrids with broad structural diversity and biological activities like enzyme inhibitors, immunosuppressants, antiparasitic agents, bioherbicides, plant growth regulators, biopesticides, bioinsecticides, antitumor agents as well as in microbial survival and pathogenesis (Demain, 2006; Romero *et al.*, 2011).

Our interest in natural products from bacterial and fungal sources and confirmation of the presence of NRPSs and NRPS/PKS hybrid clusters in *P. larvae* DSM 25719 (ERIC I) and DSM 25430 (ERIC II) genome (Djukic *et al.*, 2014), allured us to examine *P. larvae* for the production of novel secondary metabolites which could be of significance to the pathogen and possibly as pharmaceuticals or agrochemicals. In this study we identified and isolated a group of related lipopeptides, paenilarvins from *P. larvae* DSM 25430 (ERIC II), elucidated the molecular structure of the major products and determined their biological activity. All the isolated paenilarvins belong to the iturin family of lipopeptides and are closely related to mojavensin A, an iturinic lipopeptide produced by marine-derived bacterium *Bacillus mojavensis* B0621A (Ma *et al.*, 2012).

B.3. Results and Discussion

B.3.1. Bioactivity screening of *P. larvae* DSM 25719 and DSM 25430

The potential of *P. larvae* for the production of bioactive secondary metabolites was confirmed following complete genome sequencing of *P. larvae* DSM 25719 (ERIC I) and DSM 25430 (ERIC II) which has been recently reported by Djukic *et al.* Four different NRPS or NRPS/PKS hybrid clusters were identified during this study based on genome analysis and comparison with variations in domain organization and size of clusters

between the two genotypes. The two strains were grown in the presence of an adsorber resin (Amberlite XAD 16) and the crude methanol extracts were tested for their antimicrobial activity against a panel of microorganisms including gram positive and gram negative bacteria, yeast and filamentous fungi in 96 well plate diffusion assay.

Crude extracts of DSM 25719 (ERIC I) and DSM 25430 (ERIC II) showed activity against *Nocardia flava*, *Staphylococcus aureus*, *Chromobacterium violaceum* and *Mucor hiemalis*. However, while the antibacterial activity was not reproducible, the antifungal activity against *M. hiemalis* was persistent in extracts from various batches of shake flasks. Also, crude extracts from DSM 25430 strain were much more bioactive in comparison to DSM 25719 extracts against *M. hiemalis* with MIC value of 2.1 µg/ml for the former strain. These results prompted us to follow the observed antifungal activity and investigate the production of these antifungal compounds by *P. larvae* DSM 25430 (ERIC II).

Paenibacillus spp. have been described as an accomplished source of biologically active secondary metabolites in a number of previous studies (Li-jing *et al.*, 2011; Raza *et al.*, 2009; Stansly *et al.*, 1947; Anandraj *et al.*, 2009; Qian *et al.*, 2011; Wu *et al.*, 2011). Therefore, bioassay guided HPLC fractionation and MS spectrometry was implemented to *P. larvae* DSM 25430 extract to detect the antifungal compounds. This displayed the presence of a group of closely related peptides ranging in their molecular masses from 1069 Da to 1112.7 Da. The mass range of the identified compounds was closely related to iturin family compounds like mycosubtilin, mojavensin produced by *Bacillus* spp. (Peypoux *et al.*, 1986; Ma *et al.*, 2012) but a detailed structural analysis was essential for complete characterization.

B.3.2. Structural analysis of paenilarvins

P. larvae DSM 25430 strain (ERIC II) was fermented in 5L scale with XAD-16 amberlite adsorber resin which was collected and eluted with methanol to give a crude extract at the end of fermentation. Successive chromatography of the crude methanol extract on silica gel and reverse phase column guided by antifungal activity against *M. hiemalis*,

yielded 7 compounds belonging to the paenilarvin group. The most active compounds, paenilarvins A and B were used for further structure elucidation and biological assays. The complete molecular structures of paenilarvins A and B were determined by mass and nuclear magnetic resonance (NMR) (1D and 2D) spectral analysis.

Paenilarvin A (**1**) was obtained by RP-HPLC as colorless amorphous powder. The positive HRESIMS spectra presented a molecular ion cluster at m/z 1112.6108 $[M+H]^+$ consistent with the molecular formula $C_{52}H_{82}N_{13}O_{14}$ (calcd. 1112.6099), which was supported by the ^{13}C NMR spectrum. The intense IR absorptions between 1600 and 1700 cm^{-1} and between 3100 and 3400 cm^{-1} showed the presence of amide C=O and NH groups, respectively. The weak UV band at 277 nm and 223 nm was in good agreement with a peptide containing aromatic amino acids. Among all 52 carbon in signals the ^{13}C NMR spectrum of **1** displayed 13 amide carbonyl signals between 172.7 and 177.9 ppm and 8 methine carbons in the range between 48.5 and 63.2 ppm as it could be expected for a small peptide. Correspondingly, the complex 1H NMR spectrum of **1** furnished 17 H/D exchangeable protons between 6.75 ppm and 8.75 ppm and at least 8 methine protons in the range 4.05 to 5.0 ppm. A detailed analysis of COSY, TOCSY, HSQC and HMBC data for paenilarvin A (**1**) (Fig.B1) in CD_3OH solution revealed the presence of four asparagine, one tyrosine, one glutamine, and one proline residues (Table B1). Furthermore, the methylene group (δ_C 44.2, δ_H 2.49, 2.41) and the methine (δ_C 48.5, δ_H 4.15) adjacent to the doublet of 23NH (δ_H 7.49, 9.5 Hz) were recognized as parts of a long β -amino-acid. The methyl doublet (δ_C 19.7, δ_H 0.86) and a methyl triplet (δ_C 11.8, δ_H 0.87) signals and the combination of the remaining methine (δ_C 35.7, δ_H 1.29) and methylene signals (δ_C 30.6, , δ_H 1.32, 1.13) by $^1H, ^1H$ COSY and $^1H, ^{13}C$ HMBC correlations completed the structure of this part as 3-amino-14-methyl-hexadecanoic acid (β -Aa). The sequence of the amino acid residues in **1** was established by analysis of HMBC and ROESY correlations showing connections of the α -methine protons of amino acid residues to carbonyl carbons of the neighboring residues as comprised in Fig.B2 and Table B1.

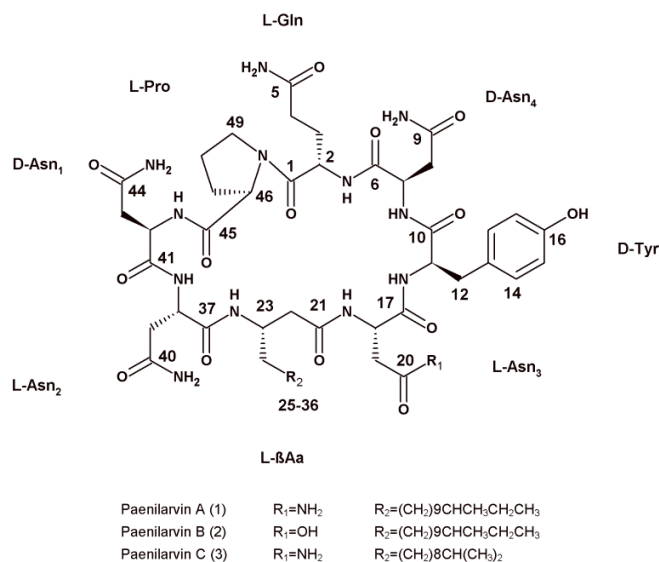


Fig. B1. Structures of paenilarvins A (1), B (2), and C (3).

B.3.3. Mass spectrometric analysis

The sequence of the amino acid residues was analyzed by ESI TOF MSMS and on Orbitrap FTMS mass spectrometer analyzer. The full scan spectrum of (1) showed a single and a doubly-charged molecular ions at m/z 1112.6108 $[M+H]^+$ and m/z 556.8098 $[M+2H]^{2+}$ (Fig.BS12) while the MS1 spectrum of Paenilarvin B (2) showed similar single and doubly-charged ions at m/z 1113.5963 $[M+H]^+$ and m/z 557.3026 $[M+2H]^{2+}$ (Fig.BS25). Equally the MS1 spectrum of (3) showed values at m/z 1084.5804 $[M+H]^+$ and m/z 542.7948 $[M+2H]^{2+}$ (Fig.BS39). For further investigations the MS2 spectra of (1) were analyzed. Based on the m/z $[M+H]^+$ 1112.610 two fragments at m/z 707.44 and m/z 406.17 were observed. These two fragments are in conclusion with the partial amino acid sequence: Pro, Asn, Asn, β -Aa, Asn and additionally the sequence Gln, Asn, Tyr, both in good agreement with the HMBC- and ROESY-NMR data. The compounds 1 and 3 showing the same amino acid sequence of Gln, Asn, Tyr, Asn, β -Aa, Asn, Asn, Pro but different β -amino-acid side chains. MS3 spectra showed the immonium ion for the side chains: $(NH_2^+=CH-CH_{14}H_{29})$ that could also be identified for compound 1 and 2 at m/z =226.167, as well as for compound 3 $(NH_2^+=CH-C_{12}H_{25})$ at m/z =198.220.

Table B1. ¹H (700 MHz) and ¹³C (175 MHz) NMR data of paenilarvin A (1) in CD₃OH

Amino acid	Position	δ_C	δ_H (J in Hz)	COSY	HMBC	ROESY Selected signals
Gln	1	172.8			2, 2NH, 46	
	2	51.7	4.65 (m)	3ab, NH	3ab, 4ab	49ab
	3a	27.9	2.11 (m)	2, 3b, 4ab	2, 4ab	2, 49b
	3b		2.06 (m)	2, 3a, 4ab		2, 4a
	4a	31.9	2.33 (m)	3ab	2, 5NH ₂	
	4b		2.32 (m)	3ab		
	5	177.8			3, 4ab, 5NH	
	2NH 5NH ₂		7.46 (d, 8.0) 7.53(s), 6.81(s)	2		2, 3ab 3ab, 4ab
Asn4	6	173.1			2, 2NH, 7, 8ab	
	7	52.5	4.64 (m)	7NH, 8ab	8ab	
	8a	36.9	2.73 (m)	7, 8b	7	7
	8b		2.70 (m)	7, 8a		7
	9	175.0			7, 8ab, 9NH ₂	
	7NH 9NH ₂		8.28 (d, 6.7) 7.54 (s), 6.85 (s)	7	11	8ab, 11 8ab
Tyr	10	174.3			7, 11NH, 12ab	
	11	58.4	4.28 (m)	11NH, 12ab	12ab	12ab, 14
	12a	36.8	3.09 (dd, 14.4, 5)	11, 12b	11, 14	11, 12b, 14
	12b		2.91 (m)	11, 12a		
	13	128.6			11, 12ab, 15	
	14*	131.3	7.06 (d, 8.4)	15	12ab	11, 12ab
	15*	116.5	6.72 (d, 8.4)	14		
	16 11NH	157.4	8.49 (d, 8.0)	11	14, 15	12ab, 18
Asn3	17	175.0			11, 11NH, 18, 19	
	18	52.7	4.61 (dd, 13.5, 7)	18NH, 19ab	19ab	
	19a	38.2	2.56 (dd, 15.3, 7.5)	18, 19b	18, 20NH ₂	18
	19b		2.48 (m)	18, 19a		18, 23, 24b
	20	174.6			18, 19, 20NH ₂	
	18NH 20NH ₂		8.01 (d, 4.7) 7.58 (s) 6.81 (s)	18		22ab, 23 19ab
β -amino- acid (β -Aa)	21	174.2			18NH	
	22a	44.2	2.49 (m)	23	23NH, 24a	23NH, 24a
	22b		2.41 (d, 14.0)	23		23, 24b
	23	48.5	4.15 (m)	22ab, 23NH, 24ab	21, 22ab	22b, 24b, 25-33
	24a	36.2	1.65 (m)	23, 25ab	22b	22a, 23, 23NH, 25-
	24b		1.50 (m)	23, 25ab		33

						22ab, 23
	25-33	27.1-31.2	1.33-1.09 (m)			
	34	35.7	1.29 (m)	34Me, 35	34Me, 36Me	
	34Me	19.7	0.86 (d, 6.2)	34	33, 35	
	35a	30.6	1.32 (m)	34,36Me	34Me, 36Me	
	35b		1.13 (m)	34,36Me		
	36Me	11.8	0.87 (t, 7.3)	35ab	34	
	23NH		7.49 (d, 9.5)	23		23, 38
Asn2	37	173.6			23NH, 39ab	
	38	51.7	4.92 (m)	38NH, 39ab	39ab	
	39a	38.8	2.97 (dd, 15.7,	38, 39b	40NH ₂	40 NH ₂
	39b		5.1)	38, 39a		39a
			2.61 (dd, 15.7,			
			8.6)			
	40	174.9			39ab, 40NH ₂	
	38NH		7.73 (d, 7.5)	38		38, 39b
	40NH ₂		7.44 (s), 6.85 (s)			39ab
Asn1	41	172.9			38,43	
	42	52.0	4.48 (m)	42NH, 43ab	43ab	
	43a	36.7	2.92 (m)	42, 43b	42, 44NH ₂	42, 44NH ₂
	43b		2.84 (dd, 16, 4.5)	42, 43a		42
	44	175.4			42, 44NH ₂	
	42NH		8.55 (d, 6.9)	42		46, 47
	44NH ₂		7.61(s), 6.85(s)			43ab
Pro	45	175.4			46, 47ab	
	46	63.3	4.23 (dd, 7.5, 7.5)	47ab	47, 48, 49ab	47a, 48b
	47a	30.6	2.25 (m)	46, 48ab	46	46, 48b
	47b		1.91 (m)	46, 48ab		
	48a	26.2	2.10 (m)	47ab, 48b,	46, 47a, 49b	47a
	48b		1.96 (m)	49ab		
				47ab, 48a,		
				49ab		
	49a	49.1	4.01 (m)	48ab, 49b	2, 47a, 48b	2, 48b, 49b
	49b		3.75 (ddd, 17, 7,	48ab, 49a		2, 48a, 49a
			6)			

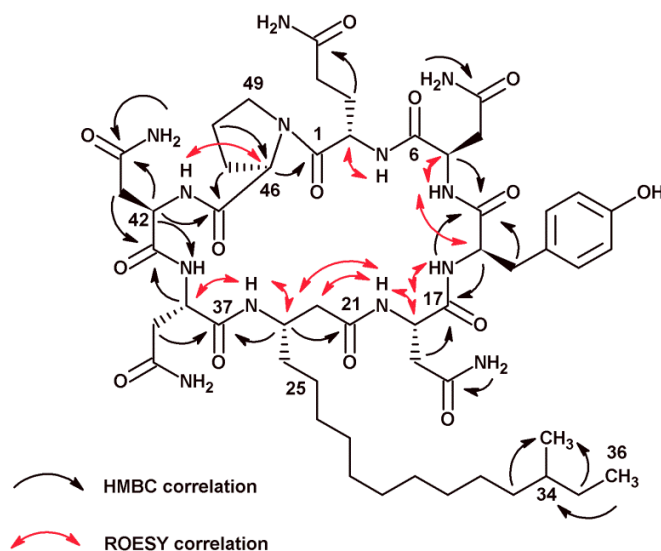


Fig. B2. Key HMBC and ROESY correlations of paenilarvin A (1)

The stereochemistry of paenilarvin A (1) was determined by Marfey's method (Marfey, 1984; Bhushan and Bruckner, 2004). After final hydrolysis the solution was compared with standard **L**- and **D**-amino acids and authentic amino acid derivatives by co-injection. Thus, paenilarvin A (1) was found to contain 1 (**L**)-Pro, 2 (**L**)-Asn, 2 (**D**)-Asn, 1 (**L**)-Gln, and 1 (**D**)-Tyr. The positions of the **D**- and **L**-Asn residues were assigned by analysis of the 2D ROESY spectrum analogously to the cyclic lipopeptides maribasins A and B, which similarly comprise seven amino acid residues and the same type of side chain (Zhang *et al.*, 2010). Accordingly, the stereochemistry was deduced by mapping the 2D ROESY correlations between the α -proton and the amide proton of amino acid 1 (AS1) and between the amide proton of AS1 and the α -proton of AS2, that both have the same configuration. The strong ROESY correlation from the Asn₁ amide proton (δ_{H} 8.55) with the **L**-Pro α -proton (δ_{H} 4.23) and the absence of a correlation with the Asn₁ α -proton (δ_{H} 4.48) indicated that the amino acid side chain is on the opposite side of the main plane of the molecule. Thus, Asn₁ was assigned to have **D** configuration. The Asn₂ amide proton (δ_{H} 7.73) neither showed a correlation with the Asn₁ α -proton (δ_{H} 4.48) nor with the Asn₂ α -proton (δ_{H} 4.92), which implied **L** configuration for Asn₂. ROESY correlations of the amide protons and α -protons of Asn₂, β -proton of β -Aa and Asn₃ showed that they were on the same side, respectively. Thus, β -Aa and Asn₃ had **L**

configurations (Fig.B1). Corresponding to the **D** configuration of Tyr derived by Marfey's method, a ROESY correlation of the Tyr amide proton (δ_{H} 8.49) with the Asn₃ α -proton (δ_{H} 4.61) was found but no correlation with the Tyr α -proton (δ_{H} 4.28). The ROESY correlation of the amide proton (δ_{H} 8.28) of Asn₄ with the α -proton (δ_{H} 4.28) of Tyr and with the α -proton (δ_{H} 4.64) of Asn₄ suggested **D** configuration for Asn₄. In contrast, no correlation of amide proton (δ_{H} 7.46) of the **L** Gln with the α -proton of Asn₄ was observed. Consequently, the structure of paenilarvin A (**1**) was finally established as cyclo **L**-Pro-**D**-Asn₁-**L**-Asn₂-**L**- β -amino-14-methylhexadecanoic acid-**L**-Asn₃-**D**-Tyr-**D**-Asn₄-**L**-Gln.

B.3.4. Antimicrobial and cytotoxic activity of paenilarvins

Screening of pure paenilarvins, **A (1)** and **B (2)** obtained from *P. larvae* DSM 25430 (ERIC II) for antimicrobial activities against a broad panel of bacteria, fungi and yeasts showed no activity against the group of Gram positive and negative bacteria tested. However, both lipopeptides showed activity against most of the fungi and yeasts but **1** showed much better activity compared to **2** with minimum inhibitory concentration (MIC) as low as 2.1 $\mu\text{g/ml}$ against *Trichosporon oleaginous*, *Aspergillus clavatus*, *Botryotinia fuckeliana* and *Hormoconis resinae* (Table B2). Compound **2** was not significantly active against all the fungi and yeast tested with a lowest MIC value observed as 16.6 $\mu\text{g/ml}$. When **1** and **2** were tested for their cytotoxicity against mouse fibroblast cell line L929, **1** was again found to be much more active (LD_{50} 4 $\mu\text{g/ml}$) than **2** which showed no significant cytotoxic activity (LD_{50} >10 $\mu\text{g/ml}$).

Lipopeptides belonging to the iturin family (iturin, mycosubtilin, bacillomycin and bacillopeptin) have long been known to possess strong antifungal and haemolytic activity, but show only restricted antibacterial effects (Maget-Dana and Peypoux, 1994). Thus, the strong antifungal activities of iturins producing organisms make them promising candidates as biocontrol agents. Mojavensin A was also found to be active against soil borne phytopathogens like *Fusarium oxysporum* f. sp. *cucumerinum* and *Valsa mali* and weakly inhibitory to *Staphylococcus aureus* (Ma *et al.*, 2012). However,

anteiso – C15 mojavensin A is not as active against fungi as other iturins. Hence, the strong antifungal activity and no antibacterial activity of compounds **1** and **2** against our test organisms correspond to the biological activity data available for other iturins.

Table B2. Minimum inhibitory concentration (MIC) in µg/mL of paenilarvin A (1) and B (2)

	Test organisms	Paenilarvin A (1)	Paenilarvin B (2)	Control ^[a,b2,c]
Yeasts	<i>Saccharomyces cerevisiae</i> (DSM 70449)	4.2	33.3	4.2 ^[b]
	<i>Rhodotorula glutinis</i> (DSM 10134)	4.2	16.6	<0.52 ^[b]
	<i>Candida albicans</i> (DSM 1665)	4.2	n.i.	8.3 ^[b2]
	<i>Wickerhamomyces anomalus</i> (DSM 6766)	4.2	16.6	2.1 ^[b]
	<i>Nematospora coryli</i> (DSM 6981)	4.2	33.3	3.3 ^[b]
	<i>Trichosporon oleaginous</i> (DSM 11815)	2.1	16.6	0.52 ^[b]
	<i>Debaryomyces hansenii</i> (DSM 3428)	4.2	n.i.	8.3 ^[b]
	<i>Pichia membranifaciens</i> (DSM 21959)	4.2	33.3	0.052 ^[b]
Filamentous fungi	<i>Mucor hiemalis</i> (DSM 2656)	4.2	33.3	2.1 ^[b]
	<i>Aspergillus clavatus</i> (DSM 816)	2.1	8.3	2.1 ^[b]
	<i>Botryotinia fuckeliana</i> (DSM 877)	2.1	16.6	2.1 ^[b]
	<i>Hormoconis resinae</i> (DSM 1203)	2.1	16.6	< 0.25 ^[b]
	<i>Penicillium capsulatum</i> (DSM 2210)	4.2	33.3	16.6 ^[b]
Gram +ve bacteria	<i>Nocardioides simplex</i> (DSM 20130)	n.i.	n.i.	16.6 ^[a]
	<i>Nocardia sp.</i> (DSM 43069)	n.i.	n.i.	<0.52 ^[a]
	<i>Staphylococcus aureus</i> (DSM 346)	n.i.	n.i.	0.1 ^[a]
	<i>Micrococcus luteus</i> (DSM 20030)	n.i.	n.i.	3.3 ^[a]
	<i>Paenibacillus polymyxa</i> (DSM 36)	n.i.	n.i.	6.7 ^[a]
Gram -ve bacteria	<i>Pseudomonas aeruginosa</i> (DSM 50071)	n.i.	n.i.	0.13 ^[c]
	<i>Chromobacterium violaceum</i> (DSM 30191)	n.i.	n.i.	1.0 ^[a]

^[a] Oxytetracyclin hydrochloride, (1mg/ml); ^[b] Nystatin, (1mg/ml in MeOH); ^[b2] Nystatin, (1mg/ml in DMSO); ^[c] Gentamycin (1mg/ml); Paenilarvin A and B (1mg/ml in MeOH); n.i. – no inhibition

B.4. Conclusion

P. larvae is pathogen of great economic as well as environmental concern because of its ability to cause one of the most serious and contagious diseases of honey bees, American foulbrood. We have come a far way in understanding *P. larvae* and its

pathogenicity in the last century but several aspects of the biology of the pathogen still remain elusive. In our study, we explored the secondary metabolite potential of *P. larvae* owing to the identification of genome segments homologous to putative NRPSs and PKSs clusters of closely related organisms like *Bacillus subtilis* (Fünfhaus *et al.*, 2009; Chan *et al.*, 2011).

Out of the four NRPS or NRPS/PKS hybrid clusters identified during complete genome sequencing and annotation of *P. larvae* DSM 25719 (ERIC I) and DSM 25430 (ERIC II), one of the clusters was found to show significant similarity to the NRPS/PKS hybrid clusters encoding for iturin family synthetases present in *Bacillus subtilis* (Djukic *et al.*, 2014). Iturin family compounds have been characterized as lipopeptides with a β -amino fatty acid chain linked to a circular heptapeptide produced by *Bacillus* sp. (Maget-Dana and Peypoux, 1994). The first report of production of an iturin like compound by a *Paenibacillus* sp. came in 2000 from a chitinolytic bacterial strain, *Paenibacillus koreensis* YC300^T, isolated from a compost sample collected from Chinju, Republic of Korea (Chung *et al.*, 2000) but the complete molecular structure of the compound was not described.

In the course of this study, we were able to identify a group of antifungal compounds within the mass range from 1069.7 Da to 1112.7 Da in our bioactivity guided assays with crude extracts of *P. larvae* DSM 25430 (ERIC II). Purification and molecular characterization of the compounds using mass spectrometry and NMR spectroscopy clarified that the compounds belong to iturin family and the complete structure elucidation of the purified compounds revealed two major cyclic compounds produced by the strain, paenilarvins A and B. Paenilarvin A has the same amino acid sequence as mojavensin A (Ma *et al.*, 2012) except that the β -Aa side chain is extended by two methylene units. Paenilarvin B has the same side chain as paenilarvin A but contains an aspartic acid instead of asparagine in position Asn₂.

Paenilarvins A and B showed no antibacterial activity but strong antifungal activity against rare human pathogenic species like *Aspergillus clavatus* and *Penicillium*

capsulatum and phytopathogens like *Nematospora coryli* and *Botryotinia fuckeliana*. Paenilarvins also exhibited significant activity against a commercially important fuel contaminant fungus, *Hormoconis resinae* (Haggett and Morchat, 1992). Cytotoxic activity against mouse fibroblast cell line L929 was also observed during the study.

Production of paenilarvins by the pathogen *in vitro* raises the question of their potential involvement and function in the pathogenicity of *P. larvae*. Production of secondary metabolites usually serves survival functions in the producing organisms in their ecological niche (Demain and Fang, 2000) as these compounds can generate competitive advantage in nature but may also be employed by a producing microorganism for an entirely different purpose. Considering the fact that honey bees are exposed to a lot of pathogens like parasitic mites, small hive beetle, microsporidian parasites, viruses and fungi, (Campano *et al.*, 1999; Murray and Aronstein, 2008) it can be speculated that *P. larvae* produces paenilarvins to be dominant amongst these potential pathogens. Certain microbes also show entomopathogenic activity, infecting and killing insects by production of secondary metabolites (Kanoaka *et al.*, 1977). However, these hypothesis can only be ascertained by examining the inhibitory effects of these compounds against prospective honey bee pathogens and honey bee larvae.

It is also known that antibiotics can exert diverse effects at subinhibitory concentrations and their response depends upon the concentration used, a concept called as hormensis (Calabrese and Baldwin, 2002; Davies *et al.*, 2006). The analysis of effect of subinhibitory antibiotic concentrations have demonstrated regulation of key biological processes including transcription, translation, transport of exoproteins, stress response, quorum sensing, and biofilm formation (Romero *et al.*, 2011). This has also been studied in regard to virulence and pathogenic properties of a number of bacteria (Aminov, 2009). In 2011, aureusimine A and aureusimine B were determined to be regulators of virulence factor expression for exotoxins, γ hemolysin, regulatory, redox associated superantigen like genes in *S. aureus* (Wyatt *et al.*, 2011). Paenilarvins A and B could also be involved in regulation of physiological processes in *P. larvae* which can only be confirmed upon a deep investigation on molecular level.

It is noteworthy that production of paenilarvins was only detected in *P. larvae* ERIC II (DSM 25430, DSM 16116) and none at all in ERIC I (DSM 25719, DSM 7030). This observation is supported by the genome sequencing and annotation data revealing the presence of an incomplete NRPS/PKS cluster in the DSM 25719 (ERIC I) genome. However, we still observed some antibacterial and antifungal activity in crude extracts of *P. larvae* DSM 25719 strains during our preliminary experiments indicating that they have the potential to produce some other biologically active secondary metabolites which still need to be discovered.

In this study, we could purify and characterize one group of secondary metabolites produced by *P. larvae* DSM 25430 (ERIC II), which possibly plays an important role for the pathogen. However, their precise function in pathogenesis needs still to be determined. The presence of other biosynthetic clusters is obvious from the genomic data obtained for the pathogen suggesting that other important secondary metabolites remain undiscovered (Djukic *et al.*, 2014; Fünfhaus *et al.*, 2009). Further studies are needed to unravel the products of these biosynthetic clusters and to investigate their exact role in pathogenesis. A comprehensive understanding of *P. larvae* pathogenesis combined with molecular evidence on virulence factors can pave the way for effectively dealing with this devastating honey bee disease in the future.

B.5. Experimental Section

B.5.1. General Experimental Procedures

Spectral and physico-chemical data were obtained with the following instruments: NMR spectra were recorded on a Bruker Ascend 700 TCI cryo probe spectrometer (^1H 700 MHz, ^{13}C 176 MHz) using CD_3OH as solvent. All 2D NMR spectra were analyzed using ACD NMR Spectrus software. IR spectra were recorded on a Perkin-Elmer FT-IR spectrometer. UV spectra were measured on a Shimadzu UV/Vis-2102 spectrometer with methanol as solvent. Optical rotation: Perkin Elmer 241 MC spectrometer, solvent methanol. Mass spectra were obtained on a Bruker maXis UHRTOF using electrospray

ionization (ESI) in positive mode, molecular formulae were calculated including the isotope pattern (Smart Formula algorithm) and in addition ESI TOF MSMS on Finnigan LTQ Orbitrap Mass spectrometer. Analytical HPLC: Gradient in 25 min. Solvent A: 5% acetonitrile 95% water + 5mM $\text{NH}_4\text{CH}_3\text{COO}$, pH 5.5 (40 μL $\text{CH}_3\text{COOH/L}$); Solvent B: 95% acetonitrile 5% water + 5mM $\text{NH}_4\text{CH}_3\text{COO}$, pH 5.5 (40 μL $\text{CH}_3\text{COOH/L}$); flow: 600 $\mu\text{L/min.}$; Temperature 40 $^\circ\text{C}$; column: Waters Acquity BEH C18, 50 x 2.1mm, 1.7 μm equipped with the corresponding pre-column.

B.5.2. Bacterial strain and growth conditions

Four *P. larvae* isolates representing genotypes ERIC I (DSM 25719, DSM 7030) and ERIC II (DSM 25430, DSM 16116) were used for the study. The strains had been cryopreserved at -80 $^\circ\text{C}$. DSM 25430 was reactivated in 20mL of modified MYPGP broth (Nordström and Fries, 1995) with beef infusion replaced by 2% meat extract and 0.2% vitamin solution at neutral pH. The strain was then sub-cultured to 600mL in the same medium in Erlenmeyer's flasks and used as a seed culture. Scale-up fermentation (5.2L) of the strain was performed in 1L Erlenmeyer's flasks each containing 350ml of the modified MYPGP media supplemented with 2% Amberlite XAD-16 resin and incubated at 30 $^\circ\text{C}$, 160rpm for 6 days. The XAD resin was separated and collected from the culture at the end of fermentation by sieving.

B.5.3. Extraction and isolation of active compounds

1L of methanol was used for elution from the adsorber XAD resin packed in a glass column. Methanol was evaporated from the extract to give a dry crude material of 6.14g. This extract was separated on 120g of silica gel in an open column equilibrated with ethyl acetate. Elution from the silica gel was made using ethyl acetate and increasing percentage of methanol from 100% ethyl acetate to 100% methanol to obtain mainly 4 fractions. The organic solvent from each fraction was evaporated.

Fractions 3 (1.19g) which was eluted with 2L of 50/50 (v/v) ethyl acetate and methanol from silica gel was dissolved in methanol and passed through RP cartridge [Strata™-X 33 μm , Polymeric Reversed Phase, 200mg/6 mL] and concentrated to 6mL. Processed

sample was further purified by four runs of preparative RP-HPLC [column 250 × 21.2mm, Phenomenex Gemini® C18, 10µm, 110Å; solvent A: acetonitrile/H₂O 37/63 + 0.1% formic acid; solvent B: acetonitrile/H₂O 40/60 + 0.1% formic acid; gradient: 0% B for 35min and 100% B from 35 to 80min; flow rate 20mL/min; UV detection at 210nm]. The fractions contained pure paenilarvin A (**1**) 6.8mg, paenilarvin B (**2**) 3.9mg, and paenilarvin C (**3**) 12.8mg along with other related peptides.

B.5.4. Assignment of absolute stereochemistry of amino acid residues

Marfey's method was used for determining the stereochemistry of amino acid residues in paenilarvins. 1.1 mg of the lipopeptide was hydrolysed in 0.5 mL of 6 N HCL at 110°C overnight. Then, the sample was dried in vacuum. 50 µL Water, FDAA (Marfey's reagent, 100 µL) in acetone and 1 M sodium-hydrogen carbonate (20 µL) were added to the hydrolyzed products and the mixture heated at 41°C for one hour. 10 µL 2M HCL was added later to stop the reaction and the mixture was evaporated to dryness. The residue was dissolved in 0.5 mL Water/ DMSO 1:1 and analyzed with reversed-phase chromatography [column 2.1x50 mm, Waters Acquity UPLC BEH C18, 1.7µm; gradient acetonitrile/water 5/95 + 0.1% formic acid to acetonitrile/water 40/60 + 0.1% formic acid in 30 min; flow rate 0.6 mL/min; UV detection: DAD, MS-spectrometer Amazon™ Bruker ESI mode.

B.5.5. Structural characteristics of paenilarvins

Paenilarvin A (**1**) white, solid; UV (methanol) λ_{\max} (log ϵ) 223 (4.27 sh), 277 (3.35) nm; $[\alpha]_D +15.4^\circ$ ($c = 0.039$, DMSO); R_t : 10.9min; $\nu = 3383, 2927, 2855, 1668, 1541, 1517, 1384\text{cm}^{-1}$; ^1H and ^{13}C NMR (see Table B1); HRESIMS: m/z 1112.6108 [$\text{M}+\text{H}^+$] (calcd. for $\text{C}_{52}\text{H}_{82}\text{N}_{13}\text{O}_{14}$, 1112.6099).

Paenilarvin B (**2**) white, solid; UV (methanol) λ_{\max} (log ϵ) 223 (4.23), 277 (3.35) nm; $[\alpha]_D +6.4^\circ$ ($c = 0.075$, methanol); R_t : 11.1min; ^1H NMR ($\text{CD}_3\text{OH} + 5\mu\text{L HCOOH}$, 700 MHz) selected signals: for Asp: δ_C 173.0ppm (C37), n.o. (C38), 37.6 (C39), 175.4ppm (C40), δ_H 4.87 (m, H38), 3 and 2.84 (m, H39a,b), 7.78 (38NH); HRESIMS: m/z 1113.5953 [$\text{M} + \text{H}^+$] (calcd. for $\text{C}_{52}\text{H}_{81}\text{N}_{12}\text{O}_{15}$, 1113.5939).

Paenilarvin C (**3**) white, solid; UV (methanol) λ_{\max} (log ϵ) 223 (4.80), 277 (3.35) nm; $[\alpha]_D^{25} +11.8^\circ$ ($c = 0.221$, DMSO); R_f : 9.6min; $^1\text{H NMR}$ (DMSO- d_6 , 700MHz) selected signals: end of the side chain: $-\text{CH}_2$ (δ_C 38.5, δ_H 1.24, 1.13), $-\text{CH}$ (δ_C 27.4, δ_H 1.49, m), $-(\text{CH}_3)_2$ (δ_C 22.5, δ_H 0.84, d, 6.7, Hz); HRESIMS: m/z 1084.5790 [$\text{M} + \text{H}^+$] (calcd. for $\text{C}_{50}\text{H}_{78}\text{N}_{13}\text{O}_{14}$, 1084.5785).

B.5.6. Antimicrobial assay

The MIC of compounds **1** and **2** was determined against the Gram-positive bacteria (*Staphylococcus aureus*, *Nocardia flava*, *Micrococcus luteus*, *Nocardioides simplex* and *Paenibacillus polymyxa*), Gram-negative bacteria (*Chromobacterium violaceum*, *Pseudomonas aeruginosa*), filamentous fungi (*Mucor hiemalis*, *Aspergillus clavatus*, *Hormoconis resinae*, *Penicillium capsulatum*, *Botryotinia fuckeliana*) and yeasts (*Saccharomyces cerevisiae*, *Candida albicans*, *Rhodotorula glutinis*, *Nematospora coryli*, *Trichosporon oleaginous*, *Debaryomyces hansenii*, *Pichia membranifaciens* and *Wickerhamomyces anomalus*). Bacterial test strains were cultivated in EBS medium (0.5% casein peptone, 0.5% protease peptone, 0.1% meat extract, 0.1% yeast extract, pH 7.0) and fungi in MYC medium (1.0% phytone peptone, 1.0% glucose, 50 mM HEPES [11.9g/L] pH 7.0) at 30 – 37°C, 160rpm for 24 -48hrs and the cell concentration adjusted to OD₆₀₀ 0.01 for bacteria and OD₅₄₈ 0.1 for yeasts. 10 μL aliquots (conc. 1mg/mL in MeOH) of **1**, **2** and 5 μl aliquots of reference drugs (oxytetracycline hydrochloride (Sigma), 1mg/mL in water; nystatin dihydrate (Sigma), 1mg/mL in MeOH or DMSO and gentamycin (Serva), 1mg/ml in water) were used. The MIC values were determined in 96 well microtitre plates by 1:1 serial dilution, as previously described (Okanya *et al.*, 2011). The lowest concentration of the drug preventing visible growth of the test strains was taken as the MIC.

B.5.7. Cytotoxicity assay

Compounds **1** and **2** were also tested for their cytotoxic activity against mouse fibroblast cell line L929. The IC₅₀ value was determined using MTT assay as previously described (Okanya *et al.*, 2011).

Acknowledgements

S.S. is highly indebted to Erasmus Mundus External Cooperation Window for a PhD scholarship and all their support. We acknowledge Christel Kakoschke for recording the NMR spectra and Silke Reineke, Aileen Teichmann, Diana Telkemeyer and Wera Collisi for their technical assistance. We are grateful to Dr. Alberto Plaza for proofreading of this manuscript.

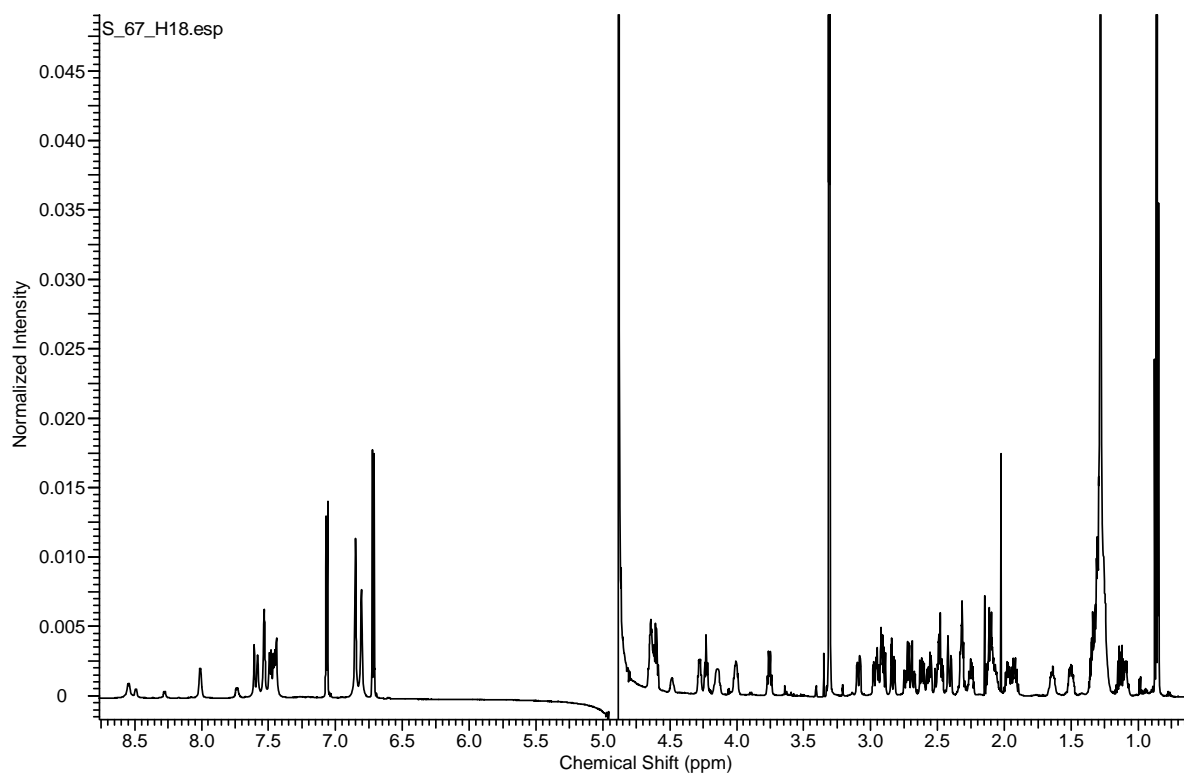
References

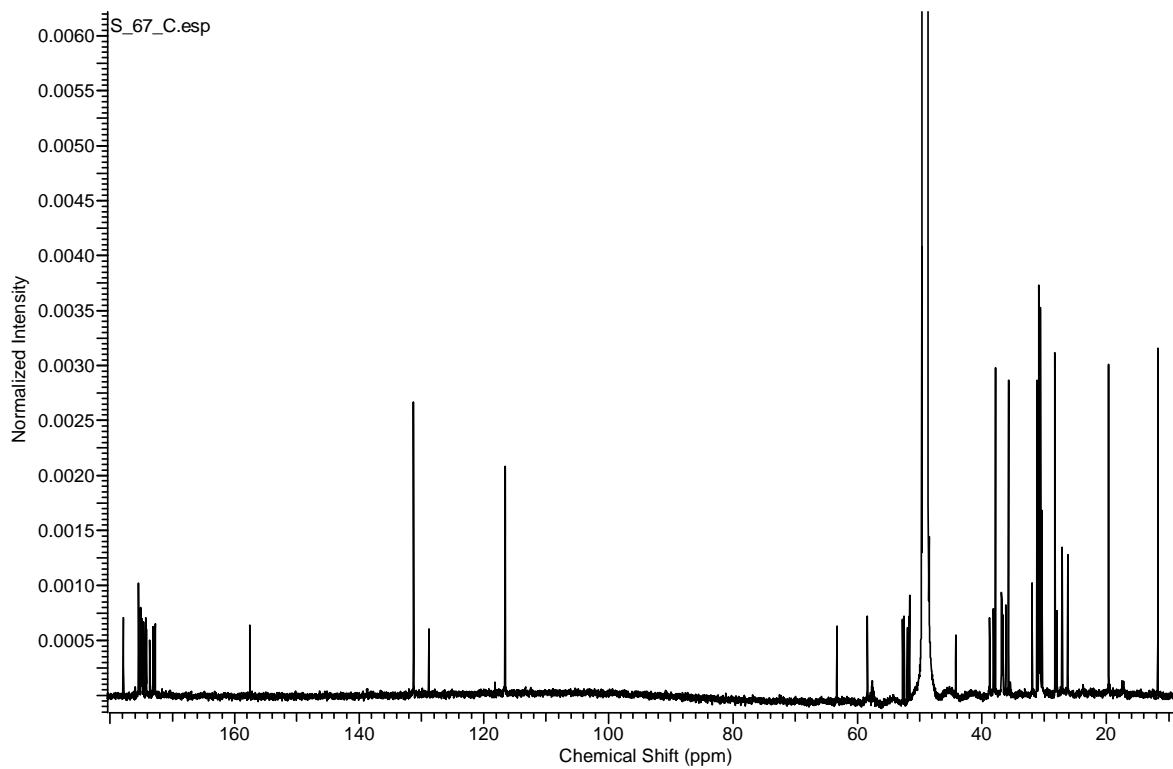
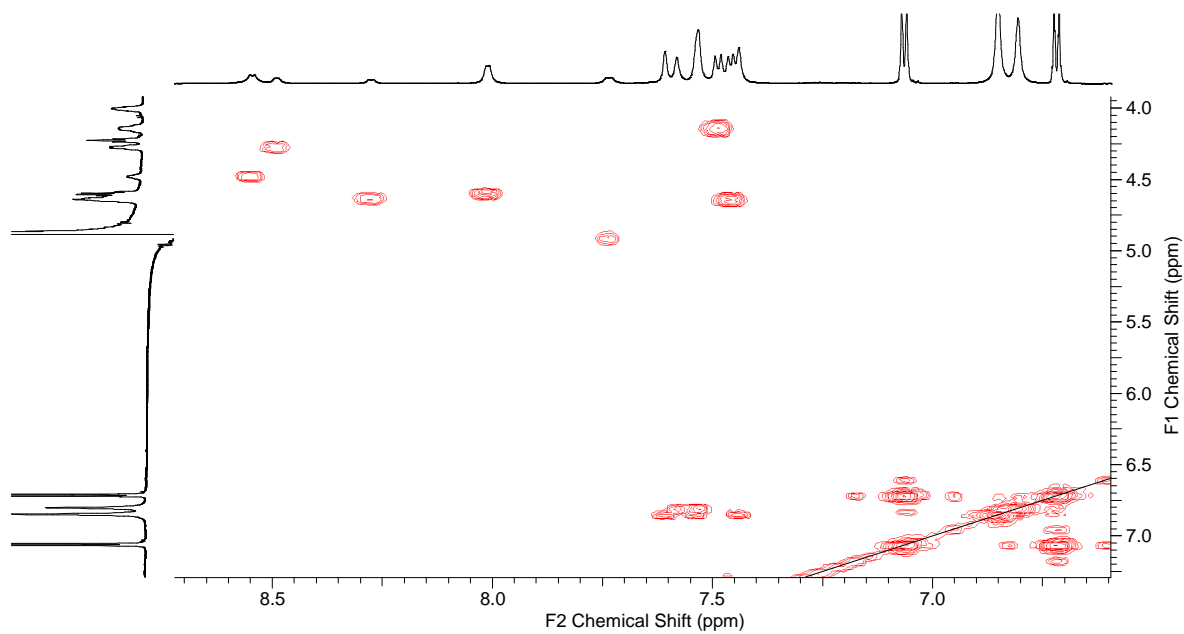
- Aminov, R. I. (2009) The role of antibiotics and antibiotic resistance in nature. *Environ. Microbiol.* 11(12), 2970–2988
- Antunez, K., Anido, M., Evans, J. D., and Zunino, P. (2010) Secreted and immunogenic proteins produced by the honeybee bacterial pathogen, *Paenibacillus larvae*. *Vet. Microbiol.* 141, 385-389
- Antunez, K., Anido, M., Arredondo, D., Evans, J. D., and Zunino, P. (2011a) *Paenibacillus larvae* enolase as a virulence factor in honey bee larvae infection. *Vet. Microbiol.* 147, 83-89
- Antunez, K., Arredondo, D., Anido, M., and Zunino, P. (2011b) Metalloprotease production by *Paenibacillus larvae* during the infection of honeybee larvae. *Microbiol.* 157, 1474-1480
- Bhushan, R., and Bruckner, H. (2004) Marfey's reagent for chiral amino acid analysis: A review. *Amino Acids* 27, 231-247
- Calabrese, E. J., and Baldwin, L. A. (2002) Defining hormesis. *Hum. Exp. Toxicol.* 21, 91-97
- Campano, F., Flores, J. M., Puerta, F., Ruiz, J. A., and Ruz, J. M. (1999) Fungal diseases of the honeybee (*Apis mellifera* L.). In: Colin M. E., Ball B. V., Kilani M. (eds.). *Bee disease diagnosis*. Zaragoza: CIHEAM, 61-68. (Options Méditerranéennes: Série B. Etudes et Recherches; n. 25)
- Chan, Q. W., Cornman, R. S., Birol, I., Liao, N.Y., Chan, S. K., Docking, T. R., *et al.* (2011) Updated genome assembly and annotation of *Paenibacillus larvae*, the agent of American foulbrood disease of honey bees. *BMC Genomics* 12, 450
- Chung, Y. R., Kim, C. H., Hwang, I., and Chun, J. (2000) *Paenibacillus koreensis* sp. nov., a new species that produces an iturin-like antifungal compound. *Int. J. Syst. Evol. Micro.* 50, 1495–1500
- Davies, J., Spiegelman, G. B., and Yim, G. (2006) The world of subinhibitory antibiotic concentrations. *Curr. Opin. Microbiol.* 9, 445–453
- Demain, A. L. (2006) From natural products discovery to commercialization: a success story. *J Ind Microbiol. Biotechnol.* 33, 486-495
- Demain, A. L., and Fang, A. (2000) The Natural Functions of Secondary Metabolites. *Advances in Biochemical Engineering/ Biotechnology*, Vol. 69 Managing Editor: Th. Scheper
- Djukic, M., Brzuszkiewicz, E., Fünfhaus, A., Voss, J., Gollnow, K., Poppinga, L., Liesegang, H., Garcia-Gonzalez, E., Genersch, E., and Daniel, R. (2014) How to Kill the Honey Bee Larva: Genomic Potential and Virulence Mechanisms of *Paenibacillus larvae*. *PLoS Pathogens* (In Press)
- Fünfhaus, A., Ashiralieva, A., Borriss, R., and Genersch, E. (2009) Use of suppression subtractive hybridization to identify genetic differences between differentially virulent genotypes of *Paenibacillus larvae*, the etiological agent of American Foulbrood of honeybees. *Environ. Microbiol.* Rep 1, 240-250
- Fünfhaus, A., Poppinga, L., and Genersch, E. (2013) Identification and characterization of two novel toxins expressed by the lethal honey bee pathogen *Paenibacillus larvae*, the causative agent of American foulbrood. *Environ. Microbiol.* 15(11), 2951–2965
- Genersch, E. (2010) American Foulbrood in honeybees and its causative agent, *Paenibacillus larvae*. *J Invert. Path.* 103 (2010) S10–S19

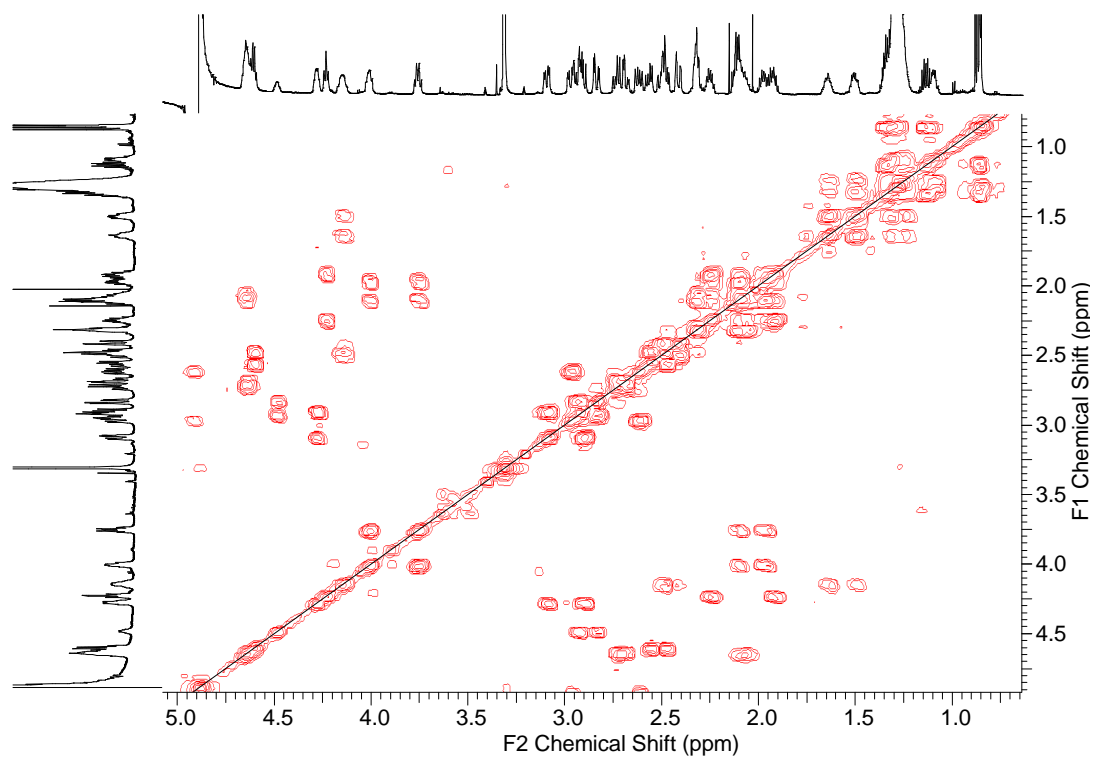
- Genersch, E., Forsgren, E., Pentikainen, J., Ashiralieva, A., Rauch, S., Kilwinski, J., and Fries, I. (2006) Reclassification of *Paenibacillus larvae* subsp. *pulvifaciens* and *Paenibacillus larvae* subsp. *larvae* as *Paenibacillus larvae* without subspecies differentiation *Intern. J. Sys. Evol. Microb.* 56, 501-511
- Genersch, E., Ashiralieva, A., and Fries, I. (2005) Strain- and genotype-specific differences in virulence of *Paenibacillus larvae* subsp. *larvae*, a bacterial pathogen causing American foulbrood disease in honeybees. *App. Environ. Microbiol.* 71, 7551–7555
- Haggett, R. D. and Morchat, R. M. (1992) Microbiological contamination: Biocide treatment in naval distillate fuel. *Int. Biodeterior. Biodegrad.* 29(1), 87-99
- Kanoaka, M., Isogai, A., Murakoshi, S., Ichjinoe, M., Suzuki, A., and Tamura, S. (1977) Bassianolide, a new insecticidal cyclodepsipeptide from *Beauveria bassiana* and *Verticillium lecanii*. *Agric. Biol. Chem.* 42(3), 629-635
- Ma, Z., Wang, N., Hu, J., and Wang, S. (2012) Isolation and characterization of a new iturinic lipopeptide, mojavensin A produced by a marine-derived bacterium *Bacillus mojavensis* B0621A. *J. antib.* 65, 317–322
- Maget-Dana, R., and Peypoux, F. (1994) Iturins, a special class of pore forming lipopeptides: biological and physicochemical properties. *Toxicology* 87, 151–174
- Marfey, P. (1984) Determination of D-amino acids. II. Use of a bifunctional reagent, 1,5-difluoro-2,4-dinitrobenzene. *Carlsberg Res. Commun.* 49, 591–596
- Murray, K. D., and Aronstein, K. A. (2008) Transformation of the Gram-positive honey bee pathogen, *Paenibacillus larvae*, by electroporation. *J. Microbiol. Meth.* 75, 325–328
- Nordström, S., and Fries, I. (1995) A comparison of media and cultural conditions for identification of *Bacillus larvae* in honey. *J. Apic. Res.* 34, 97–103
- Okanya, P. W., Mohr, K. I., Gerth, K., Jansen, R., and Müller, R. (2011) Marinoquinolines A-F, pyrroloquinolines from *Ohtaekwangia kribbensis* (Bacteroidetes) *J. Nat. Prod.* 74, 603-608
- Poppinga, L., Janesch, B., Fünfhaus, A., Sekot, G., Garcia-Gonzalez, E., Hertlein, G., et al. (2012) Identification and Functional Analysis of the S-Layer Protein SplA of *Paenibacillus larvae*, the Causative Agent of American Foulbrood of Honey Bees. *PLoS Pathog.* 8(5): e1002716. doi:10.1371/journal.ppat.1002716
- Romero, D., Traxler, M. F., López, D., and Kolter, R. (2011) Antibiotics as Signal Molecules. *Chem. Rev.* 111(9), 5492–5505
- Rauch, S., Ashiralieva, A., Hedtke, K., and Genersch, E. (2009) Negative correlation between individual-insect-level virulence and colony-level virulence of *Paenibacillus larvae*, the etiological agent of American Foulbrood of honeybees. *Appl. Environ. Microbiol.* 75, 3344–3347
- Wyatt, M. A., Wang, W., Roux, C. M., Beasley, F. C., Heinrichs, D. E., Dunman, P. M. and Magarvey, N. A. (2010) Clarification of “*Staphylococcus aureus* Nonribosomal Peptide Secondary Metabolites Regulate Virulence”. *Science* 329, 294 (Corrected 2011)

Yue, D., Nordhoff, M., Wieler L. H. and Genersch, E. (2008) Fluorescence in situ hybridization (FISH) analysis of the interactions between honeybee larvae and *Paenibacillus larvae*, the causative agent of American foulbrood of honeybees (*Apis mellifera*). *Environ. Microbiol.* 10, 1612-1620

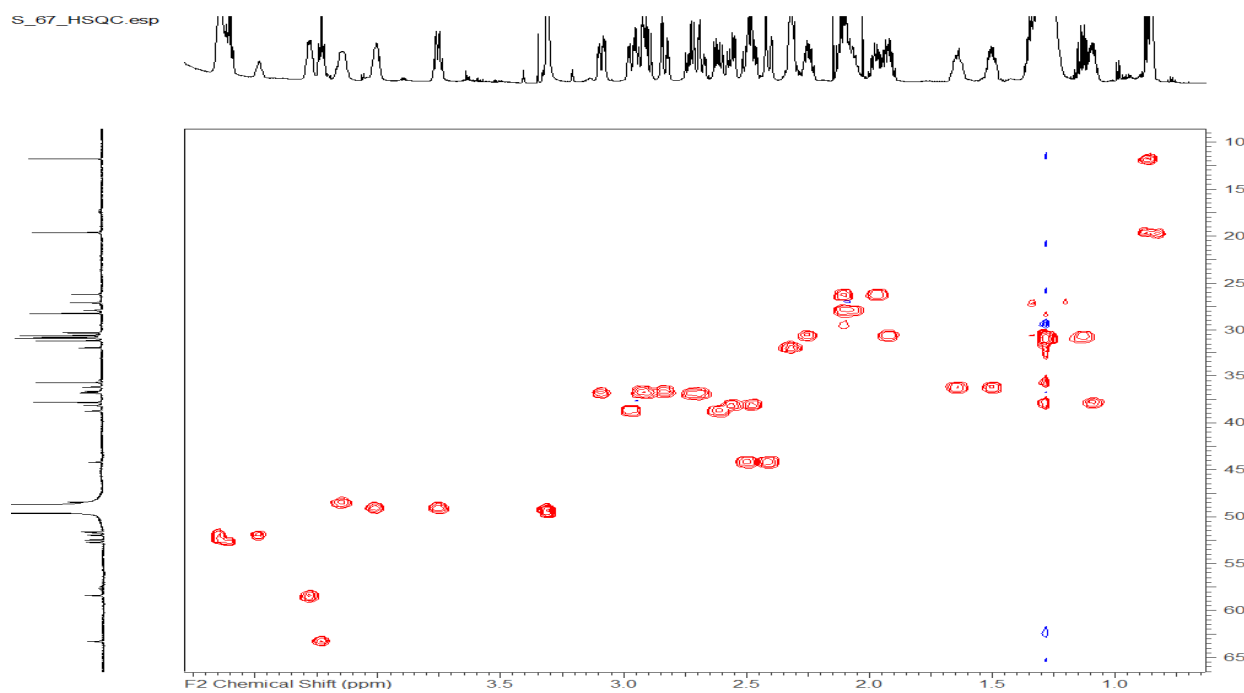
Zhang, D. J., Liu, R. F., Li, Y. G., Tao, L. M., and Tian, L. L. (2010) Two New Antifungal Cyclic Lipopeptides from *Bacillus marinus* B-9987. *Chem. Pharm. Bull.* 58(12), 1630-1634

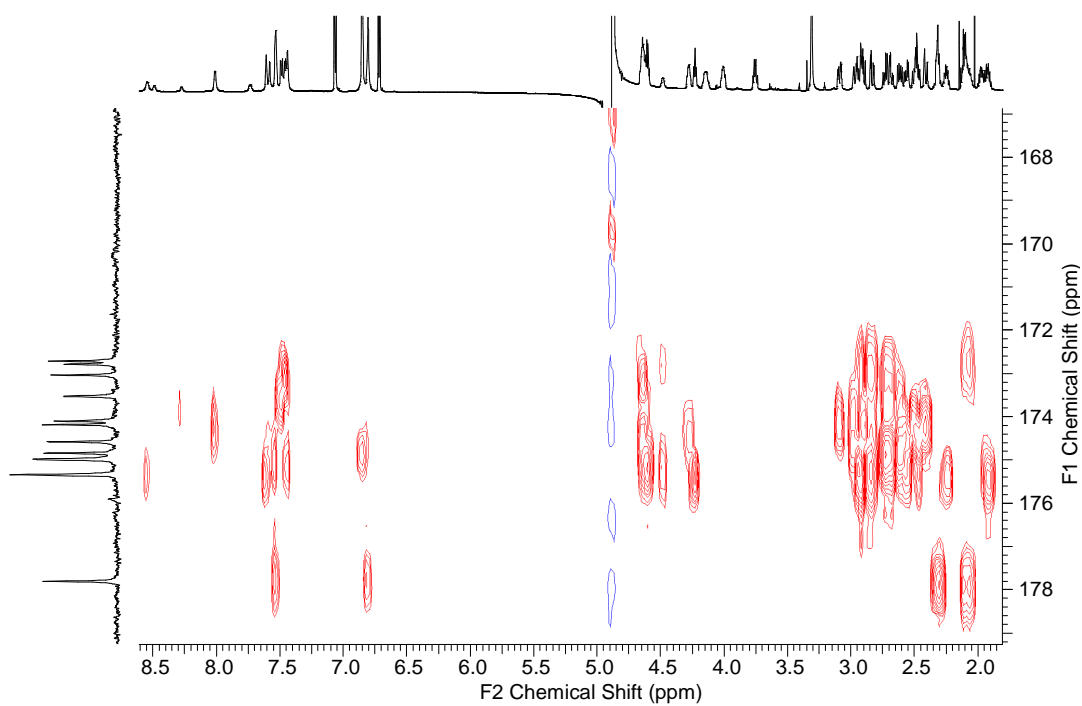
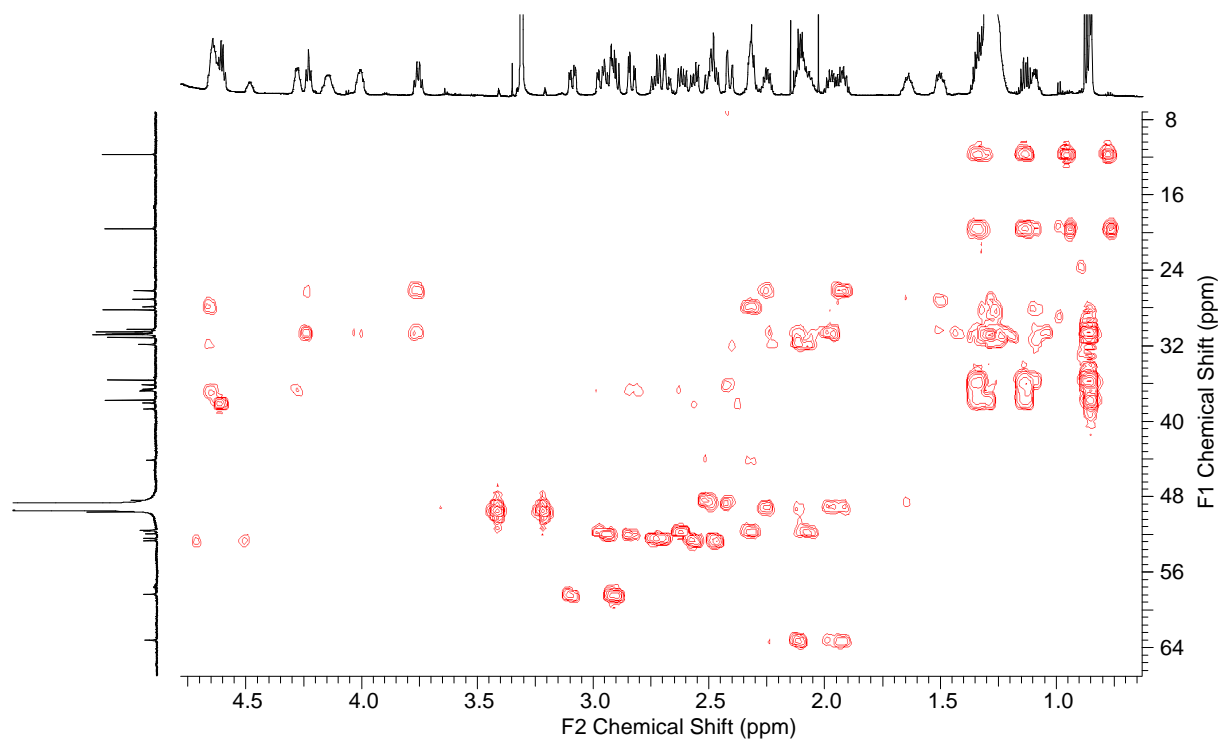
Supplemental information**Figure BS1. ¹H NMR of 1 in CD₃OH, 700 MHz**

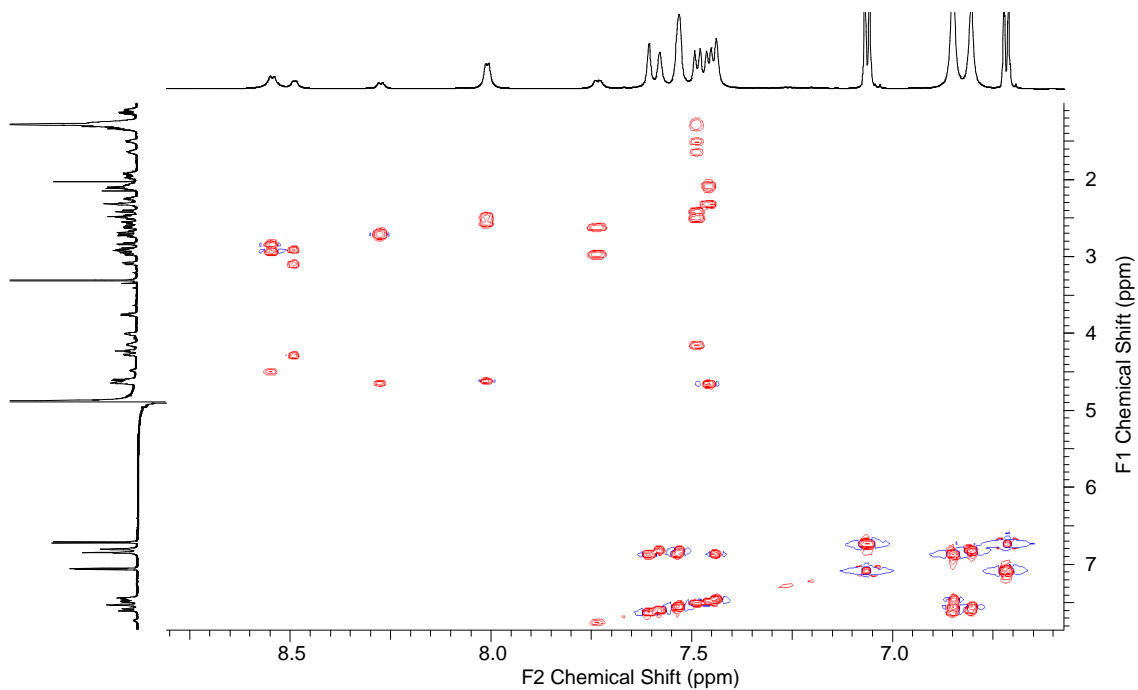
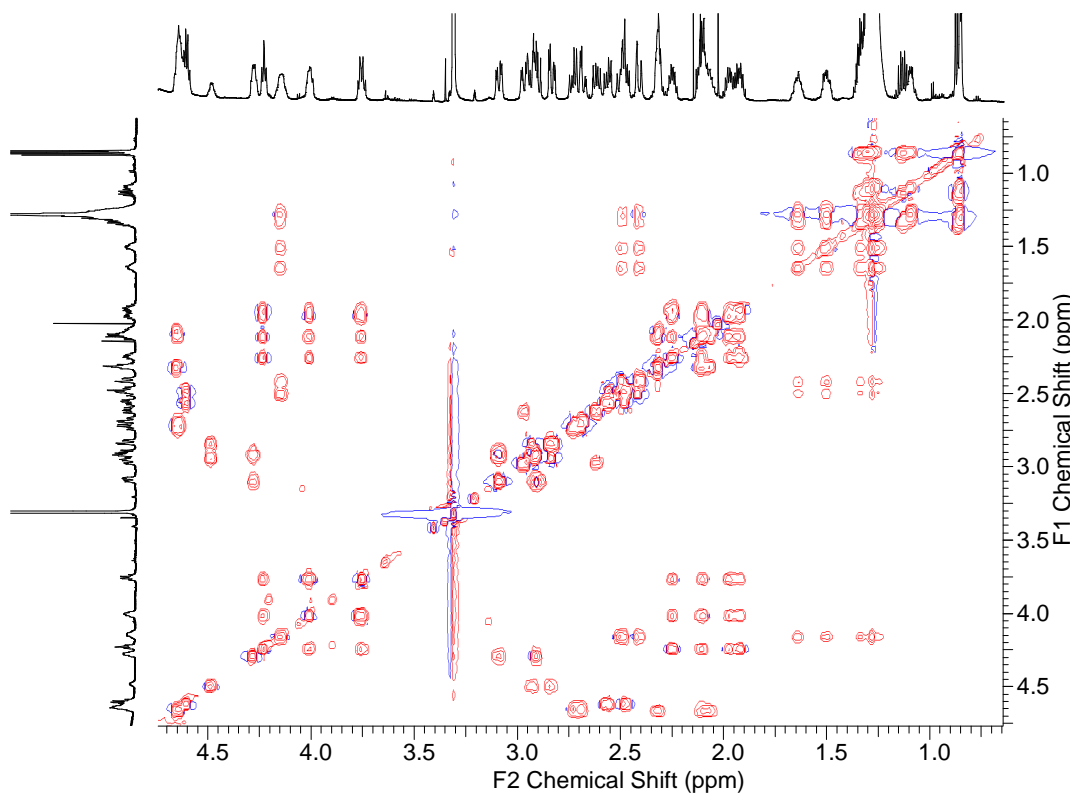
Figure BS2. ^{13}C NMR of 1 in CD_3OH , 176 MHzFigure BS3. ^1H - ^1H COSY NMR of 1 in CD_3OH , selected area

Figure BS4. ^1H - ^1H COSY NMR of **1** in CD_3OH , selected area

S_67_HSQC.esp

Figure BS5. HSQC NMR of **1** in CD_3OH , selected area



Figure BS8. TOCSY NMR of 1 in CD₃OH, selected areaFigure BS9. TOCSY NMR of 1 in CD₃OH, selected area

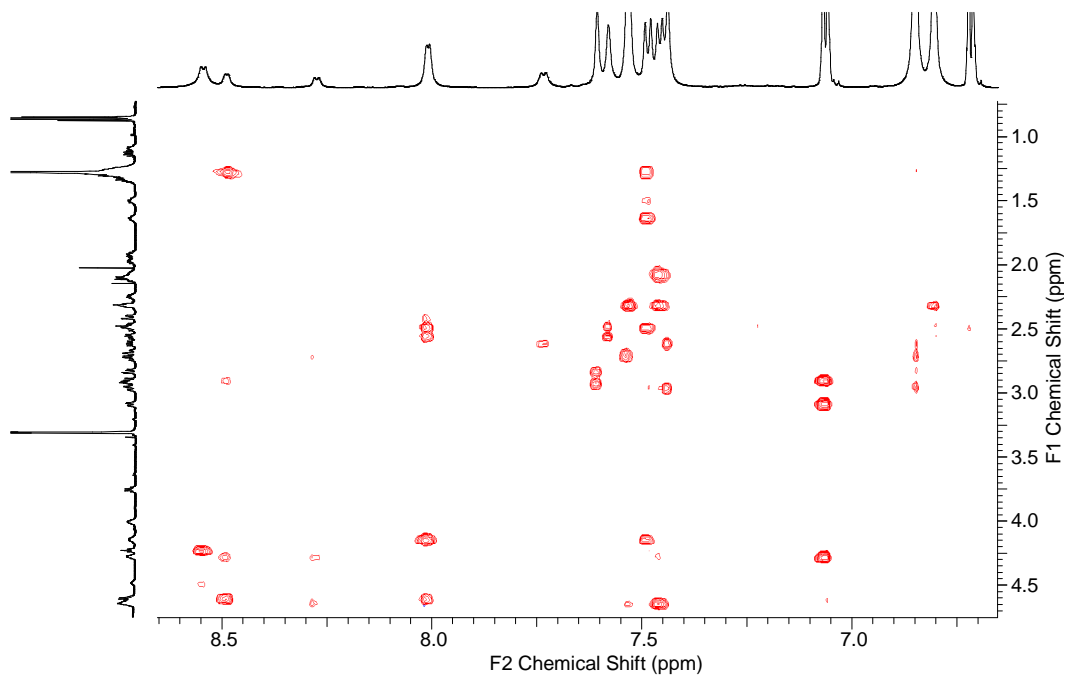


Figure BS10. ROESY NMR of 1 in CD₃OH, selected area

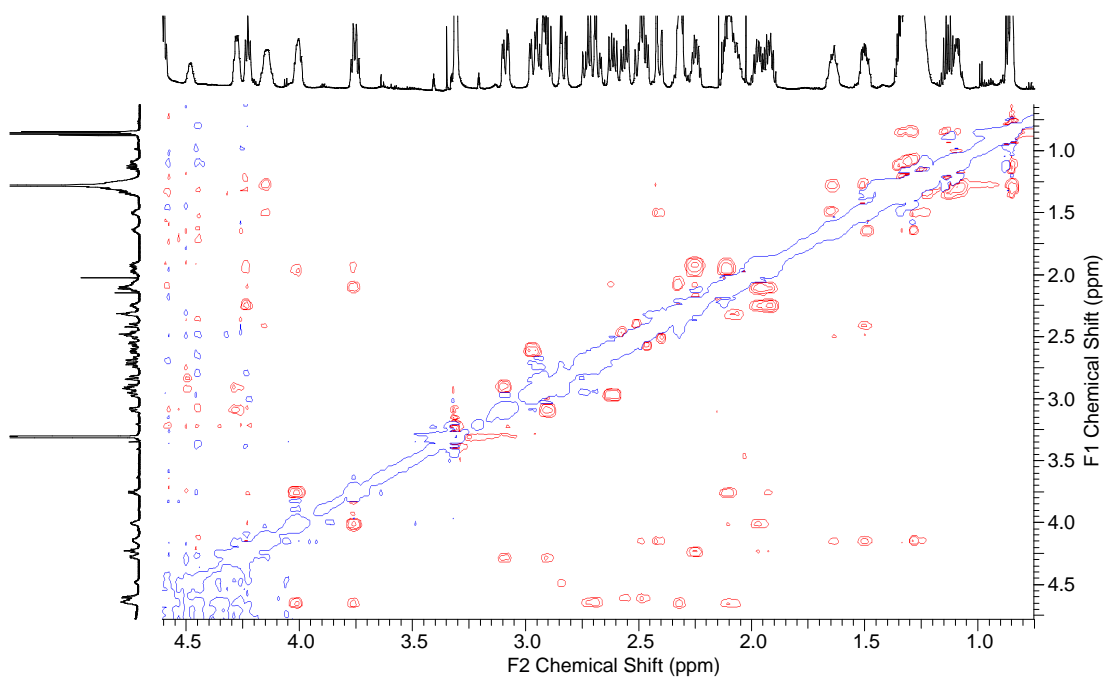


Figure BS11. ROESY NMR of 1 in CD₃OH, selected area

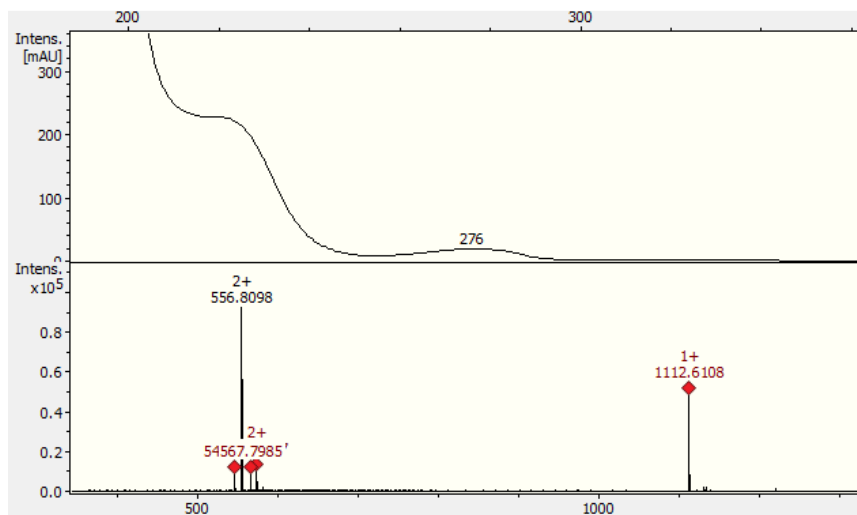
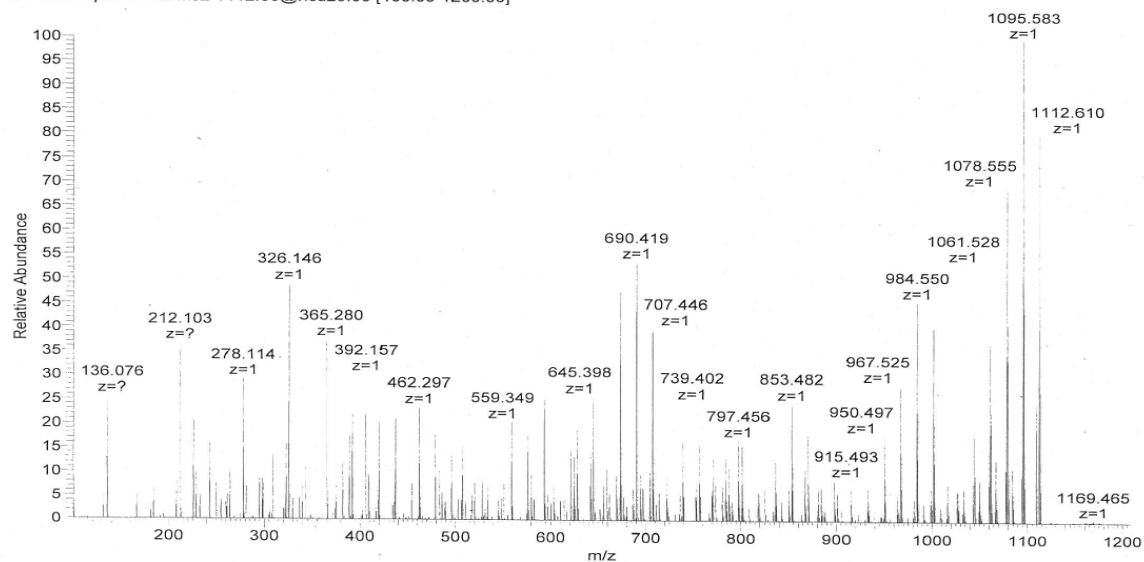


Figure BS12: ESI HRMS of paenilarvin A (1)

N0112B #25-89 RT: 0.192-0.986 AV: 65 NL: 7.44E6
T: FTMS + p NSI Full ms2 1112.60@hcd25.00 [100.00-1200.00]



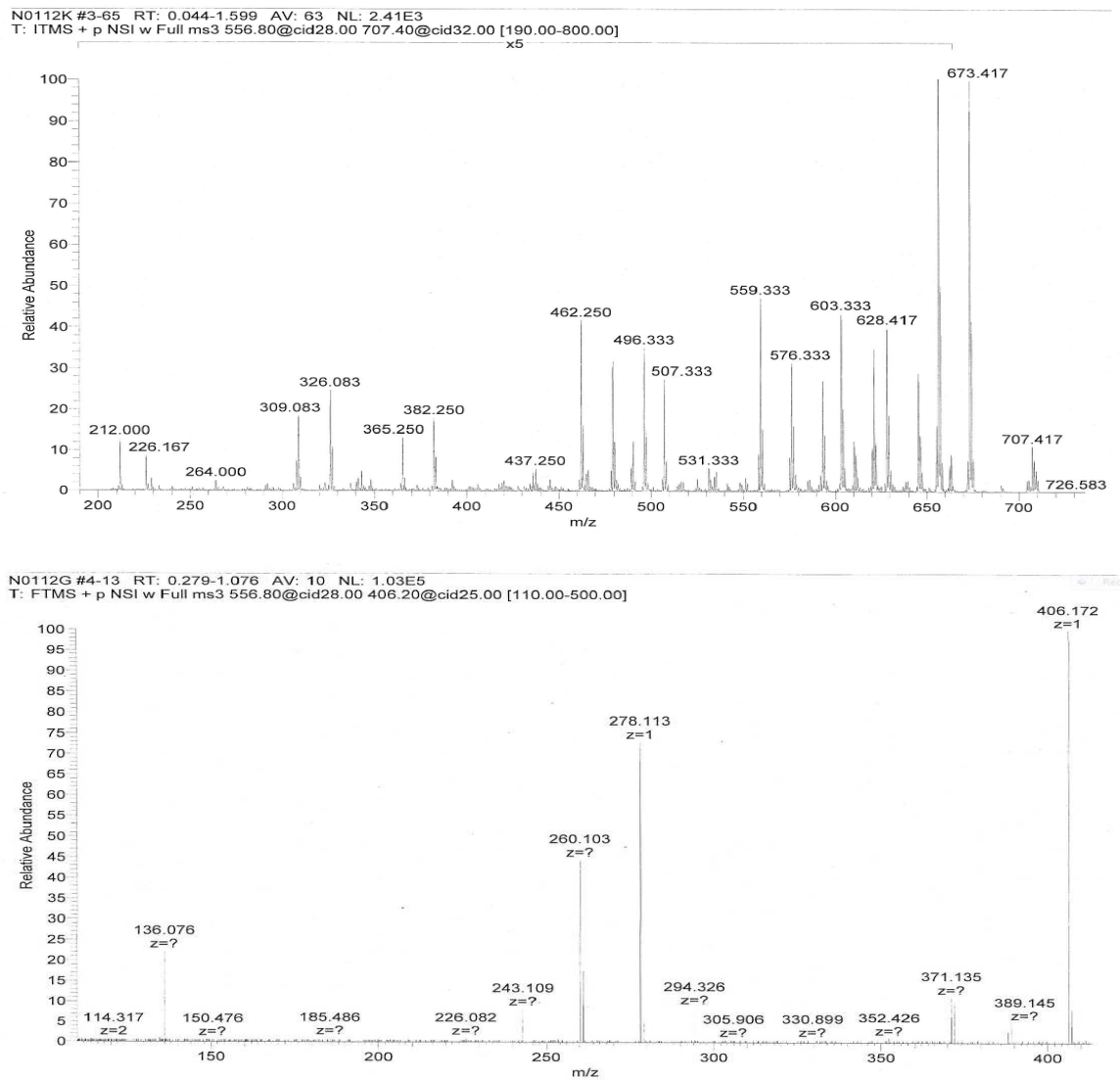


Figure BS13. MS/MS spectra of (1)

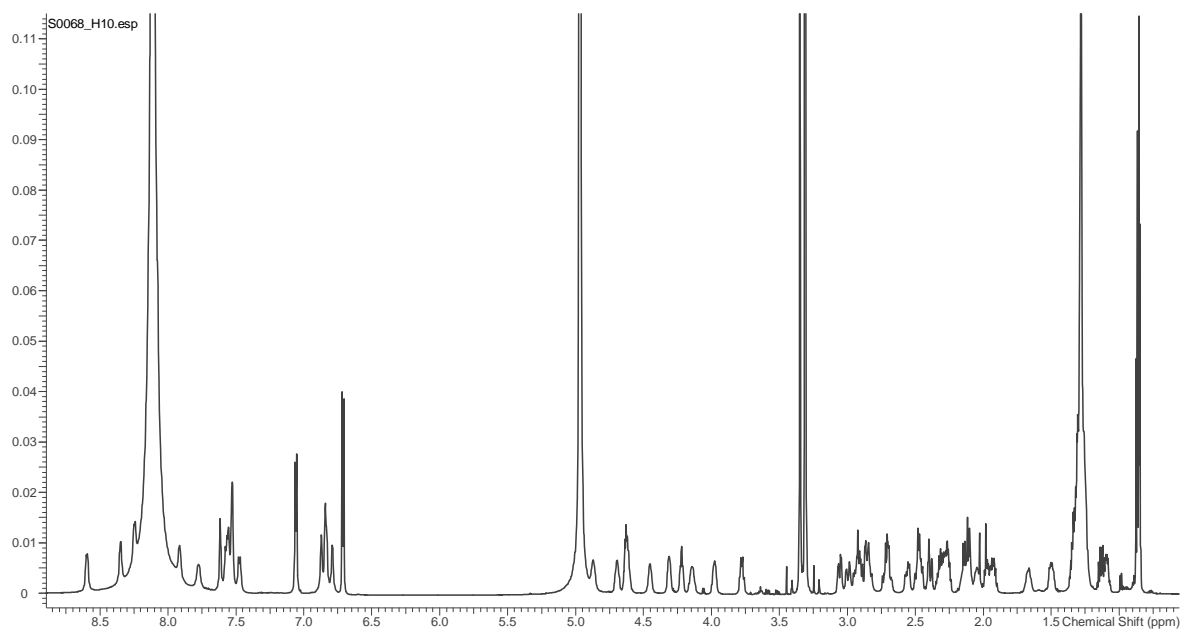


Figure BS14. ^1H NMR of 2 in $\text{CD}_3\text{OH} + 5 \mu\text{L HCOOH}$, 700 MHz

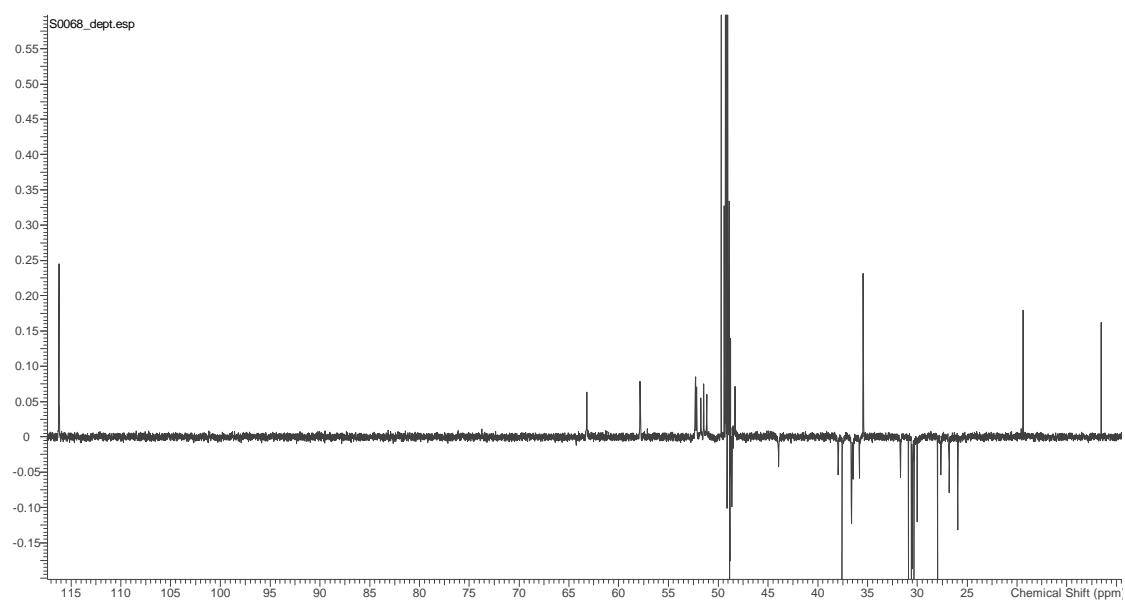


Figure BS15. ^{13}C NMR DEPT of 2 in $\text{CD}_3\text{OH} + 5 \mu\text{L HCOOH}$, 176 MHz, selected area

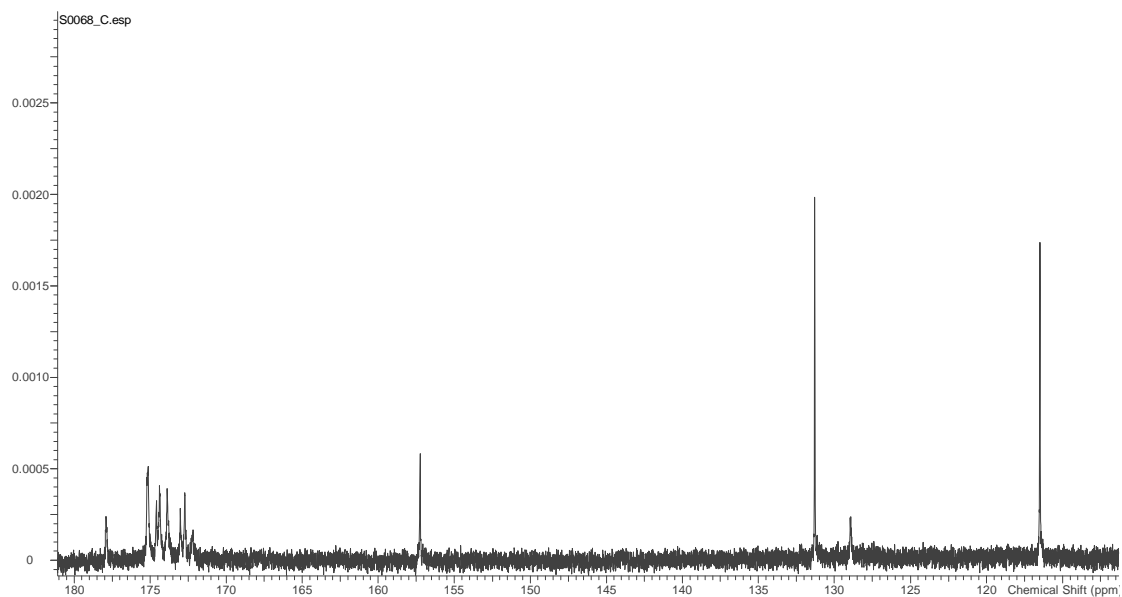


Figure BS16. ^{13}C NMR of 2 in $\text{CD}_3\text{OH} + 5 \mu\text{L HCOOH}$, 176 MHz, selected area

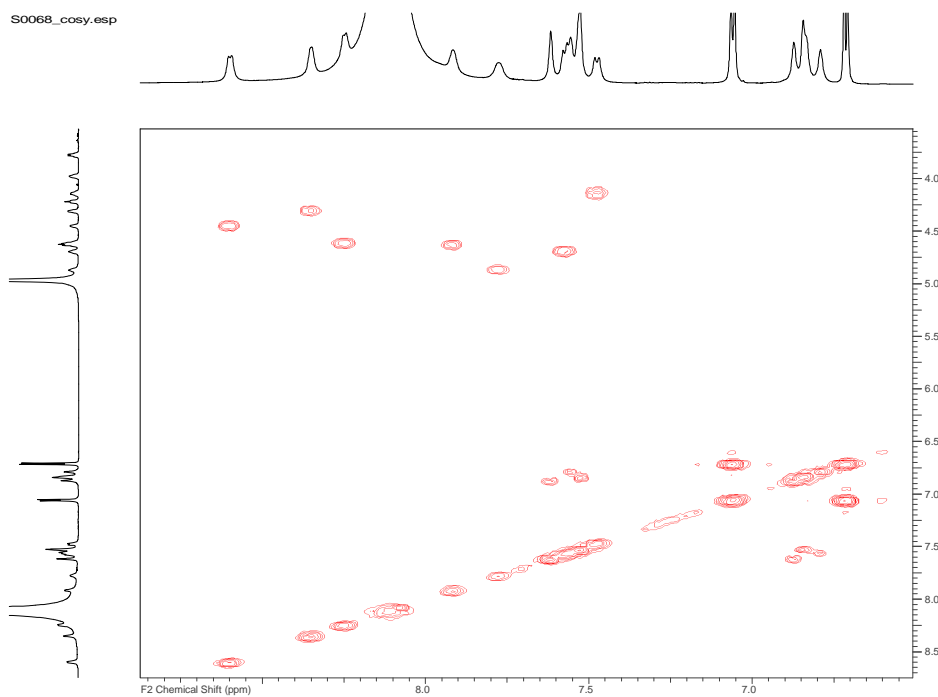


Figure BS17. ^1H - ^1H COSY NMR of 2 in $\text{CD}_3\text{OH} + 5 \mu\text{L HCOOH}$, 700 MHz, selected area

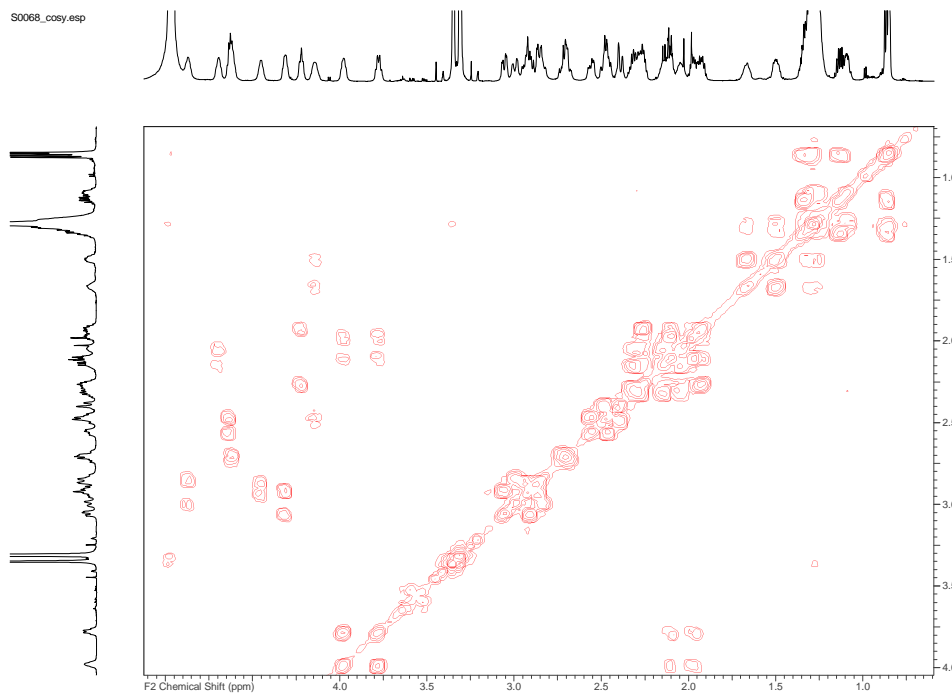


Figure BS18. ^1H - ^1H COSY NMR of 2 in $\text{CD}_3\text{OH} + 5 \mu\text{L HCOOH}$, 700 MHz, selected area

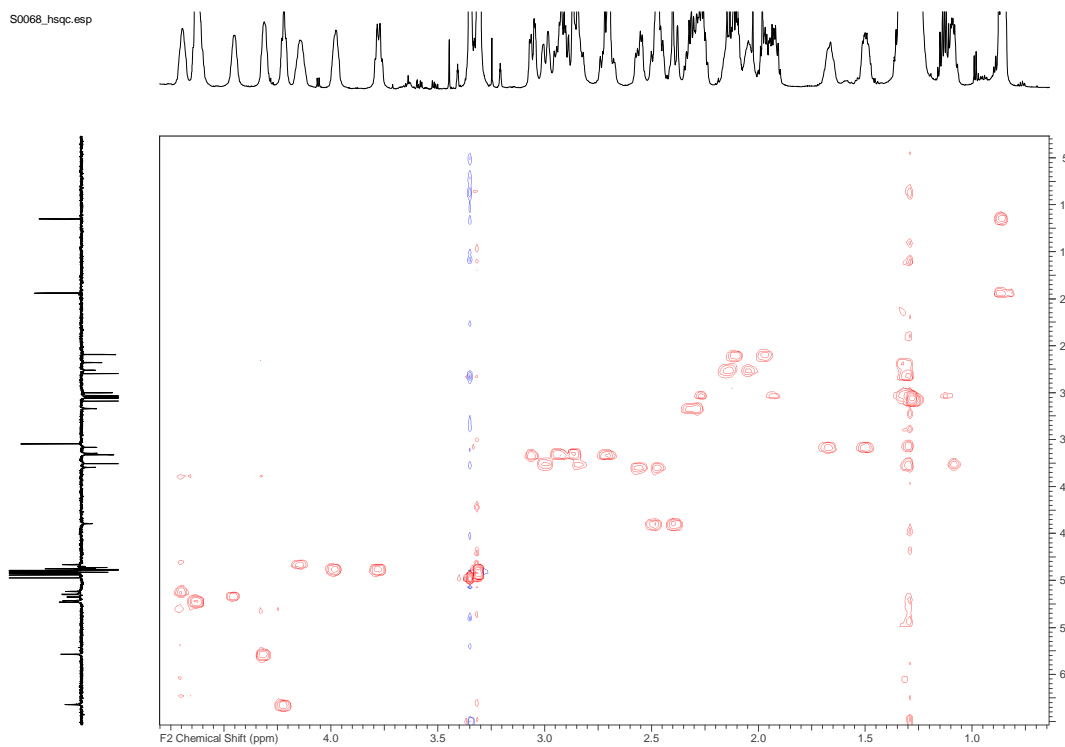


Figure BS19. HSQC NMR of 2 in $\text{CD}_3\text{OH} + 5 \mu\text{L HCOOH}$, 700 MHz, selected area

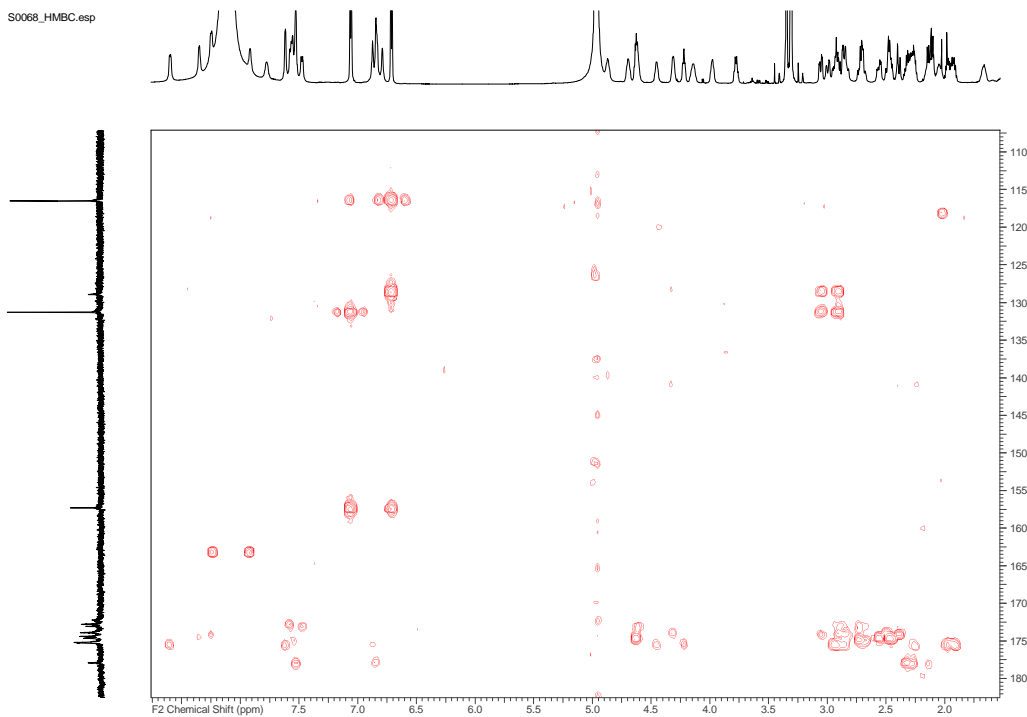


Figure BS20. HMBC NMR of 2 in CD₃OH + 5 μL HCOOH, 700 MHz, selected area

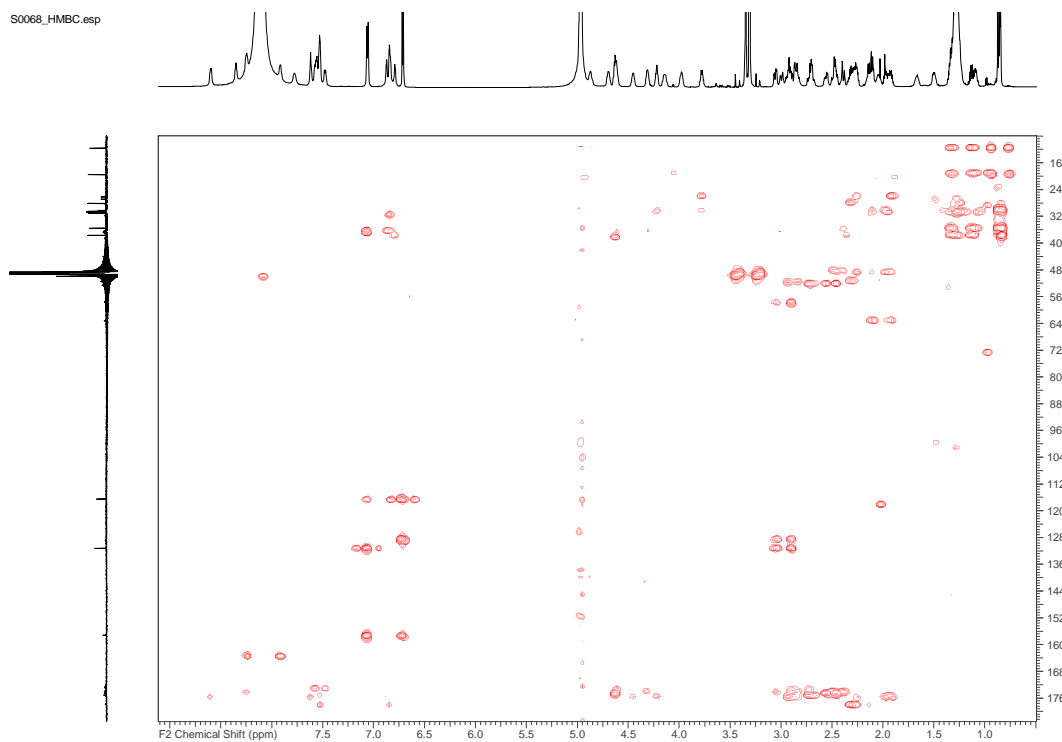


Figure BS21. HMBC NMR of 2 in CD₃OH + 5 μL HCOOH, 700 MHz, selected area

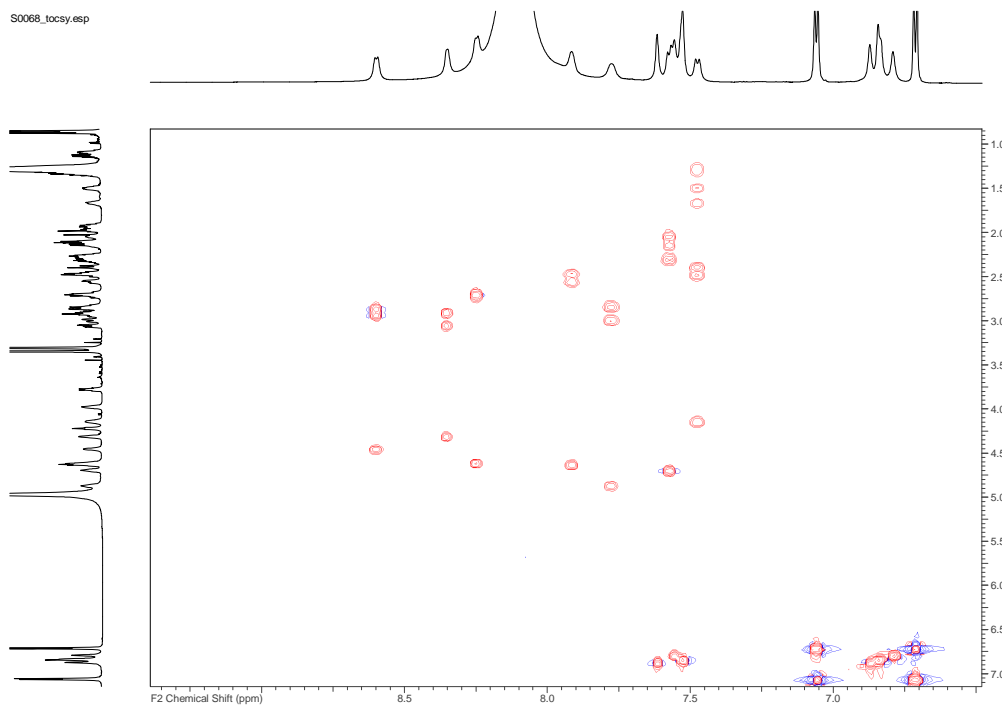


Figure BS22. TOCSY NMR of 2 in CD_3OH + 5 μL HCOOH , 700 MHz, selected area

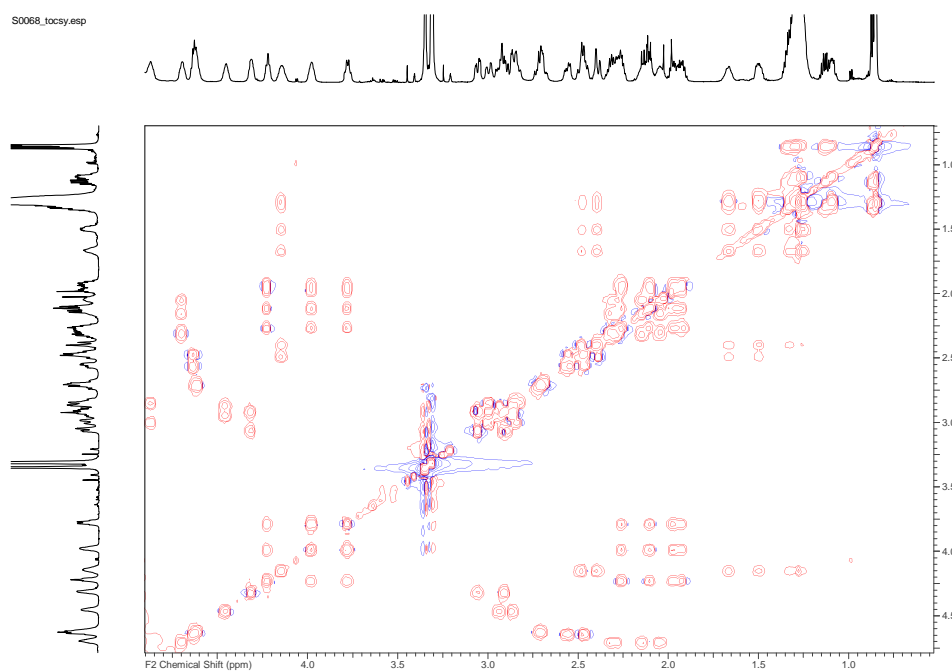


Figure BS23. TOCSY NMR of 2 in CD_3OH + 5 μL HCOOH , 700 MHz, selected area

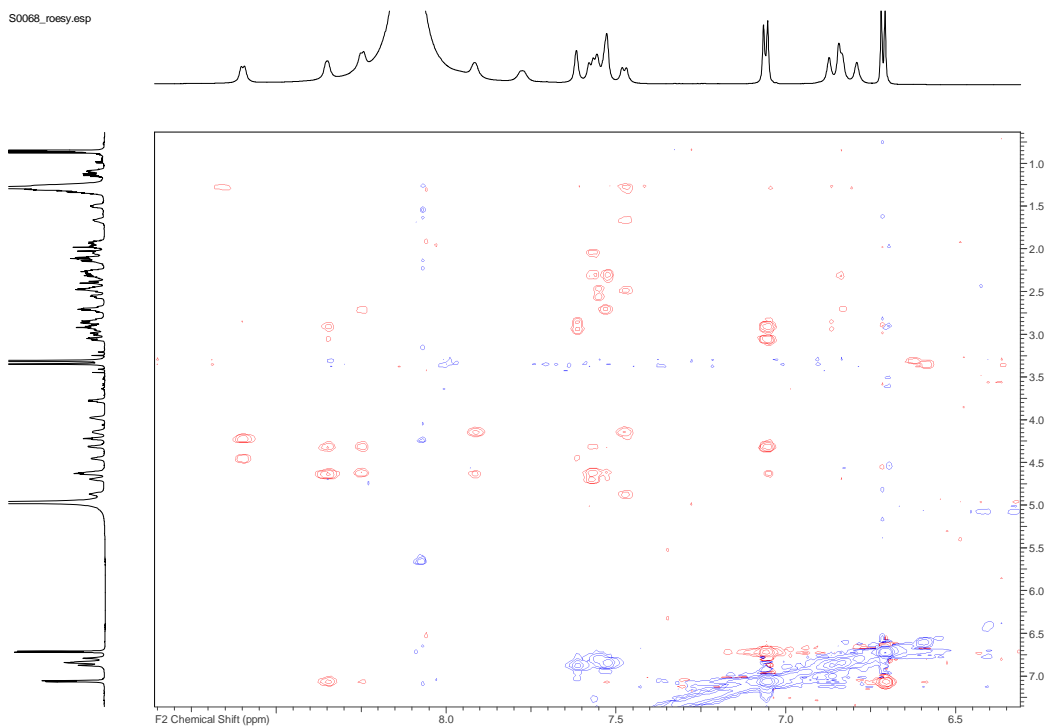


Figure BS24. ROESY NMR of 2 in CD₃OH +5 µL HCOOH, 700 MHz, selected area

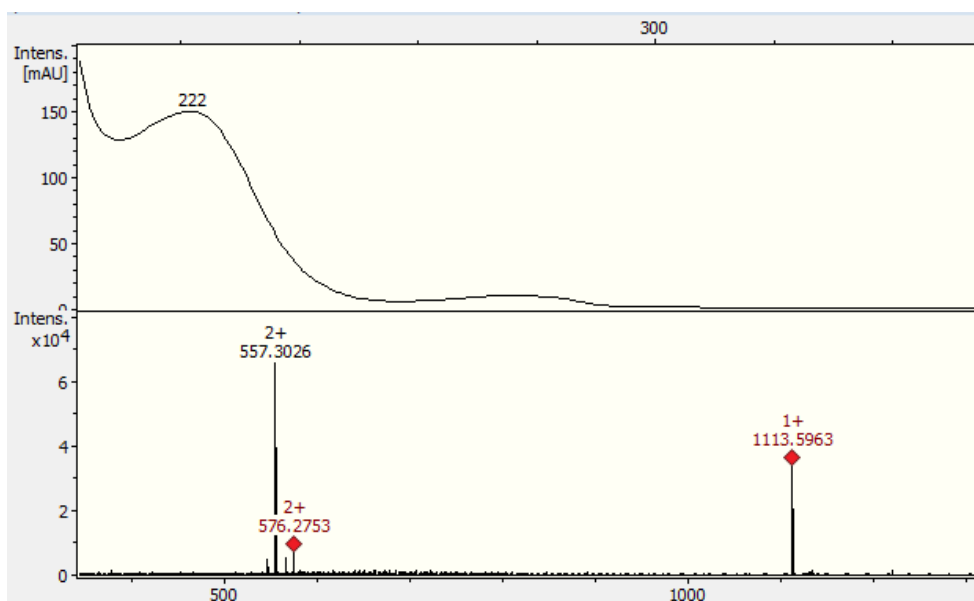
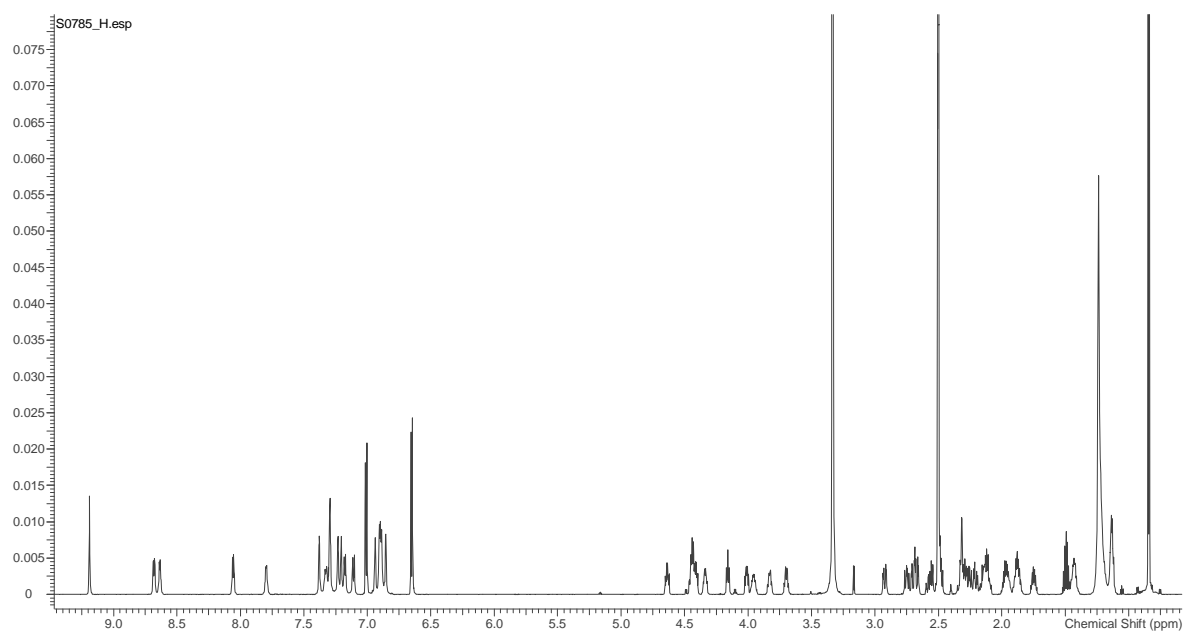
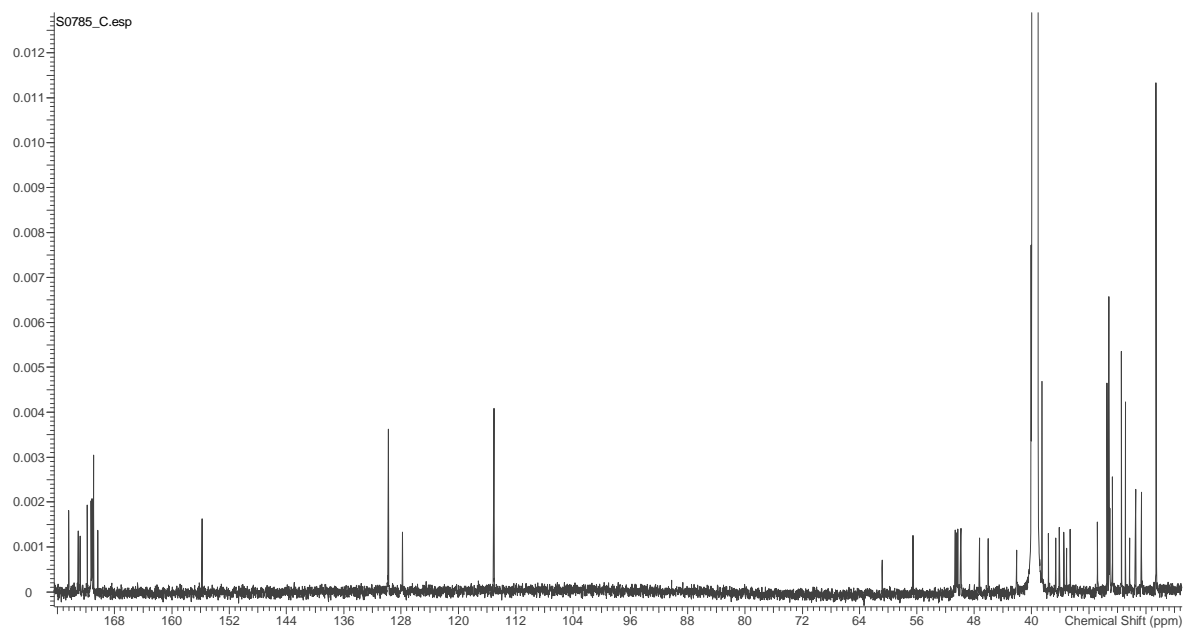


Figure BS25. ESI HRMS of paenilarvin B (2)

Figure BS26: ¹H NMR of 3 in DMSO-d₆, 700 MHzFigure BS27. ¹³C NMR of 3 in DMSO-d₆, 176 MHz

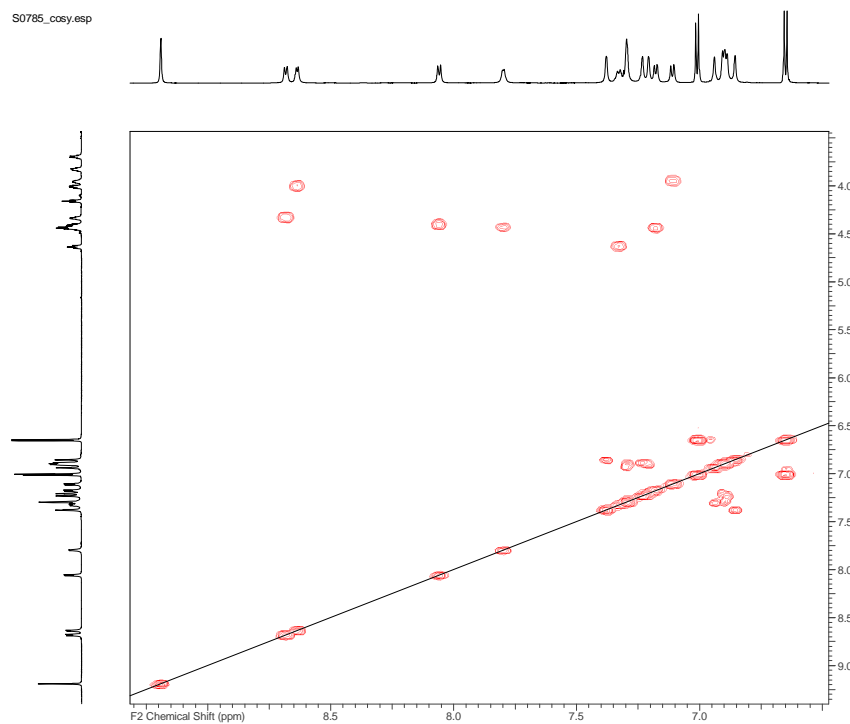


Figure BS28. ^1H - ^1H COSY NMR of 3 in DMSO- d_6 , selected area

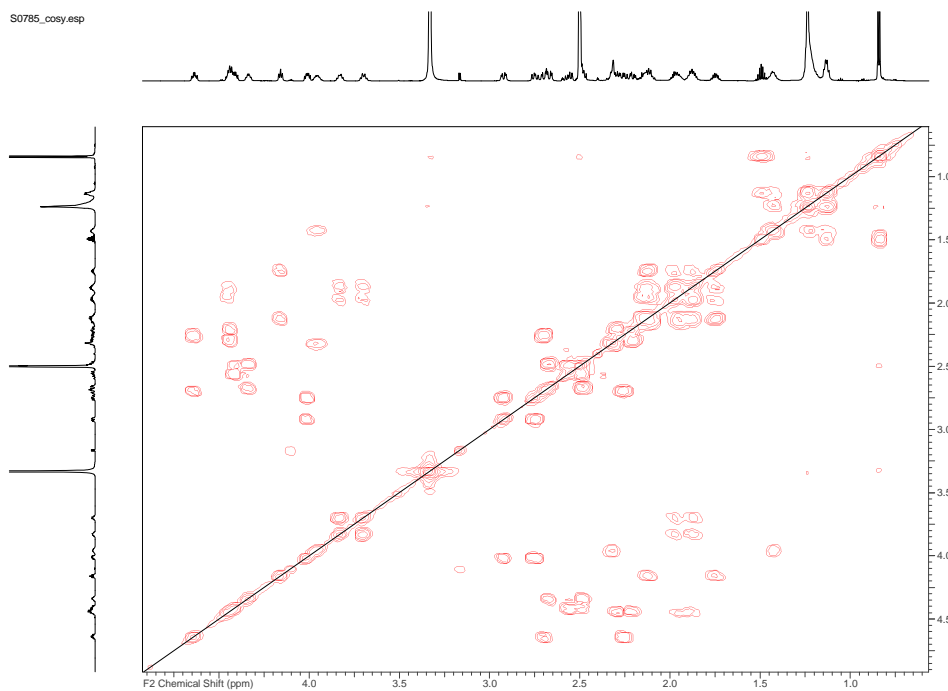


Figure BS29. ^1H - ^1H COSY NMR of 3 in DMSO- d_6 , selected area

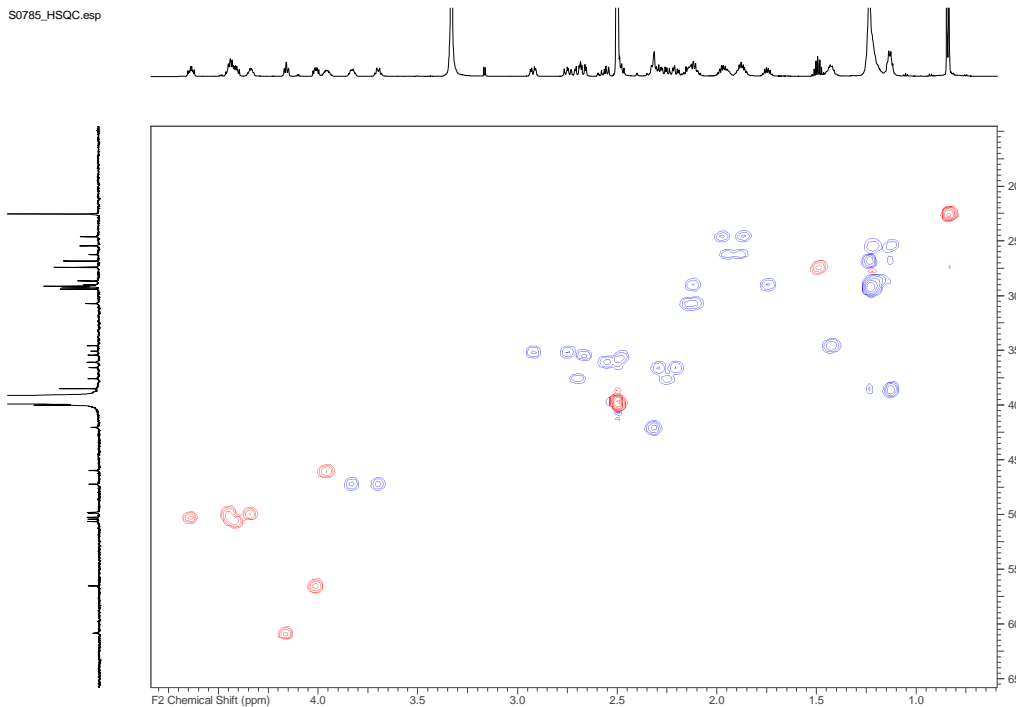


Figure BS30. HSQC NMR of 3 in DMSO-d₆ +5 μL HCOOH, 700 MHz, selected area

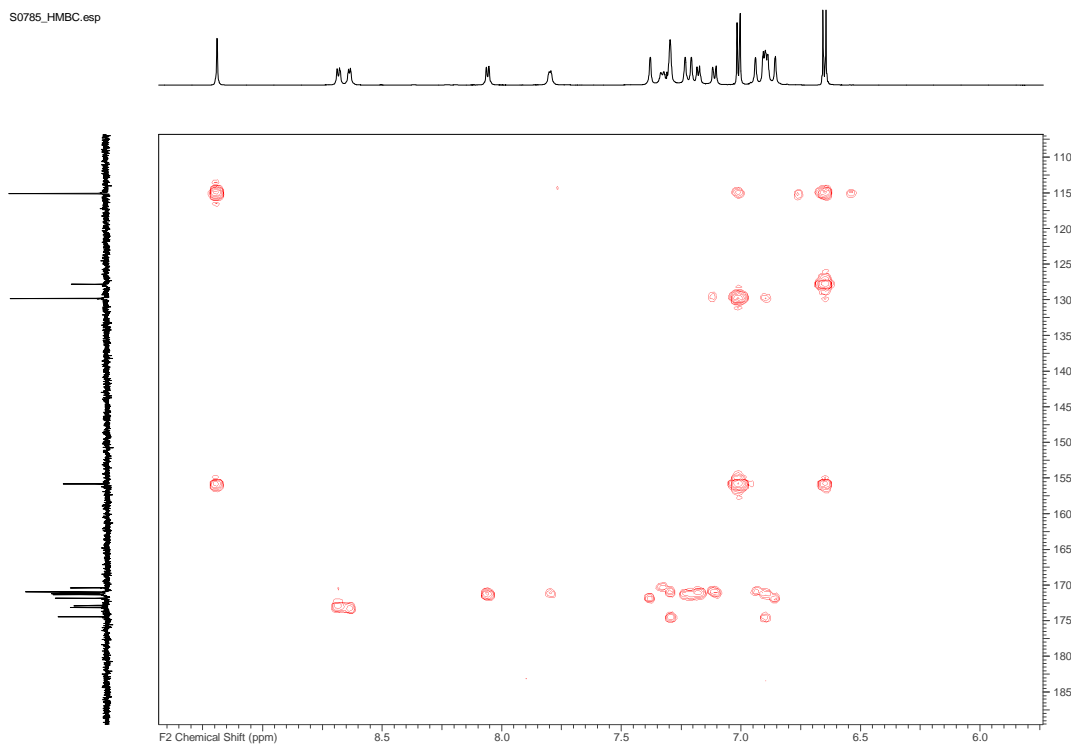


Figure BS31. HMBC NMR of 3 in DMSO-d₆, 700 MHz, selected area

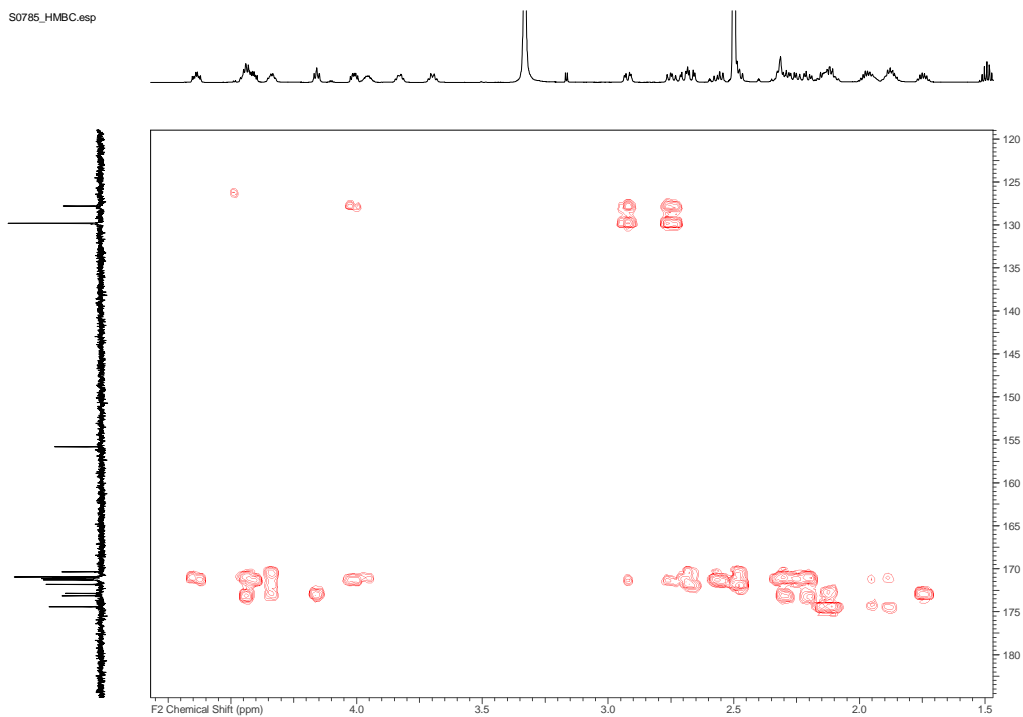


Figure BS32. HMBC NMR of 3 in DMSO-d₆, 700 MHz, selected area

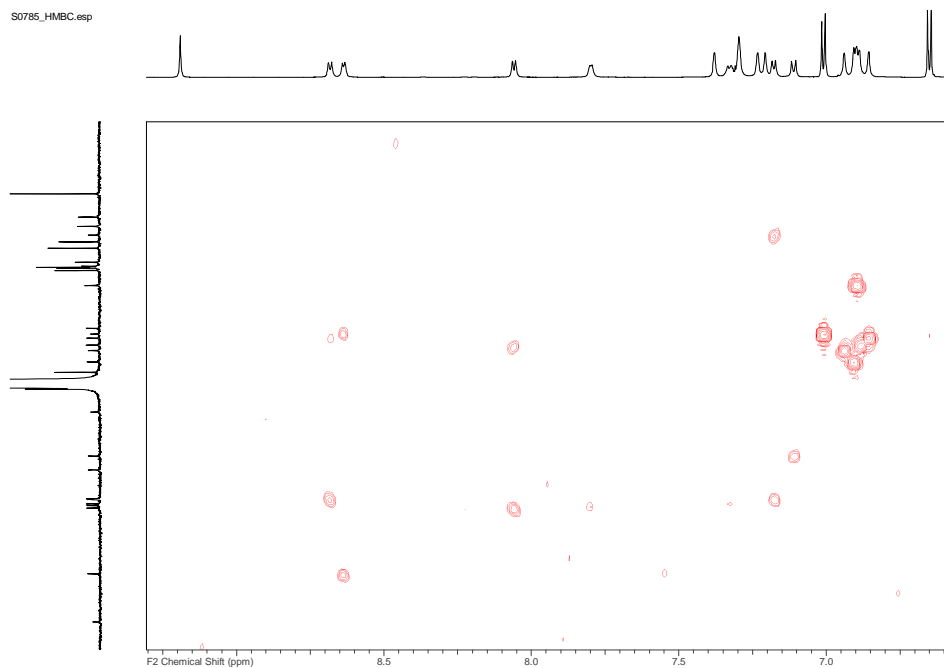


Figure BS33. HMBC NMR of 3 in DMSO-d₆, 700 MHz, selected area

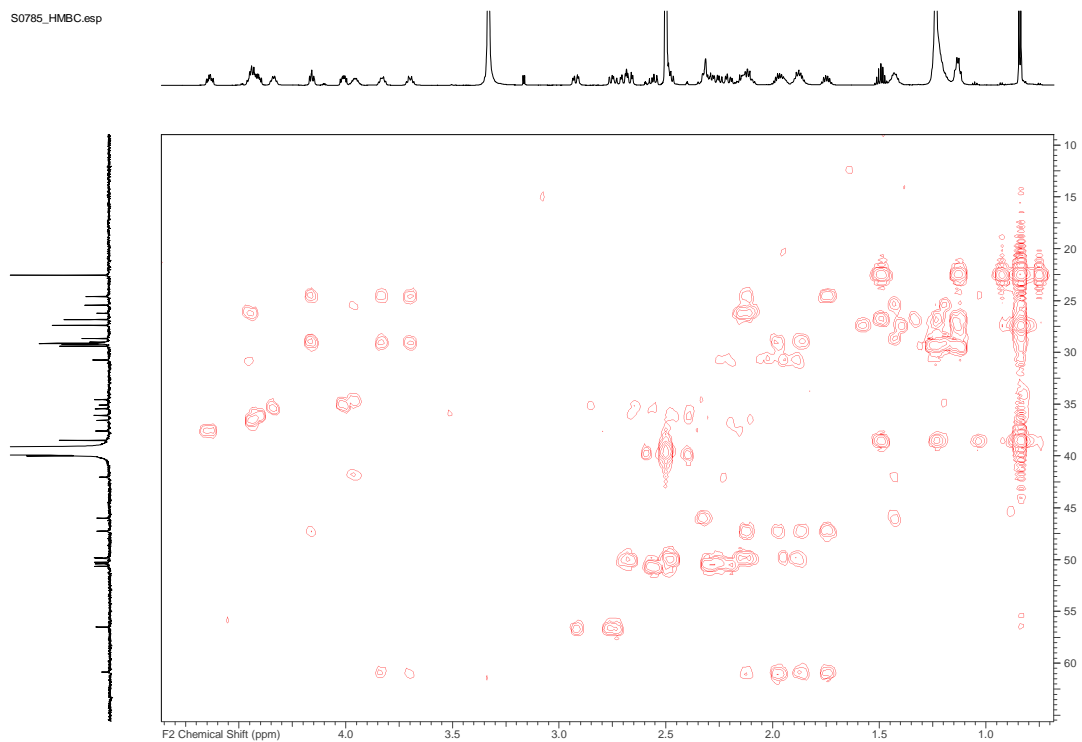


Figure BS34. HMBC NMR of 3 in DMSO-d₆, 700 MHz, selected area

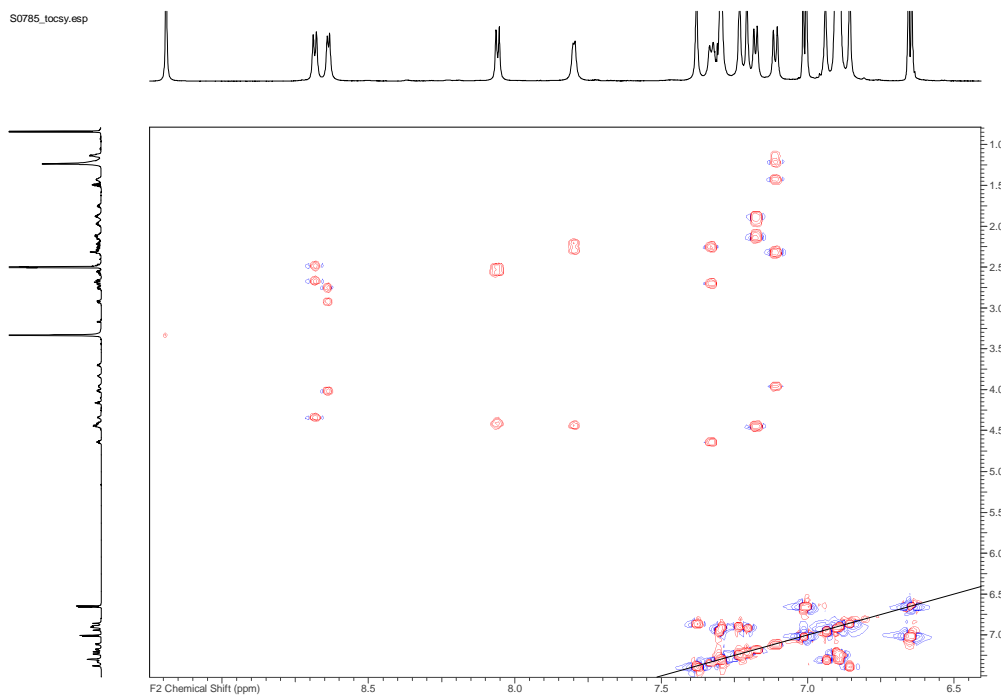


Figure BS35. TOCSY NMR of 3 in DMSO-d₆, 700 MHz, selected area

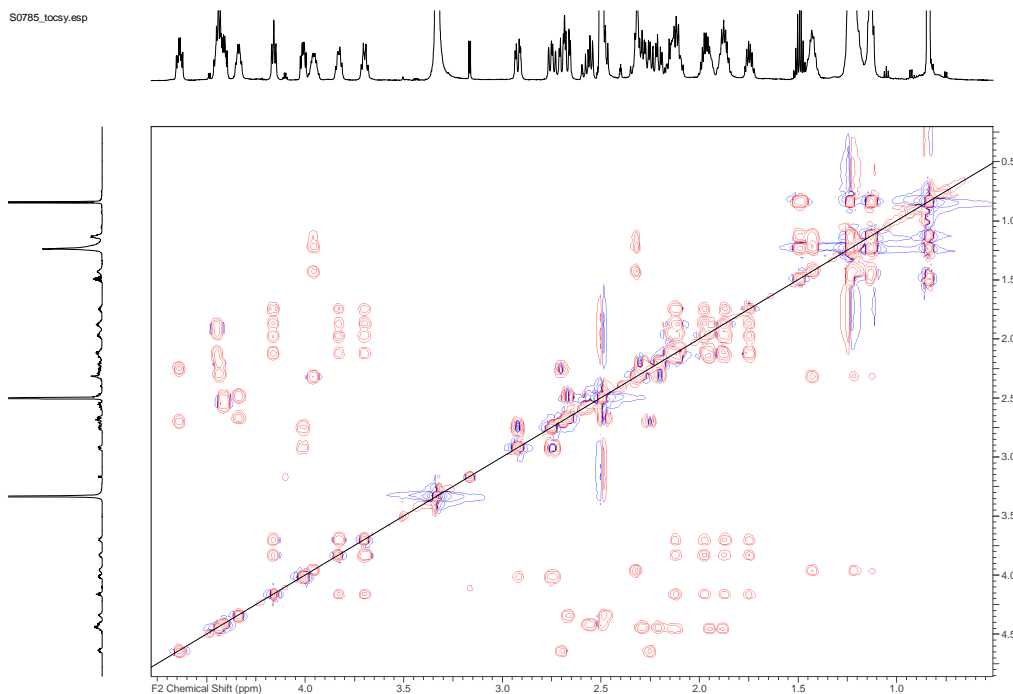


Figure BS36. TOCSY NMR of 3 in DMSO-d₆, 700 MHz, selected area

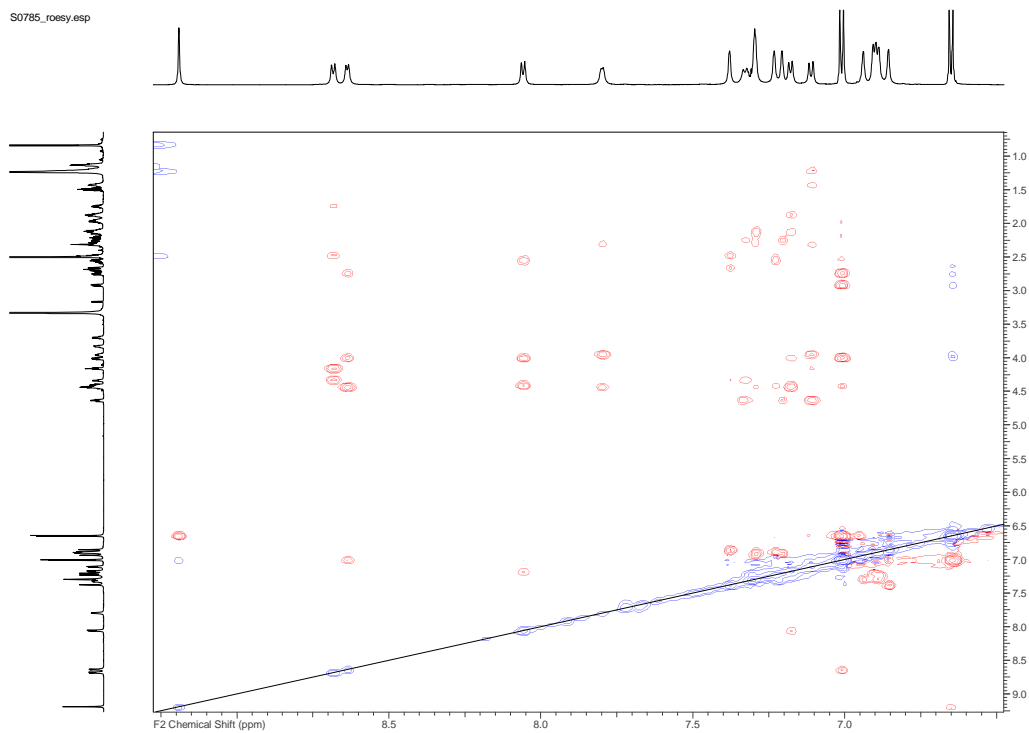


Figure BS37. ROESY NMR of 3 in DMSO-d₆, 700 MHz, selected area

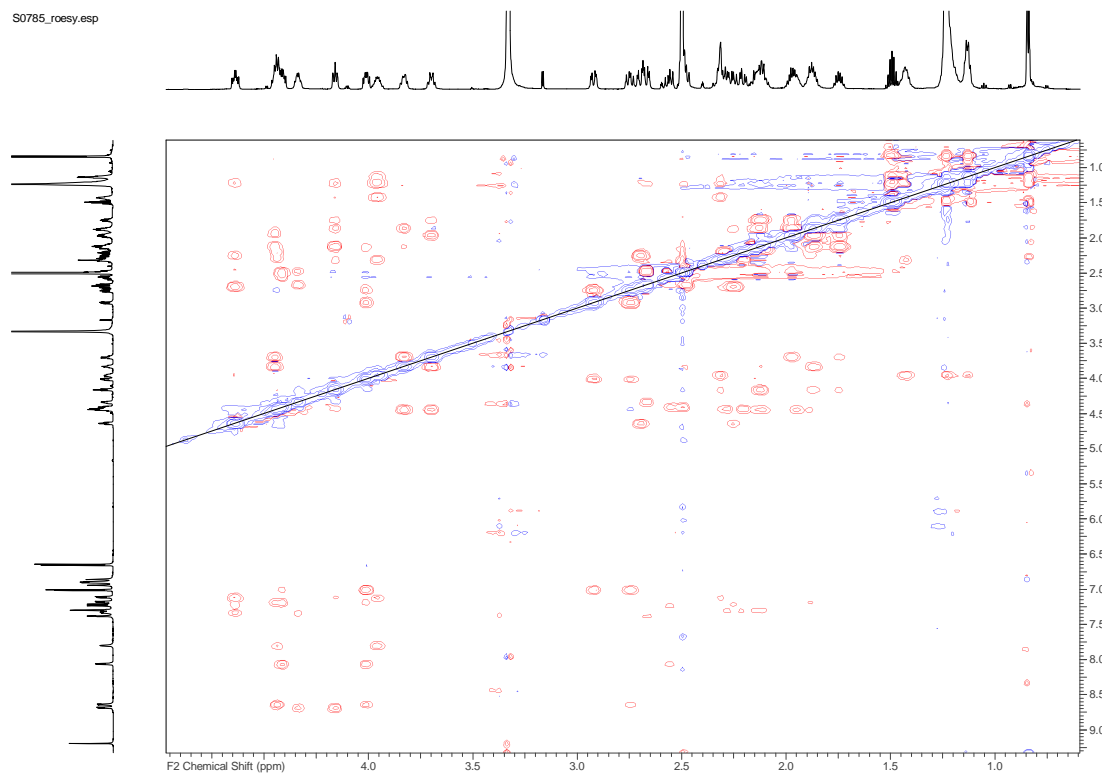


Figure BS38. ROESY NMR of 3 in DMSO-d₆, 700 MHz, selected area

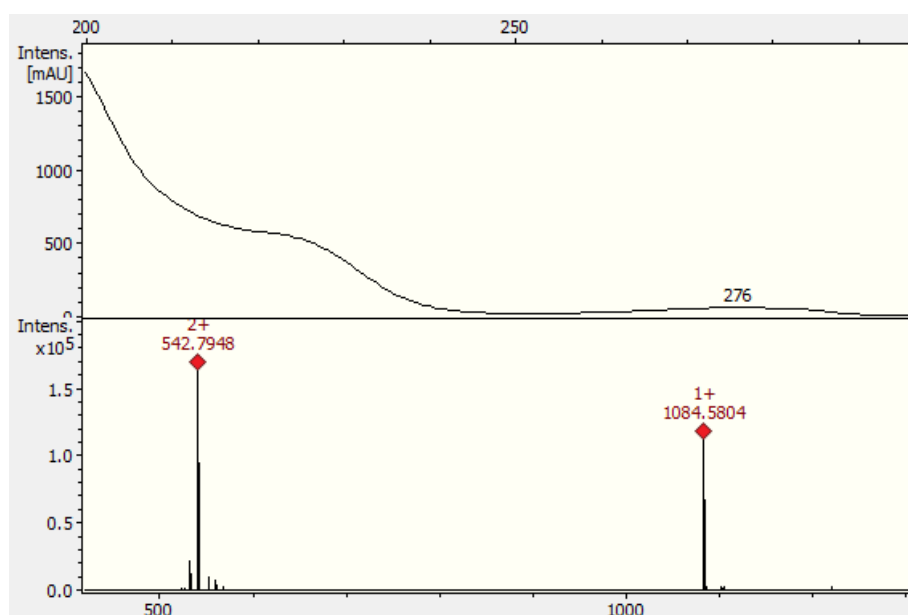


Figure BS39. ESI HRMS of paenilarvin C (3)

Chapter C

Aggregicoccus edonensis gen. nov., sp. nov.,
an unusually aggregating myxobacterium
isolated from a soil sample

Sakshi Sood*, Ram Prasad Awal*, Joachim Wink, Kathrin I. Mohr, Manfred Rohde,
Marc Stadler, Peter Kämpfer, Stefanie P. Glaeser, Peter Schumann, Ronald Garcia
and Rolf Müller

Submitted to International Journal of Systematic and Evolutionary Microbiology on
December 13th, 2013

Last revised on February 5th, 2014

(Current status – Published online on March 3rd, 2014)

Author's contribution to this work

*Contributed equally

Morphological, physiological and sequencing experiments and analysis: SS, RA

SEM Images: MR

DNA-DNA hybridization experiments and analysis: PK, SG

MALDI-TOF experiments and analysis: HB

Fatty acid profile experiments: RG

Wrote the paper: SS, RPA

Provided research facilities: JW, MS, RM

Conceived and designed the experiments: JW, KM

C.1. Abstract

A novel myxobacterium MCy1366^T (Ar1733) was isolated in 1981 from a soil sample collected from a region near Tokyo, Japan. It displayed general myxobacterial features like Gram negative staining, rod shaped vegetative cells, gliding on solid surfaces, microbial lytic activity, fruiting body-like aggregates and myxospore-like structures. The strain was mesophilic, aerobic and showed chemoheterotrophic mode of nutrition. It was resistant to many antibiotics like cephalosporin C, kanamycin, gentamycin, hygromycin B, polymyxin and bacitracin and the key fatty acids of whole cell hydrolysates were *iso*-C_{15:0}, *iso*-C_{17:0}, and *iso*-C_{17:0} 2-OH. The genomic G+C content of the novel strain is 65.6 mol%. The 16S rRNA gene sequence showed highest similarity (97.60%) to “*Stigmatella koreensis*” strain KYC-1019 (not validly described taxon, GenBank accession no. EF112185). The phylogenetic analysis based on 16S rRNA gene sequences and MALDI-TOF data revealed a novel branch in the family *Myxococcaceae*. DNA-DNA hybridization showed only 28% similarity between the novel strain and the closest species, *Coralloccoccus exiguus* DSM 14696^T (97% 16S rRNA gene sequence similarity). A recent isolate from a Switzerland soil sample and designated reference strain, MCy10622 displayed 99.9% 16S rRNA gene similarity and showed almost the same characteristics with MCy1366^T. Since some morphological features like fruiting body like aggregates were barely reproducible in the type strain, the newly isolated strain MCy10622 was also intensively studied. On the basis of a comprehensive taxonomic study, we propose a novel genus and species, *Aggregicoccus edonensis* gen. nov., sp. nov., for strain MCy1366^T and MCy10622. The type strain for the genus *Aggregicoccus* is MCy1366^T (=DSM 27872^T =NCCB 100468^T).

C.2. Introduction

Myxobacteria are known for their unique life cycle and the ability to produce natural products with unique structures and bioactivities (Weissman and Müller, 2010). They form a phylogenetically coherent group within the class δ -*proteobacteria* based on 16S rRNA gene sequence analysis (Garcia *et al.*, 2010). Three suborders, 7 families, 23 genera and 55 species with valid names have been published within the order

Myxococcales until today (Approved List of Bacterial Names). Myxobacterial systematics is mainly based on morphological characteristics like shape and size of vegetative cells and myxospores, swarming colonies and fruiting bodies. However, their morphological characteristics are often unstable and may vary or be lost on repeated subculturing under laboratory conditions (Garcia *et al.*, 2010). 16S rRNA gene sequences are also quite conservative for fine discrimination between closely related taxa (Fox *et al.*, 1992). Hence, a polyphasic approach should be followed in order to clearly delineate a potential new taxon from its closest relatives. Recently, fatty acid analysis with respect to different taxonomic clades within myxobacteria helped to establish chemotaxonomic-phylogenetic correlations (Garcia *et al.*, 2011). In the future, other molecular markers and approaches also need to be identified and applied to establish a modern myxobacterial systematics.

Using divergent approaches based on genotypic, phenotypic and chemotaxonomic analysis performed together with the reference strain MCy10622 and selected type strains belonging to the genera *Myxococcus*, *Corallocooccus*, *Pyxidicoccus*, and *Melittangium*, we propose a new genus for a soil bacterium from Japan, MCy1366^T.

C.3. Results and Discussion

Two strains described here were isolated from different geographical locations in different time and place. MCy1366^T was isolated at the Helmholtz Centre for Infection Research (HZI; formerly GBF, Gesellschaft für Biotechnologische Forschung, Braunschweig, Germany) in 1981 from a soil sample, collected in 1980 near Tokyo, Japan. The reference strain MCy10622 was isolated in July 2013 at the Helmholtz Institute for Pharmaceutical Research Saarland (HIPS, Saarbrücken, Germany) from a soil sample collected from Zürich, Switzerland. Standard isolation and purification protocols were used for both strains (Reichenbach and Dworkin, 1992). The type and neotype strains used in this study are listed in Table S1 in the supplementary information. All strains were continuously maintained on CY/H medium supplemented with 1 ml l⁻¹, 500 fold diluted vitamin solution after autoclaving (Mohr *et al.*, 2011; Schlegel, 1992) and VY/2 agar. All cultures were incubated at 30°C, liquid cultures at 160 – 200 rpm unless specified otherwise.

Morphology of vegetative cells and myxospores was studied with phase-contrast microscopy (Olympus BX51). Fruiting body like aggregates (for MCy1366^T), fruiting bodies (for MCy10622) and swarming colonies were observed under an Olympus SZX12 stereomicroscope and Zeiss Discovery.V20 stereomicroscope on P (Garcia *et al.*, 2009), VY/2 and CY agar (Shimkets *et al.*, 2006). All photographs were taken using the image analysis software “AxioVision LE” and AxioCam MRc camera (Carl Zeiss). Fruiting body aggregate morphology of MCy1366^T was also studied by field emission scanning electron microscopy using a Zeiss Merlin, aldehyde fixed, critical-point dried and gold palladium sputtered samples. Images were taken with the Everhart-Thornley SE-detector and Inlens-SE detector in a 25:75% ratio applying the SEMSmart software version 5.05. Formation of myxospore-like structures by strain MCy1366^T was observed in myxo media broth (10 g casein peptone, 1 mg CoCl₂, 0.05 g CaCl₂·2H₂O, 0.25 g MgSO₄·7H₂O, 23.6 g HEPES, 1 litre distilled water, pH 7.0) after incubation for at least 3 days.

The swarm colony of both isolates on VY/2 agar was transparent, soft, thin, and surrounded by a clear halo, owing to the lysis of yeast cells as often described for most members of *Myxococcaceae* (Reichenbach, 2005) but the salmon orange color of the MCy1366^T cells was evident upon scraping the swarm with the loop. Swarm colony on P agar was yellow to orange colored with large flame-like outward extensions at the periphery (Fig.C1d) and surrounded by a clear halo suggesting starch hydrolysis. Swarm on CY agar was with shades of orange to brown color (Fig.C1b), ripples and flat ridges like structures in the center and intricate wavy veins at the edges (Fig.C1c). Such an undulating vein structure is typical for *Myxococcaceae* swarms on peptone containing agar (Reichenbach, 2005). Radiating veins in the swarm or corrosion of agar, typical for *Cystobacteraceae* and *Nannocystaceae*, respectively, were not observed on any medium.

Vegetative cells were slender rods with slight tapering ends, mostly measuring 0.72-0.82 µm x 5.71-10.73 µm except few which were as long as 20 µm upon cultivation in myxo media for 2 days (Fig.CS1b). Numerous optically refractile, irregular spherical to ellipsoidal myxospore-like structures (1.3-1.7 µm in size) surrounded by a conspicuous dark capsule were observed in the same media after longer (10-20

days) incubation period (Fig.C1h). Cultivation in CY/H and myxo media broth displayed salmon orange and beige color of the vegetative cells of MCy1366^T and MCy10622, respectively, which often gathered into a huge aggregate of cells. Such a massive aggregation of cells often into a single clump with a branching morphology pattern is a peculiar characteristic of both isolates in liquid media (Fig.C1a).

Fruiting bodies like aggregates of MCy1366^T could only be observed on P and CY agar after prolonged incubation (8-10 weeks) (Fig.C1e). They mostly appeared solitary as yellowish orange spherical heads and lacked sporangioles and stalk. Immature fruiting bodies had the appearance of humps or knobs on the agar, as in *Myxococcus* spp. (Reichenbach, 2005). Cell aggregation on the agar, presumably in an attempt to form the fruiting bodies was clearly visible under stereomicroscope as well as by scanning electron microscopic imaging (Fig.C1g). No fruiting bodies were observed on buffered VY/2 agar, while the new isolate MCy10622 could form reproducible fruiting bodies on the same agar within one week of incubation (Fig.C1f). However, the fruiting bodies of MCy10622 were irregularly shaped, cushion like cell mounds formed in groups clearly distinguishing themselves from MCy1366^T fruiting bodies (Fig.C1f). Myxospores similar to spherical structures observed in liquid myxo media were also observed upon teasing of fruiting bodies and fruiting body like aggregates on a glass slide.

Reaction of 3 week old swarm colonies of MCy1366^T and MCy10622 on VY/2 agar to Congo Red stain was determined using the method of McCurdy (McCurdy, 1969). Enzyme activity was determined using APIZym strips (BioMérieux) inoculated with the cells grown in CY/H broth and further diluted with sterile water (1:10) and incubated aerobically at 30°C overnight. Starch hydrolysis, cellulose and agar degradation was studied as described by Mohr *et al.* (2011). The chitin degradation assay was performed using CT-6 (Reichenbach, 2006) and synthetic S agar (0.5 g CaCl₂.2H₂O, 0.5 g MgSO₄.7H₂O, 0.06 g K₂HPO₄, 8 mg Ferric EDTA, 50 mM HEPES, 1 liter distilled water, pH 7.2) with 0.7% (w/v) chitin as the sole nutrient source. Salt tolerance to 1.5% (w/v) sodium chloride was tested on CY agar after incubation for 3-4 weeks at 30°C.

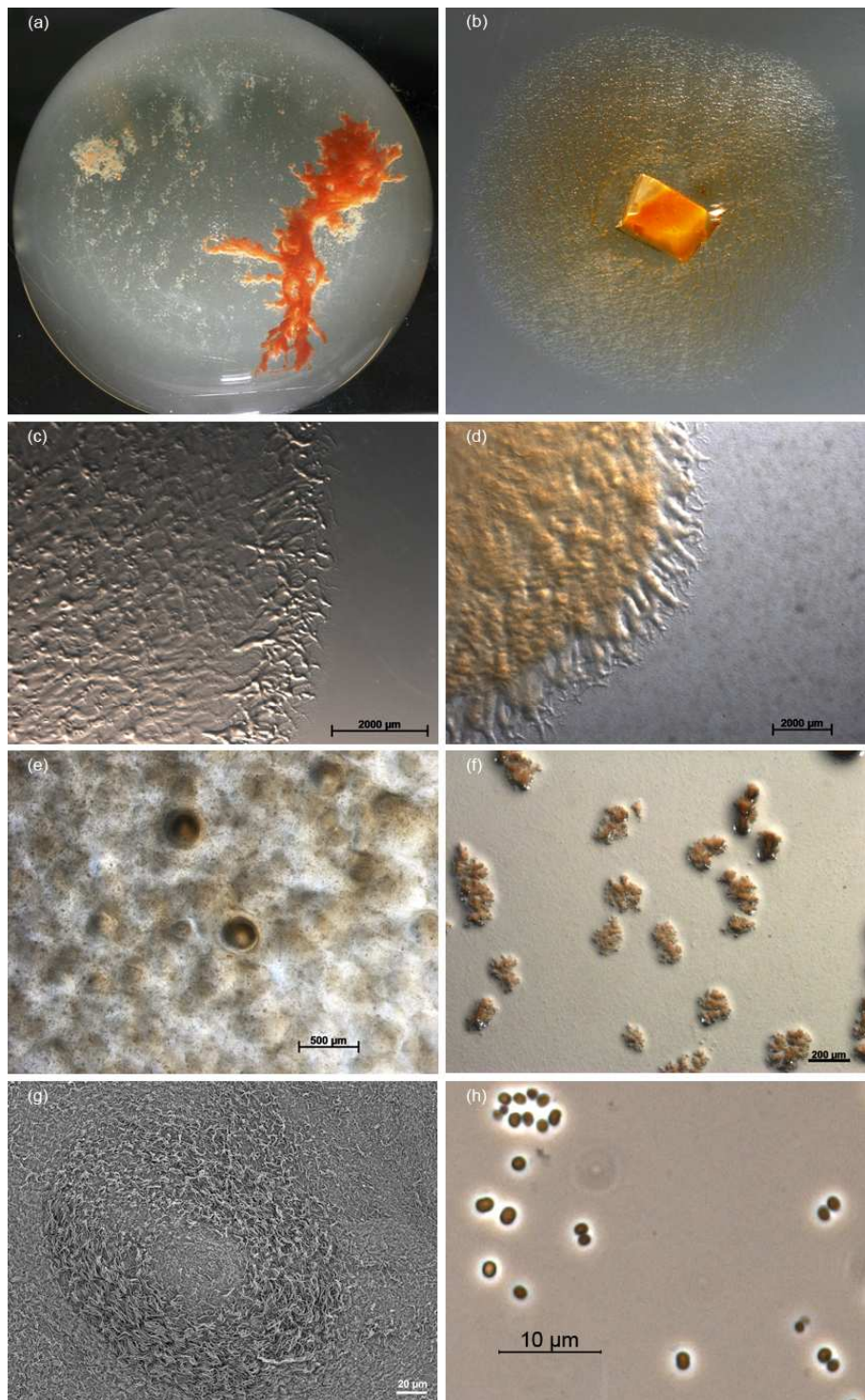


Fig.C1. Photographs showing morphology of strain MCy1366^T and MCy10622. (a) Photograph of huge bright orange cell aggregate of MCy1366^T in 11 day old culture in CY+H broth. (b) Saffron orange coloured 4-week-old swarming colony of MCy1366^T on CY agar. Stereophotomicrograph of (c) 4-week-old swarm of MCy1366^T on CY agar (bar, 2000 µm), (d) 3 week old swarm of MCy1366^T on P agar (bar, 2000 µm), (e) fruiting body-like aggregates of MCy1366^T on P agar (bar, 500 µm), (f) mature fruiting bodies of MCy10622 on VY/2 agar (bar, 200 µm). (g) SEM image showing cell aggregation of MCy1366^T on agar surface for initiation of fruiting body formation (bar, 20 µm) (h) Phase contrast image of myxospore-like structures in liquid myxo media (bar, 20 µm)

The Congo Red reaction was very weak and displayed light pink color (Fig.CS1a) in contrast to strong reactions observed for *Corallocooccus* spp., *Pyxidicooccus* sp., and some *Myxococcus* spp. Both the isolates could not degrade cellulose, chitin or agar. No cell growth was observed for MCy1366^T and MCy10622 under 1.5% NaCl concentration same as observed for *Corallocooccus* spp. and *Melittangium lichenicola* while fair to good growth was observed for *Pyxidicooccus fallax* and all *Myxococcus* spp. except *M. fulvus* (Table CS2). The colorless haloes on P agar plate after staining with Lugol's solution was limited to the size of MCy1366^T and MCy10622 swarms as opposed to *Corallocooccus* spp. depicting weak starch hydrolysis ability (Fig.CS1c). Ability to degrade starch and salt tolerance are often used as characteristics to differentiate between species of *Myxococcus* and *Corallocooccus* (Lang and Stackebrandt, 2009).

The reactions on the APIZym strips by MCy1366^T were reasonably similar to the reactions observed for *Corallocooccus* spp. suggesting close relationship between both (Table CS3). Alkaline phosphatase, esterase lipase, leucine arylamidase and acid phosphatase were positive and β -galactosidase, α -mannosidase and α -fucosidase were negative for MCy1366^T along with all the other strains used during this study (Table CS1). Trypsin was negative for MCy1366^T along with *Corallocooccus* spp. and *M. lichenicola* while it was positive for three *Myxococcus* spp. and *P. fallax*. All the reactions for MCy1366^T on APIZym strips were same to the reactions from MCy10622 except cysteine arylamidase which was found to be negative for the former and positive for the latter. All these similar reactions observed for all the members of the family *Myxococcaceae* strengthened the supposition that both new isolates belong to the same family. Detailed results from the APIZym test system for all strains are given in supplementary information (Table CS3).

Cross streaked microbial baits of live bacteria (*Paenibacillus polymyxa* DSM 36^T), yeasts (*Candida albicans* DSM 1665, *Wickerhamomyces anomalus* DSM 6766) and autoclaved *E. coli* K12 cells on water agar was used for testing the ability of MCy1366^T and MCy10622 to lyse microorganisms as described by Mohr *et al.* (2011). *E. coli* and *C. albicans* cells were completely lysed by both the strains. *W. anomalus* and *P. polymyxa* supported the growth of MCy1366^T on water agar but

clearing of cells could not be observed, making it difficult to assess the ability of MCy1366^T to lyse the cells of these organisms.

Growth response of MCy1366^T and MCy10622 to different temperatures was tested at 20°C, 30°C, 37°C and 42°C on VY/2 agar. The pH optima for both strains were tested between pH 5.0 to 10.0 at intervals of 0.5 pH units in CY liquid media. Optimum growth temperatures for MCy1366^T and MCy10622 were near 30°C like most myxobacteria. Both isolates could not grow at 42°C. They tolerated wide range of pH 6.0-10.0 but the maximum growth was seen at pH 6.5-7.0 (Table CS8). No evidence of growth was found below pH 5.5.

Antibiotic resistance of strains MCy1366^T and MCy10622 was tested along with the other related strains as described by Mohr *et al.* (2011) against 13 antibiotics. The final concentration was adjusted to 50 (µg ml⁻¹) for most antibiotics except oxytetracycline (10), chloramphenicol (30), ampicillin (100) and hygromycin B (150). MCy1366^T was sensitive to spectinomycin, thiostrepton and chloramphenicol and resistant to cephalosporin C, kanamycin, gentamycin, hygromycin B, polymyxin and bacitracin similar to the *Corallococcus* spp. used in this study. However, it was sensitive to fusidic acid and ampicillin as opposed to the *Corallococcus* spp. which showed little growth on fusidic acid but good growth on ampicillin. MCy10622 was found to be sensitive to spectinomycin and thiostrepton whereas resistant to most of the other antibiotics tested. MCy1366^T and MCy10622, both grew poorly on trimethoprim. A detailed description of the antibiotic resistance test is given in the supplementary information (Table CS4).

Synthetic liquid medium S containing 0.25% (w/v) casitone and supplemented with 0.25% (w/v) of various sugars and starch was used for testing the carbon sources favored for growth. Nitrogen requirement was tested on a minimal casitone medium (C) (Mohr *et al.*, 2011) with addition of 0.25% (w/v) of some organic and inorganic nitrogen sources. Utilization of various peptones was also tested by addition to synthetic S medium individually at a concentration of 0.25% (w/v). These experiments were performed in duplicates and all flasks were incubated at 30°C, 200 rpm for 7 days. Cell pellets were collected and washed with sterile water in order to remove salt contents, dried and the dry weight was noted.

Table C1. Differential characteristics of strain MCy1366^T, MCy10622 and their closely related strains

Features	<i>Myxococcus</i> spp.	<i>Corallococcus</i> spp.	MCy1366 ^T	MCy10622	<i>Pyxidicoccus fallax</i>	<i>Melittangium lichenicola</i>
No. of strains used for study	5	2			1	1
Resistance to:						
Ampicillin (100ug/ml)	V(3)	+	-	+	+	-
Kanamycin (50ug/ml)	V(2)	+	+	+	-	+
Spectinomycin (50ug/ml)	+	-	-	-	+	+
Trimethoprim (50ug/ml)	V(2)	+	+	+	+	+
Fusidic acid (50ug/ml)	V(3)	+	-	+	+	-
Growth at 1.5% salt	V(4)	-	-	-	+	-
Starch hydrolysis	Weak positive	Strong positive	Weak positive	Weak positive	Positive	n.i.
Congo red reaction	Weak/Strong	Strong	Very weak	Very weak	Strong	Weak
ApiZym Test						
Trypsin	V(3)	-	-	-	+	-
Fatty acid analysis						
C _{15:0}	0.0-2.7	0.2-0.8	1.8	1.6	1.1	0
C _{15:1} isomer 2	0.0-2.5	0.1-0.4	3.3	0	0.9	0
C _{16:1} isomer 2	6.1-14.5	0.2-0.6	1.1	0	21.0	5.5
C _{17:1} ω7cis	0.0-1.0	1.5-2.2	0.40	0	0.2	0
iso C _{15:0}	13.5-39.7	17.5-22.3	23.2	25.3	14.0	13.0
iso C _{17:0}	1.3-11.7	4.3-10.1	16.6	10.4	7.7	0.8
iso C _{17:0} 2-OH	0.2-12.4	32.9-34.4	26.1	14.1	9.3	0.5
iso C _{15:0} OAG	0.0-10.3	3.4-7.2	1.9	1.3	2.9	0
iso C _{15:0} DMA	0.0-2.1	1.6-4.2	2.0	4.4	4.7	0

* Results for individual strains are given in Supplementary Tables S2, S3, S4 and S7. V, Variable results (numbers of positive strains given in parentheses); n.i., not determined; for reactions to antibiotics, + (positive) indicates resistance, growth; and - (negative) indicates sensitivity, inhibition of growth; fatty acids analysis, isomer 2, position isomer of a monounsaturated fatty acid; ω7cis, Omega-7 fatty acid with cis double bond; 2-OH, Hydroxy fatty acid; OAG, *O*-alkylglycerol fatty acids; DMA, Dimethylacetal fatty acids. Strain used for the study: *Myxococcus* spp. (*M. xanthus* DSM 16526^T, *M. fulvus* DSM 16525^T, *M. stipitatus* DSM 14675^T, *M. virescens* DSM 2260^T, *M. macrosporus* DSM 14697^T); *Corallococcus* spp. (*C. exiguus* DSM 14696^T, *C. coralloides* DSM 2259^T); *Pyxidicoccus fallax* DSM 14698^T and *Melittangium lichenicola* DSM 2275^T.

MCy1366^T as well as MCy10622 could not utilize any of the monosaccharides or disaccharides under the tested conditions (Table CS5). This is also true for most of the members of the family *Myxococcaceae* (Reichenbach, 2005). However, growth was observed on molasses (Juchem) which could be due to presence of other supplements. They could utilize polysaccharides viz. potato starch, soluble starch and pyruvate. But the two strains differ slightly in their peptone requirements. Strain MCy1366^T yielded high cell densities in neopeptone (Becton Dickinson), phytone peptone (BD) and skimmed milk (Oxoid) whereas MCy10622 grew better in tryptone enzymatic digest from casein (BD). No growth was observed in synthetic media S supplemented with casamino acids (BD). All the organic and inorganic nitrogen sources tested resulted in moderate to fair growth of both the strains (Table CS6).

For fatty acid analysis, all the strains used in the study (Table CS7) were cultivated in 50 ml of CY medium in 300 ml flasks shaken at 160 rpm at 30°C. Cellular fatty acid extraction, GC-MS analysis and peak identification was done in duplicates using the method described by Garcia *et al.* (2011). All the strains had substantially high amounts of *iso*-C_{15:0}, which is true for most myxobacteria (Garcia *et al.*, 2009). The fatty acid pattern of strains MCy1366^T and MCy10622 was significantly distinct from all the other strains used in the study. Strain MCy10622 differed from MCy1366^T because of the presence of significant amounts of *iso*-C_{17:1} (10.9 %) while it was completely absent in the fatty acid profile of the latter. Strain MCy1366^T showed highest percentage of the branched chain fatty acid, *iso*-C_{17:0}2-OH (26.1%) followed by *iso*-C_{15:0} (23.2%) (Table C1). Indeed, high amounts of *iso*-C_{17:0}2-OH has been recommended as a determinative chemotaxonomic marker for *Corallococcus* spp. in the family *Myxococcaceae* (Garcia *et al.*, 2011). Strain MCy1366^T possessed a significant amount of *iso*-C_{17:0} (16.6 %) and higher amounts of C_{15:1 isomer2} (3.3%) compared to all the other strains. MCy1366^T also differed from *Corallococcus* spp. because of the lower amounts (1.9%) of O-alkylglycerol (OAG) FAs. In addition, MCy1366^T and MCy10622 clearly distinguished from *M. lichenicola* DSM 2275^T because of the presence of much higher amounts of C_{16:0} (9.8%), C_{18:0} (20.6%) and unspecified fatty acid alcohol (32.1%) as well as much lower amounts of *iso*-C_{15:0} (13.0%) and *iso*-C_{17:0}2-OH (0.5%) in the latter compared to the former two strains. The total amount of SCFAs and BCFAs for strain MCy1366^T was 15.4% and 84.4%,

respectively, while MCy10622 showed 10.0% and 76.3% of total SCFAs and BCFAs, respectively (Table CS7).

For 16S rRNA gene amplification, genomic DNA was extracted from actively growing cells of MCy1366^T and MCy10622 using the protocol for gram-negative bacteria of the Puregene CoreKit A (Qiagen). 16S rRNA gene was amplified by PCR using universal primers (forward 5'-GAGTTTGATCCTGGCTCAGGA-3'; reverse 5'-AAGGAGGTGATCCAGCCGCA-3'). The PCR product was purified using Nucleospin Gel and PCR clean-up (Macherey Nagel) following analysis of PCR product by gel electrophoresis using 0.8% (w/v) agarose gel at 95 V for 35 min. The same set of primers along with forward primers F27, F945, F357, F1100 and reverse primers R336, R518, R1078 and R1525 was applied for sequencing of the 16S rRNA gene (Lane, 1991; Turner *et al.*, 1999; Stackebrandt and Liesack, 1993; Weidner *et al.*, 1996). The consensus sequences were produced using the Cap contig assembly function of the BioEdit Sequence Alignment Editor Version 7.1.3.0. and compared to the NCBI-BLAST nucleotide data bank using FASTA search tool and showed highest similarity (MCy1366^T, 97.60%, and MCy10622, 97.47%) to invalidly described taxon, "*Stigmatella koreensis*" strain KYC-1019 (GenBank accession no. EF_112185).

The complete sequences of MCy1366^T and MCy10622 were aligned with sequences of their close relatives using ClustalW (Larkin *et al.*, 2007). A phylogenetic analysis with type and representative myxobacterial strains was calculated using two tree-making algorithms; neighbor joining (Saitou and Nei, 1987) and maximum likelihood (Guindon and Gascuel, 2003) methods by using the software package Geneious 7.0.3 version (Biomatters, New Zealand). A sulfate-reducing bacterium, *Desulfovibrio desulfuricans* DSM 642^T (GenBank accession no. NR_036778) was chosen as an out-group to root the phylogenetic tree. Jukes Cantor model (Jukes and Cantor, 1969) was applied to calculate evolutionary distance matrices of the neighbor joining and maximum likelihood method. The topology of the phylogenetic tree was evaluated by bootstrap support based on 1000 resamplings (Felsenstein, 1985).

The tree constructed by maximum likelihood (Fig. C2) method showed that both strains (MCy1366^T and MCy10622), formed a separate cluster within the family *Myxococcaceae* close to *C. exiguus* DSM 14696^T, *C. coralloides* DSM 2259^T and

Melittangium lichenicola DSM 2275^T. Their separate branching from the known myxobacterial taxa in the suborder *Cystobacterineae* was also clear in the phylogenetic tree constructed with the neighbor joining method (Fig.CS2). The delineation of the two isolates from closely related strains and clustering within *Myxococcaceae*, clearly indicate that they represent a new taxon in the same family.

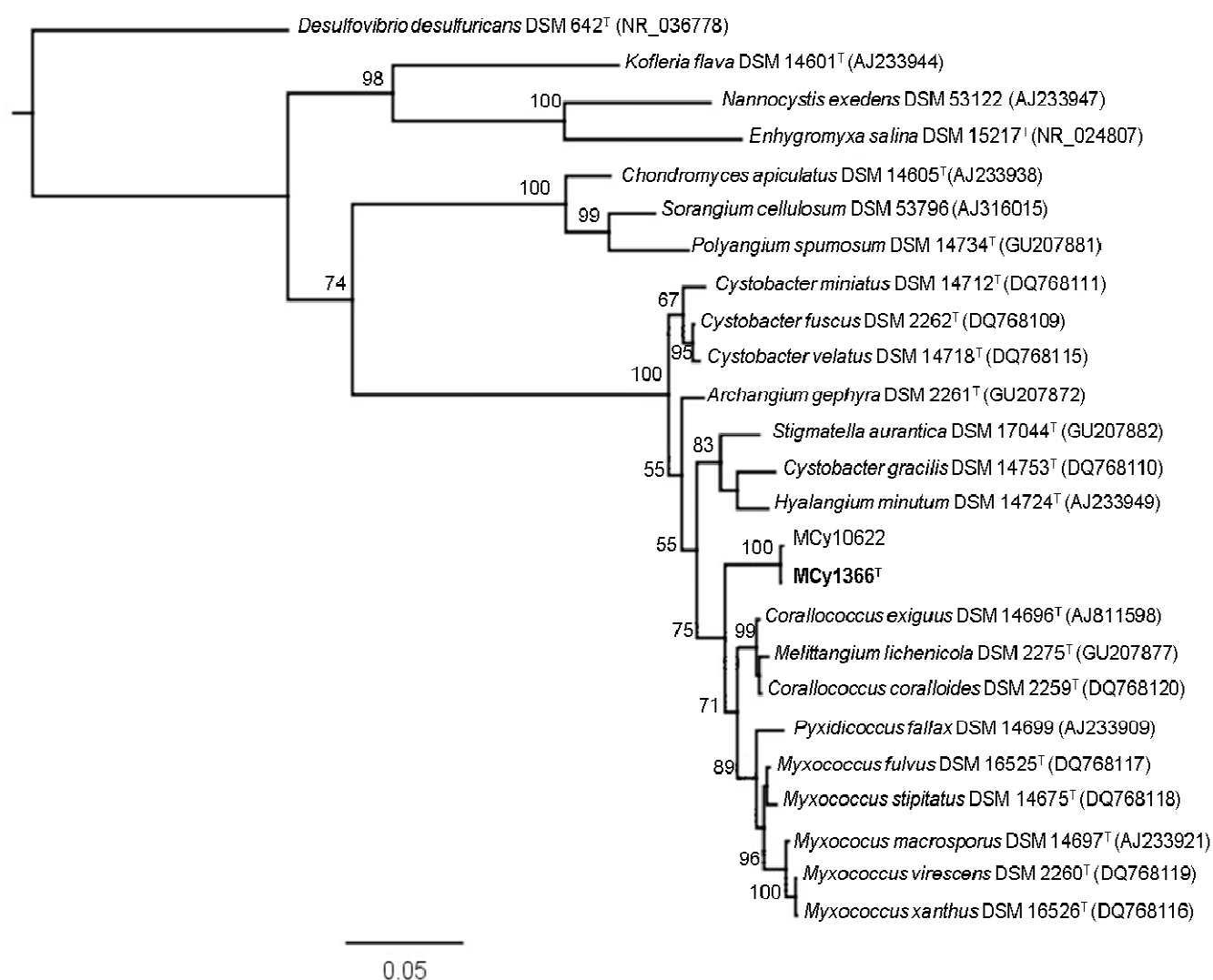


Fig.C2. Maximum likelihood phylogenetic tree (PHYML) based on 16S rRNA gene sequences of strains *MCy1366^T* and *MCy10622* and related taxa. Numbers at the branch points indicate bootstrap support based on 1000 resamplings. Bar, 0.05 substitutions per nucleotide position. The GenBank accession number of strains used in the tree is shown in parentheses. *Desulfovibrio desulfuricans* DSM 642^T was used as an outgroup.

The two closest relatives of *MCy1366^T* and *MCy10622* according to the 16S rRNA gene sequence-based phylogenetic tree, *C. exiguus* DSM 14696^T and *C. coralloides* DSM 2259^T were chosen for DNA-DNA hybridization assay and DNA G+C mol% content analysis. A method adapted from Kieser *et al.* (2000) but modified and

optimized especially for myxobacteria was used for isolation of high yields of genomic DNA. 100 ml cultures in myxo media, CY+H media and A media (8 g starch, 4 g soymeal, 2 g yeast, 1 g CaCl₂, 1 g MgSO₄, 100 mM HEPES, 8 mg Ferric EDTA, 4 ml glycerol, 1 liter distilled water, pH 7.4), respectively, were harvested by centrifugation at 12000 rpm for 5 min. The cell pellets were re-suspended in 10 ml Tris buffer after discarding the supernatant. The cell aggregates were dispersed and homogenized with an Ultraturrax (Art Moderne Labortechnik). After addition of 200 µl proteinase K (20 mg ml⁻¹ in 50 mM Tris-HCl, 1 mM CaCl₂·2H₂O, pH 7.5) and 200 µl SDS (20% (w/v) solution), the solution was mixed gently and kept in hybridization oven for continuous shaking and incubation at 41°C for 30 min–2 hrs until the solution became slightly clear. 3.5 ml of 5 M NaCl was added to the solution with gentle mixing followed by 4 ml CTAB extraction buffer (4.1% (w/v) NaCl, 10% (w/v) Cetyl trimethylammonium bromide, water). The cell solutions were again shaken and incubated at 65°C for another 20 min inside the hybridization oven. The cell solution was incubated at room temperature from 1 hr to 12 hrs in an overhead shaker after addition of chloroform up to 35 ml. Phase separation of the solution was then achieved by centrifugation at 12000 rpm for 20 min and the upper phase was carefully transferred into new falcon tubes. The acquired upper phase was mixed with equal volume of isopropanol and mixed gently. The precipitated DNA was aspirated and rinsed with 70% (v/v) ethanol twice. DNA was then air dried and dissolved in 2 ml TE buffer.

DNA-DNA hybridizations (DDH) was performed as described by Ziemke *et al.* (1998), with the modification that for nick translation, 2 µg of DNA was labeled during a 3 hr incubation at 15°C. The G+C mol% was determined using a fluorimetric thermal denaturation temperature determining method described by Gonzalez & Saiz-Jimenez (2002). Analysis was performed in a total volume of 20 µl, including 5 µg genomic DNA, 0.1X SSC buffer (0.03 M NaCl, 0.03 M sodium citrate), 10% (v/v) deionized formamide and 0.25X SYBR Green I (Molecular probes). Thermal denaturation was performed in a CFX384 Touch™ Real-Time PCR Detection System (BioRad) starting with 15 min at 25°C, followed by a ramp from 65 to 98°C with an increase of 0.1°C cycle⁻¹. Each cycle holds for 5 s including a fluorescence measurement (SYBR channel). Analysis was performed at least in duplicates. Five

reference strains were used to generate a standard curve of G+C mol% versus melting temperature (T_m). A linear regression analysis was used to calculate the G+C mol%.

The DNA G+C content of strain MCy1366^T was found to be same as *Corallococcus coralloides* DSM 2259^T i.e. 65.6 mol% in our analysis. The type strains of *C. exiguus* DSM 14696^T and *C. coralloides* DSM 2259^T are very closely related species with 99.9% 16S rRNA gene sequence similarity and sharing 61.5% DNA-DNA similarity (Stackebrandt *et al.*, 2007). However, these high values did not hold true for the pairs MCy1366^T and DSM 14696^T (28%; with 97% 16S rRNA gene sequence similarity) and MCy1366^T and DSM 2259^T (35.15%; with 96.9% 16S rRNA gene sequence similarity) clearly revealing that strain MCy1366^T does not belong to *C. exiguus* or *C. coralloides* (Wayne *et al.*, 1987). MCy1366^T and MCy10622 showed 99.9% 16S rRNA gene sequence similarity and 100% DNA-DNA similarity.

Biomass for matrix-assisted laser desorption/ionization time-of-flight mass spectrometry (MALDI-TOF MS) analysis was collected from one week old, 100 ml cultures of MCy1366^T, MCy10622 and the reference strains in CY+H broth, centrifuged at 12000 rpm for 10 min. Whole-cell protein extracts were analyzed by using a Microflex L20 mass spectrometer (Bruker Daltonics) equipped with a N₂ laser. Sample preparation for MALDI-TOF MS protein analysis was carried out according to the ethanol/formic acid extraction protocol recommended by Bruker Daltonics as described in detail by Tóth *et al.* (2008). The MALDI-TOF mass spectra were analyzed with the BioTyper software (version 3.1, Bruker Daltonics). The dendrogram generated on the basis of MALDI-TOF mass spectra (Fig. C3) confirms the close relationship of the strains MCy1366^T and MCy10622 as revealed by DNA-DNA hybridization and demonstrates that both strains can be differentiated by MALDI-TOF MS from related type strains of the genera *Corallococcus*, *Myxococcus*, *Pyxidicoccus* and *Melittangium*.

In addition to the 3% phylogenetic distance based on 16S rRNA gene sequences and low DNA-DNA relatedness to the closest known myxobacterial neighbors (*C. exiguus* and *C. coralloides*); strain MCy1366^T also delineates into a novel branch in the MALDI-TOF MS dendrogram, show distinct cellular fatty acid profile and biochemical

characteristics compared to other members of *Myxococcaceae*. Therefore, we propose strain MCy1366^T as a representative of a new genus *Aggregicoccus* gen. nov., and a new species *Aggregicoccus edonensis* sp. nov. based on these distinguishing characteristics.

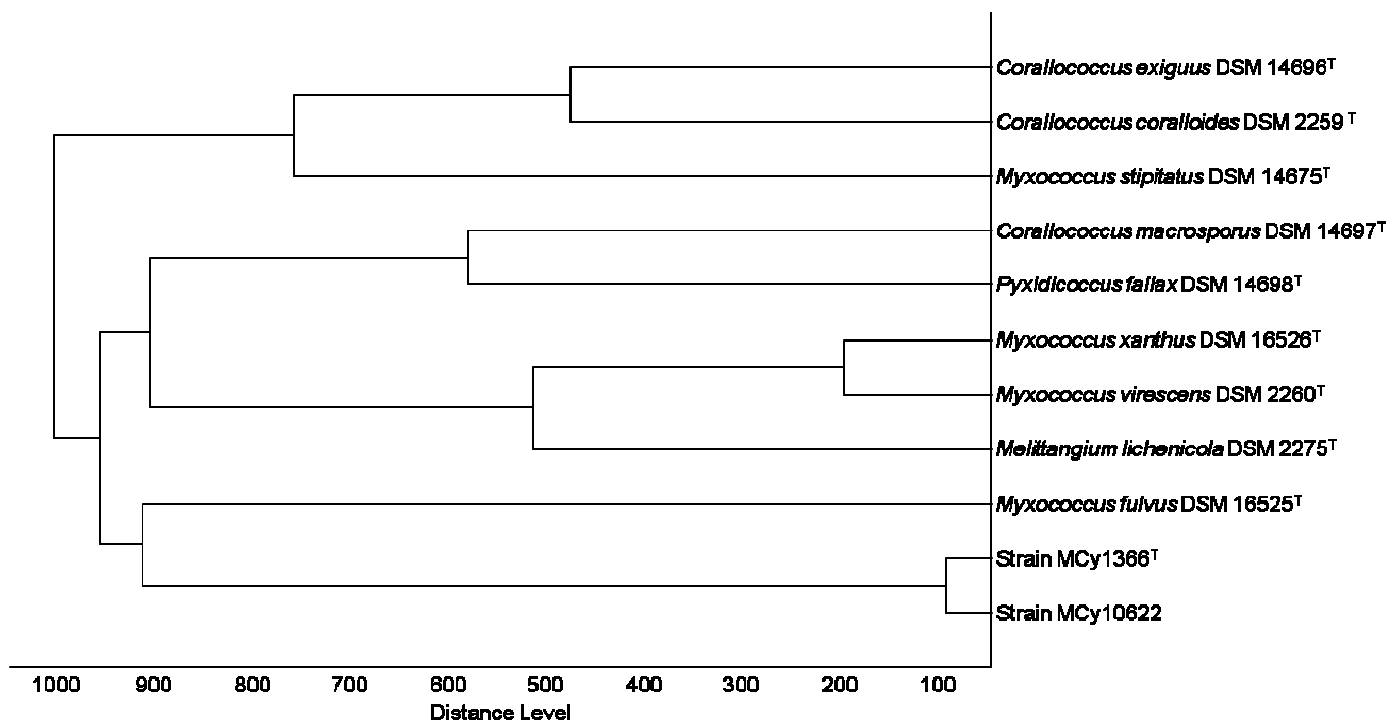


Fig.C3. Score-oriented dendrogram generated by the BioTyper software (version 3.1, Bruker Daltonics) showing the similarity of MALDI-TOF mass spectra of cell extracts of strains MCy1366^T, MCy10622 and type strains of related species within the genera *Corallocooccus*, *Myxococcus*, *Pyxidicoccus* and *Melittangium*.

C.4. Description of *Aggregicoccus* gen. nov.

Aggregicoccus gen. nov. (Ag.gre.gi.cocc'us. Lat. v. aggrego, to aggregate, form clumps; N.L. masc. n. coccus (from Gr. masc. n. kokkos, grain, seed, coccus); N.L. masc. n. *Aggregicoccus*, an aggregating coccus referring to massively aggregating cells in liquid culture)

The vegetative cells are rod-shaped with slight tapering ends (*Myxococcaceae* type). Transparent swarms on VY/2 yeast agar. Produce wavy, rippling structures with intricate veins on edges on CY agar. Colonies are very weak positive in Congo Red stain. Fruiting bodies like aggregates and fruiting bodies are spherical to irregularly shaped, cushion like, yellow orange colored, lacking sporangioles and stalks. Myxospores are optically refractive, irregularly spherical. Myxospore-like structures

are also produced in peptone containing liquid media upon longer incubation. Does not utilize monosaccharides and disaccharides. Bacteria and yeast are lysed. Aerobic, chemoorganotrophic and strictly mesophilic. Hydrolyses starch, but not cellulose, chitin or agar. The G + C content is 65.6 mol%. The phylogenetic position is in the family *Myxococcaceae*, suborder *Cystobacterineae*, Order *Myxococcales*. The type species is *Aggregicoccus edonensis*.

C.5. Description of *Aggregicoccus edonensis* sp. nov.

Aggregicoccus edonensis (e.do.nen'sis. N.L. masc. adj. *edonensis*, belonging to Edo, former name of Tokyo, where the soil sample was collected from which the type strain was isolated).

In addition to the characteristics of the genus, the vegetative cells are 0.72-0.82 μm x 5.71-10.73 μm in size. The swarm colony varies from yellow orange to almost transparent color depending upon the medium. Myxospore-like structures, 1.3-1.7 μm in size and covered with outer capsule were obtained in liquid media. Cell aggregates are beige to saffron orange in color with extreme branching in peptone or casitone media. Growth optimal temperature is between 30°C and 37°C. pH tolerance is between 6.0–10.0, and optimum at 6.0-7.0. Cannot tolerate high salt concentrations. Best nutritional sources are media with peptones. Can utilize L-asparagine monohydrate, ammonium sulfate, potassium nitrate, urea, L- glutamic acid, glycine, L-lysine monohydrate and L-arginine as nitrogen sources in the presence of casitone. Major fatty acids are C_{17:0} 2-OH, *iso*-C_{15:0} and *iso*-C_{17:0}. Alkaline phosphatase, esterase lipase, leucine arylamidase and acid phosphatase production was positive while β -galactosidase, α -mannosidase and α -fucosidase showed negative reaction in APIZym test system. The type strain is MCy1366^T (=DSM 27872^T, =NCCB 100468^T), isolated from soil collected in 1981 from a region near Tokyo, Japan.

Acknowledgements

S.S. is highly indebted to Erasmus Mundus External Cooperation Window for a PhD scholarship and all their support. R.P.A. wishes to acknowledge Deutscher Akademischer Austauschdienst (DAAD) for the PhD fellowship. We thank D. Telkemeyer, S. Schulz and K. Gemperlein for their technical assistance.

References

- Felsenstein, J. (1985) Confidence limits on phylogenies: An approach using the bootstrap. *Evolution* 39, 783-791
- Fox, G. E., Wisotzkey, J. D. and Jurtshuk, P. (1992) How close is close: 16S rRNA sequence identity may not be sufficient to guarantee species identity, *Int. J. Syst. Bacteriol.* 42, 166–170
- Garcia, R., Gerth, K., Stadler, M., Dogma, I. J. Jr., and Müller, R. (2010) Expanded phylogeny of myxobacteria and evidence for cultivation of the 'unculturables'. *Mol. Phylogenet. Evol.* 57, 878-887
- Garcia, R., Pistorius, D., Stadler, M., and Müller, R. (2011) Fatty acid related phylogeny of myxobacteria as an approach to discover polyunsaturated omega-3/6 fatty acids. *J. Bacteriol.* 193, 1930-1942
- Garcia, R., Reichenbach, H., Ring, M. W. and Müller, R. (2009) *Phaselicystis flava* gen. nov., sp. nov., an arachidonic acid-containing soil myxobacterium, and the description of *Phaselicystidaceae* fam. nov. *Int. J. Syst. Evol. Microbiol.* 59, 1524-1530
- Gonzales, J. M. and Saiz-Jimenez, C. (2002) A fluorimetric method for the estimation of G+C mol% content in microorganism by thermal denaturation temperature. *Environ. Microbiol.* 4, 770-773
- Guindon, S. and Gascuel, O. (2003) A simple, fast, and accurate algorithm to estimate large phylogenies by maximum likelihood. *Systematic Biology* 52, 696-704
- Jukes, T. H. and Cantor, C. R. (1969) Evolution of protein molecules. In *Mammalian Protein Metabolism*, pp. 21–123. Edited by H. N. Munro. New York: Academic Press
- Kieser, T., Bibb, M. J., Buttner, M. J., Chater, K. F. and Hopwood, D. A. (2000) Preparation and analysis of genomic and plasmid DNA. *Practical Streptomyces Genetics*, pp. 161-210. John Innes Foundation Norwich
- Lane, D. J. (1991) 16S/23S rDNA sequencing. In *Nucleic Acid Techniques in Bacterial Systematics*, pp. 115–175. Edited by E. Stackebrandt & M. Goodfellow. Chichester: Wiley
- Lang, E. and Stackebrandt, E. (2009) Emended descriptions of the genera *Myxococcus* and *Corallococcus*, typification of the species *Myxococcus stipitatus* and *Myxococcus macrosporus* and a proposal that they be represented by neotype strains. Request for an Opinion. *Int. J. Syst. Evol. Microbiol.* 59, 2122-2128
- Larkin, M. A., Blackshields, G., Brown, N. P., Chenna, R., McGettigan, P. A., McWilliam, H., Valentin, F., Wallace, I. M., Wilm, A., and others (2007) Clustal W and clustal X version 2.0. *Bioinformatics* 23, 2947-2948
- McCurdy, H. D. (1969) Studies on taxonomy of the Myxobacterales. I. Record of Canadian isolates and survey of methods. *Can. J. Microbiol.* 15, 1453–1461
- Mohr, K. I., Garcia, R. O., Gerth, K., Irschik, H. and Müller, R. (2011) *Sandaracinus amylolyticus* gen. nov., sp. nov., a starch degrading soil myxobacterium, and description of *Sandaracinaceae* fam. nov. *Int. J. Syst. Bacteriol.* 62, 1191-1198
- Reichenbach, H. and Dworkin, M. (1992). The myxobacteria. In *The Prokaryotes*, 2nd edn, pp. 3416–3487. Edited by A. Balows, H. G. Trüper, M. Dworkin, W. Harder & K.-H. Schleifer. Berlin: Springer-Verlag

- Reichenbach, H. (2005) Order VIII. *Myxococcales* Tchan, Pochon and Pre´vot 1948, 398AL. In *Bergey's Manual of Systematic Bacteriology*, 2nd edn, vol. 2, part C, pp. 1059–1072. Edited by D. J. Brenner, N. R. Krieg, J. T. Staley, & G. M. Garrity. New York: Springer
- Reichenbach, H. (2006) The genus *Lysobacter*. In *The Prokaryotes: A Handbook on the Biology of Bacteria*, 3rd edn, vol. 6, pp. 939–957. Edited by M. Dworkin, S. Falkow, E. Rosenberg, K. H. Schleifer & E. Stackebrandt. New York: Springer
- Saitou, N., and Nei, M. (1987) The neighbor-joining method: a new method for reconstructing phylogenetic trees. *Mol. Biol. Evol.* 4, 406–425
- Schlegel, H. G. (1992) *Allgemeine Mikrobiologie*, 7th edn. Stuttgart: Georg Thieme Verlag
- Shimkets, L. J., Dworkin, M. and Reichenbach, H. (2006) The myxobacteria. In *The Prokaryotes: A Handbook on the Biology of Bacteria*, 3rd edn, vol. 7, pp. 31-115. Edited by M. Dworkin, S. Falkow, E. Rosenberg, K. H. Schleifer & E. Stackebrandt, New York: Springer
- Stackebrandt, E., and Liesack, W. (1993) Nucleic acids and classification. In *Handbook of New Bacterial Systematics*, pp. 152-189. Edited by M. Goodfellow & A.G. O'Donnell. London: Academic Press
- Stackebrandt, E., Pauker, O., Steiner, U., Schumann, P., Straubler, B., Heibei, S., and Lang, E. (2007) Taxonomic characterization of members of the genus *Coralloccoccus*: Molecular divergence versus phenotypic coherency. *Syst. App. Microbiol.* 30, 109–118
- Toth, E. M., Schumann, P., Borsodi, A. K., Keki, Z., Kovacs, A. L., and Marialigeti, K. (2008) *Wohlfahrtiimonas chitiniclastica* gen. nov., sp. nov., a new gammaproteobacterium isolated from *Wohlfahrtia magnifica* (Diptera: Sarcophagidae). *Int. J. Syst. Evol. Microbiol.* 58, 976-981.
- Turner, S., Pryer, K. M., Miao, V. P. W., and Palmer, J. D. (1999) Investigating deep phylogenetic relationships among cyanobacteria and plastids by small subunit rDNA sequence analysis. *J. Eukar. Microbiol.* 46, 327–338
- Wayne, L. G., Brenner, D. J., Colwell, R. R., Grimont, P. A. D., Kandler, O., Krichevsky, M. I., Moore, L. H., Moore, W. E. C., Murray, R. G. E., and other authors (1987) International Committee on Systematic Bacteriology. Report of the ad hoc committee on reconciliation of approaches to bacterial systematics. *Int. J. Syst. Bacteriol.* 37, 463-464
- Weidner, S., Arnold, W., and Puhler, A. (1996) Diversity of uncultured microorganisms associated with the seagrass *Halophila stipulacea* estimated by restriction fragment length polymorphism analysis of PCR-amplified 16S rRNA genes. *Appl. Env. Microbiol.* 62, 766–71
- Weissman, K. J., and Muller, R. (2010) Myxobacterial secondary metabolites: bioactivities and modes-of-action. *Nat. Prod. Rep.*, 27, 1276–1295
- Ziemke, F., Hofle, M. G., Lalucat, J., and Rossello-Mora, R. (1998) Reclassification of *Shewanella putrefaciens* Owen's genomic group II as *Shewanella baltica* sp. nov. *Int. J. Syst. Bacteriol.* 48, 179–186

Supplemental information

Table CS1. Type and neotype strains used in this study

Strain name	Strain no.
<i>Corallocooccus exiguus</i>	DSM 14696 ^T (Cc e167 ^T)
<i>Corallocooccus coralloides</i>	DSM 2259 ^T (M2 ^T)
<i>Myxococcus virescens</i>	DSM 2260 ^T (M22 ^T)
<i>Myxococcus fulvus</i>	DSM 16525 ^T (M17 ^T)
<i>Myxococcus xanthus</i>	DSM 16526 ^T
<i>Myxococcus stipitatus</i>	DSM 14675 ^{NT} (Mx s8 ^{NT})
<i>Myxococcus macrosporus</i>	DSM 14697 ^T (Cc m8 ^T)
<i>Pyxidococcus fallax</i>	DSM 14698 ^T (Py fl ^T)
<i>Melittangium lichenicola</i>	DSM 2275 ^T (M155 ^T)

Table CS2. Salt tolerance

Strain name	Growth on CY agar with 1.5% NaCl (w/v)
MCy1366 ^T	-
MCy10622	-
<i>C. exiguus</i> DSM 14696 ^T	-
<i>C. coralloides</i> DSM 2259 ^T	-
<i>M. virescens</i> DSM 2260 ^T	+++
<i>M. fulvus</i> DSM 16525 ^T	-
<i>M. xanthus</i> DSM 16526 ^T	++
<i>M. stipitatus</i> DSM 14675 ^{NT}	+
<i>M. macrosporus</i> DSM 14697 ^{NT}	+++
<i>P. fallax</i> DSM 14698 ^T	+
<i>M. lichenicola</i> DSM 2275 ^T	-

*Assessment of growth levels. -, no growth; +, poor growth; ++, moderate; +++, very good growth

Table CS3. Differential physiological reactions in APIZym tests

Enzyme	<i>M. stipitatus</i> DSM 14675 ^{NT}	<i>M. virescens</i> DSM 2260 ^T	<i>M. xanthus</i> DSM 16526 ^T	<i>M. fulvus</i> DSM 16525 ^T	<i>M. macrosporus</i> DSM 14697 ^T	MCy1366 ^T	MCy10622	<i>C. coralloides</i> DSM 2259 ^T	<i>C. exiguus</i> DSM 14696 ^T	<i>P. fallax</i> DSM 14698 ^T	<i>M. lichenicola</i> DSM 2275 ^T
Control	C	C	C	C	C	C	C	C	C	C	C
Esterase(C4)	+	+	+	+	+	V	+	-	+	+	+
Lipase(C14)	-	+	+	-	+	+	+	+	+	+	+
Valine arylamidase	+	+	+	+	+	+	+	+	-	-	+
Cystine arylamidase	+	+	+	+	-	-	+	+	-	-	+
Trypsin	+	-	+	-	+	-	-	-	-	+	-
α -chymotrypsin	+	-	+	-	-	V	+	+	-	-	-
Naphthol- AS-BI- phosphohydrolase	-	+	+	+	+	+	+	+	+	+	+
α -galactosidase	-	-	-	+	-	-	-	-	-	-	-
β -glucuronidase	-	-	-	+	-	-	-	-	-	-	-
α -glucosidase	-	-	-	+	-	-	-	-	-	-	+
β -glucosidase	-	-	-	+	-	-	-	-	-	-	-
N-acetyl- β - glucosaminidase	+	-	-	+	-	-	-	-	-	-	+

Reactions on APIZym strips: +, positive; -, negative; V, variable. All the tested strains were positive for alkaline phosphatase, esterase lipase, leucine arylamidase, and acid phosphatase and negative for β -galactosidase, α -mannosidase, and α -fucosidase.

Table CS4. Antibiotic resistance test for MCy1366^T and MCy10622 along with related type and neotype strains

Antibiotic	<i>M. stipitatus</i> DSM 14675 ^{NT}	<i>M. virescens</i> DSM 2260 ^T	<i>M. xanthus</i> DSM 16526 ^T	<i>M. fulvus</i> DSM 16525 ^T	<i>M. macrosporus</i> DSM 14697 ^T	MCy1366 ^T	MCy10622	<i>C. coralloides</i> DSM 2259 ^T	<i>C. exiguus</i> DSM 14696 ^T	<i>P. fallax</i> DSM 14698 ^T	<i>M. lichenicola</i> DSM 2275 ^T
Control agar	VY/2 +	+	+	+	+	+	+	+	+	+	+
Ampicillin	+	-	+	-	+	-	+	+	+	+	-
Kanamycin	+	-	-	+	-	+	+	+	+	-	+
Spectinomycin	+	+	+	+	+	-	-	-	-	+	+
Trimethoprim	+	-	-	-	+	+	+	+	+	+	+
Bacitracin	+	+	+	+	+	+	+	+	+	+	-
Oxytetracyclin	-	-	-	-	-	-	n.c.	-	-	-	-
Fusidic acid	+	+	+	-	-	-	+	+	+	+	-
Thiostreptone	+	-	-	-	-	-	-	-	-	+	-
Chloramphenicol	-	+	-	-	-	-	n.c.	-	-	+	-

+, Growth; -, Inhibition of growth; n.c., not clear. All the tested strains were resistant to cephalosporin C, gentamycin, hygromycin B and polymyxin.

Table CS5. Dry weight biomass (mg) of MCy1366^T and MCy10622 obtained in synthetic S medium with casitone supplemented with various carbon sources.

Carbon sources	Average dry biomasses (MCy1366 ^T)	Average dry biomasses (MCy10622)
1. Sucrose	16.05	14.25
2. Fructose	15.15	16.0
3. Maltose	14.15	16.7
4. Potato starch	41.05	43.85
5. Molasses	29.95	29.85
6. Xylose	15.05	14.4
7. Soluble starch	29.6	31.35
8. Cellobiose	16.1	15.2
9. Lactose	16.35	17.25
10. Mannose	14.35	15.35
11. Galactose	20.5	14.75
12. Glucose	15.45	15.0
13. Pyruvate	20.2	25.35
14. Control	15	14.25

Table CS6. Dry weight biomass (mg) of MCy1366^T and MCy10622 in minimal casitone (C) medium with various inorganic nitrogen sources, amino acids or peptones sources.

Nitrogen sources	Average dry biomasses (MCy1366 ^T)	Average dry biomasses (MCy10622)
1. L-asparagine monohydrate	16.7	24.55
2. Urea	15.6	15.55
3. L-arginine	13.25	19
4. KNO ₃	13.25	12.5
5. (NH ₄) ₂ SO ₄	11.5	14.85
6. L-lysine monohydrate	14.8	14.5
7. Glycine	12.7	12.45
8. L-glutamic acid	15.3	24.35
9. Procion FM 582	61.1	60.65
10. Tryptone enzymatic digest of casein	7.9	20.35
11. Casitone	19.75	25.75
12. Soytone	23.4	13.9
13. Yeast extract	13.4	21.15
14. Tryptone	18.95	33.05
15. Neopeptone	9.1	4.15
16. Phytone peptone	10.75	3.1
17. Skimmed milk	16.3	7.3
18. Gluten from wheat	32.85	39.6
19. Corn Steep solid	28.65	83.45
20. Meat extract	15.25	14.7
21. Casamino acid	1.5	1.4
22. Control	1.3	1.25

C _{16:2}	-	-	-	-	3.4	3.5	-	3.0	0.6	-	-
C _{18:3w6,cis9,12}	-	-	-	0.2	-	-	-	-	-	-	-
Hydroxy FAs											
C _{13:0 3-OH}	-	-	-	-	-	-	-	-	-	-	-
C _{14:0 3-OH}	-	-	-	-	0.4	0.7	-	0.5	0.6	0.6	0.1
C _{15:0 3-OH}	-	-	-	-	0.1	0.1	0.3	0.1	0.1	-	-
C _{16:0 2-OH}	-	-	-	-	0.2	1.1	-	0.2	0.7	1.2	-
C _{16:0 3-OH}	-	-	-	-	0.4	0.6	0.5	0.3	0.6	0.4	0.2
C _{16:1 3-OH}	-	-	-	-	-	-	-	-	-	0.2	-
C _{24:0 2-OH}	-	-	-	-	-	-	-	-	-	-	-
Total SCFAs	9.6	8.2	15.4	10.0	37.8	41.3	38.0	35.2	33.6	37.7	39.5
BCFAs											
<i>iso</i> -C _{13:0}	1.9	0.8	0.2	1.5	0.7	0.4	-	0.5	0.2	0.1	-
<i>iso</i> -C _{14:0}	0.7	0.3	-	0.4	-	-	-	-	0.1	-	-
<i>iso</i> -C _{15:0}	17.6	22.3	23.2	25.3	39.8	34.5	13.5	30.7	16.3	14.0	13.0
<i>iso</i> -C _{15:1}	-	-	-	1.0	-	-	-	-	-	-	-
<i>iso</i> -C _{15:1ω9cis}	-	1.1	-	-	0.8	-	-	0.4	-	-	-
<i>iso</i> -C _{16:0}	1.9	1.4	2.6	3.3	0.1	0.8	0.2	0.4	1.1	0.9	0.1
<i>iso</i> -C _{16:1}	-	1.1	-	0.4	-	0.3	-	0.1	-	-	-
<i>iso</i> -C _{17:0}	10.1	4.3	16.6	10.4	3.3	3.2	1.4	8.1	11.8	7.7	0.8
<i>iso</i> -C _{17:1}	-	-	-	10.9	-	-	-	-	-	-	-
<i>iso</i> -C _{17:1ω5cis}	12.8	8.2	9.5	-	1.9	1.2	7.3	2.9	2.5	1.9	6.1
<i>iso</i> -C _{17:1ω11cis}	-	2.0	0.2	-	0.7	0.5	-	-	0.3	-	-
<i>iso</i> -C _{17:2}	-	-	-	2.3	-	-	-	-	-	-	-
<i>iso</i> -C _{17:2ω5cis,cis11}	1.0	3.7	-	-	2.4	0.9	-	1.4	0.1	-	-

<i>anteiso</i> -C _{15:0}	-	-	0.3	0.3	-	-	6.0	0.2	-	-	0.8
<i>anteiso</i> -C _{17:0}	0.1	-	0.4	-	-	-	-	0.1	-	-	-
Branched-chain hydroxy FAs											
<i>iso</i> -C _{15:0} 3-OH	2.8	1.6	1.2	0.7	3.1	3.3	4.4	2.9	3.5	1.9	2.7
<i>iso</i> -C _{16:0} 2-OH	0.1	0.2	0.1	-	-	-	-	-	-	-	-
<i>iso</i> -C _{16:0} 3-OH	-	-	-	-	-	-	-	-	-	-	-
<i>iso</i> -C _{17:0} 2-OH	34.4	33.0	26.1	14.1	4.2	7.1	0.2	3.3	12.4	9.3	0.5
<i>iso</i> -C _{17:0} 3-OH	0.3	-	0.1	-	1.2	1.3	3.7	1.2	1.1	0.4	3.2
<i>iso</i> -C _{17:1} 2-OH	0.0	-	-	-	-	-	-	-	-	-	-
Branched chain OAG FAs											
C _{14:0}	-	-	-	-	-	-	-	0.1	0.3	0.4	-
C _{15:0}	-	-	-	-	-	-	-	0.1	-	2.9	-
C _{16:0}	-	-	-	-	-	-	-	0.1	0.4	7.4	-
<i>iso</i> -C _{15:0}	3.4	7.2	1.9	1.3	3.0	3.9	-	10.3	10.1	10.8	-
Branched chain DMA FAs											
<i>iso</i> -C _{15:0}	1.6	4.2	2.0	4.4	1.0	0.7	-	1.7	2.1	4.7	-
Total BCFAs	88.7	91.4	84.4	76.3	62.2	58.1	36.7	64.5	62.3	62.4	27.2
Fatty alcohols											
<i>iso</i> Pentadecanol	0.1	0.3	0.0	-	-	0.0	0.8	0.0	0.2	0.0	0.9
Hexadecanol	-	-	-	-	-	0.0	0.0	-	-	-	-
Unspecified fatty alcohol	-	-	-	-	-	-	24.4	-	-	-	32.1

(Abbreviations: SCFAs, Short chain fatty acids; PUFAs, Polyunsaturated fatty acids; BCFAs, Branched chain fatty acids; OAG FAs, *O*-alkylglycerol fatty acids; DMA FAs, Dimethylacetal fatty acids)

*Percentages of major fatty acids in MCy1366^T and MCy10622 are distinguished in boldface type.

Table CS8. Dry weight biomass (mg) of MCy1366^T and MCy10622 at different pH.

pH	Average dry biomasses (MCy1366 ^T)	Average dry biomasses (MCy10622)
5.0	0.10	0.25
5.5	0.15	0.20
6.0	34.30	27.50
6.5	50.15	52.00
7.0	41.40	38.05
7.5	24.55	25.15
8.0	12.35	21.30
8.5	12.40	15.15
9.0	11.55	14.50
9.5	9.55	14.35
10.0	9.25	14.25

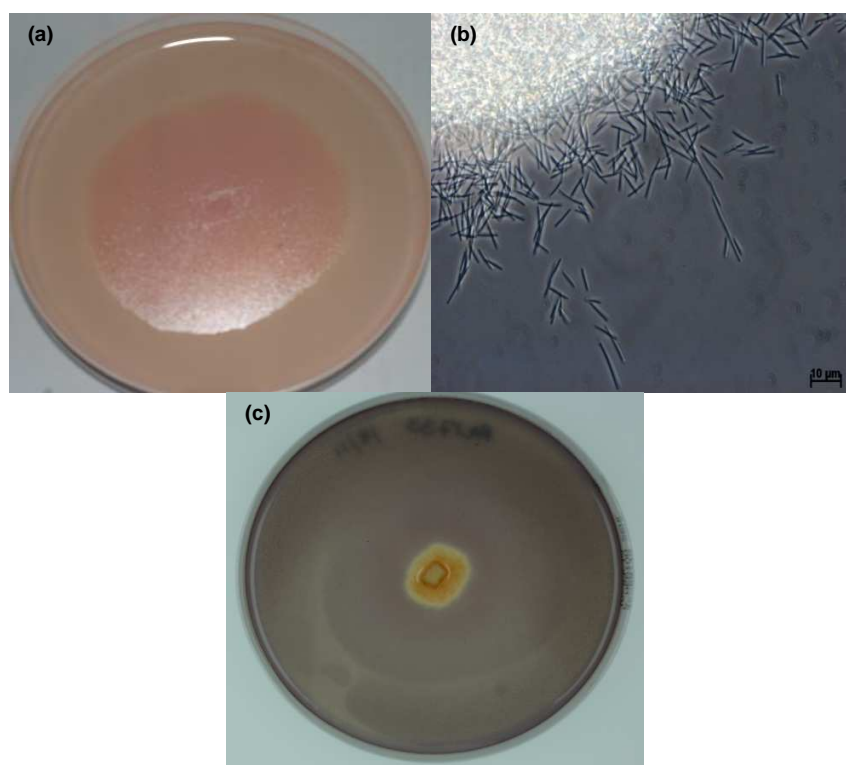


Fig.CS1. (a) Congo Red staining of 3 week old swarm of strain MCy1366^T on VY/2 agar displaying a weak positive reaction (b) Phase contrast microscopic image of vegetative cells of MCy1366^T in myxo media (bar, 10µm) (c) Lugol's solution staining of 2 week old swarm of strain MCy1366^T on P agar displaying a weak positive reaction.

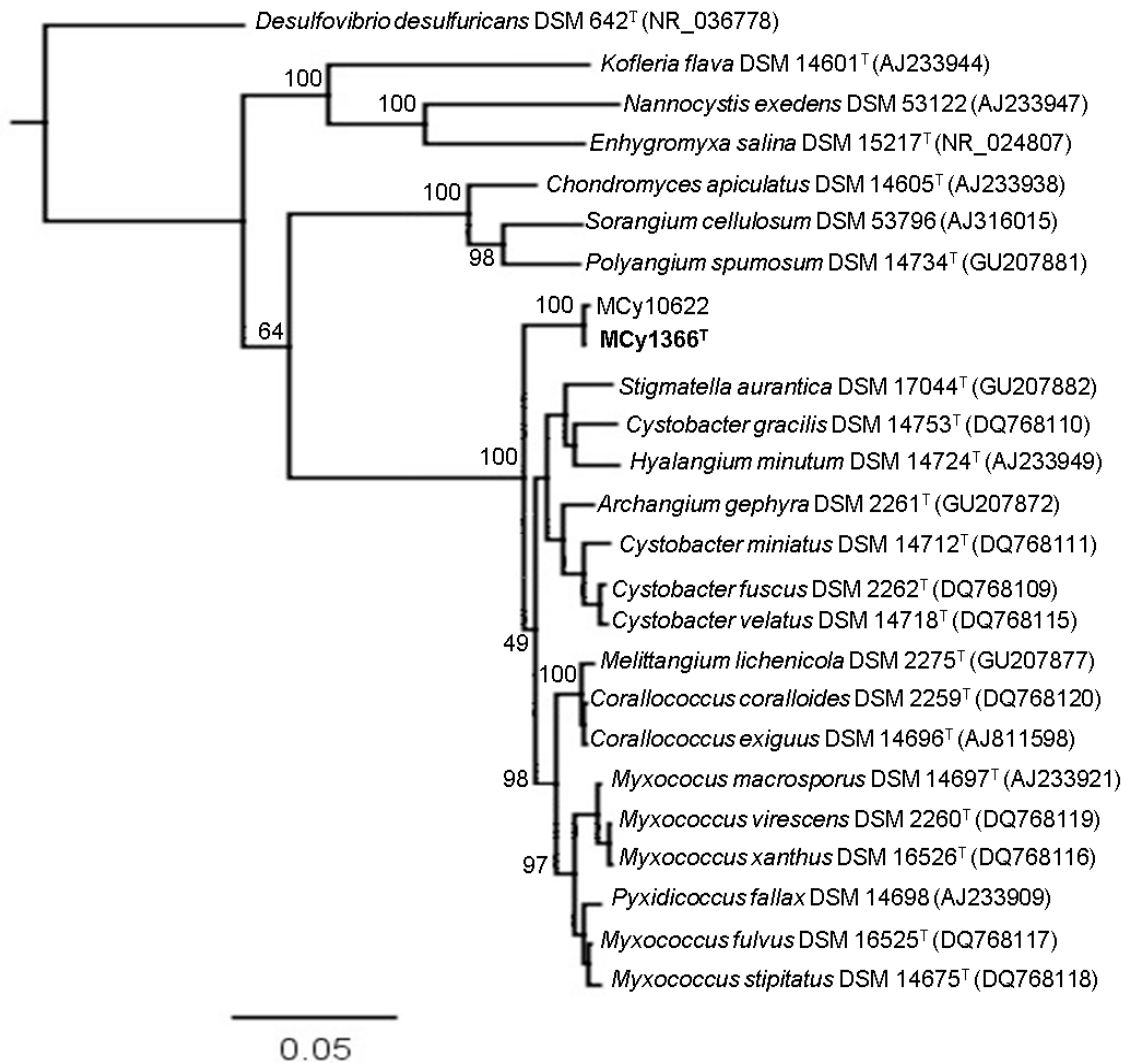


Fig.CS2. Neighbor-joining tree based on 16S rRNA gene sequence showing the phylogenetic position of MCy1366^T and MCy10622. The numbers at branch points indicate bootstrap support based on 1000 resamplings. Bar, 0.05 substitutions per nucleotide position. The GenBank accession number for each strain is shown in parentheses. *Desulfovibrio desulfuricans* DSM 642^T was used as an out group.

Chapter D

Pyrronazols, Metabolites from the Myxobacteria
Nannocystis pusilla and *N. exedens* are Unusual
Chlorinated Pyrone-Oxazole-Pyrroles

Rolf Jansen, **Sakshi Sood**, Volker Huch, Brigitte Kunze, Marc Stadler and Rolf Müller

Submitted to Journal of Natural Products on October 16th, 2013

Accepted on January 24th, 2014

(**Current status** – Published on February 24th, 2014)

Author's contribution to this work

Performed the experiments: SS, RJ, BK

Analyzed chemical and NMR data: RJ

Analyzed X-Ray data: VH

Wrote the paper: SS, RJ

Provided research facilities: MS, RM

Conceived and designed the experiments: RJ

D.1. Abstract

The chlorinated pyrrole-oxazole-pyrones, pyrronazol A (**1**), pyrronazol A2 (**2**) and pyrronazol B (**3**) were isolated from *Nannocystis pusilla* strain Ari7 as well as two chlorinated pyrrole-oxazole isomers, pyrronazol C1 (**4**) and C2 (**5**), from *N. pusilla* strain Na a174. HRESIMS, NMR, and X-ray crystallographic analysis was used in the structure elucidation including the absolute configuration of pyrronazol A (**1**). In addition to pyrronazols, 1,6-phenazine-diol (**6**) and its glycosyl derivative, 1-hydroxy-phenazine-6-yl- α -D-arabinofuranoside (**7**) were isolated and identified from the culture broth of *N. pusilla* strain Ari7. When tested for biological activity against bacteria, fungi, and yeasts, **1** showed weak antifungal activity against *Mucor hiemalis* (MIC 33.3 μ g/mL) but no antibacterial activity, while **6** showed weak antibacterial and antifungal activity (MIC 33.3 μ g/mL) against some of the strains tested. In cell culture experiments **1** showed no significant cytotoxicity while **6** was active against several cell lines, especially the human ovarian carcinoma cells SK-OV-3 (LD₅₀ 2.59 μ M).

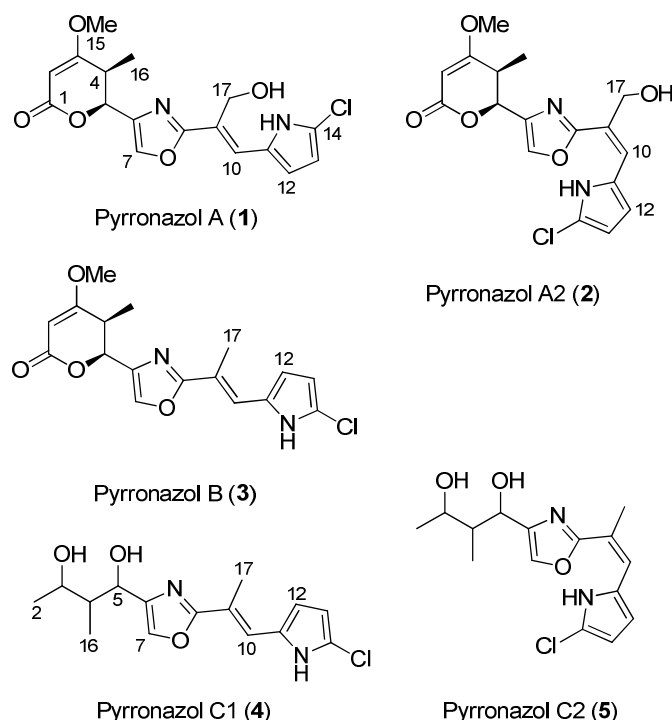
D.2. Introduction

Myxobacteria have been used as a source of new natural products for almost three decades (Bode and Müller, 2007; Wenzel and Müller, 2009). In our quest to find valuable and structurally diverse natural products, we constantly engage in screening strains from our continuously expanding in-house collection of myxobacteria. Pyrronazols were identified from our screening program and isolated as novel secondary metabolites from strain Ari7. The 16S rRNA gene sequence analysis of the producing strain Ari7 showed 99.9% similarity to *Nannocystis pusilla* (DSM 14622^T). Previously, *N. pusilla* strain B150 and *N. exedens* have been reported as producers of phenylnannolones, inhibitors of P-glycoprotein mediated efflux of drugs from eukaryotic cells (Oehlendorf *et al.*, 2008). Further, the siderophores nannochelins (Kunze *et al.*, 1992), steroids (Kohl *et al.*, 1983), germacrane (Reichenbach and Höfle, 2000) and geosmin (Trowitzsch *et al.*, 1981) were reported as *Nannocystis* metabolites.

Herein, we report the isolation and structure elucidation of three secondary metabolites, pyrronazol A (**1**), pyrronazol A2 (**2**) and pyrronazol B (**3**) from *Nannocystis pusilla*, strain Ari7, as well as pyrronazol C1 (**4**) and C2 (**5**) from *N. pusilla* strain Na a174. Extensive HRESIMS, NMR, and X-ray crystallographic analysis was used for the structure elucidation of pyrronazol A (**1**). In addition to pyrronazols, 1,6-phenazine-diol (**6**) and its glycosyl derivative, 1-hydroxy-phenazine-6-yl- α -D-arabinofuranoside (**7**) were isolated and identified from the culture broth of *N. pusilla* strain Ari7.

D.3. Results and Discussion

For metabolite production *N. pusilla*, strain Ari7 was inoculated in a liquid medium supplemented with Amberlite XAD 16 resin and fermented in a 10 L bioreactor for 7 days. The resin was recovered from the culture broth by sieving and the crude extract was eluted from the resin using methanol. The products were isolated from the crude extract using a series of solvent partitioning, silica gel chromatography, preparative RP-MPLC and RP-HPLC, and thin layer chromatography.



Scheme D1. Natural pyrronazol variants

Pyrronazol A (**1**) was isolated from both strains as crystals melting under decomposition at 150 °C. HRESIMS presented the molecular ion clusters for $[M+H]^+$ and $[M+Na]^+$, and a prominent fragment ion $[M-H_2O]^+$ in positive mode as well as $[M-H]^-$ in the negative mode, all pointing to the chlorine-containing elemental formula $C_{17}H_{17}ClN_2O_5$ with ten double bond equivalents. Accordingly, the UV spectrum displayed two chromophores at 348 and 232 nm. All carbons and protons were visible in the 1D NMR spectra in $CDCl_3$ and those directly connected with each other were correlated by the $^1H, ^{13}C$ HMQC spectrum defining the singlets at $\delta_H = 10.6$ and 4.08 as NH and OH signals, respectively. The COSY NMR spectrum revealed only two small structural elements (Figure D1), i.e., methines H-4 and H-5 with methyl group C-16 and methines H-12 and H-13, which showed a long-range correlation to the NH signal. A further long-range correlation was observed between H-5 and H-7. Thus, the carbon skeleton was derived from the $^1H, ^{13}C$ HMBC NMR data (Table D1) as illustrated in Figure D1. The connection of the chlorine atom was required from the elemental formula and the ^{13}C chemical shift of the C-14 atom, while the closure of the 2-pyrone ring was mainly assigned due to the acyl shift of the oxymethine H-5 at δ 5.34 ppm. The ROESY NMR spectrum offered only a few correlations, although, the proximity of 2-H and the methoxy group C-15 as well as of methines H-10 and H-12 was indicated. The latter revealed the *cis* relative configuration of the substituted double bond and the pyrrole H-12. A supporting NOE effect was observed between H-17b and the NH signal on the opposite side. The absence of NOE effects between methylene C-17 and methine C-10 suggested the *trans* configuration of the $\Delta^{9,10}$ double bond, whereas the absence of an NOE effect between methine H-5 and methyl C-16 and methine H-7 required their H-5/C-16 *trans* configuration and a H-5/H-7 *transoidal* conformation of the 5,6-dihydro-2H-pyran-2-one ring, respectively.

Since **1** could be crystalized from methanol, an X-ray crystal analysis was conducted. Fortunately the crystal was of real good quality to allow the determination of the absolute configuration from structure refinement (Flack $x = -0.001(22)$ from 2103 selected quotients (Parsons' method), which indicated the absolute 4*S*,5*S*-configuration (Figure D2). The conspicuous inclination of the primary alcohol C-17 towards the pyrrole

NH is caused by a hydrogen bond between 17-O and the pyrrole NH. The gross conformation in the crystal is fully compatible with the results of the NMR experiments in solution.

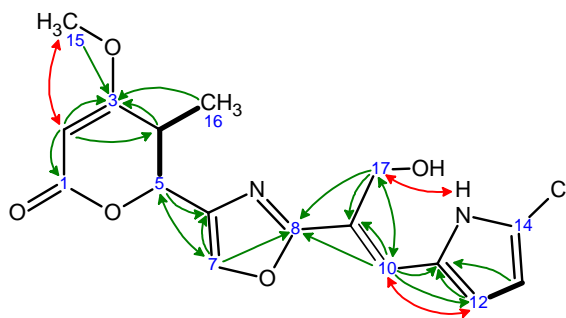


Figure D1. Selected $^1\text{H},^{13}\text{C}$ HMBC (green arrows) and ROESY NMR Correlations (red arrows) of Pyrronazol A (1). (bold bonds show vicinal COSY correlations)

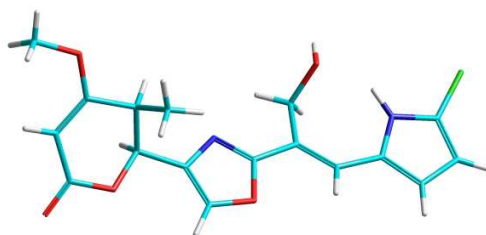


Figure D2. Absolute 4*S*,5*S*-Configuration of Pyrronazol A (1) (red: O; blue: N; green: Cl)

Interestingly, as a byproduct from *N. pusilla* strain Ari7, an isomer **2** of $\text{C}_{17}\text{H}_{17}\text{ClN}_2\text{O}_5$ was isolated showing the same HRESIMS molecular ion clusters as **1**. The NMR data (Table D1) of pyrronazole A2 (**2**) suggested a similar carbon skeleton, though with a *cis* configuration of the methyl substituted $\Delta^{9,10}$ double bond, that was indicated by a strong ROESY correlation between methylene protons H-17 and H-10. While the correlation between H-10 and H-12 was still present, the ROESY correlation of methylene H-17b with the pyrrole NH was lost. As a consequence of the lost fixation by the hydrogen bond the methylene proton signals no longer appeared separated ($\Delta\delta \sim 0.2$ ppm) but as a narrow A,B multiplet at $\delta = 4.66$ ppm in **2**.

The presence of another pyrronazol **3** was suggested by a more lipophilic peak in the RP-HPLC analyses of strains *N. pusilla* or *N. exedens* exhibiting a related UV spectrum.

This however, had the elemental formula $C_{17}H_{17}ClN_2O_4$ indicated by molecular ion clusters for $[M+H]^+$ and $[M+Na]^+$, and a conspicuous pyrone fragment ion $[M-44 = M-CO_2]^+$ in positive mode as well as $[M-H]^-$ in negative mode. The loss of one oxygen atom and the appearance of a new methyl group C-17 in the NMR spectra suggested the absence of the primary alcohol function in pyrronazole B (**3**) (Table D2). This small difference resulted in a surprising consequence in the solution conformation of **3** compared to **1**; supported by a weak ROESY correlation between H-10 and the pyrrole NH, the unambiguously strong correlation between methyl group C-17 and the pyrrole H-12 required a 180 degree turn of the pyrrole ring, positioning both in a *cisoidal* relation (Scheme D1).

Table D1. NMR Data of Pyrronazol A1 (**1**) and A2 (**2**)

Pos.	1^a							2^a						
	δ_H	m	<i>J</i> [Hz]	ROESY	δ_C	m	H in HMBC	δ_H	M	<i>J</i> [Hz]	ROESY	δ_C	m	H in HMBC
1					166.1	C	2					165.9	C	2
2	5.07	s		15	88.9	CH		5.22	s		15	89.2	CH	4
3					178.5	C	16, 4, 15, 2					178.2	C	16, 4, 15, 2
4	2.79	qd	7.1, 3.6	5	35.8	CH	16, 2	2.99	qd	7.1, 3.7	5	36.2	CH	16, 2
5	5.34	dd	3.6, 1.5	4	75.0	CH	16	5.64	m		4, 7	74.6	CH	16
6					137.9	C	5, 7					137.1	C	5
7	7.66	d	1.5		135.9	CH	5	7.85	d	1.5	5	135.5	CH	5
8					163.6	C	17b, 17a, 10, 7					162.6	C	17, 10, 7
9					118.3	C	17b, 17a, 10					115.1	C	17, 10
10	7.38	s		12	126.6	CH	17b, 17a	6.79	s		17	126.1	CH	17
11					128.0	C	13, 12, 10					127.7	C	13, 12, 10
12	6.45	dd	3.6, 2.0	10, 13	116.9	CH	10	6.46	dd	3.6, 2.3	13	117.8	CH	13, 10
13	6.16	dd	3.8, 1.8	12	109.1	CH		6.16	dd	3.6, 2.5	12	108.6	CH	12
14					120.3	C						117.9	C	
15	3.75	s			56.3	CH ₃		3.84	s		2	56.5	CH ₃	
16	0.96	d	7.1	2, 4	11.4	CH ₃	5	1.10	d	7.3	2, 5	11.8	CH ₃	4, 5
17a	4.93	d	13.2	17b	58.6	CH ₂	10	4.66	m		10	65.8	CH ₂	10
17b	4.74	d	13.2	17a, NH										
NH	10.60	br. s		17b				13.94	br. s					
OH	4.08	br. s						n.o.						

^ain CDCl₃ (¹H 600 MHz, ¹³C 100 MHz)

Table D2. NMR Data of Pyrronazol B (3) in CDCl₃

No.	$\delta_{\text{H}}^{\text{a}}$	m	J [Hz]	ROESY	δ_{C}	m ^b	H in HMBC
1					166.45	C	2
2	5.16	s		15	89.11	CH	
3					178.81	C	16, 4, 15, 2
4	2.91	qd	7.0, 3.4	5	35.93	CH	16, 2
5	5.52	dd	3.4, 1.5	4, 7	75.44	CH	16
6					138.23	C	5
7	7.71	d	1.5	5	135.67	CH	5
8					164.66	C	17, 10, 7
9					118.47	C	17, 10
10	7.21	m		NH	121.11	CH	17
11					128.74	C	17, 12
12	12	t	3.4	17	113.33	CH	10
13	6.17	dd	3.8, 2.6	-	108.77	CH	
14					117.11	C	
15	3.80	s		2, 16, 4	56.36	CH ₃	
16	1.01	d	7.2		11.56	CH ₃	5
17	2.34	d	1.1	12	14.79	CH ₃	10
NH	8.47	s	br.				

^a ¹H 300 and 600 MHz; ^b ¹³C 75 MHz from DEPT and HMQC

When *N. pusilla* strain Na a174 was used for large-scale production of **1**, a late eluting fraction from LH-20 chromatography of the extract showed the typical conjugated oxazol-pyrrole chromophore at 340-350 nm in the UV spectrum for two peaks in the analytical RP-HPLC-HRESIMS at 9.7 min and 11.8 min for **4** and **5**, respectively. Both were isomers with the elemental composition C₁₅H₁₉ClN₂O₃ derived from their molecular ion clusters [M+H]⁺ at 311.1158. Their NMR spectra revealed the presence of the pyrrole and oxazol units like pyrronazol B (**3**) but lacked the 2-pyrone part of the molecule (Table D3). Instead, identical 2-methylbutane-1,3-diol residues were suggested from the COSY NMR spectra of pyrronazol C1 (**4**) and C2 (**5**). Suspicious shift differences of 0.7 ppm for H-10 in the ¹H NMR spectra and of 6.8 ppm for C-17 in the ¹³C NMR spectra indicated different configurations of the methyl-substituted $\Delta^{9,10}$ double bond. Actually, **4** was recognized as the *E* configured pyrronazol C isomer from NOESY correlations between CH₃-17 and H-12 and between H-10 and the NH proton. Conversely, ROESY correlations were observed between CH₃-17 and H-10 and between H-10 and H-12 in the *Z* isomer, pyrronazol C2 (**5**).

Table D3. NMR-Data of Pyrronazol C1 (**4**) and C2 (**5**) in CDCl₃^b

4 ^a							5 ^b							
No.	δ _H	m	J [Hz]	NOESY	δ _C	m	HMBC	δ _H	m	J [Hz]	ROESY	δ _C	m	HMBC
2	1.27	d	6.9		21.6	CH ₃		1.34	d	6.4	>4	22.0	CH ₃	-
3	4.33	qd	6.5, 1.7	5 >4	70.7	CH	16, 2, 5	4.38	qd	6.4, 2.3	5 >4	72.6	CH	5, 2, 16
4	1.98	qdd	7.1, 3.2, 1.7	>3, 5	42.6	CH	16, 2	2.20	qt	7.1, 2.3	>3,5	42.3	CH	16, 2 >5
5	4.98	dd	3.2, 0.7	4, 3 >7	72.8	CH	16, 3	5.17	dd	2.3, 1.3	3 >4 >7	73.4	CH	3, 16
6					143.5	C	5, 7	-				142.9	C	5, 7
7	7.53	d	0.7		134.5	CH	5	7.62	d	1.3		134.2	CH	5
8					164.0	C	17, 10, 7	-				163.0	C	17, 7, 10
9					118.7	C	17, 10	-				112.2	C	17, 10
10	7.20	br.s		NH	120.8	CH	17	6.50	br.q	1.1	12 >17	124.2	CH	17
11					128.8	C	13, 12	-				128.6	C	10 >13
12	6.42	br. t	3.3	17, 13	113.3	CH	10	6.28	br.dd	3.4, 2.6	10	115.1	CH	10
13	13	dd	3.7, 2.6	12	108.7	CH	12	6.10	dd	3.6, 2.6		107.6	CH	
14					117.0	C	12	-				115.9	C	
16	0.90	d	7.1	2	5.2	CH ₃	3, 5	0.95	d	7.1		4.4	CH ₃	3, 5 >4
17	2.34	d	0.9	12	14.8	CH ₃	10	2.27	d	1.1	10	21.6	CH ₃	10
NH	8.29	br.s		10				14.27	br.s					

^a ¹H at 700.5 MHz, ¹³C at 176.1 MHz; ^b ¹H at 300.1 MHz, ¹³C at 75.5 MHz. ^b The numbering scheme of pyrronazols A – B was retained in the smaller C1 and C2 variants.

A strongly preferred conformation in solution was expected from the substitution pattern of the 2-methylbutane-1,3-diol residue of the isomers. In the ¹H NMR spectra only small coupling constants $J_{3,4}$ and $J_{4,5}$ between 1.7 and 3.2 Hz were observed for **4** and **5**, together with a strong NOE effect between H-3 and H-5. Assuming the relative position of the substituents on C-4 and C-5 are similar to **1** – **3**, the 4*R*,5*S* configuration was used to calculate the preferred conformations of the 3*R* and 3*S* isomers of pyrronazol C1 (**4**) using the conformational search module of HyperChem (Ver. 8.0). While none of the *R,R,S* conformations were compatible with the NMR restrictions, the conformation of the *S,R,S* configuration of **4** shown in Fig. D3 provided calculated coupling constants of 2.7 and 2.3 Hz for $J_{3,4}$ and $J_{4,5}$, respectively. The strong NOE effects between H-3 and H-5 and the weaker one between H-5 and H-7 were compatible with the atom distances of 2.4 and 3.0 Å in the model. Additionally, the absence of any NOE effect between H-5 and the methyl groups C-2 and C-16 was explained by the conformation of the 3*S*,4*R*,5*S* isomer **4** as shown in Fig. D3.

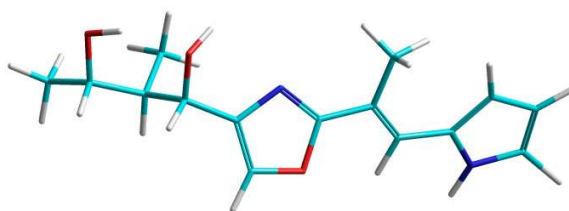
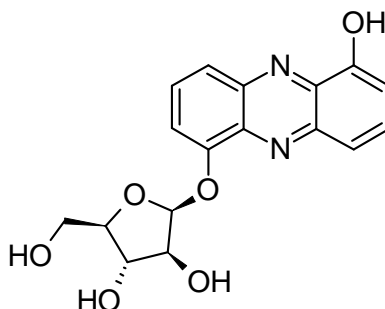


Figure D3. Calculated Solution Conformation of Pyrronazol C1 (4)
(HyperChem Ver. 8.0, Conformational Search (MM+), followed by optimization (pm3))

1,6-Phenazinediol (**6**) was isolated by Si-flash chromatography of a fraction from Sephadex LH-20 chromatography in dichloromethane/methanol (1:1). **6** was identified by HPLC-HRESI mass spectrometry and ^1H and ^{13}C NMR spectroscopy as a metabolite of *N. pusilla*, strain Ari7 (Breitmaier and Hollstein, 1976; Alonso *et al.*, 2005).



Scheme D2. 1-Hydroxy-phenazine-6-yl- α -D-arabinofuranoside (7)

The corresponding glycoside **7** (Scheme D2) was identified by HPLC-UV-MS in a Si-flash chromatography fraction from its similar UV spectrum and the molecular ion cluster $[\text{M}+\text{H}]^+$ at m/z 345.1081 providing the elemental composition $\text{C}_{17}\text{H}_{17}\text{N}_2\text{O}_6$. The molecular ion cluster was accompanied by a typical fragment ion $[\text{M}+\text{H}-\text{C}_5\text{H}_8\text{O}_4]^+$ at m/z 213.0659 indicating the loss of a pentosyl residue. Since the carbon nuclei in furanose sugars are generally less shielded than in related pyranoses and the anomeric configuration can be differentiated by their ^{13}C chemical shifts (Table DS6), the carbohydrate residue was assigned by NMR spectroscopy as an α -arabinofuranosyl residue (observed δ_{C} 109.1, 83.1, 78.9, 87.8, 63.1; methyl- α -furanoside δ_{C} 109.3, 81.9, 77.5, 84.9, 62.4) (Agrawal, 1992; Bubb, 2003). The absolute configuration was

determined to be D-arabinose by GC-MS comparison of the (–)-2-butyl glycoside derivative to authentic standards (Gerwig *et al.*, 1978).

Pyrronazol A (**1**), 1,6-phenazine-diol (**6**) and 1-hydroxy-phenazine-6-yl- α -D-arabinofuranoside (**7**) were tested for their biological activity against bacteria, fungi and yeasts. **1** showed weak antifungal activity against *Mucor hiemalis* with a minimum inhibitory concentration (MIC) of 33 μ g/mL but no antibacterial activity, while **6** showed weak antibacterial and antifungal activity with a MIC of 33 μ g/mL against some of the strains tested (Table D4). When both the compounds were assessed for cytotoxicity against growing cancer and primary cell lines, **1** showed no significant activity but **6** was active against all cell lines tested with a minimum LD₅₀ value of 2.59 μ M against SKOV3 cells (Human ovarian carcinoma cells) (Table D5).

Table D4. In-vitro Antibacterial and Antifungal Activity of Pyrronazol A (1), 1,6-Phenazine-diol (6) and 1-Hydroxy-phenazine-6-yl- α -D-arabinofuranoside (7) (MIC [μ g/mL])

Test Organism (DSM No.)	1	6	7	Control
<i>Chromobacterium violaceum</i> (30191)	n.i.	66.7	n.i.	2.1 ^a
<i>Nocardia sp.</i> (43069)	n.i.	33.3	n.i.	<0.52 ^a
<i>Paenibacillus polymyxa</i> (36)	n.i.	66.7	n.i.	6.7 ^d
<i>Mycobacterium sp.</i> (43270)	n.i.	66.7		2.1 ^a
<i>Mycobacterium diernhoferi</i> (43542)	n.i.	33.3	66.6	<0.52 ^a
<i>Mucor hiemalis</i> (2656)	33.3	33.3	n.i.	2.1 ^b
<i>Trichosporon oleaginosus</i> (11815)	n.i.	n.i.	n.i.	0.1 ^a
<i>Wickerhamomyces anomalus</i> (6766) ^e	n.i.	33.3	n.i.	0.52 ^b
<i>Aspergillus flavus</i> (1959)	n.i.	n.i.	n.i.	1.0 ^c
<i>Aspergillus fumigatus</i> (15966)	n.i.	n.i.	33.3	<0.52 ^c

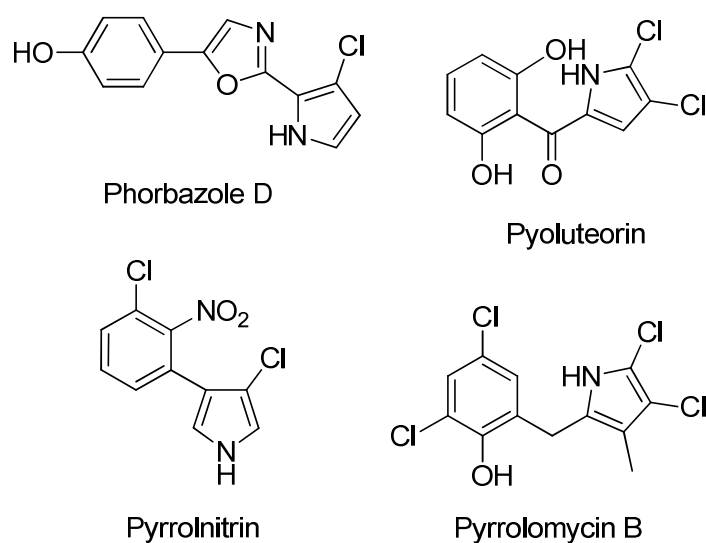
^a Streptomycin sulfate; ^b Nystatin dihydrate; n.i. no inhibition; ^c Amphotericin B; ^d Oxytetracyclin hydrochloride; ^e formerly *Pichia anomala*.

Table D5. Cytotoxicity (LD₅₀ [μ M]) of Pyrronazol A (1) and 1,6-Phenazine-diol (6) against growing cell lines.

Cell lines	Pyrronazol A (1)	1,6-Phenazine-diol (6)	Ref. ^a
L-929	>27.41	11.31	0.008
KB-3-1	>27.41	5.18	0.002
HUVEC	>27.41	3.81	-
SK-OV-3	>27.41	2.59	0.0026
A-549	>27.41	5.65	0.0014

^a Epothilon

With their tricyclic carbon skeleton the pyrronazols A (**1**, **2**) and B (**3**) represent a novel structural class of secondary metabolites. The minor byproducts pyrronazol C1 (**4**) and C2 (**5**) observed with *N. pusilla* strain Na a174 are probably degradation products, which are sometimes observed to a greater extent after a prolonged cultivation period. As next related natural products (Scheme D3) pyoluteorin (Takeda, 1958), a pyrrole antibiotic from *Pseudomonas aeruginosa* and *P. fluorescens* with antibacterial, antifungal and herbicidal properties might be seen, or pyrrolomycin B (Kaneda *et al.*, 1981) from *Actinosporangium vitaminophilum* with antibiotic, antifungal and immune-potentiator properties as well as the phorbazole D variants (Rudi *et al.*, 1994), immunomodulators from the marine sponge *Phorbas aff. clathrata*. Another antifungal pyrrole antibiotic, the 3-chloro derivative pyrrolnitrin was isolated among others from the myxobacterium *Myxococcus fulvus* (Gerth *et al.*, 1982).



Scheme D3. Pyrrole antibiotics

1,6-Phenazine-diol (**6**) belongs to a phenazine family of compounds and has been reported previously from of diverse microorganisms such as *Brevibacterium iodinum*, *Microbispora aerata*, *Streptomyces thioluteus*, *Pseudomonas iodine* and *Nocardioopsis dassonvillei* (Gerber and Lechevalier, 1965; Podojil and Gerber, 1967; Tsujibo, 1988). The glycosyl derivative, 1-hydroxy-phenazine-6-yl- α -D-arabinofuranoside (**7**) was isolated from *Nannocystis pusilla* strain Ari7 for the first time.

D.4. Experimental Section

D.4.1. General Experimental Procedures. Melting points were measured on a Büchi-510 melting point apparatus; UV data were recorded on a Shimadzu UV/Vis-2450 spectrophotometer in methanol (UVASOL, Merck); IR data were recorded on a Bruker Tensor 27 IR spectrophotometer. ^1H NMR and ^{13}C NMR spectra were recorded on Bruker Avance DMX 600 or DPX 300 NMR spectrometers, locked to the deuterium signal of the solvent. Data acquisition, processing and spectral analysis were performed with standard Bruker software and ACD/NMR Spectrus. Chemical shifts are given in parts per million (ppm) and coupling constants in Hertz (Hz). HRESIMS data were recorded on a Maxis ESI TOF mass spectrometer (Bruker Daltonics), molecular formulae were calculated including the isotopic pattern (Smart Formula algorithm). Analytical RP HPLC was carried out with an Agilent 1260 HPLC system equipped with a diode-array UV detector (DAD) and a Corona Ultra detector (Dionex) or a Maxis ESI TOF mass spectrometer (Bruker Daltonics). HPLC conditions: Waters Acquity C_{18} column 50x2 mm, 1.7 μm , solvent A: H_2O , 0.1% HCOOH ; solvent B: acetonitrile, 0.1% HCOOH ; gradient system: 5% B for 1 min, increasing to 95% B in 20 min; flow rate 0.6 mL/min; 40 °C.

The myxobacterial strain *Nannocystis pusilla*, strain Ari7 was isolated in 1980 from a soil sample collected on Langeoog island, Germany, in 1977 and strain Na a174 was isolated from soil with plant residues from Rhodos island, Greece in 1999.

D.4.2. Isolation of Pyrronazols A, A2 and B from *N. pusilla*, strain Ari 7

Fermentation. The strain was stored at -80 °C. It was reactivated in 20 mL of liquid media consisting of 0.3% probion (single cell protein, Hoechst), 0.3% starch (Cerestar), 0.2% $\text{MgSO}_4 \times 7 \text{H}_2\text{O}$, 0.05% $\text{CaCl}_2 \times 2 \text{H}_2\text{O}$, 50 mM HEPES at pH 7.2. 20 μL of vitamin solution was added to the culture. The culture was scaled up to 1L and used as inoculum for a fermentation of strain Ari7 that was performed in the same media as above but supplemented with 2% Amberlite XAD-16 resin in a 10 L bioreactor. The bioreactor was kept at 30 °C, aerated at 0.05 vvm per minute, pH regulated at 7.2, and

agitated with a flat blade turbine stirrer at 100 rpm for 7 days. At the end of fermentation the XAD resin (181 g) was collected from the culture by sieving.

Extraction and Isolation. The XAD adsorber resin was stored overnight in methanol and extracted three times in a glass column with 3 bed volumes of methanol. The methanol extract was evaporated to an aqueous mixture, diluted with water and extracted with ethyl acetate (three times with 150 mL). The combined ethyl acetate was dried with Na_2SO_4 . It was evaporated to give 1.34 g of crude extract. A further solvent-solvent partitioning was done between methanol and n-heptane to eliminate lipophilic compounds. Methanol–n-heptane (100 mL) partitioning was repeated twice to give 914 mg of an enriched crude methanol extract. This crude extract was further separated by Sephadex LH-20 chromatography [column 4×84 cm; solvent dichloromethane - methanol (1:1); flow rate 3.6 mL/min, UV detection at 275nm] to obtain two fractions with crude 1,6-phenazinediol (**4**) (62 mg) and a fraction 2 (325 mg) after evaporation of the organic solvent.

Crude **4** was dissolved in methanol (50 mL) and evaporated with silica gel (11 g). The dried silica gel was used in a solid loader for further purification by silica gel flash chromatography (Reveleris Flash Chromatography System; column 12 g silica 40 μ), solvent dichloromethane for 10 min; flow rate 36 mL/min; UV detection at 350 nm and 270 nm) yielding pure 1,6-phenazinediol (**4**) (17 mg).

The fraction 2 was dissolved in methanol and purified subsequently by RP-MPLC chromatography [column 480×30 mm (Kronlab), ODS-AQ C_{18} (YMC), S 16 μ m; solvent A: H_2O -methanol 1/1; solvent B: methanol; gradient: 15% B to 40% B in 120 min; flow rate 30 mL/min; UV detection at 350 nm] to give four fractions; fraction 2 (58 mg), fraction 3 (13 mg), fraction 4 containing pure pyrronazol A2 (**2**) (3.5 mg), and fraction 5 with pure pyrronazol B (**3**) (2 mg). Fraction 2 was dissolved in DMSO and ultimately purified by two preparative RP-HPLC runs [column 250×21 mm, Nucleodur 100-10 C_{18} EC, S 10 μ m; solvent A: H_2O -methanol 1/1; solvent B: methanol; gradient: 15% B to 30% B in 60 min; flow rate 20 mL/min; UV detection at 350 nm] yielding pure pyrronazol A (**1**) (43 mg) and pyrronazol A2 (**2**) (4.5 mg). **1** was crystalized from methanol at 4 $^\circ\text{C}$.

Fraction 3 was purified by preparative TLC [20 × 20 cm, 0.25 mm, silica gel 60 F254 nm (Merck), dichloromethane-MeOH (9:1), UV detection at 254 nm]. The UV active zone was eluted and to yield 3.2 mg of 1-Hydroxy-phenazine-6-yl- α -D-arabinofuranoside (**7**).

D.4.3. Isolation of Pyrronazol C1 and C2 from *N. pusilla*, strain Na a174

Fermentation. Strain Naa174 was cultivated in 65 L of a medium consisting of 1 % probion (single cell protein, Hoechst), 0.1% MgSO₄ × 7 H₂O, 0.05% CaCl₂ × 2 H₂O, and 50 mM HEPES in the presence of 1 % Amberlite XAD-16 in a 100 L bioreactor. The bioreactor was kept at 30 °C, aerated at 0.05 vvm per minute, pH regulated at 7.2, and agitated with a flat blade turbine stirrer at 110 rpm for 4 days. At the end of fermentation the XAD resin and cells (1.6 kg) were collected from the culture by sieving.

Isolation. Amberlite XAD 16 from a fermentation of strain Naa174 was extracted with acetone (three times, 6 L each) under stirring and filtered through filter paper on a Buchner funnel. The combined extracts were evaporated providing aqueous oil, which was extracted with dichloromethane. After evaporation 22.5 g of a raw extract remained, that was partitioned between methanol and heptane (1:1, 3 times). After evaporation of the methanol, 8.1 g of a raw product was obtained and separated by LH-20 column chromatography (column 70×600 mm, dichloromethane-methanol 8:2, flow rate 10 mL/min; 3 runs). Five fractions were collected guided by TLC and UV absorption (365 nm). Fraction 2 contained pyrronazol A1 (**1**) (3.1 g with about 0.5 g of **1**). Fraction 5 (82 mg) was separated by RP-HPLC [column 22×250 mm, RP-18, solvent gradient 50 to 100% MeOH in 30 min, flow 23 mL/Min; UV detection 350 nm) to give fraction 5.1 (5.6 mg) containing enriched pyrronazol C1 (**4**) and fraction 5.3 (3.4 mg) containing enriched pyrronazol C2 (**5**). Both fractions were again purified by RP-HPLC.

D.4.4. X-Ray Structure Determination of Pyrronazol A (**1**)

Crystals suitable for single-crystal x-ray analysis were obtained from methanol. Although chlorine is not sufficient normally, fortunately in this case the crystal was of real good quality and allowed the determination of the absolute configuration from structure refinement. The data were collected at 132 K on a BrukerAXS X8Apex CCD diffractometer operating with graphite-monochromatized Mo K α radiation. Frames of

0.5° oscillation were exposed; deriving data in the θ range of 2 to 33° with a completeness of ~95%. Structure solution and full least-squares refinement with anisotropic thermal parameters of all non-hydrogen atoms and free refinement of the hydrogen were performed using SHELX (Sheldrick, 2008). The final refinement resulted in: R1= 0.039, wR2= 0.087, S = 1.009 and Flack = 0.00(4) for the correct structure and R1 = 0.041, wR2= 0.093, S= 1.075 and Flack = 0.99(6) for the opposite configuration.

D.4.5. Structural characteristics of compounds isolated

Pyrronazol A1 (1) 6-{2-[(1*E*)-1-(5-chloro-1*H*-pyrrol-2-yl)prop-1-en-2-yl]-1,3-oxazol-4-yl}-4-methoxy-5-methyl-5,6-dihydro-2*H*-pyran-2-one: C₁₇H₁₇ClN₂O₅ M = 364.78; HPLC System A: R_t 10.2 min; mp. 150 °C decomp.; [α]_D²² - 134.4 (*c* = 8 mg/cm⁻³, CH₃OH); UV (MeOH): λ_{\max} (log ϵ) 232 (4.229), 346 (4.484) nm; IR (KBr) ν_{\max} 1681 (s), 1617 (s), 1223 (s), 781 (m) cm⁻¹; NMR data, see Table D1; HRESIMS *m/z* 365.0903 [M+H]⁺ (calcd. for C₁₇H₁₈ClN₂O₅, 365.0899), *m/z* 387.0726 [M+Na]⁺ (calcd. for C₁₇H₁₇ClN₂O₅Na, 387.0718), *m/z* 347.0798 [M-H₂O+H]⁺ (calcd. for C₁₇H₁₆ClN₂O₄, 437.0793), *m/z* 363.0751 [M-H]⁻ (calcd. for C₁₇H₁₆ClN₂O₅, 363.0753).

Pyrronazol A2 (2) 6-{2-[(1*Z*)-1-(5-chloro-1*H*-pyrrol-2-yl)-3-hydroxyprop-1-en-2-yl]-1,3-oxazol-4-yl}-4-methoxy-5-methyl-5,6-dihydro-2*H*-pyran-2-one: C₁₇H₁₇ClN₂O₅ M = 364.78; [α]_D²² - 366 (*c* = 0.0038 g/cm⁻³, CH₃OH); UV (MeOH): λ_{\max} (log ϵ) 233 (4.313), 353 (4.266) nm; NMR data, see Table D1; HRESIMS *m/z* 365.0900 [M+H]⁺ (calcd. for C₁₇H₁₈ClN₂O₅, 365.0899), *m/z* 347.0793 [M-H₂O+H]⁺ (calcd. for C₁₇H₁₆ClN₂O₄, 437.0793).

Pyrronazol B (3) (5*R*,6*R*)-6-{2-[(1*E*)-1-(5-chloro-1*H*-pyrrol-2-yl)prop-1-en-2-yl]-1,3-oxazol-4-yl}-4-methoxy-5-methyl-5,6-dihydro-2*H*-pyran-2-one: C₁₇H₁₇ClN₂O₄ M = 348.78; HPLC System A: R_t 11.8 min; m.p. 215-6 °C; [α]_D²² - 132.3 (*c* = 5.3 mg/cm⁻³, CH₃OH); UV (MeOH): λ_{\max} (log ϵ) 231 (3.852), 338 (4.038) nm; IR (KBr) ν_{\max} 1704 (s), 1629 (s), 1618 (s), 1379 (s) 1222 (s), 765 (m) cm⁻¹; NMR data, see Table D2; HRESIMS *m/z* 349.0954 [M+H]⁺ (calcd. for C₁₇H₁₈ClN₂O₄, 349.0950), *m/z* 305.1057 [M+H-CO₂]⁺ (calcd. for C₁₆H₁₈ClN₂O₂, 305.1051), *m/z* 371.0756 [M+Na]⁺ (calcd. for C₁₇H₁₇ClN₂O₄Na, 371.0769), *m/z* 347.0801 [M-H]⁻ (calcd. for C₁₇H₁₆ClN₂O₄, 347.0804).

Pyrronazol C1 (4) 1-{2-[(1*E*)-1-(5-chloro-1*H*-pyrrol-2-yl)prop-1-en-2-yl]-1,3-oxazol-4-yl}-2-methylbutane-1,3-diol: C₁₅H₁₉ClN₂O₃ M = 310.78; HPLC System A: R_t 9.7 min; α²²_D UV (MeOH): λ_{max} (log ε) 341 (3.381) nm; NMR data, see Table D3; HRESIMS *m/z* 311.1167 [M+H]⁺ (calcd. for C₁₅H₂₀ClN₂O₃, 311.1157).

Pyrronazol C2 (5) 1-{2-[(1*Z*)-1-(5-chloro-1*H*-pyrrol-2-yl)prop-1-en-2-yl]-1,3-oxazol-4-yl}-2-methylbutane-1,3-diol: C₁₅H₁₉ClN₂O₃ M = 310.78; HPLC System A: R_t 11.85 min; α²²_D UV (MeOH): λ_{max} (log ε) 349 (3.851) nm; NMR data, see Table D3; HRESIMS *m/z* 311.1158 [M+H]⁺ (calcd. for C₁₅H₂₀ClN₂O₃, 311.1157).

1,6-Phenazine-diol (6): HPLC System A: R_t 7.3 min, UV λ_{max} 271, 373, 442 nm; ¹H NMR (400 MHz, DMSO-*d*₆) δ 10.48 (2H, br. s., OH), 7.76 (2H, dd, J = 8.6 Hz, J = 7.1 Hz, CH), 7.72 (2H, dd, J = 8.6 Hz, J = 1.5 Hz, CH), 7.19 (2H, dd, J = 6.9 Hz, J = 1.8 Hz, CH); ¹³C NMR (101 MHz, DMSO-*d*₆) δ 110.52 (CH), 119.12 (CH), 131.27 (CH), 135.66, 142.06, 153.37; HRESIMS *m/z* 213.0662 [M+H]⁺ (calcd. for C₁₂H₈N₂O₂, 213.0659).

1-Hydroxy-phenazine-6-yl-α-D-arabinofuranoside (7): C₁₇H₁₆N₂O₆ M = 344.32; HPLC System A: R_t 5.47 min; UV (MeOH): λ_{max} (log ε) 270 (4.698), 371 (3.496), 436 (3.232) nm; NMR data, see Table DS6; HRESIMS *m/z* 345.1081 [M+H]⁺ (calcd. for C₁₇H₁₇N₂O₆, 345.1081), *m/z* 213.0659 [M+H-C₅H₈O₄]⁺ (calcd. for C₁₂H₉N₂O₂, 213.0659).

D.4.6. Antimicrobial Testing

20 μl aliquots (conc. 1 mg/mL) of compound **1**, **6**, **7** and reference drugs (streptomycin against bacteria and nystatin against yeast and fungi) were tested against 5 bacteria (*Chromobacterium violaceum*, *Nocardia* sp., *Paenibacillus polymyxa*, *Mycobacterium* sp., *Mycobacterium diernhoferi*), fungi (*Mucor hiemalis*, *Aspergillus fumigatus*), and two yeasts (*Pichia anomala* (recently the name *P. a.* was changed to *Wickerhamomyces anomalus*). The MIC values were determined in 96 well microtitre plates by 1:1 serial dilution in EBS medium (0.5 % casein peptone, 0.5 % protease peptone, 0.1 % meat extract, 0.1 % yeast extract, pH 7.0) for bacteria and MYC medium (1.0 % glucose, 1.0 % phytone peptone, 50 mM HEPES [11.9 g/L], pH 7.0) for yeasts and fungi, as

previously described (Okanya *et al.*, 2011). The test organisms were cultivated at 30 °C and 160 rpm for 24-48 hrs and the cell concentration adjusted to OD₆₀₀ 0.01 for bacteria and OD₅₄₈ 0.1 for yeasts before the test. The lowest concentration of the drug preventing visible growth of the test organism was taken as the MIC.

D.4.7. Cytotoxicity assay

In-vitro cytotoxicity (IC₅₀) was determined for compound **1** and **6** against a number of mammalian cell lines including the mouse fibroblast cell line L929, the cervix carcinoma cell line KB-3-1, non-transformed human umbilical vein endothelial cell line HUVEC, human ovarian carcinoma cell line SKOV3, adenocarcinomic human alveolar basal epithelial cell A549. KB-3-1, A549 and L929 were cultured in DMEM (Lonza), HUVEC was cultured in EBM-2 (Lonza) and SKOV3 was cultured in McCoy's (Lonza) media, all supplemented with 10% of fetal bovine serum (Gibco) and incubated under 10% CO₂ at 37 °C. The MTT (2-(4,5-dimethylthiazol-2-yl)-2,5-di phenyltetrazolium bromide) method was used for the cytotoxicity assay on 96 well microplates as described previously. Methanol was used as negative control.

Acknowledgements

S. S. is highly indebted to Erasmus Mundus External Cooperation Window for a PhD scholarship and all their support. We thank C. Kakoschke for measuring the NMR spectra, Dr. M. Nimtz for GC-MS analysis, W. Kessler and his team for large-scale fermentation, and K. Schober, A. Teichmann, D. Telkemeyer, and W. Collisi for technical assistance.

References

- Agrawal, P. K. (1992) *Phytochemistry* 31, 3307-3330
- Alonso, A. M., Horcajada, R. H., Groombridge, J., Chudasama, R., Motavali, M., Utley, J. H. P., and Wyatt, P. B. (^1H NMR) (2005) *Org. Biomol. Chem.* 3, 2832-2841
- Bode, H. B., and Müller, R. (2007) *Myxobacteria: Multicellularity and Differentiation*; ASM Press: Washington, DC, 259–282
- Bouhired, S. M. (2012) *Biosynthesis of Phenylnannolone A, a MDR Reversal Agent from Nannocystis pusilla*; Rheinischen Friedrich-Wilhelms-Universität Bonn, Bonn, 2012
[hss.ulb.unibonn.de/2013/3127/3127.pdf]
- Breitmaier, E., and Hollstein, U. (^{13}C NMR)(1976) *J. Org. Chem.* 41, 2104-2108
- Bubb, W. A. (2003) *Concepts Magn. Reson. A* 19, 1-19
- Gerber, N. N., and Lechevalier, M. P. (1965) *Biochemistry* 4, 176-180
- Gerth, K., Trowitzsch, W., Wray, V., Höfle, G., Irschik, H., and Reichenbach, H. (1982) *J. Antibiot.* 35, 1101-1103
- Gerwig, G. J., Kamerling, J. P., and Vliegthart J.F.G. (1078) *Carbohydr. Res.* 62, 349-357
- Kaneda, M., Akamura, S., Ezaki, N., and Iitaka, Y. (1981) *J. Antibiot.* 34, 1366-1368
- Kohl, W., Gloe, A., and Reichenbach, H. (1983) *J. Gen. Microbiol.* 129, 1629-1635
- Kunze, B., Trowitzsch-Kinast, W., Höfle, G., and Reichenbach, H. (1992) *J. Antibiot.* 45, 147-150
- Ohlendorf, B., Leyers, S., Krick, A., Kehraus, S., Wiese, M., and König, G.M. (2008) *ChemBioChem* 9, 2997-3003
- Okanya, P.W., Mohr, K.I., Gerth, K., Jansen, R., and Müller, R. (2011) *J. Nat. Prod.* 74, 603-608
- Podojil, M., and Gerber, N. N. (1967) *Biochemistry* 6, 2701-2705
- Reichenbach, H., and Höfle, G. in *Drug Discovery from Nature* (Eds. Grabley, S.; Thierecke, R.), Springer, Heidelberg, 2000, p. 173.
- Rudi, A., Stein, Z., Green, S., Goldberg, I., Kashman, Y., Benayahu, Y., and Schleyer, M. (1994) *Tetrahedron. Lett.* 35, 2589-2592
- Sheldrick, G. M. (2008) *Acta Cryst. A* 64, 112-122
- Takeda, R. (1958) *J. Am. Chem. Soc.* 80, 4749-4750
- Trowitzsch, W., Witte, L., and Reichenbach, H. (1981) *FEMS Microbiol. Lett.* 12, 257-260
- Tsujibo H., Sato T., Inui M., Yamamoto H., and Inamori Y. (1988) *Agric. Biol. Chem.* 52, 301-306
- Wenzel, S.C., and Müller, R. (2009) *Curr. Opin. Drug Discov. & Devel.* 12, 220-230

Supplemental information

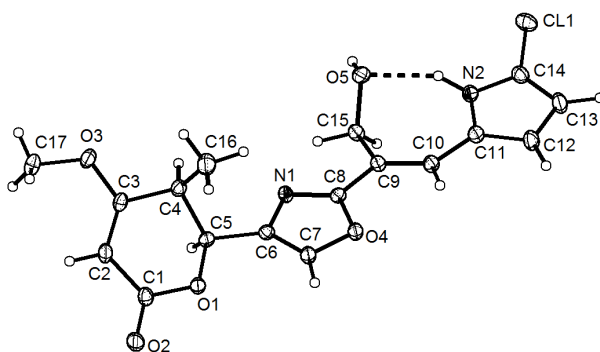


Figure DS1. ORTEP presentation of the X-ray analysis of Pyrronazol A1 (1)

Table DS1. Crystal data and structure refinement for Pyrronazol A1 (1)

Identification code	sh3288
Empirical formula	C ₁₇ H ₁₇ Cl N ₂ O ₅
Formula weight	364.78
Temperature	132(2) K
Wavelength	0.71073 Å
Crystal system	Monoclinic
Space group	P2(1)
Unit cell dimensions	a = 7.6925(7) Å α = 90° b = 10.9091(8) Å β = 90.238(5)° c = 10.2880(8) Å γ = 90°
Volume	863.34(12) Å ³
Z	2
Density (calculated)	1.403 Mg/m ³
Absorption coefficient	0.252 mm ⁻¹
F(000)	380
Crystal size	1.13 x 0.84 x 0.32 mm ³
Theta range for data collection	1.98 to 32.92°
Index ranges	-11 ≤ h ≤ 6, -16 ≤ k ≤ 16, -15 ≤ l ≤ 15
Reflections collected	9117
Independent reflections	5584 [R(int) = 0.0203]
Completeness to theta = 32.92°	92.9 %
Absorption correction	Semi-empirical from equivalents
Max. and min. transmission	0.9229 and 0.7649
Refinement method	Full-matrix least-squares on F ²
Data / restraints / parameters	5584 / 66 / 294
Goodness-of-fit on F ²	1.009
Final R indices [I > 2σ(I)]	R1 = 0.0346, wR2 = 0.0841
R indices (all data)	R1 = 0.0393, wR2 = 0.0875
Absolute structure parameter	0.00(4)
Largest diff. peak and hole	0.438 and -0.412 e.Å ⁻³

Table DS2. Atomic Coordinates ($\times 10^4$) and Equivalent Isotropic Displacement Parameters ($\text{\AA}^2 \times 10^3$) for Pyrronazol A1 (1).U(eq) is defined as one third of the trace of the orthogonalized U^{ij} tensor.

	x	y	z	U(eq)
Cl(1)	-294(1)	5373(1)	1719(1)	24(1)
O(1)	13021(1)	7434(1)	6425(1)	17(1)
O(2)	15685(1)	7783(1)	7123(1)	23(1)
O(3)	12371(2)	4636(1)	9087(1)	22(1)
O(4)	8339(1)	8248(1)	4529(1)	17(1)
O(5)	4504(1)	4925(1)	4266(1)	18(1)
N(1)	8965(2)	6303(1)	4989(1)	15(1)
N(2)	2599(2)	6376(1)	2658(1)	16(1)
C(1)	14397(2)	7130(1)	7177(1)	18(1)
C(2)	14250(2)	6084(1)	8048(1)	19(1)
C(3)	12714(2)	5527(1)	8227(1)	16(1)
C(4)	11130(2)	5904(1)	7474(1)	17(1)
C(5)	11739(2)	6482(1)	6195(1)	14(1)
C(6)	10280(2)	7050(1)	5456(1)	14(1)
C(7)	9911(2)	8233(1)	5181(1)	17(1)
C(8)	7854(2)	7053(1)	4451(1)	14(1)
C(9)	6227(2)	6737(1)	3814(1)	14(1)
C(10)	5098(2)	7626(1)	3450(1)	16(1)
C(11)	3436(2)	7484(1)	2820(1)	16(1)
C(12)	2389(2)	8376(1)	2261(2)	22(1)
C(13)	895(2)	7800(1)	1747(2)	22(1)
C(14)	1075(2)	6578(1)	2035(1)	18(1)
C(15)	5969(2)	5387(1)	3556(1)	16(1)
C(16)	9968(2)	6739(2)	8293(1)	26(1)
C(17)	13732(2)	4272(2)	9966(2)	28(1)

Table DS3. Bond lengths [\AA] and angles [$^\circ$] for Pyrronazol A1 (1)

Cl(1)-C(14)	1.7149(14)
O(1)-C(1)	1.3496(15)
O(1)-C(5)	1.4516(15)
O(2)-C(1)	1.2218(17)
O(3)-C(3)	1.3415(16)
O(3)-C(17)	1.4357(18)
O(4)-C(8)	1.3592(15)
O(4)-C(7)	1.3805(17)
O(5)-C(15)	1.4363(17)
O(5)-H(11)	0.79(3)
N(1)-C(8)	1.3044(16)
N(1)-C(6)	1.3840(16)
N(2)-C(14)	1.3524(17)

N(2)-C(11)	1.3796(17)
N(2)-H(8)	0.92(2)
C(1)-C(2)	1.4554(19)
C(2)-C(3)	1.3425(19)
C(2)-H(1)	0.945(19)
C(3)-C(4)	1.4991(18)
C(4)-C(16)	1.531(2)
C(4)-C(5)	1.5338(18)
C(4)-H(2)	0.99(2)
C(5)-C(6)	1.4891(17)
C(5)-H(3)	0.928(18)
C(6)-C(7)	1.3501(17)
C(7)-H(4)	0.95(2)
C(8)-C(9)	1.4519(18)
C(9)-C(10)	1.3535(18)
C(9)-C(15)	1.5094(18)
C(10)-C(11)	1.4396(18)
C(10)-H(5)	0.94(2)
C(11)-C(12)	1.3858(19)
C(12)-C(13)	1.410(2)
C(12)-H(6)	0.95(2)
C(13)-C(14)	1.373(2)
C(13)-H(7)	1.01(2)
C(15)-H(9)	0.983(16)
C(15)-H(10)	0.981(19)
C(16)-H(12)	1.00(2)
C(16)-H(13)	0.90(3)
C(16)-H(14)	0.97(2)
C(17)-H(15)	0.92(2)
C(17)-H(16)	0.86(2)
C(17)-H(17)	1.00(2)
C(1)-O(1)-C(5)	116.60(10)
C(3)-O(3)-C(17)	118.08(13)
C(8)-O(4)-C(7)	104.84(10)
C(15)-O(5)-H(11)	106(2)
C(8)-N(1)-C(6)	104.71(10)
C(14)-N(2)-C(11)	108.48(11)
C(14)-N(2)-H(8)	125.9(14)
C(11)-N(2)-H(8)	123.5(14)
O(2)-C(1)-O(1)	117.66(12)
O(2)-C(1)-C(2)	123.38(12)
O(1)-C(1)-C(2)	118.90(12)
C(3)-C(2)-C(1)	120.66(12)
C(3)-C(2)-H(1)	121.7(13)
C(1)-C(2)-H(1)	116.9(13)
O(3)-C(3)-C(2)	126.46(12)
O(3)-C(3)-C(4)	112.23(12)
C(2)-C(3)-C(4)	121.27(12)

C(3)-C(4)-C(16)	110.77(11)
C(3)-C(4)-C(5)	107.78(11)
C(16)-C(4)-C(5)	114.13(11)
C(3)-C(4)-H(2)	107.2(12)
C(16)-C(4)-H(2)	112.5(12)
C(5)-C(4)-H(2)	104.0(11)
O(1)-C(5)-C(6)	107.18(10)
O(1)-C(5)-C(4)	111.36(10)
C(6)-C(5)-C(4)	112.16(11)
O(1)-C(5)-H(3)	107.6(12)
C(6)-C(5)-H(3)	109.1(11)
C(4)-C(5)-H(3)	109.2(11)
C(7)-C(6)-N(1)	109.75(11)
C(7)-C(6)-C(5)	131.46(12)
N(1)-C(6)-C(5)	118.70(10)
C(6)-C(7)-O(4)	107.25(11)
C(6)-C(7)-H(4)	139.8(12)
O(4)-C(7)-H(4)	112.9(12)
N(1)-C(8)-O(4)	113.45(11)
N(1)-C(8)-C(9)	127.19(11)
O(4)-C(8)-C(9)	119.36(11)
C(10)-C(9)-C(8)	120.40(11)
C(10)-C(9)-C(15)	124.49(11)
C(8)-C(9)-C(15)	115.06(10)
C(9)-C(10)-C(11)	128.01(12)
C(9)-C(10)-H(5)	116.9(12)
C(11)-C(10)-H(5)	115.1(12)
N(2)-C(11)-C(12)	107.19(12)
N(2)-C(11)-C(10)	124.12(12)
C(12)-C(11)-C(10)	128.69(13)
C(11)-C(12)-C(13)	108.31(13)
C(11)-C(12)-H(6)	125.2(13)
C(13)-C(12)-H(6)	126.5(13)
C(14)-C(13)-C(12)	105.70(12)
C(14)-C(13)-H(7)	122.8(12)
C(12)-C(13)-H(7)	131.3(12)
N(2)-C(14)-C(13)	110.30(12)
N(2)-C(14)-Cl(1)	119.69(10)
C(13)-C(14)-Cl(1)	130.01(11)
O(5)-C(15)-C(9)	110.80(11)
O(5)-C(15)-H(9)	110.2(11)
C(9)-C(15)-H(9)	108.2(12)
O(5)-C(15)-H(10)	109.3(11)
C(9)-C(15)-H(10)	108.8(11)
H(9)-C(15)-H(10)	109.4(15)
C(4)-C(16)-H(12)	111.3(14)
C(4)-C(16)-H(13)	110.1(19)
H(12)-C(16)-H(13)	107(2)

C(4)-C(16)-H(14)	108.5(15)
H(12)-C(16)-H(14)	111(2)
H(13)-C(16)-H(14)	109(2)
O(3)-C(17)-H(15)	112.6(11)
O(3)-C(17)-H(16)	105.3(13)
H(15)-C(17)-H(16)	111.8(19)
O(3)-C(17)-H(17)	111.4(12)
H(15)-C(17)-H(17)	110.1(17)
H(16)-C(17)-H(17)	105.3(17)

Table DS4. Anisotropic displacement parameters ($\text{\AA}^2 \times 10^3$) for Pyrronazol A1 (1). The anisotropic displacement factor exponent takes the form: $-2\pi^2 [h^2 a^{*2} U^{11} + \dots + 2 h k a^* b^* U^{12}]$

	U ¹¹	U ²²	U ³³	U ²³	U ¹³	U ¹²
Cl(1)	19(1)	27(1)	25(1)	-3(1)	-1(1)	-7(1)
O(1)	15(1)	13(1)	24(1)	3(1)	-5(1)	-2(1)
O(2)	18(1)	18(1)	34(1)	4(1)	-6(1)	-4(1)
O(3)	24(1)	20(1)	24(1)	9(1)	-5(1)	-1(1)
O(4)	16(1)	11(1)	24(1)	1(1)	-5(1)	-1(1)
O(5)	19(1)	11(1)	26(1)	1(1)	2(1)	-1(1)
N(1)	14(1)	11(1)	18(1)	-1(1)	-3(1)	0(1)
N(2)	14(1)	15(1)	21(1)	0(1)	-2(1)	0(1)
C(1)	16(1)	14(1)	22(1)	0(1)	-5(1)	1(1)
C(2)	18(1)	16(1)	22(1)	2(1)	-6(1)	0(1)
C(3)	20(1)	12(1)	18(1)	1(1)	-4(1)	1(1)
C(4)	17(1)	15(1)	18(1)	2(1)	-4(1)	-1(1)
C(5)	14(1)	11(1)	18(1)	0(1)	-2(1)	-1(1)
C(6)	14(1)	12(1)	16(1)	-1(1)	-1(1)	0(1)
C(7)	15(1)	12(1)	23(1)	1(1)	-4(1)	-1(1)
C(8)	14(1)	9(1)	18(1)	-1(1)	0(1)	0(1)
C(9)	13(1)	12(1)	18(1)	-1(1)	-2(1)	0(1)
C(10)	16(1)	13(1)	21(1)	0(1)	-2(1)	1(1)
C(11)	15(1)	13(1)	20(1)	-1(1)	-2(1)	0(1)
C(12)	18(1)	17(1)	30(1)	2(1)	-4(1)	3(1)
C(13)	16(1)	23(1)	26(1)	2(1)	-6(1)	4(1)
C(14)	14(1)	21(1)	18(1)	-1(1)	-2(1)	-1(1)
C(15)	13(1)	12(1)	23(1)	-2(1)	0(1)	0(1)
C(16)	25(1)	33(1)	20(1)	3(1)	3(1)	9(1)
C(17)	29(1)	29(1)	24(1)	11(1)	-5(1)	4(1)

Table DS5. Hydrogen coordinates ($\times 10^4$) and isotropic displacement parameters ($\text{\AA}^2 \times 10^3$) for Pyrronazol A1 (1)

	x	y	z	U(eq)
H(1)	15230(30)	5902(18)	8573(18)	23(5)
H(2)	10530(30)	5140(20)	7199(18)	27(5)
H(3)	12260(30)	5884(16)	5685(16)	16(4)
H(4)	10420(30)	9020(20)	5261(18)	23(5)
H(5)	5420(30)	8441(19)	3637(18)	19(4)
H(6)	2660(30)	9230(20)	2220(20)	33(5)
H(7)	-90(30)	8130(19)	1200(20)	27(5)
H(8)	2900(30)	5680(20)	3110(20)	36(6)
H(9)	5780(20)	5275(18)	2617(16)	16(4)
H(10)	7020(30)	4944(17)	3825(17)	19(4)
H(11)	4360(30)	4240(20)	4030(30)	47(7)
H(12)	8860(30)	6930(20)	7830(20)	38(6)
H(13)	10510(40)	7450(30)	8450(20)	52(8)
H(14)	9740(30)	6330(20)	9120(20)	35(5)
H(15)	14650(30)	3912(19)	9548(17)	21(5)
H(16)	13250(30)	3780(18)	10506(18)	18(4)
H(17)	14150(30)	4980(19)	10501(19)	27(5)

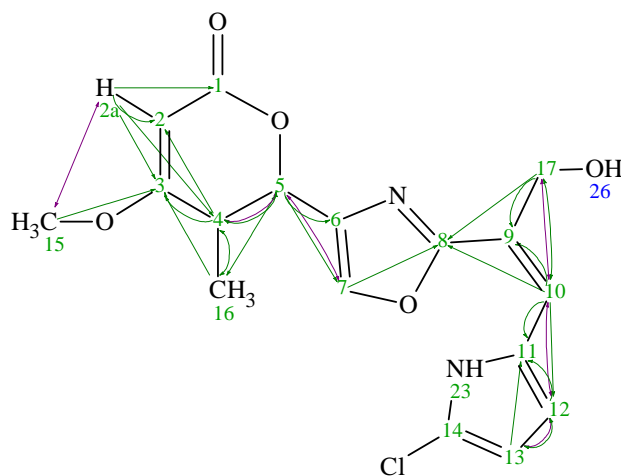


Figure DS2. HMBC-correlations of Pyrronazol A2 (2)

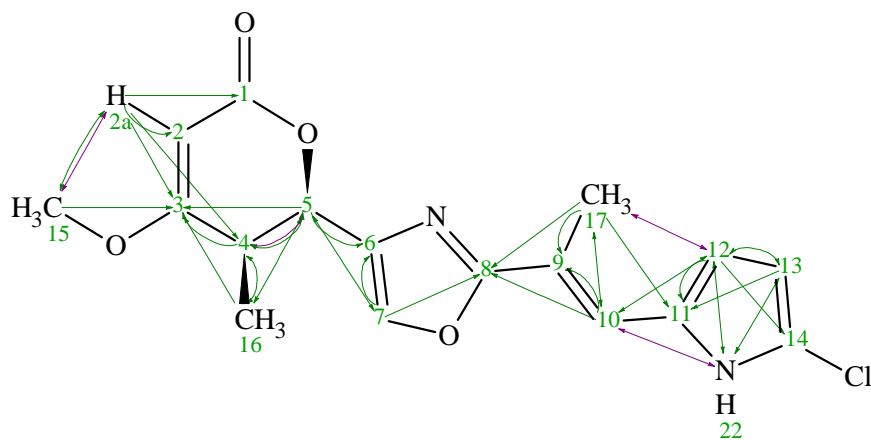


Figure DS3. HMBC-correlations of Pyrronazol B (3)

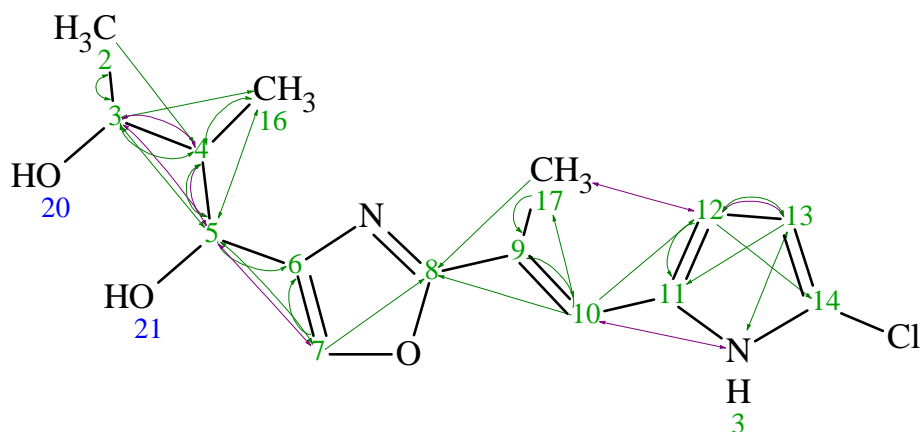


Figure DS4. HMBC-correlations of Pyrronazol C1 (4)

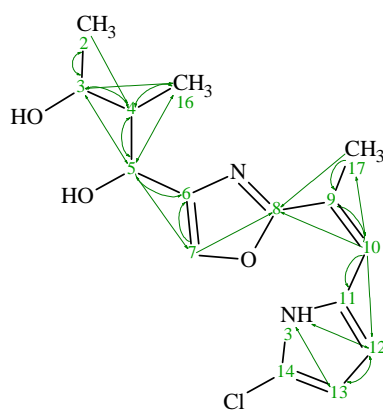
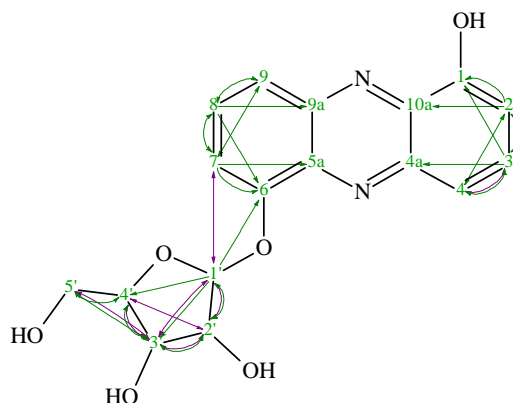
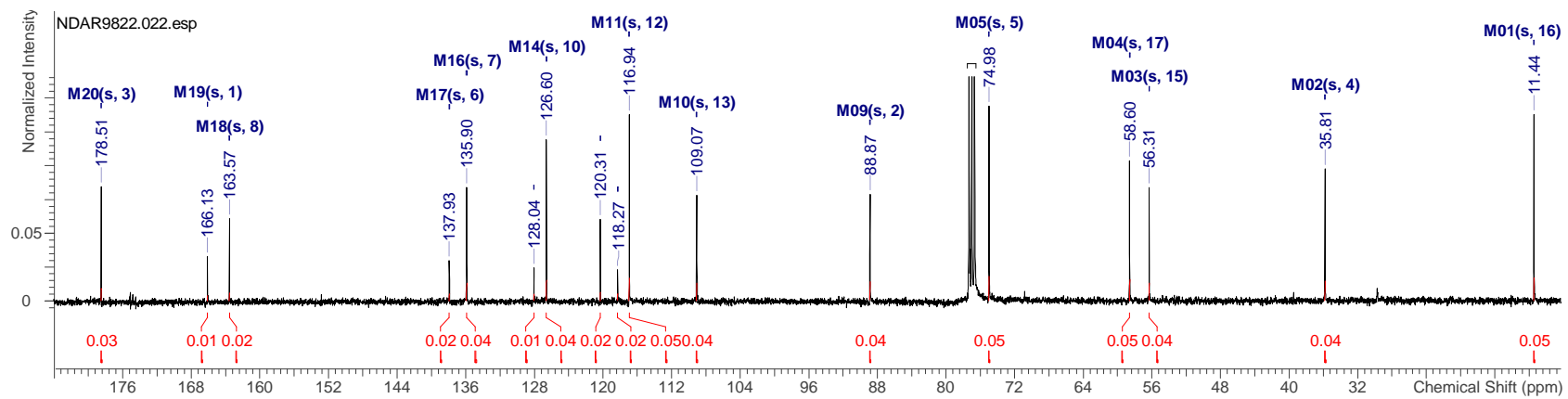
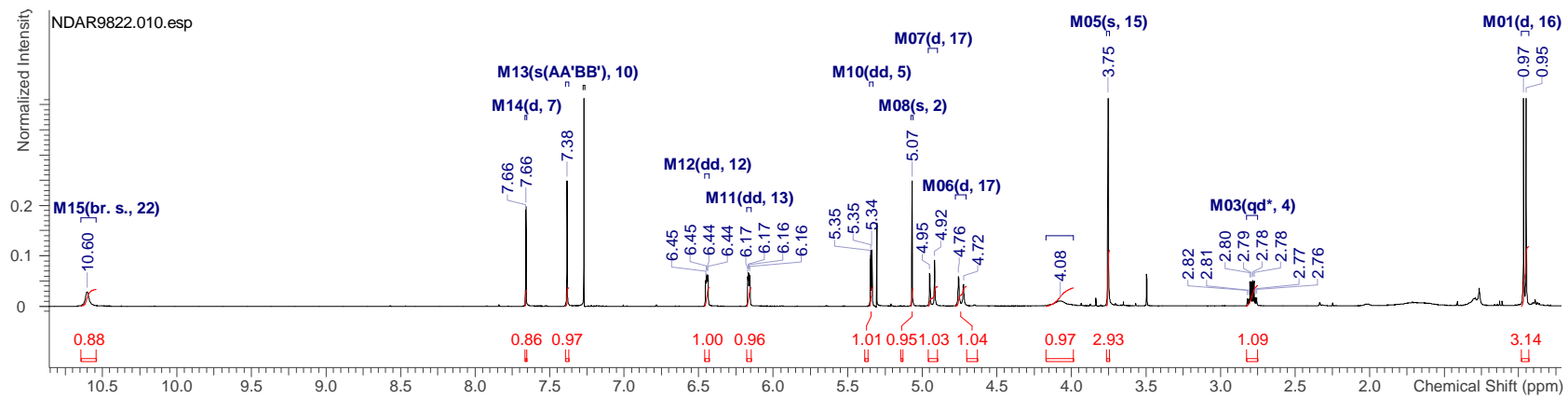


Figure DS5. HMBC-correlations of Pyrronazol C2 (5)

Figure DS6. HMBC- (green) and ROESY (violet) correlations of 1,6-Phenazine-diol- α -D-arabinofuranoside (7)Table DS6. NMR Data of 1,6-Phenazine-diol- α -D-arabinofuranoside (7) in CD₃OD [¹H 600 MHz; ¹³C 100 MHz]

Pos.	δ_{H}	H	J [Hz]	ROESY	δ_{C}	m	H in HMBC
1					154.73	C	2, 3
10a					137.45	C	2
2	7.22	br. d	6.2		111.69	CH	
3	7.80	m		4	133.51	CH	
4	7.78	m		3	120.10	CH	2
4a					144.14	C	3
5a					138.48	C	7
6					152.94	C	1', 7, 8
7	7.57	br. d	7.3	1'	115.07	CH	9
8	7.82	m			131.60	CH	
9	8.01	br. d	7.7		124.10	CH	7
9a					143.91	C	8
1'	5.95	br. s		3', 2', 7	109.09	CH	
2'	4.65	dd	3.3, 1.1	3', 4', 1'	83.09	CH	3'
3'	4.08	dd	5.5, 3.3	5'ab, 4', 1', 2'	78.90	CH	5'ab, 4', 2', 1'
4'	4.18	td	5.2, 3.5	3', 2'	87.84	CH	5'b, 1'
5'a	3.78	dd	12.1, 3.3	5'b, 3'			3'
5'b	3.70	dd	12.1, 5.5	5'a, 3'	63.05	CH ₂	3'



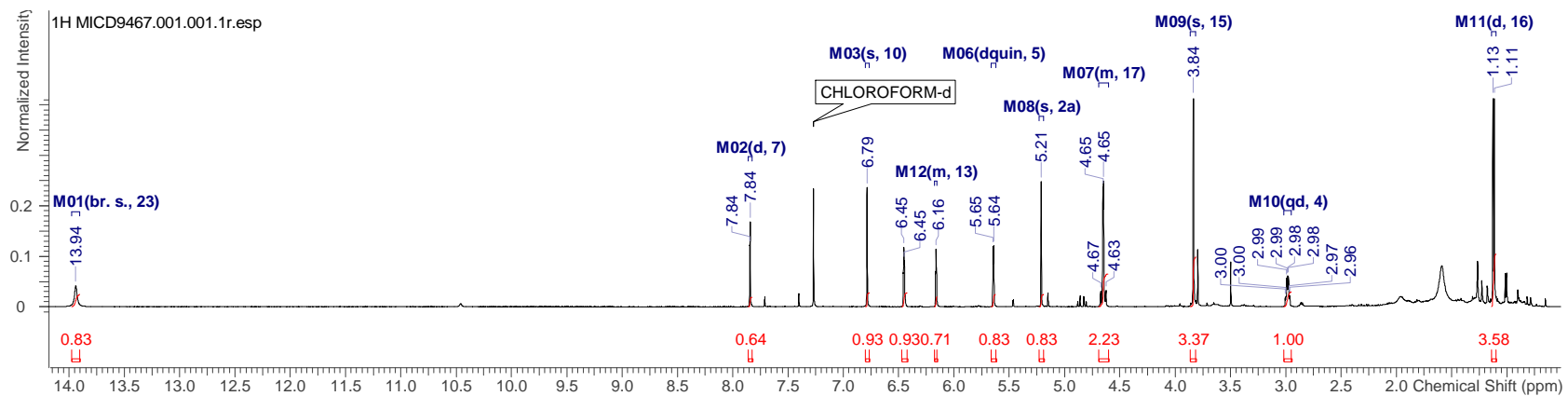


Figure DS9. ¹H NMR spectrum of Pyrronazol A2 (2) in CDCl₃ (600 MHz)

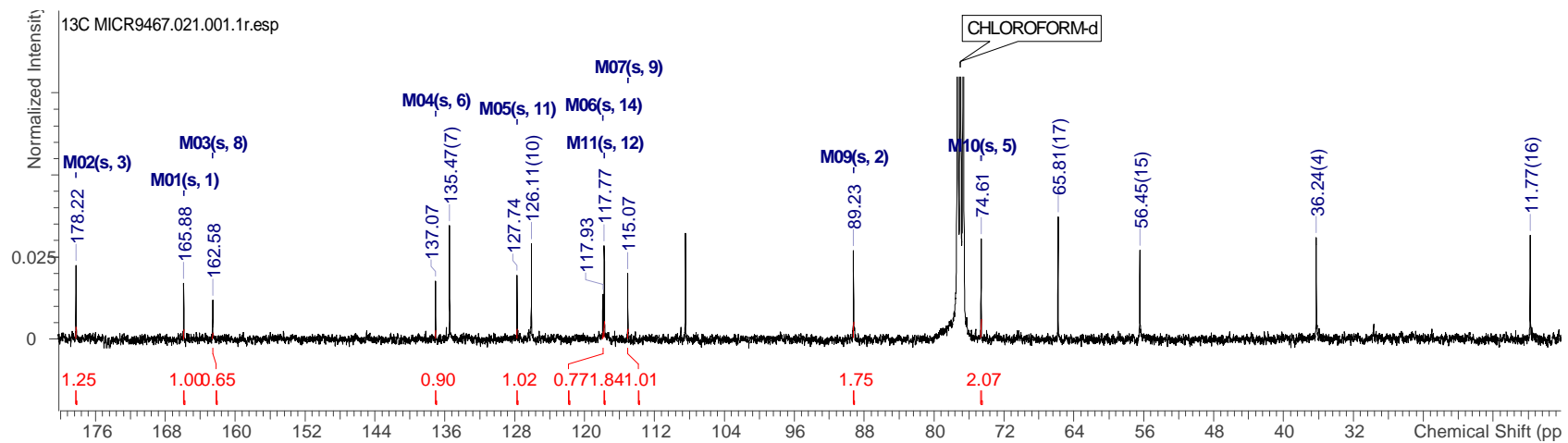


Figure DS10. ¹³C NMR spectrum of Pyrronazol A2 (2) in CDCl₃ (100.6 MHz)

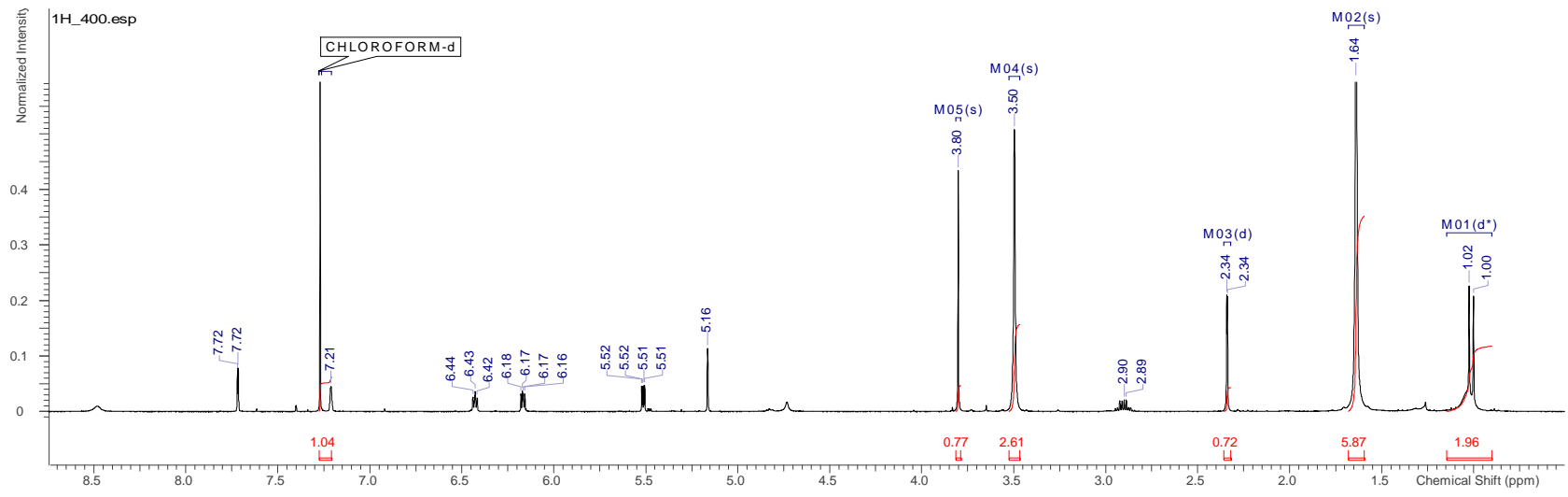


Figure DS11. ¹H NMR spectrum of Pyrronazol B (3) in CDCl₃ (400 MHz)

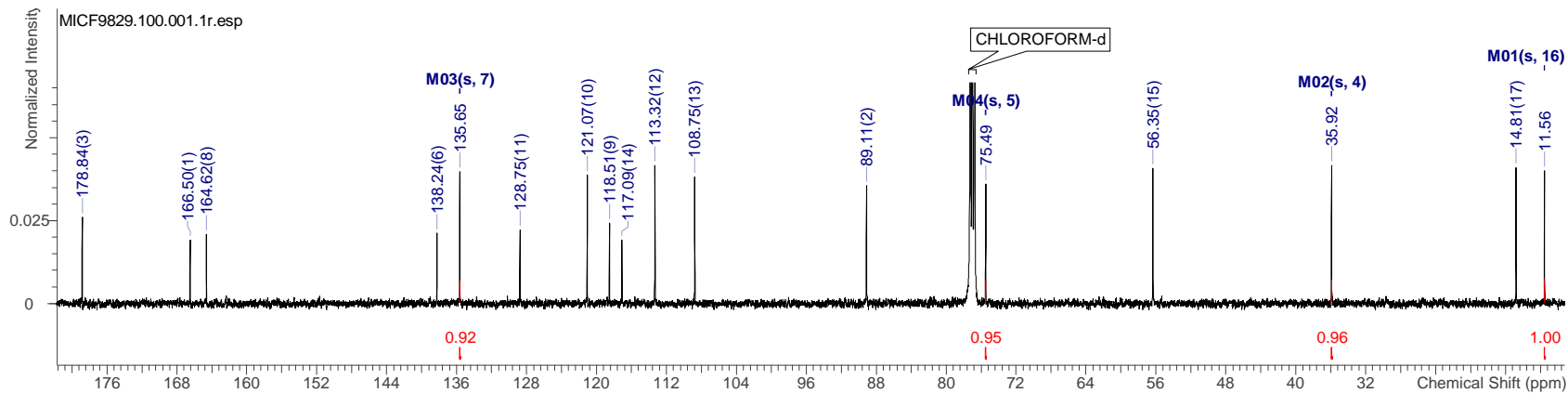
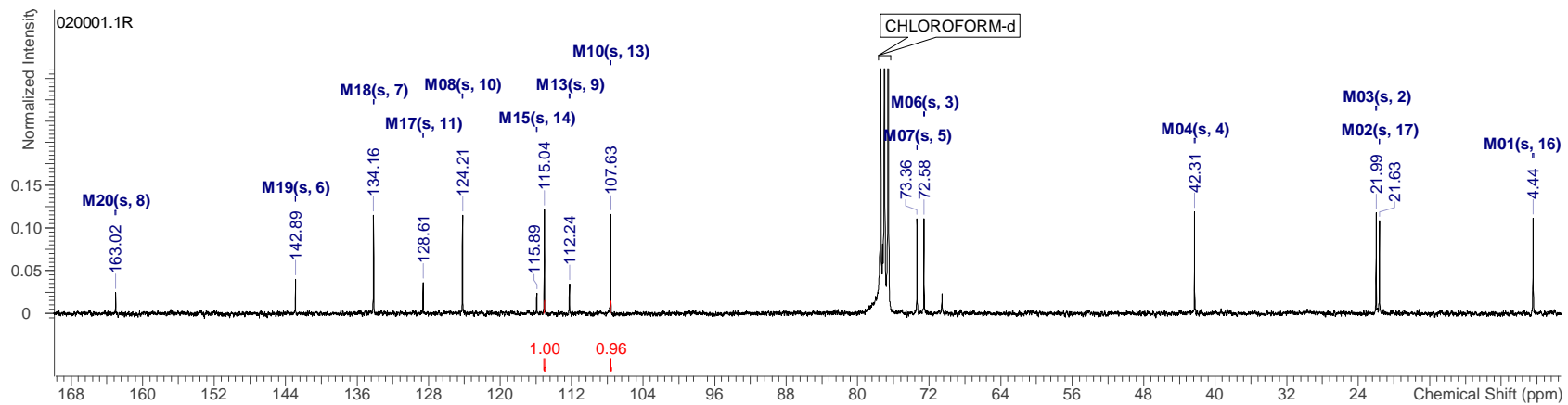
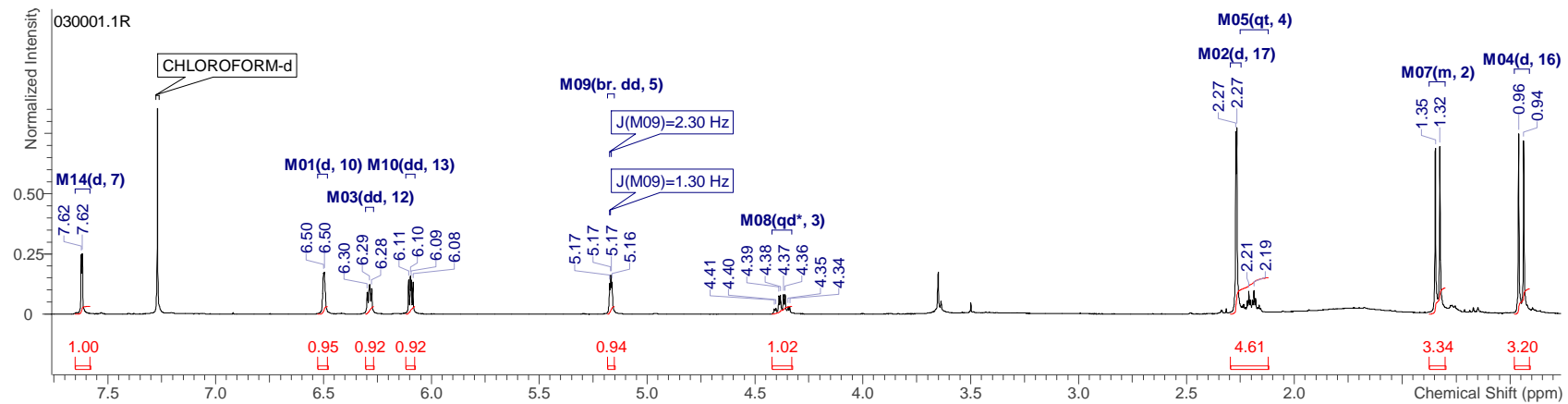
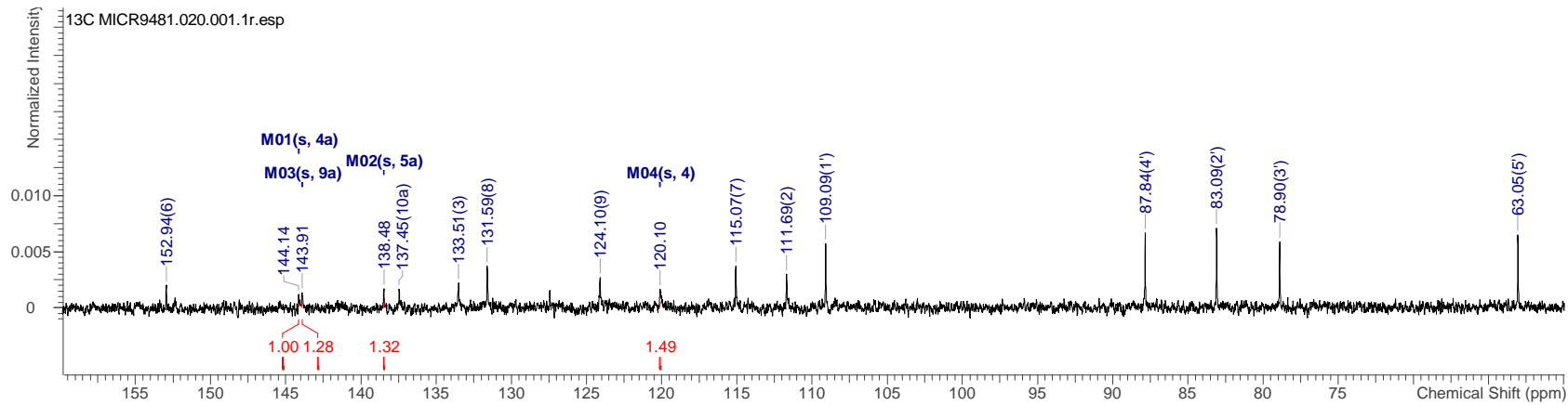
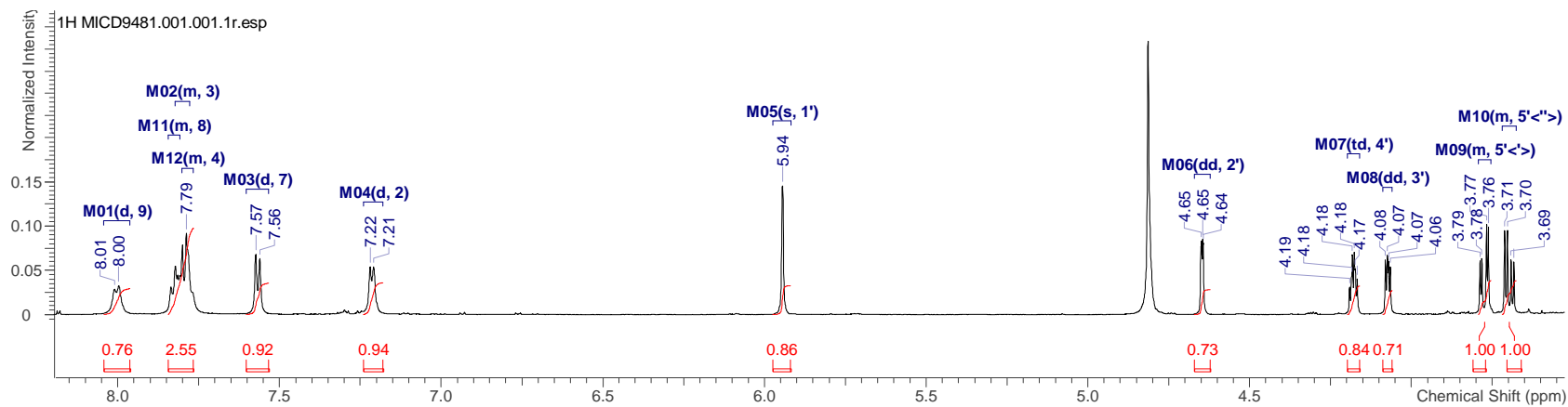


Figure DS12. ¹³C NMR spectrum of Pyrronazol B (3) in CDCl₃ (125.8 MHz)





Chapter E

Discussion

It is evident that microbes are accountable for plethora of human and animal ailments but the fact that most drugs currently in clinical application have been derived from microorganisms is also undeniable (Newman and Cragg, 2012). While fungi and actinobacteria have long established themselves as two of the most renowned sources of microbial drugs, other groups like *Bacillus*, cyanobacteria and myxobacteria are slowly emerging as the future potential sources for microbial drugs (Berdy, 2012). New technologies based on genome mining, high throughput screening and modern purification methods complement the age old culture based methods of drug discovery and aid to explore the metabolic diversity of the microbial world. This study mainly focused on discovery of novel microbial natural products and myxobacterial taxons and the outcome and future prospects of the study are discussed in this chapter.

E.1. Paenilarvins, antifungal peptides from honey bee pathogen, *Paenibacillus larvae*

Paenibacillus larvae has been the subject of studies since many decades to unravel the virulence factors and the strategies it employs during infection of the host i.e. honey bee larvae. The partial genome sequences available and the proteomics studies have helped to determine some important virulence factors and their role in pathogenesis including toxins, proteases, and S-layer protein (Fünfhaus *et al.*, 2009; Antunez *et al.*, 2010). It is also evident from the results that both prominent genotypes of *P. larvae*, ERIC I and II adapt different approaches for infection (Poppinga *et al.*, 2012; Fünfhaus *et al.*, 2013).

Complete genome sequencing and annotation of *P. larvae* ERIC I and II in the group of Prof. Rolf Daniel, University of Göttingen, brought into light an astounding arsenal of virulence factors that could possibly allow the pathogen to conquer various sites in the host throughout the course of infection (Djukic *et al.*, unpublished). One of the

most interesting sequences confirmed from this study with respect to pathogenicity were the NRPS and NRPS/PKS hybrid biosynthetic gene clusters which putatively coded for some secondary metabolites (Fünfhaus *et al.*, 2009).

With the aim of finding the bioactive products of these biosynthetic gene clusters,



Fig.E1. Antifungal activity of crude methanol extract of *P. larvae* ERIC II (DSM 25430) against *Mucor hiemalis* after HPLC fractionation

methanol extracts from *P. larvae* ERIC I and ERIC II were screened for antimicrobial activity and exhibited antifungal activity. Bioactivity guided HPLC and LC-MS data analysis of *P. larvae* ERIC II extracts indicated production of a group of lipopeptides with masses ranging from 1069 to 1112 Da. Characterization of the pure compounds based on molecular

formulae and UV spectra revealed their affiliation to iturin family compounds including iturins, mycosubtilin and bacillomycin which are known to be produced by most *Bacillus* species (Ongena and Jacques, 2008). This family of compounds along with other *Bacillus* lipopeptides plays an important role in control of fungal phytopathogens in their natural environments (Romero *et al.*, 2007) establishing their producers as versatile biocontrol agents (Zerriouh *et al.*, 2011).

The complete structure elucidation of some of the lipopeptides produced by *P. larvae* using NMR spectroscopy and MS-MS fragmentation firmly established the resemblance of these lipopeptides to Mojavensin A, produced by *Bacillus mojavensis* B0621A (Ma *et al.*, 2012) except the length of the β -Aa side chain in one of the compounds and replacement of asparagine by aspartic acid in another. All the other compounds obtained were found to be derivatives of these two major classes with the difference in the length of the β -Aa side chain.

These lipopeptides were named paenilarvins and the major products were paenilarvins A-C. The antifungal activity observed for paenilarvins against certain fungi was significantly higher than reported for Anteiso-C15 mojavensin A (1) against some soil-borne phytopathogens like *Valsa mali*, *Fusarium oxysporum* f. sp. *cucumerinum*, and *Fusarium verticillioides* (Ma *et al.*, 2012). However, *P. larvae* can never be utilized for phytopathogen control because of its lethal effects on *Apis mellifera* whereas in fact the simultaneous production of many lipopeptides like

surfactins, fengycins and iturins, with good biological activity by the marine- derived bacterium *Bacillus mojavensis* B0621A makes it a potential biocontrol agent (Ma *et al.*, 2012).

Paenilarvins exhibited no antibacterial activity but some cytotoxic activity against mouse fibroblast cell line L929. Further experiments using different concentrations of compounds on honey bee larvae can help to determine their larval toxicity. Paenilarvins could be directly insecticidal to the bee larvae like bassianolide, an insecticidal cyclodepsipeptide produced by the fungus, *Beauveria bassiana* and *Verticillium lecanii* (currently known as *Lecanicillium lecanii*), which elicits atonic symptoms in silkworm larvae (Kanoaka *et al.*, 1977) or they could indirectly assist in disease progression.

Production of secondary metabolites with antibiotic activity by a pathogen is very common in order to eliminate other potential pathogens of the same host (Axelrod *et al.*, 1988). Many infectious agents like parasites, mites, fungi and viruses apart from *P. larvae* pose a serious threat to honey bee larvae (Murray and Aronstein, 2008; Puerta *et al.*, 1999) and production of paenilarvins could help the producer to establish its dominance over other pathogens. They might also give a growth advantage to the pathogen in the competitive environment of larval gut microflora.

It has been proven that antibiotics can act at much lower concentrations than their lethal dose in natural environments and target and regulate different genes including virulence genes (Aminov, 2009). A polypeptide encoded by a NRPS in the citrus pathogen *Alternaria alternata*, can regulate siderophore and melanin production, iron uptake under low iron conditions, oxidative stress resistance, conidia formation and virulence (Chen *et al.*, 2013).

Thus, it can be speculated that paenilarvins aid the pathogen during infection using any of the above mentioned or any other mechanism but their exact role in disease progression still needs to be thoroughly investigated. Construction of *P. larvae* mutants lacking expression of NRPS/PKS gene cluster responsible for paenilarvin production can help to ascertain their role as virulence factors. An insight into the biosynthesis of paenilarvins in *P. larvae* and their precise molecular mechanism of action inside the bee larvae is also essential. Another main objective for future should

be identification, purification and characterization of the products of other NRPS/PKS gene clusters in the *P. larvae* genome and to establish their role in pathogenesis.

E.2. *Aggregicoccus edoensis* gen. nov., sp. nov., a soil myxobacterium with characteristic aggregation

Myxococcaceae include four genera of myxobacteria, namely, *Myxococcus*, *Corallocooccus*, *Pyxidicooccus* and *Anaeromyxobacter*. No new genus has been added to the family since the description of facultative anaerobic *Anaeromyxobacter dehalogenans* in 2002 (Sanford *et al.*, 2002). Hereby we describe a novel genus in the *Myxococcaceae*, *Aggregicoccus* represented by two strains of the novel species *A. edoensis*, MCy1366^T (Ar1733^T) and MCy10622 (SBCy015) which were isolated from soil samples from different locations (Japan, Switzerland resp.) and at different times (1980, 2013 resp.) at HZI in our continuing efforts to isolate new myxobacteria.

The 16S rRNA gene sequence of strain MCy1366^T was analyzed together with other 50 myxobacterial strains selected from our in house myxobacterial strain collection. It exhibited only 97.56% 16S rRNA gene sequence similarity to *Stigmatella koreensis* strain KYC-1019 (no valid description available, accession no. EF112185) in BLAST N analysis and branched out notably from all other known genera of myxobacteria in the phylogenetic tree. Hence, it was chosen for further study as a novel taxon.

Strain MCy10622 was isolated by Ram Awal Prasad, Helmholtz Institute for Pharmaceutical Research, Saarbrücken and characterized as strain belonging to *Myxococcaceae*. It was upon comparison of the 16S rRNA gene sequence of MCy1366^T with MCy10622 that they were found to be 99.9% similar and hence, representing the same taxon. The morphological characteristics like swarming pattern and shape and size of fruiting body like structures, vegetative cells and myxospore like structures indicated that the two strains belong to the family *Myxococcaceae*.

A polyphasic approach including genotypic, phenotypic and chemotypic features was followed to investigate the reliable taxonomic status of MCy1366^T and MCy10622 because of their close relation to *Corallocooccus* species (97%) on the basis of 16S rRNA gene sequences and similar G+C content (65.6%). The 3% sequence

divergence suggested the two novel strains to represent a new species but in depth analysis was needed to confirm the results.

The two isolates under study were checked for their physiological characteristics like antibiotic resistance, carbon and nitrogen source requirements, optimum temperature and pH for growth, starch, chitin and cellulose degradation, Congo Red reaction, salt tolerance, microbial predation and APIZym assay for enzyme production. Most of the results from the physiological studies like positive Congo Red reaction, inability to degrade monosaccharides, disaccharides, chitin and cellulose definitely placed them in the family *Myxococcaceae* but could not provide any clear delineation from the already known genera in the family.

Fatty acid content including FA types, FA ratio and major FA markers have been successfully used to determine the chemo-phylogenetic relationship within the order Myxococcales (Garcia *et al.*, 2011). Around 34 FAs have been reported in members of the family Myxococcaceae (Garcia *et al.*, 2011), but only 26 could be detected in MCy1366^T and 27 in MCy10622, some of which were present in very minute quantities. The close divergence of MCy1366^T and MCy10622 from *Corallococcus exiguus* and *C. coralloides* was reflected in their SCFAs to BCFAs ratio. An extensive analytical study of FA profiles of MCy1366^T and MCy10622 along with other closely related strains in comparison to the FA profiles of other myxobacteria already illustrated in literature supported the taxonomic placement of the new isolate into a new taxon.

DNA-DNA hybridization is based on comparison between whole genomes of two bacterial strains and has been applied as one of the most important tools for bacterial systematics since almost 50 years (Goris *et al.*, 2007). A group of bacteria showing 70% or more DNA-DNA relatedness is often regarded as belonging to same species (Prakash *et al.*, 2007). So, DNA-DNA hybridization was employed to ascertain the status of MCy1366^T and MCy10622 as a new genus or a new species. 28-35% DNA-DNA relatedness of MCy1366^T with *Corallococcus* spp. and 100% DNA-DNA relatedness of MCy1366^T with MCy10622 clearly advocated their description as two isolates of one species in a new genus.

Matrix assisted laser desorption ionization time-of-flight (MALDI-TOF) mass spectrometric analysis has become an important tool in chemotaxonomic classification of bacteria using some proteins as biomarkers or the comparison of the proteomics spectra of a group of related bacteria (Lay, 2000). MALDI-TOF MS has been successfully used for classification up to genus, species and subspecies level (Murray, 2010). The ability of this technique to differentiate between methicillin - sensitive and methicillin-resistant *Staphylococcus aureus* projects its true potential in bacterial strain typing as well (Edwards-Jones *et al.*, 2000). When MALDI-TOF MS was used to study the chemotaxonomic relations between MCy1366^T with MCy10622 and the other members of the family *Myxococcaceae*, the dendrogram obtained after data analysis showed clear delineation of the new isolates from *Corallococcus Myxococcus* and *Pyxidicoccus* spp.

Based on the polyphasic analysis, especially 16S rRNA gene sequences, DNA-DNA hybridization and MALDI-TOF data, it could be determined that novel strains, MCy1366^T and MCy10622 represent a new genus (*Aggregicoccus*) and species (*Aggregicoccus edoensis*).

As exemplified in section 5.1, screening of novel taxa for secondary metabolites is a promising approach towards discovery of novel natural products. This suggests that screening of the novel isolates, MCy1366^T and MCy10622 under optimum growth conditions and methodical analysis of its metabolome can lead to detection of yet unexplored products.

E.3. Pyrroazols and phenazines from *Nannocystis pusilla*

Bacteria of the genus *Nannocystis* represent the family *Nannocystaceae* within Myxococcales and are closely related to marine myxobacteria like *Enhygromyxa*, *Pseudenhygromyxa* and *Plesiocystis*. The secondary metabolite potential of *Nannocystis* spp. has not been thoroughly exploited. They have been reported to produce only few compounds like phenylannolones (Ohlendorf *et al.*, 2008), germacran (Reichenbach and Höfle, 2000), geosmin (Trowitzsch *et al.*, 1981) and the siderophores called nannochelins (Kunze *et al.*, 1992). This could be due to the description and availability of only two species in this genus, *N. exedens* and *N. pusilla* till date.

Nannocystis pusilla, strain Ari7 was selected from the 50 myxobacterial strains which were screened when it showed some antifungal activity in the course of preliminary screening. During HPLC-UV-HRESIMS data analysis, it was found to produce pyrronazols, which had been identified previously in another *Nannocystis* strain but remained unpublished. Pyrronazols represent a novel structural class of secondary metabolites constituting chlorinated pyrrole-oxazole-pyrones showing very weak activity against the filamentous fungi, *Mucor hiemalis*. Three pyrronazol variants, pyrronazol A, A2 and B were isolated and characterized from strain Ari7. The other known derivatives of pyrronazol, pyrronazol C1 and pyrronazol C2 had been isolated from *N. pusilla*, strain Na 174. Pyrronazols were detected in extracts from both species of *Nannocystis*, *N. pusilla* and *N. exedens* but not from any other myxobacteria screened during our screening program, which leads us to speculate that pyrronazols production is limited to this genus only and thus has the potential to be used as a chemotaxonomic biomarker in future.

N. pusilla strains Ari7 and Na a174 were isolated from Langeoog Island in Germany and Rhodos Island in Greece, respectively, which suggests their close association with the marine environment. In this perspective, it is very fascinating to note the resemblance in the molecular structures of pyrronazols and phorbazoles, which have been isolated from the marine sponge, *Phorbis aff. clathrata* (Rudi *et al.*, 1994) and the marine mollusk, *Aldisa andersoni* (Nuzzo *et al.*, 2012). The detection of phorbazoles in *A. andersoni* extracts can be mostly accredited to their feeding on *Phorbis* sponges. Phorbazoles are chlorinated phenyl-pyrrolyl-oxazoles which differ in the number and position of the chlorine atoms.

The two phorbazole derivatives, 9-chloro-phorbazole D and N1-methyl-phorbazole A exhibited good inhibitory activity against many human cancer cell lines (Nuzzo *et al.*, 2012) while pyrronazol A failed to show any significant activity against the cell lines tested. The similarity between the structures for both these classes of compounds suggests that chemical modification of pyrronazols might help to enhance their biological activity.

Three other natural compounds closely related to pyrronazols are pyroluteorin (Takeda, 1958), pyrrolomycin B (Kaneda *et al.*, 1981) and pyrrolnitrin (Arima *et al.*,

1964). Pyrrolnitrin and its derivatives were long known to be produced by *Pseudomonas* species but were discovered for the first time from a myxobacterial strain of *Myxococcus fulvus* (Gerth *et al.*, 1982). Pyrrolnitrin was later detected in many other myxobacteria from the suborder *Cystobacterineae* including *Coralloccoccus* and *Cystobacter* (Gerth *et al.*, 1982).

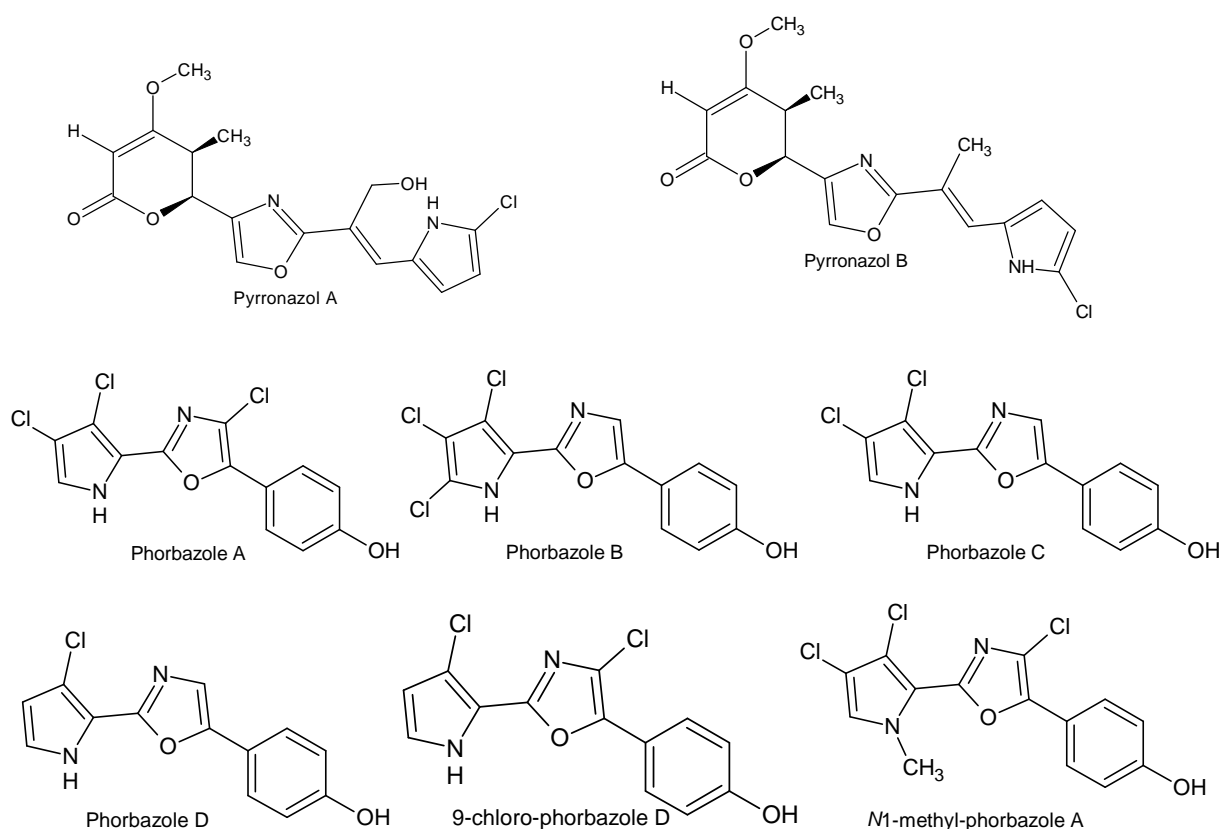


Fig.E2. Structures of pyrronazols and phorbazoles

Natural products containing heterocyclic rings can also be found from other sources like fungi and plants besides bacteria and marine organisms (Gribble, 1996). The fungus *Auxarthron umbrinum* along with other members of order Onygenales are known to produce a pyrrolylpolyene called rumbrin (Yamagishi *et al.*, 1993). Rumbrin structurally resembles pyrronazol with the presence of a pyrrole and a pyrone ring, here completely unsaturated. Rumbrin was found to possess potent cytoprotective (Yamagishi *et al.*, 1993) and calcium-accumulation inhibitory activities (Yamagishi and Shindo, 1993). An isomer of rumbrin, 12*E*-isorumbrin also showed potent anticancer activity (Clark *et al.*, 2006). It can be speculated that pyrronazols may also

exhibit such distinct biological activities if tested in some exclusive screening program.

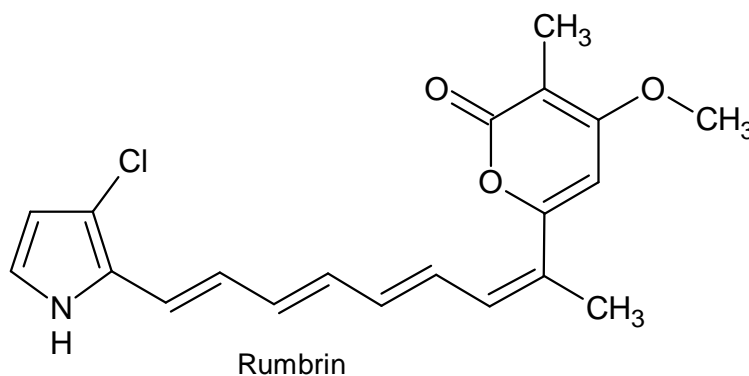


Fig. E3. Structure of Rumbrin

N. pusilla, strain Ari7 also produced two phenazine compounds, 1,6-phenazinediol and 1-hydroxy-phenazine-6-yl- α -D-arabinofuranoside in addition to pyrrolozols. Phenazines have been reported from a wide variety of bacteria like *Nocardia*, *Brevibacterium*, *Burkholderia*, *Pseudomonas* and *Streptomyces* (Dwivedi and Johri, 2003,). The phenazine antibiotic, myxin was first isolated from *Sorangium sp.* and reported to exhibit potent antimicrobial activity (Peterson *et al.*, 1966). 1,6-phenazinediol was first reported from *Streptomyces thioluteus* (Akabori and Nakamura, 1959).

Though phenazines are versatile natural compounds and more than 100 structural derivatives have been identified from numerous bacteria, phenazine glycosides are rarely encountered as natural products (Abdelfattah *et al.*, 2011). Izuminosides (Abdelfattah *et al.*, 2011), phenazoviridine (Kato *et al.*, 1993), aestivopheonins (Shin-Ya *et al.*, 1995) and L-quinovose esters of saphenic acid (Pathirana *et al.*, 1992) are amongst the few phenazine glycosides which have been primarily known to be produced by actinomycetes. This is the first report of the production of a phenazine glycoside from myxobacteria.

Pseudomonads are known to suppress the growth and survival of competitive microbes by production of many secondary metabolites including pyrroles and phenazines (Dwivedi and Johri, 2003) and the occurrence of both these classes of compounds from a single myxobacterial strain suggest that the biosynthetic gene

clusters or biosynthetic pathways for these two classes of compounds could be linked in some way. It also explains the antifungal effects of crude methanol extract of strain Ari7 and implicates the possibility of use of these compounds by the producer for its competitive fitness in its natural environment.

References

- Abdelfattah, M.S., Toume, K., and Ishibashi, M. (2011) Isolation and structure elucidation of izuminosides A–C: a rare phenazine glycosides from *Streptomyces* sp. IFM 11260. *J. Antibiot.* 64, 271–275
- Akabori, H., and Nakamura, M. (1959) 1,6-Dihydroxyphenazine, an antibiotic produced by *Streptomyces thioluteus*. *J. Antibiot.* 12, 17-20
- Aminov, R. I. (2009) The role of antibiotics and antibiotic resistance in nature. *Environ. Microbiol.* 11(12), 2970–2988
- Antunez, K., Anido, M., Evans, J. D., and Zunino, P. (2010) Secreted and immunogenic proteins produced by the honeybee bacterial pathogen, *Paenibacillus larvae*. *Vet. microbiol.* 141, 385-389
- Arima, K., Imanaka, H., Kausaka, M., Fukuda, A., and Tameera, C. (1964) Pyrrolnitrin, a new antibiotic substance, produced by *Pseudomonas*. *Agric. Biol. Chem.* 28, 575–576
- Axelrod, P.E., Rella, M. and Schroth, M.N. (1988) Role of antibiosis in competition of *Erwinia* strains in potato infection courts. *Applied and Environmental microbiology*, 54(5), 1222-1229
- Berdy, J. (2012) Thoughts and facts about antibiotics: Where we are now and where we are heading. *J. Antibiot.* 65, 385–395
- Chen, L., Lin, C., and Chung, K. (2013) A nonribosomal peptide synthetase mediates siderophore production and virulence in the citrus fungal pathogen *Alternaria alternate*. *Molecular Plant Pathology.* 14(5), 497–505
- Clark, B. R., Capon, R. J., Lacey, E., Tennant, S., and Gill, J. H. (2006) Polyenylpyrroles and Polyenylfurans from an Australian Isolate of the Soil Ascomycete *Gymnoascus reessii*. *Org. Lett.*, 8, 701–704
- Dwivedi, D., and Johri, B.N. (2003) Antifungals from fluorescent pseudomonads: Biosynthesis and regulation. *Current Science.* 85(12), 1693-1703
- Edwards-Jones, V., Claydon, M., Evason, D., Walker, J., Fox, A. J., and Gordon, D. B. (2000) Rapid discrimination between methicillin-sensitive and methicillin-resistant *Staphylococcus aureus* by intact cell mass spectrometry. *J. Med. Microbiol.* 49, 295–300
- Fünfhaus, A., Ashiralieva, A., Borriss, R. and Genersch, E. (2009) Use of suppression subtractive hybridization to identify genetic differences between differentially virulent genotypes of *Paenibacillus larvae*, the etiological agent of American Foulbrood of honeybees. *Environ. Microbiol. Rep.* 1, 240-250
- Fünfhaus, A., Poppinga, L., and Genersch, E. (2013) Identification and characterization of two novel toxins expressed by the lethal honey bee pathogen *Paenibacillus larvae*, the causative agent of American foulbrood. *Environ. Microbiol.* doi:10.1111/1462-2920.12229
- Garcia, R., Pistorius, D., Stadler, M. & Müller, R. (2011) Fatty acid related phylogeny of myxobacteria as an approach to discover polyunsaturated omega-3/6 fatty acids. *J. Bacteriol.* 193, 1930-1942
- Genoveffa Nuzzo, G., Ciavatta, M. L., Kiss, R., Mathieu, V., Leclercqz, H., Manzo, E., Villani, G., Mollo, E., Lefranc, F., D'Souza, L., Gavagnin, M., and Cimino, G. (2012) Chemistry of the Nudibranch *Aldisa andersoni*: Structure and Biological Activity of Phorbazole Metabolites. *Mar. Drugs* 10, 1799-1811

- Gerth, K., Trowitzsch, W., Wray, V., Höfle, G., Irschik, H., and Reichenbach, H. (1982) Pyrrolnitrin from *Myxococcus fulvus*. *J. Antibiot.* 35, 1101-1103
- Goris, J., Konstantinidis, K. T., Klappenbach, J. A., Coenye, T., Vandamme, P., and Tiedje, J. M. (2007) DNA–DNA hybridization values and their relationship to whole-genome sequence similarities. *Intern. J. Syst. Evol. Microb.* 57, 81–91
- Gribble, G. W. (1996) Pyrroles and their Benzo Derivatives: Applications. Reference Module in Chemistry, Molecular Sciences and Chemical Engineering-Comprehensive Heterocyclic Chemistry II. Pages 207–257
- Kaneda, M., Akamura, S., Ezaki, N., and Iitaka, Y. (1981) Structure of Pyrrolmycin B, a chlorinated nitro-pyrrole antibiotic. *J. Antibiot.* 34, 1366-1368
- Kanoaka, M., Isogai, A., Murakoshi, S., Ichinoe, M., Suzuki, A. and Tamura, S. (1977) Bassianolide, a new insecticidal cyclodepsipeptide from *Beauveria bassiana* and *Verticillium lecanii*. *Agric. Biol. Chem.*, 42(3), 629-635
- Kato, S., Shindo, K., Yamagishi, Y., Matsuoka, M., Kawai, H., and Mochizuki, J. (1993) Phenazoviridin, a novel free radical scavenger from *Streptomyces* sp. *J. Antibiot.* 46, 1485–1493
- Kunze, B., Trowitzsch-Kinast, W., Höfle, G. and Reichenbach, H. (1992) Nannocheline A, B and C, new iron chelating compounds from *Nannocystis exedens* (Myxobacteria). *J. Antibiot.* 45, 147-150
- Lay, J. O. (2000) MALDI-TOF mass spectrometry and bacterial taxonomy. *Trends in analytical chemistry*. 19, 8
- Ma, Z., Wang, N., Hu, J., and Wang, S. (2012) Isolation and characterization of a new iturinic lipopeptide, mojavensin A produced by a marine-derived bacterium *Bacillus mojavensis* B0621A. *J. Antib.* 00, 1-6
- Murray, K. D., Aronstein, K. A. (2008) Transformation of the Gram-positive honey bee pathogen, *Paenibacillus larvae*, by electroporation. *J. Microbiol. Meth.* 75, 325–328
- Murray, P.R. (2010) Matrix-assisted laser desorption ionization time-of-flight mass spectrometry: usefulness for taxonomy and epidemiology. *Clin. Microbiol. Infect.* 16, 1626–1630
- Newman, D.J., and Cragg, G.M. (2012) Natural products as sources of new drugs over the 30 years from 1981 to 2010. *J. Nat. Prod.* 75, 311–335
- Ohlendorf, B., Leyers, S., Krick, A., Kehraus, S., Wiese, M., and König, G. M. (2008) Phenylannolones A–C: Biosynthesis of New Secondary Metabolites from the Myxobacterium *Nannocystis exedens*. *ChemBioChem.* 9, 2997 – 3003
- Ongena, M., and Jacques, P. (2008) Bacillus lipopeptides: versatile weapons for plant disease biocontrol. *Trends Microbio.* 16, 115–125
- Pathirana, C., Jensen, P. R., Dwight, R., and Fenical, W. (1992) Rare phenazine L-quinovose esters from a marine actinomycete. *J. Org. Chem.* 57, 740–742
- Peterson, E. A., Gillespie, D. C., and Cook, F. D. (1966) A wide spectrum antibiotic produced by a species of *Sorangium*. *Can. J. Microbiol.* 12, 221–230
- Poppinga, L., Janesch, B., Fünfhaus, A., Sekot, G., Garcia-Gonzalez, E., et al. (2012) Identification and Functional Analysis of the S-Layer Protein SplA of *Paenibacillus larvae*, the Causative Agent of American Foulbrood of Honey Bees. *PLoS Pathog.* 8(5): e1002716. doi:10.1371/journal.ppat.1002716

- Prakash, O., Verma, M., Sharma, P., Kumar, M., Kumari, K., Singh, A., Kumari, H., Jit, S., Gupta, S.K., Khanna, M., and Lal, R. (2007) Polyphasic approach of bacterial classification – An overview of recent advances. *Indian J. Microbiol.* 47:98–108
- Puerta, F., Flores, J. M., Ruiz, J. A., Ruz J. M. and Centro, C. (1999) Fungal diseases of the honeybee (*Apis mellifera* L.). In: Colin M.E. (ed.), Ball B.V. (ed.), Kilani M. (ed.). *Bee disease diagnosis*. Zaragoza : CIHEAM, 61-68
- Reichenbach, H., and Höfle, G.(2000) in *Drug Discovery from Nature* (Eds. Grabley, S.; Thierecke, R.), Springer, Heidelberg, p. 173
- Romero, D., de Vicente, A., Rakotoaly, R. H., Dufour, S. E., Veening, J. W., Arrebola, E., Cazorla, F. M., Kuipers, O. P., Paquot, M., and Pérez-García, A. (2007) The iturin and fengycin families of lipopeptides are key factors in antagonism of *Bacillus subtilis* toward *Podosphaera fusca*. *Mol. Plant Microbe Interac.* 20, 430–440
- Rudi, A., Stein, Z., Green, S., Goldberg, I., Kashman, Y., Benayahu, Y., and Schleyer, M. (1994) Phorbazoles A-D, Novel Chlorinated Phenylpyrrolyloxazoles from the Marine Sponge *Phorbos aff. clathrata*. *Tetrahedron. Lett.* 35, 2589-2592
- Sanford, R. A., Cole, J. R., and Tiedje, J. M. (2002) Characterization and Description of *Anaeromyxobacter dehalogenans* gen. nov., sp. nov., an Aryl-Halorespiring Facultative Anaerobic Myxobacterium. *App. Env. Microb.* 893–900
- Shin-Ya, K. Shimizu, S., Kunigami, T., Furihata, K., Hayakawa, Y., and Seto, H. (1995) Novel neuronal cell protecting substances, aestivophoenins A and B, produced by *Streptomyces purpeofuscus*. *J. Antibiot.* 48, 1378–1381
- Takeda, R. (1958) Structure of new antibiotic, Pyoluteorin. *J. Am. Chem. Soc.* 80, 4749-4750
- Trowitzsch, W., Witte, L., and Reichenbach, H. (1981) Geosmin from earthy smelling cultures of *Nannocystis exedens* (Myxobacterales). *FEMS Microbiol. Lett.* 12, 257-260
- Yamagishi, J., and Shindo, K. (1993) Japanese Patent 5039288-A
- Yamagishi, Y., Matsuoka, M., Odagawa, A., Kato, S., Shindo, K., and Mochizuki, J. (1993) Rumbrin, a new cytoprotective substance produced by *Auxarthron umbrinum*. *J. Antibiot.* 46 (6), 884-887
- Zeriuoh, H., Romero, D., García-Gutiérrez, L., Cazorla, F. M., de Vicente, A. and Pérez-García, A. (2011) The Iturin-like lipopeptides are essential components in the biological control arsenal of *Bacillus subtilis* against bacterial diseases of Cucurbits. *Mol. Plant Microbe Interac.* 24, 12, 1540–1552

Summary

With the advent of new pathogens and upsurge in the number of antibiotic resistant microbes, concerted efforts need to be made by pharmaceutical, biotechnological and academic communities to pace up the antibiotic discovery programs and combat these deadly pathogens to ensure progress in health sector. Natural products continue to be a plenteous source of new chemical entities with distinct biological activities in extended screening programs. Microbe derived natural products and analogues have found applications in wide range of fields from pharmaceuticals to agriculture.

The present thesis mainly focused on natural products isolation and characterization from myxobacteria and *Paenibacillus larvae* and identification and description of a novel myxobacterial taxon, *Aggregicoccus edoensis*. In order to find new compounds, 50 myxobacterial strains from our in house myxobacterial collection and two genotypes (ERIC I and ERIC II) of *Paenibacillus larvae* were cultivated and screened by biological assays, HPLC and HPLC-HRESIMS analysis. The compounds recognized as new metabolites were subsequently purified and characterized followed by structure elucidation.

Pyrronazols and phenazine derivatives purified from *Nannocystis pusilla*, strain Ari7 give an insight of yet unexhausted metabolic diversity of microbes, specifically, of myxobacteria. Furthermore, description of paenilarvins from *P. larvae* is the first report of purification of secondary metabolites from this deadly honey bee pathogen. It is known that novel microbial taxa have a huge potency to detect new secondary metabolites. Hence, with an aim to identify novel myxobacterial taxa amongst the group of myxobacteria screened for natural products, their 16S rRNA genes were analyzed and compared to representative strains of the validly published taxa to determine their position in the myxobacterial phylogeny. One strain which delineated from other myxobacterial strains during phylogenetic studies was compared to the type strains of closely related genera for proteomics, fatty acid content and antibiotic resistance and described as a representative of a new genus, *Aggregicoccus edoensis*. Comprehensive screening of this novel taxon can possibly grant access to new myxobacterial metabolites.

List of Figures

Figure A1. Structure of Polymyxin B isolated from <i>B. subtilis</i>	5
Figure A2. Systematic description of myxobacteria within order Myxococcales	10
Figure A3. Natural compounds from myxobacteria with cytotoxic, antifungal and antibacterial activity	12
Figure B1. Structures of paenilarvins A (1), B (2), and C (3)	32
Figure B2. Key HMBC and ROESY correlations of paenilarvin A (1)	35
Figure BS1. ^1H NMR of 1 in CD_3OH , 700 MHz	48
Figure BS2. ^{13}C NMR of 1 in CD_3OH , 176 MHz	49
Figure BS3. ^1H - ^1H COSY NMR of 1 in CD_3OH , selected area	49
Figure BS4. ^1H - ^1H COSY NMR of 1 in CD_3OH , selected area	50
Figure BS5. HSQC NMR of 1 in CD_3OH , selected area	50
Figure BS6. HMBC NMR of 1 in CD_3OH , selected area	51
Figure BS7. HMBC NMR of 1 in CD_3OH , selected area	51
Figure BS8. TOCSY NMR of 1 in CD_3OH , selected area	52
Figure BS9. TOCSY NMR of 1 in CD_3OH , selected area	52
Figure BS10. ROESY NMR of 1 in CD_3OH , selected area	53
Figure BS11. ROESY NMR of 1 in CD_3OH , selected area	53
Figure BS12: ESI HRMS of paenilarvin A (1)	54
Figure BS13. MS/MS spectra of (1)	54
Figure BS14. ^1H NMR of 2 in CD_3OH + 5 μL HCOOH , 700 MHz	56
Figure BS15. ^{13}C NMR DEPT of 2 in CD_3OH +5 μL HCOOH , 176 MHz, selected area	56
Figure BS16. ^{12}C NMR of 2 in CD_3OH +5 μL HCOOH , 176 MHz, selected area	57
Figure BS17. ^1H - ^1H COSY NMR of 2 in CD_3OH +5 μL HCOOH , 700 MHz, selected area	57
Figure BS18. ^1H - ^1H COSY NMR of 2 in CD_3OH +5 μL HCOOH , 700 MHz, selected area	58
Figure BS19. HSQC NMR of 2 in CD_3OH +5 μL HCOOH , 700 MHz, selected area	58
Figure BS20. HMBC NMR of 2 in CD_3OH +5 μL HCOOH , 700 MHz, selected area	59
Figure BS21. HMBC NMR of 2 in CD_3OH +5 μL HCOOH , 700 MHz, selected area	59
Figure BS22. TOCSY NMR of 2 in CD_3OH +5 μL HCOOH , 700 MHz, selected area	60
Figure BS23. TOCSY NMR of 2 in CD_3OH +5 μL HCOOH , 700 MHz, selected area	60
Figure BS24. ROESY NMR of 2 in CD_3OH +5 μL HCOOH , 700 MHz, selected area	61
Figure BS25. ESI HRMS of paenilarvin B (2)	61
Figure BS26: ^1H NMR of 3 in DMSO-d_6 , 700 MHz	62

Figure BS27. ¹³ C NMR of 3 in DMSO-d ₆ , 176 MHz	62
Figure BS28. ¹ H- ¹ H COSY NMR of 3 in DMSO-d ₆ , selected area	63
Figure BS29. ¹ H- ¹ H COSY NMR of 3 in DMSO-d ₆ , selected area	63
Figure BS30. HSQC NMR of 3 in DMSO-d ₆ +5 μL HCOOH, 700 MHz, selected area	64
Figure BS31. HMBC NMR of 3 in DMSO-d ₆ , 700 MHz, selected area	64
Figure BS32. HMBC NMR of 3 in DMSO-d ₆ , 700 MHz, selected area	65
Figure BS33. HMBC NMR of 3 in DMSO-d ₆ , 700 MHz, selected area	65
Figure BS34. HMBC NMR of 3 in DMSO-d ₆ , 700 MHz, selected area	66
Figure BS35. TOCSY NMR of 3 in DMSO-d ₆ , 700 MHz, selected area	66
Figure BS36. TOCSY NMR of 3 in DMSO-d ₆ , 700 MHz, selected area	67
Figure BS37. ROESY NMR of 3 in DMSO-d ₆ , 700 MHz, selected area	67
Figure BS38. ROESY NMR of 3 in DMSO-d ₆ , 700 MHz, selected area	68
Figure BS39. ESI HRMS of paenilarvin C (3)	68
Figure C1. Photographs showing morphology of strain MCy1366T and MCy10622	74
Figure C2. Maximum likelihood phylogenetic tree (PHYML) based on 16S rRNA gene sequences	80
Figure C3. Score-oriented dendrogram showing the similarity of MALDI-TOF mass spectra of cell extracts	83
Figure CS1. (a) Congo Red staining of 3 week old swarm of strain MCy1366T on VY/2 agar displaying a weak positive reaction (b) Phase contrast microscopic image of vegetative cells of MCy1366T in myxo media (bar, 10μm) (c) Lugol's solution staining of 2 week old swarm of strain MCy1366T on P agar displaying a weak positive reaction	94
Figure CS2. Neighbor-joining tree based on 16S rRNA gene sequence	95
Scheme D1. Natural pyrronazol variants	98
Scheme D2. 1-Hydroxy-phenazine-6-yl-α-d-arabinofuranoside (7)	104
Scheme D3. Pyrrole antibiotics	106
Figure D1. Selected ¹ H, ¹³ C HMBC (green arrows) and ROESY NMR Correlations (red arrows) of Pyrronazol A (1)	100
Figure D2. Absolute 4S,5S-Configuration of Pyrronazol A (1)	100
Figure D3. Calculated Solution Conformation of Pyrronazol C1 (4)	104
Figure DS1. ORTEP presentation of the X-ray analysis of Pyrronazol A1 (1)	114
Figure DS2. HMBC-correlations of Pyrronazol A2 (2)	119
Figure DS3. HMBC-correlations of Pyrronazol B (3)	120
Figure DS4. HMBC-correlations of Pyrronazol C1 (4)	120

Figure DS5. HMBC-correlations of Pyrronazol C2 (5)	120
Figure DS6. HMBC- and ROESY correlations of 1-hydroxy-phenazine-6-yl- α -d-arabinofuranoside (7)	121
Figure DS7. ¹ H NMR spectrum of Pyrronazol A (1) in CDCl ₃ (400 MHz)	122
Figure DS8. ¹³ C NMR spectrum of Pyrronazol A (1) in CDCl ₃ (100.6 MHz)	122
Figure DS9. ¹ H NMR spectrum of Pyrronazol A2 (2) in CDCl ₃ (600 MHz)	123
Figure DS10. ¹³ C NMR spectrum of Pyrronazol A2 (2) in CDCl ₃ (100.6 MHz)	123
Figure DS11. ¹ H NMR spectrum of Pyrronazol B (3) in CDCl ₃ (400 MHz)	124
Figure DS12. ¹³ C NMR spectrum of Pyrronazol B (3) in CDCl ₃ (125.8 MHz)	124
Figure DS13. ¹ H NMR spectrum of Pyrronazol C2 (5) in CDCl ₃ (300 MHz)	125
Figure DS14. ¹³ C NMR spectrum of Pyrronazol C2 (5) in CDCl ₃ (75.5 MHz)	125
Figure DS15. ¹ H NMR spectrum of 1-hydroxy-phenazine-6-yl- α -d-arabinofuranoside (7) in CD ₃ OD	126
Figure DS16. ¹³ C NMR spectrum of 1-hydroxy-phenazine-6-yl- α -d-arabinofuranoside (7) in CD ₃ OD	126
Figure E1. Antifungal activity of crude methanol extract of <i>P. larvae</i> ERIC II (DSM 25430) against <i>Mucor hiemalis</i> after HPLC fractionation	128
Figure E2. Structures of pyrronazols and phorbazoles	134
Figure E3. Structure of Rumbrin	135

List of Tables

Table B1. ^1H (700 MHz) and ^{13}C (175 MHz) NMR data of paenilarvin A (1) in CD_3OH	33
Table B2. Minimum inhibitory concentration (MIC) in $\mu\text{g}/\text{mL}$ of paenilarvin A (1) and B (2)	37
Table C1. Differential characteristics of strain MCy1366T, MCy10622 and their closely related strains	77
Table CS1. Type and neotype strains used in this study	87
Table CS2. Salt tolerance	87
Table CS3. Differential physiological reactions in APIZym tests	88
Table CS4. Antibiotic resistance test for MCy1366T and MCy10622 along with related type and neotype strains	89
Table CS5. Dry weight biomass (mg) of MCy1366T and MCy10622 obtained in synthetic S medium with casitone supplemented with various carbon sources	90
Table CS6. Dry weight biomass (mg) of MCy1366T and MCy10622 in minimal casitone (C) medium with various inorganic nitrogen sources, amino acids or peptones sources	90
Table CS7. Fatty acid analysis of MCy1366T, MCy10622 and closely related type strains	91
Table CS8. Dry weight biomass (mg) of MCy1366T and MCy10622 at different pH	94
Table D1. NMR Data of Pyrronazol A1 (1) and A2 (2)	101
Table D2. NMR Data of Pyrronazol B (3) in CDCl_3	102
Table D3. NMR-Data of Pyrronazol C1 (4) and C2 (5) in CDCl_3b	103
Table D4. In-vitro Antibacterial and Antifungal Activity of Pyrronazol A (1), 1,6-Phenazine-diol (6) and 1-Hydroxy-phenazine-6-yl- α -d-arabinofuranoside (7) (MIC [$\mu\text{g}/\text{mL}$])	105
Table D5. Cytotoxicity (LD50 [μM]) of Pyrronazol A (1) and 1,6-Phenazine-diol (6) against growing cell lines	105
Table DS1. Crystal data and structure refinement for Pyrronazol A1 (1)	114
Table DS2. Atomic Coordinates and Equivalent Isotropic Displacement Parameters for Pyrronazol A1 (1)	115
Table DS3. Bond lengths [\AA] and angles [$^\circ$] for Pyrronazol A1 (1)	115
Table DS4. Anisotropic displacement parameters ($\text{\AA}^2 \times 10^3$) for Pyrronazol A1 (1)	118
Table DS5. Hydrogen coordinates ($\times 10^4$) and isotropic displacement parameters ($\text{\AA}^2 \times 10^3$) for Pyrronazol A1 (1)	119
Table DS6. NMR Data of 1-hydroxy-phenazine-6-yl- α -d-arabinofuranoside (7) in CD_3OD	121

Acknowledgements

“Feeling gratitude and not expressing it, is like wrapping a gift and not giving it”

William Arthur Ward

It is impossible for any work to come to a conclusion without adding a warm note of thanks to all those special people who have been kind enough to encourage me throughout and to help me in completing this dissertation.

I am deeply indebted to my doctoral advisors, Prof. Dr. Rolf Müller and Prof. Dr. Rolf Daniel for giving me the opportunity to work under their guidance. I am also really thankful to Prof. Dr. Marc Stadler for his stimulating suggestions and encouragement which helped me at all times. I am grateful to them for their continuous support through my tough times and taking out time from their busy schedules for proof reading of my manuscripts and thesis. Their critical questioning, remarks and suggestions proved to be a helpful motivating force which made me think all the time and progress in the right direction.

I would also like to express my gratitude to Dr. Kathrin I. Mohr for immense personal attention, dedication, relentless energy, and optimism which enabled me to bring this dissertation to fruition. I am really thankful for her overwhelming care and affection and I will forever cherish my graduate experience working with her.

I also take this opportunity to express my heartfelt thanks to Dr. Joachim Wink, Dr. Rolf Jansen and Heinrich Steinmetz for giving me a deeper insight into subjects which were new to me like chemistry and taxonomy. Their doors were always open for attending and answering all my naïve queries on various subjects. I am also thankful to them for carefully reading and commenting on various versions of manuscripts and thesis.

I wish to reckon my gratefulness to all the members of Microbial Drugs for their unconditional support and help. I appreciate the support of Diana Telkemeyer, Wera Collisi, Klaus Conrad, Stephanie Schulz and Birte Trunkwalter in all the biological work. Special thanks to Dr. Enge Sudarman, Kerstin Schober, Sabrina Wollpers, Silke Reinecke and Aileen Teichmann for all their help in chemistry lab which was a completely new field for me. I tastefully acknowledge their unparalleled enthusiasm

demonstrated by the readiness to share the workspace under any circumstances and care and affection, which made research a pleasant experience. I would also like to acknowledge the fermentation team, the mycology team and the G2L team in Göttingen, especially Wolfgang Kessler, Steffen Bernecker, Marvin Djukic, John Vollmers, Sandra Wiegand for always helping me out in lab and administrative procedures.

This acknowledgment is incomplete without acknowledging my friends in HZI, Vinay Pawar, Smita Bhuyan, Abhinay Sharma, Pratibha Gaur with whom research even during the stressful conditions was a pleasant learning experience. I thank them all for providing resourceful suggestions to many aspects during the preparation of the thesis.

Most importantly, I am thankful to my family in India, particularly my parents for their unconditional love, encouragement and unending patience. I would also like to express my heartfelt appreciation to Sriharsha Puranik for his constant belief in me and for being there with me at every step of the way.

Finally, I acknowledge Erasmus Mundus External Cooperation Window for providing great opportunity in the form of EurIndia fellowships for my PhD.

Promovierenden-Erklärung der Georg-August-Universität Göttingen

Name: Sood, Sakshi

Anschrift: Jüdelstraße 13, 38126 Braunschweig

Ich beabsichtige, eine Dissertation zum Thema „Natural products from Myxococcales and Bacillales & Description of a new myxobacterial taxon“ an der Georg-August-Universität Göttingen anzufertigen. Dabei werde ich von Herrn Prof. Rolf Daniel und Prof. Rolf Müller betreut.

Ich gebe folgende Erklärung ab:

1. Die Gelegenheit zum vorliegenden Promotionsvorhaben ist mir nicht kommerziell vermittelt worden. Insbesondere habe ich keine Organisation eingeschaltet, die gegen Entgelt Betreuerinnen und Betreuer für die Anfertigung von Dissertationen sucht oder die mir obliegenden Pflichten hinsichtlich der Prüfungsleistungen für mich ganz oder teilweise erledigt.

2. Hilfe Dritter wurde bis jetzt und wird auch künftig nur in wissenschaftlich vertretbarem und prüfungsrechtlich zulässigem Ausmaß in Anspruch genommen. Insbesondere werden alle Teile der Dissertation selbst angefertigt; unzulässige fremde Hilfe habe ich dazu weder unentgeltlich noch entgeltlich entgegengenommen und werde dies auch zukünftig so halten.

3. Die Richtlinien zur Sicherung der guten wissenschaftlichen Praxis an der Universität Göttingen werden von mir beachtet.

4. Eine entsprechende Promotion wurde an keiner anderen Hochschule im In- oder Ausland beantragt; die eingereichte Dissertation oder Teile von ihr wurden nicht für ein anderes Promotionsvorhaben verwendet.

Mir ist bekannt, dass unrichtige Angaben die Zulassung zur Promotion ausschließen bzw. später zum Verfahrensabbruch oder zur Rücknahme des erlangten Grades führen.

Göttingen,

Curriculum Vitae

Name: Sakshi Sood

Nationality: Indian

Birth Date: 2nd March, 1987

Email: Sakshi.sood@helmholtz-hzi.de

Sakshisood87@gmail.com

Since 08/2010

Doctorate studies

Department of Microbial Drugs, Helmholtz Centre for infection Research, Braunschweig, Germany

Department of Genomic and Applied Microbiology & Göttingen Genomics Laboratory, Institute of Microbiology and Genetics, Georg-August University of Göttingen, Germany

08/2009-05/2010

Masters thesis

“Isolation and characterization of an antibacterial small molecule from a soil bacterium”

Department of Biotechnology, Indian Institute of Technology Roorkee, India

08/2008-05/2010

M.Sc. Biotechnology

Department of Biotechnology, Indian Institute of Technology Roorkee, India

07/2005 – 05/2008

B.Sc. (Hons.) Microbiology

Department of Microbiology, Institute of Home Economics, University of Delhi, India

03/2008

High School

St. Luke’s Sen. Sec. School, Solan, India